NEXT THERAPEUTIC TARGETS IN OCULAR DISEASES

EDITED BY: Ryoji Yanai, Yoko Okunuki, Dong Ho Park and Embong Zunaina

PUBLISHED IN: Frontiers in Medicine

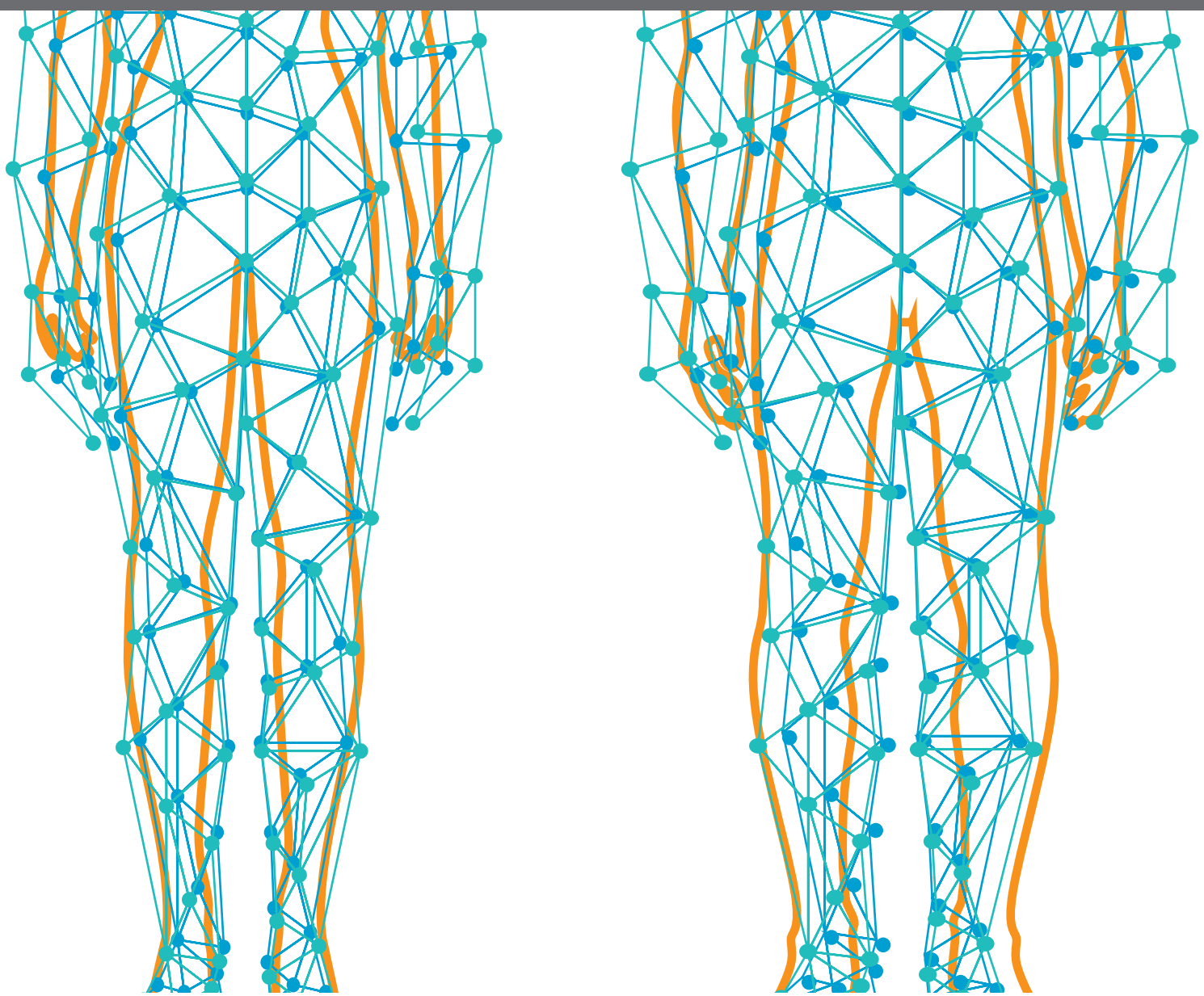

frontiers Research Topics

ISSN 1664-8714
ISBN 978-2-88976-586-7
DOI 10.3389/978-2-88976-586-7

About Frontiers

Frontiers is more than just an open-access publisher of scholarly articles: it is a pioneering approach to the world of academia, radically improving the way scholarly research is managed. The grand vision of Frontiers is a world where all people have an equal opportunity to seek, share and generate knowledge. Frontiers provides immediate and permanent online open access to all its publications, but this alone is not enough to realize our grand goals.

Frontiers Journal Series

The Frontiers Journal Series is a multi-tier and interdisciplinary set of open-access, online journals, promising a paradigm shift from the current review, selection and dissemination processes in academic publishing. All Frontiers journals are driven by researchers for researchers; therefore, they constitute a service to the scholarly community. At the same time, the Frontiers Journal Series operates on a revolutionary invention, the tiered publishing system, initially addressing specific communities of scholars, and gradually climbing up to broader public understanding, thus serving the interests of the lay society, too.

Dedication to Quality

Each Frontiers article is a landmark of the highest quality, thanks to genuinely collaborative interactions between authors and review editors, who include some of the world's best academicians. Research must be certified by peers before entering a stream of knowledge that may eventually reach the public - and shape society; therefore, Frontiers only applies the most rigorous and unbiased reviews.
Frontiers revolutionizes research publishing by freely delivering the most outstanding research, evaluated with no bias from both the academic and social point of view. By applying the most advanced information technologies, Frontiers is catapulting scholarly publishing into a new generation.

What are Frontiers Research Topics?

Frontiers Research Topics are very popular trademarks of the Frontiers Journals Series: they are collections of at least ten articles, all centered on a particular subject. With their unique mix of varied contributions from Original Research to Review Articles, Frontiers Research Topics unify the most influential researchers, the latest key findings and historical advances in a hot research area! Find out more on how to host your own Frontiers Research Topic or contribute to one as an author by contacting the Frontiers Editorial Office: frontiersin.org/about/contact

NEXT THERAPEUTIC TARGETS IN OCULAR DISEASES

Topic Editors:
Ryoji Yanai, Yamaguchi University, Japan
Yoko Okunuki, Janssen Biopharma, United States
Dong Ho Park, Kyungpook National University Hospital, South Korea
Embong Zunaina, Universiti Sains Malaysia, Malaysia

Citation: Yanai, R., Okunuki, Y., Park, D. H., Zunaina, E., eds. (2022). Next Therapeutic Targets in Ocular Diseases. Lausanne: Frontiers Media SA. doi: 10.3389/978-2-88976-586-7

Table of Contents

frontiers | Frontiers in Medicine

EDITORIAL
published: 23 June 2022
doi: 10.3389/fmed.2022.953377

Editorial: Next Therapeutic Targets in Ocular Diseases

Ryoji Yanai[1]*, *Yoko Okunuki*[2], *Dong Ho Park*[3,4] and *Embong Zunaina*[5]

[1] Department of Ophthalmology, Yamaguchi University Graduate School of Medicine, Yamaguchi, Japan, [2] Janssen Biopharma, South San Francisco, CA, United States, [3] Department of Ophthalmology, School of Medicine, Kyungpook National University, Kyungpook National University Hospital, Daegu, South Korea, [4] Cell and Matrix Research Institute, Kyungpook National University, Daegu, South Korea, [5] Department of Ophthalmology and Visual Science, School of Medical Sciences, Universiti Sains Malaysia, Kubang Kerian, Malaysia

Keywords: diabetic macular edema, glaucoma, uveitis, pediatric cataract, inherited retinal diseases, age-related macular degeneration, digitally assisted vitreoretinal surgery, 27-gauge vitrectomy

Editorial on the Research Topic

Next Therapeutic Targets in Ocular Diseases

Vision impairment significantly impacts the length and quality of life (QOL). Over the last several decades, there has been a revolution in our understanding of ocular diseases and an advance in the development of medical and surgical treatment for patients. Particularly in developed countries, the leading causes of vision impairment are diabetic retinopathy, glaucoma, and age-related macular degeneration (AMD).

The most recent medical treatment in ocular diseases is anti-vascular endothelial growth factor (VEGF) therapy for AMD, diabetic macular edema (DME), and neovascular glaucoma. However, the currently available treatments are ineffective for some ocular diseases. These inefficacies in the treatment of vision impairments need to be addressed.

Given these unmet medical needs, it is imperative to investigate the pathological factors that constitute the risks of vision impairment. It is this important topic that provides a platform for this collection of papers to explore the next therapeutic targets in ocular diseases with visual impairment. The inquiry can be sub-divided into three categories:

1. Cutting-edge treatments for DME and diabetic retinopathy: VEGF and next related factors.
2. Next medical applications of treatment options for ocular diseases: gene therapy, new or existing anti-inflammatory therapy.
3. Advanced surgical technologies for ocular diseases: exploring novel usages of these medical devices, and also the application of VEGF.

The first category, *Cutting*-edge *treatments for DME and diabetic retinopathy,* involves the selective accumulation of clinical studies in patients with DME, or diabetic retinopathy, in order to investigate future therapeutic options. As mentioned in the introduction section, anti-VEGF agents such as ranibizumab are the most successful treatment options for DME, which are pathologically linked to the disruption of the blood retinal barrier broken by VEGF. Nonetheless, monthly injections of ranibizumab are impractical as the cost of anti-VEGF agents and the requirement of frequent clinic visits can be serious barriers to patient compliance to the treatment regimen. Lai et al. demonstrated that a treat-and-extend (T&E) regimen with ranibizumab at 4-week intervals effectively improved best corrected visual acuity (BCVA) and reduced central retinal thickness (CRT) for 91 eyes from the 64 patients they studied. In their contribution, Chen et al. found that erythropoietin has an angiogenic potential equal to VEGF, and that intravitreal injection of

OPEN ACCESS

Edited and reviewed by:
Jodhbir Mehta,
Singapore National Eye Center, Singapore

***Correspondence:**
Ryoji Yanai
yanai@yamaguchi-u.ac.jp

Specialty section:
This article was submitted to Ophthalmology, a section of the journal Frontiers in Medicine

Received: *26 May 2022*
Accepted: *02 June 2022*
Published: *23 June 2022*

Citation:
Yanai R, Okunuki Y, Park DH and Zunaina E (2022) Editorial: Next Therapeutic Targets in Ocular Diseases. Front. Med. 9:953377. doi: 10.3389/fmed.2022.953377

ranibizumab (IVR) discernibly reduced the erythropoietin level, but not enough to the normal level when they compared 24 proliferative diabetic retinopathy patients with 11 non-diabetic patients.

To determine the prognostic factors in vitrectomized eyes with DME, which is not the effect of anti-VEGF therapy, Liang et al. demonstrated that intraocular inflammation has an important influence on the pathogenesis of DME in 36 vitrectomized eyes when compared with 71 treatment-naïve eyes and suggested that anti-inflammatory therapies may represent another strategy for the treatment of DME in vitrectomized eyes. Moreover, Hsia et al. evaluated the effectiveness and safety of anti-inflammatory therapies as intravitreal dexamethasone (DEX) implants in refractory DME treated by intravitreal ranibizumab. They concluded that switching to a DEX implant is not only feasible but also safe for treating patients of DME refractory with intravitreal ranibizumab.

In an insightful work using acrolein, a highly reactive aldehyde that covalently binds to cellular macromolecules, Fukutsu et al. demonstrated that Rho-associated coiled-coil-containing protein kinases-1 (ROCK-1) mediated the migration of retinal glial cells: a pathological hallmark of diabetic retinopathy. Although VEGF is one of the prominent participants in the pathological factors in diabetic ocular disease, the current data suggests that inflammation is the next therapeutic target in the mechanisms of progressive and encouraging factors in DME and diabetic retinopathy.

The second category of papers in this collection, *Medical applications of ocular diseases*, explores the next medical treatment options, including gene therapy, biologics, and immune mediators. Inherited retinal dystrophies represent a clinical and Research Topic of great interest. This is because of the lack of approved treatments in most cases and also because of the increasing prevalence related to the evolution of diagnostic approaches to detect these diseases early. In their paper, Amato et al. reviewed the current state-of-the-art, and the rapidly evolving future perspectives regarding gene therapy in the primary inherited retinal dystrophies in order to provide an updated, broad, and comprehensive scenario regarding the present situation and future attitudes.

As is now widely known, and generally accepted, uveitis is one of the significant causes of vision loss and is estimated to cause ∼10% blindness in developed countries. Immunosuppressive therapy, including local or systemic corticosteroids, is the primary treatment for non-infectious uveitis. Although prolonged corticosteroid used leads to severe ocular and systemic side effects, it is now increasingly hoped corticosteroid-sparing agents will be the next effective and practical therapeutic agents in ocular inflammatory diseases. Harada et al. performed clinical studies and found the efficacy and safety of methotrexate in treating Japanese patients with non-infectious uveitis. Hiyama et al. also investigated immunosuppressive therapies' clinical characteristics and efficacy in 65 eyes in 35 patients (14 male and 21 female) with Vogt-Koyanagi-Harada (VKH) disease. They proposed the treatment possibility for patients with late-stage VKH disease with adalimumab and low-dose methotrexate combination therapy. However, some severe uveitis cases are resistant to steroid treatment, multiple conventional disease-modifying antirheumatic drugs (methotrexate and salazosulfapyridine), and tumor necrosis factor-α (TNF-α) inhibitors (adalimumab and infliximab). Kaneko et al. reported the possibility of a Janus kinase (JAK) inhibitor, including baricitinib, as a viable option in treating uveitis with resistance to conventional treatment.

Some other medical procedures that can be categorized as *Medical applications for ocular diseases* are the effect of Sulforaphane (SFN), a natural isothiocyanate, reported by Sim et al. SFN effectively alleviates $PM_{2.5}$-induced oxidative damage in human ARPE-19 cells by its antioxidant effects; additionally, SFN can potentially be used as a therapeutic agent for AMD, particularly in cases related to $PM_{2.5}$ exposure. The role of oxymatrine as a transforming growth factor-β (TGF-β) and TNF-α inhibitor is to retard the development and progression of an animal model of glaucoma, as has been proposed by Das et al. in their contribution.

The third category, *Surgical technologies for ocular diseases*, is related to research efforts for the development of advanced therapeutic techniques. For instance, Kim et al. presented the data on the effectiveness and safety profile of 27-gauge pars plana vitrectomy (PPV) for various vitreoretinal conditions associated with uveitis. This study proposes that most uveitis specialists anticipate using 27-gauge PPV because of its minimally invasive nature which suit uveitis eyes.

Melega et al. conducted a randomized clinical trial to compare nylon sutures to polyglactin sutures in pediatric cataract patients and demonstrated that polyglactin 10-0 sutures in pediatric patients' cataract surgeries are safe and result in fewer post-operative complications than non-absorbable nylon 10-0 sutures.

In their innovative study on vitrectomy, Park et al. demonstrated that the customized color settings available in the digitally assisted vitreoretinal surgery (DAVS) system enabled surgeons to lower the indocyanine green (ICG) concentration as much as 3-fold, which would be helpful in reducing the ICG toxicity. This is the first study that quantitatively measured the macular color contrast according to different color channels using the DAVS color settings.

In another exciting contribution that suggests an alternative treatment to both surgery and the conventional medical treatment for pterygium, Omar et al. proposed the possible use of intralesional anti-VEGF as the future modality of adjunctive therapy for pterygium surgery.

This compendium of papers on this Research Topic provides interesting, innovative and helpful insights that can surely contribute to the development of subsequent management and treatment regimens for vision loss from ocular diseases, including DME, diabetic retinopathy, inherited retinal dystrophies, uveitis, AMD, glaucoma and pterygium. This timely collection of articles pertinently emphasizes the importance of DME and anti-VEGF therapies in basic research and clinical settings. It presents not only some novel and creative methods of anti-VEGF therapy, gene therapy, anti-inflammatory therapy, and offers improvements in current treatment practices for vitrectomy and pterygium surgery but also questions, re-considers and re-interprets widely held assumptions in the light

of these emerging therapeutic procedures, application options and advanced technologies for ocular diseases. However, one limitation of this collection is the paucity of evidence. This insufficiency may well be because of the number of subjects studied, or the size of the data. Also, in some instances, the specific mechanisms for the studies could be rendered clearer, or made more lucid, by further elaboration.

It is our expectation and hope that this collective inquiry in the form of research papers will raise the level of understanding about, and also sharpen the focus on the pathogenesis of ocular diseases, including genomic, molecular, cellular predisposition. We also hope that the contributions assembled here will play a significant catalytic role in the future development of next therapeutic options.

AUTHOR CONTRIBUTIONS

RY drafted the manuscript. YO, DP, and EZ critically proofread and edited the manuscript. All authors contributed to the article and approved the submitted version.

FUNDING

DP is financially supported by the Basic Science Research Program of the National Research Foundation of Korea (NRF) funded by the Korean government (Ministry of Science and ICT) (2019R1A2C1084371) and also supported by the Ministry of Science and ICT (MSIT) Korea under the Information Technology Research Center (ITRC) Support Program (IITP-2022-2020-0-01808) supervised by the Institute of Information and Communications Technology Planning and Evaluation (IITP). This research was supported by Korea Drug Development Fund funded by Ministry of Science and ICT, Ministry of Trade, Industry and Energy, and Ministry of Health and Welfare (HN21C0923000021, Republic of Korea).

Conflict of Interest: YO was employed by Janssen Biopharma.

The remaining authors declare that the research was conducted in the absence of any commercial or financial relationships that could be construed as a potential conflict of interest.

Publisher's Note: All claims expressed in this article are solely those of the authors and do not necessarily represent those of their affiliated organizations, or those of the publisher, the editors and the reviewers. Any product that may be evaluated in this article, or claim that may be made by its manufacturer, is not guaranteed or endorsed by the publisher.

frontiers in Medicine

ORIGINAL RESEARCH
published: 30 April 2021
doi: 10.3389/fmed.2021.649979

Short-Term Outcomes of Refractory Diabetic Macular Edema Switch From Ranibizumab to Dexamethasone Implant and the Influential Factors: A Retrospective Real World Experience

Ning-Yi Hsia[1], Chun-Ju Lin[1,2,3], Huan-Sheng Chen[4], Cheng-Hsien Chang[1,2,3], Henry Bair[1,5], Chun-Ting Lai[1], Jane-Ming Lin[1,3], Wen-Lu Chen[1,3], Peng-Tai Tien[1,6], Wen-Chuan Wu[1] and Yi-Yu Tsai[1,2,3]*

[1] Department of Ophthalmology, Eye Center, China Medical University Hospital, Taichung, Taiwan, [2] School of Medicine, College of Medicine, China Medical University, Taichung, Taiwan, [3] Department of Optometry, Asia University, Taichung, Taiwan, [4] An-Shin Dialysis Center, NephroCare Ltd., Fresenius Medical Care, Taichung, Taiwan, [5] School of Medicine, Stanford University, Stanford, CA, United States, [6] Graduate Institute of Clinical Medical Science, China Medical University, Taichung, Taiwan

OPEN ACCESS

Edited by:
Dong Ho Park,
Kyungpook National University Hospital, South Korea

Reviewed by:
Haemin Kang,
Catholic Kwandong University, South Korea
Jae Hui Kim,
Kim's Eye Hospital, South Korea

***Correspondence:**
Chun-Ju Lin
doctoraga@gmail.com

Specialty section:
This article was submitted to Ophthalmology, a section of the journal Frontiers in Medicine

Received: 06 January 2021
Accepted: 24 March 2021
Published: 30 April 2021

Citation:
Hsia N-Y, Lin C-J, Chen H-S, Chang C-H, Bair H, Lai C-T, Lin J-M, Chen W-L, Tien P-T, Wu W-C and Tsai Y-Y (2021) Short-Term Outcomes of Refractory Diabetic Macular Edema Switch From Ranibizumab to Dexamethasone Implant and the Influential Factors: A Retrospective Real World Experience. Front. Med. 8:649979. doi: 10.3389/fmed.2021.649979

Introduction: To evaluate the effectiveness and safety of intravitreal dexamethasone (DEX) implants in refractory diabetic macular edema (DME) treated by intravitreal ranibizumab.

Materials and Methods: We retrospectively analyzed DME patients who received DEX implant treatment after being refractory to at least 3 monthly intravitreal ranibizumab injections. The main outcomes were best-corrected visual acuity (BCVA), central retinal thickness (CRT), and intraocular pressure (IOP).

Results: Twenty-nine eyes of 26 patients who had previously received an average of 8.1 ± 4.4 ranibizumab injections were included. Patients received between one and three DEX implants during 12.4 ± 7.4 months of follow-up. The mean final CRT significantly decreased from $384.4 \pm 114.4\,\mu m$ at baseline to $323.9 \pm 77.7\,\mu m$ ($p = 0.0249$). The mean final BCVA was 51.4 ± 21.3 letters, which was not significant compared to baseline (44.9 ± 30.2 letters, $p = 0.1149$). Mean IOP did not increase significantly. All patients tolerated the treatment well without serious adverse events. Higher baseline CRT and worse BCVA correlated with better therapeutic responses.

Conclusion: Switching to DEX implant is feasible and safe for treating patients of DME refractory to intravitreal ranibizumab in real world. Further larger-scale or multicenter studies would be conducted to explore different DEX treatment strategies for DME, such as first-line or early switch therapy, for better BCVA improvement.

Keywords: diabetic macular edema, intravitreal dexamethasone implant, intravitreal ranibizumab, ozurdex, refractory diabetic macular edema

INTRODUCTION

Diabetes mellitus is one of the most important global health issues of the twenty-first century. At present, there are 425 million patients with diabetes worldwide, and this number is projected to reach 629 million by 2045 (1). Diabetic retinopathy, a microvascular complication of diabetes, has an estimated prevalence of 34.6% among patients with diabetes. Diabetic macular edema (DME), a manifestation of diabetic retinopathy, develops in ∼6.8% of patients with diabetes and is a major cause of visual loss in this population (2).

Hyperglycemia in diabetes increases oxidative stress, inflammation, and vascular dysfunction. Oxidative stress and inflammation induce the upregulation of growth factors, such as vascular endothelial growth factor (VEGF) and cytokines, which contribute to the breakdown of the blood-retinal barrier (BRB) by disrupting the integrity of retinal vascular endothelial cell tight junctions and increasing vascular permeability (3). The ensuing fluid accumulation, in addition to the persistent presence of inflammatory factors, causes dysfunction of the inner nuclear layer and subsequent development of DME (4).

VEGF antagonists are frequently used as intravitreal treatments for DME, as several studies reveal that patients with DME had favorable visual and anatomic responses to ranibizumab (5, 6). However, there are still patients who, after a favorable initial response to anti-VEGF agents, show decreased responses over time and became resistant to further intravitreal injections. This may be a result of inflammatory mediators other than VEGF contributing to the persistence of DME (7). Increasing dosages of intravitreal injections are needed to control the disease. However, this carries an increased risk of complications and poor compliance (8).

Corticosteroids have been demonstrated to inhibit the expression of VEGF and other inflammatory factors, thus reinforcing the BRB. The biodegradable intravitreal dexamethasone (DEX) implant provides sustained release of the anti-inflammatory corticosteroid dexamethasone into the vitreous. DEX implants have been identified as an effective treatment of DME and have recently been approved by the US Food and Drug Administration (FDA) (9–11). We thus conducted this study to investigate anatomic and functional improvements of DEX implant treatment in a group of patients with DME refractory to previous ranibizumab injections.

MATERIALS AND METHODS

This retrospective, non-comparative, consecutive case series study was approved by the Institutional Ethics Committee and conducted in compliance with the tenets of the Declaration of Helsinki. We retrospectively analyzed the eyes of patients with DME refractory to intravitreal ranibizumab treatment, were treated with DEX implant between August 2013 and October 2017. Informed oral and written consent was obtained from all patients. Before March 2020, Taiwan National Health Insurance scheme only reimbursed 3 initial plus 5 additional injections of ranibizumab for eligible patients with DME. No switch to DEX was allowed. Therefore, patients had to continue 3 to 8 ranibizumab injections unless they decide to pay for DEX out of pocket.

The inclusion criteria were as follows: (1) a diagnosis of DME (the presentation of choroidal neovascularization with macular edema, confirmed by fluorescein angiography and optical coherence tomography [OCT]); (2) a history of treatment with at least 3 monthly intravitreal ranibizumab injections, followed by increasing or persistent sub-retinal fluid or retinal edema on OCT; and (3) a CRT $>250\,\mu m$. The criteria for treatment with DEX implant were the same as the retreatment criteria for ranibizumab regarding the presence of intraretinal or subretinal fluid.

We recorded general patient data including age, sex, laterality, medical history, glycated hemoglobin (HbA1c), best-corrected visual acuity (BCVA), central retinal thickness (CRT), intraocular pressure (IOP), and results of external ocular and slit-lamp examinations. Each patient underwent a thorough bilateral fundus examination by indirect ophthalmoscopy, fundus photography, fluorescein angiography, and spectral-domain OCT (Cirrus HD-OCT; Carl Zeiss Meditec, Inc., Dublin, CA) scans. Over the course of the treatment, patients received between one and three injections of DEX implant 0.7 mg (Ozurdex, Allergan, Inc, Irvine, CA). Before each DEX implantation, the topical antibiotic levofloxacin (Cravit, Santen Pharmaceutical Co., Osaka, Japan) was applied. Topical and subconjunctival anesthesia was achieved by 0.5% proparacaine hydrochloride (Alcaine, Alcon Pharmaceuticals, Puurs, Belgium) before surgery. Each eye was prepared in a sterile manner using 5% povidone/iodine. The DEX implant was inserted intravitreally via a pars plana puncture (3.5 mm away from the limbus). Application of levofloxacin eyedrops was prescribed four times a day for 1 week after the operation. Initial management with ranibizumab and the number of subsequent treatments with DEX implant were collected. All of the patients were scheduled for monthly follow-ups.

The main outcome measures included the mean change in CRT from baseline as measured by spectral-domain OCT and mean change in BCVA (approximate Early Treatment Diabetic Retinopathy Study [ETDRS] letter scores) from baseline during monthly follow-ups. Therefore, the outcome of DEX implant after ranibizumab was evaluated by analyzing changes in retinal anatomy and vision, with reference to patient characteristics and fundus findings. Safety was evaluated by recording complications and other adverse events during the follow-up period.

For statistical analyses, SAS 9.4 was used in this study. For comparison of cross-section data, one-way ANOVA was used for continuous data and Fisher's exact test was used for categorical data. For comparison of serial data, the principle of a generalized linear mixed model (GLMM) was applied using the GLIMMIX procedure in SAS. Generalized linear mixed model is actually a method with the same concept as repeated measured ANOVA for

Abbreviations: DEX, dexamethasone; DME, diabetic macular edema; BCVA, best-corrected visual acuity; CRT, central retinal thickness; IOP, intraocular pressure; VEGF, vascular endothelial growth factor; BRB, blood-retinal barrier; FDA, Food and Drug Administration; HbA1c, glycated hemoglobin; ETDRS, Early Treatment Diabetic Retinopathy Study; GLMM, generalized linear mixed model.

serial data comparison but is more flexible and tolerant of data completeness. Shapiro-Wilk test and Kolmogorov-Smirnov tests were both used for normality test with SAS procedure univariate.

RESULTS

Study Population and Treatments

A total of 29 eyes of 26 patients with DME were included in this study. The study group comprised of 14 men and 12 women, and the mean age was 62.0 ± 9.1 (range 46–84) years. The mean baseline HbA1c was 7.5 ± 1.3 %. Before any treatment (baseline), the mean CRT was 384.4 ± 114.4 (range 248–727) μm (**Table 1**). After ranibizumab treatment, patients were followed up for an average of 12.4 ± 7.4 months. Prior to receiving DEX implant treatment, all patients had been treated with an average of 8.1 ± 4.4 (range 3–18) injections of intravitreal ranibizumab. The time between the last ranibizumab injection and the first DEX injection was a month. Each eye received an average of 1.3 ± 0.6 DEX implant (range 1–3) injections. Of the 29 study eyes, 23 eyes received only one DEX implant, four eyes received two DEX implants and two eyes received three DEX implants. The mean interval between DEX implant injections in the six eyes that received more than one injection was 5.93 ± 2.68 months (range 3.1 ∼ 10.2 months). The follow-up period before DEX was 12.39 ± 7.44 months, the follow-up period after DEX was 7.43 ± 4.60 months, and the entire follow-up period was 19.82 ± 8.96 months.

Anatomic Changes

Distribution of CRT thickness before DEX implant treatment were as follows: 16 eyes between 350 and 250 μm, 8 eyes between 450 and 350 μm, 3 eyes between 550 and 450 μm, 1 eye between 650 and 550 μm, and 1 eye >650 μm. All eyes showed anatomic improvement after switching to intravitreal DEX implant treatment, with significant postoperative changes in CRT as measured by OCT. After DEX implant treatment, the mean final CRT (323.9 ± 77.7, range 201–488 μm) was significantly lower than the baseline value (384.5 ± 114.4, range 248–727 μm) ($p = 0.0249$), and also significantly lower than the mean CRT at 1 month after the last injection of ranibizumab (375.5 ± 111.0, range 261–757 μm) ($p = 0.0265$; **Figure 1A**). The mean best CRT (the lowest CRT value recorded during follow-up)after ranibizumab treatment (302.1 ± 73.5, range 195–568 μm) was significantly lower than the baseline value ($p = 0.0004$), and it was maintained if not further improved after DEX implants (286.1 ± 56.3, range 172–414 μm) ($p < 0.0001$ compared to baseline; **Figure 1B**).

TABLE 1 | Baseline characteristics of the patients.

Baseline characteristics	Mean ± SD or (%)
Age (years)	62.0 ± 9.1
Gender ($n = 26$)	
Female	12 (46.2%)
Male	14 (53.8%)
Eyes ($n = 29$)	
OD	16 (55.2%)
OS	13 (44.8%)
Baseline BCVA (letter score)	44.9 ± 30.2
Baseline CRT (μm)	384.4 ± 114.4
Baseline IOP (mmHg)	14.9 ± 3.1
Lens status	
Phakic	20 (69%)
Pseudophakic	9 (31%)
Follow-up (months)	
Total	19.8 ± 9.0
Before ozurdex (anti-VEGF use)	12.4 ± 7.4
After ozurdex	7.4 ± 4.6

BCVA, best-corrected visual acuity; CRT, central retina thickness; IOP, intraocular pressure; VEGF, vascular endothelial growth factor.

Changes in Best-Corrected Visual Acuity

After DEX implant treatment, the mean final BCVA (51.4 ± 21.3 letters) did not significantly improve as compared to baseline (44.9 ± 30.2 letters) ($p = 0.1149$; **Figure 2A**). However, the mean maximal BCVA (the highest letter score recorded during follow-up) after DEX implant (61.2 ± 17.4 letters) was significantly higher than baseline ($p = 0.0022$; **Figure 2B**).

Predictors of Therapeutic Response

Several baseline patient parameters were analyzed to explore the correlation with the treatment responses (**Table 2**). Thicker baseline CRT (**Figure 3**), lower HbA1c, and worse BCVA (**Figure 4**) had better responses to the treatment. Multivariate logistic regression and general linear model analyses confirmed the same results that thicker baseline CRT and worse baseline BCVA had better responses to the treatment ($p < 0.0001$).

Safety Outcomes

The mean final IOP (15.3 ± 3.2 mmHg) was not significantly higher than the baseline value (14.9 ± 3.1 mmHg, $p = 0.5643$), and not significantly higher than the IOP at 1 month after the last injection of ranibizumab (15.3 ± 3.3, $p = 0.9985$). The mean maximal IOP (the highest IOP recorded during follow-up) was 20.1 ± 4.7 mmHg, which was significantly higher than the baseline (14.9 ± 3.1 mmHg, $p < 0.0001$), but not significantly higher than the IOP at 1 month after the last ranibizumab injection (20.0 ± 4.5, mmHg, $p = 0.8480$). During the study, seven patients experienced IOP increases >22 mmHg after DEX implant, but all these patients had IOP returned to ≤22 mmHg after being managed with topical IOP-lowering medications.

All patients tolerated the treatment well, and none experienced serious ocular (e.g., endophthalmitis, non-infectious endophthalmitis, vitreous hemorrhage, retinal tear, retinal detachment, or sustained IOP elevations) or systemic adverse events during the follow-up period.

DISCUSSION

This retrospective case series, carried out in a tertiary medical center in central Taiwan, studied the therapeutic effects of DEX

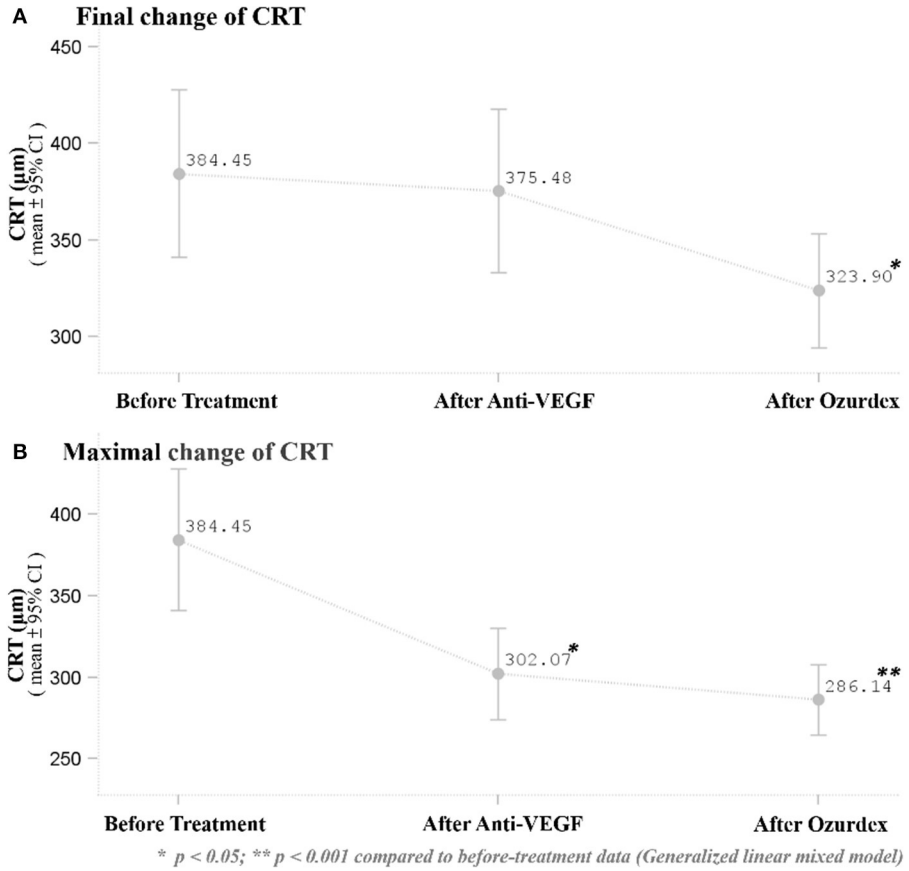

FIGURE 1 | (A) Mean baseline and final CRT after the respective treatments. The mean final CRT after DEX implant treatment was significantly lower than the CRT ($p = 0.0249$) at baseline and 1 month after the last ranibizumab injection ($p = 0.0265$). **(B)** Mean best CRT (the lowest CRT value recorded during follow-up) at baseline and after the respective treatments. The mean best CRT after DEX implant treatment was significantly lower than the CRT ($p < 0.0001$) before treatment. *$p < 0.05$; **$p < 0.001$ compared to before-treatment data (Generalized linear mixed model).

implant treatment on DME in eyes that had been unsuccessfully treated with intravitreal ranibizumab. In this study, DEX implants were effective in the anatomical improvement. Patients were assessed at monthly intervals postoperatively, and anatomic improvements as gauged by CRT were sustained throughout the entire course of follow-up. Even though improvements in CRT did not correlate with significantly improved BCVA, neither did BCVA decrease over the course of treatment and follow-up. DEX implants were well-tolerated, with only a few cases of increased IOP that were manageable with antihypertensive eyedrops.

Currently, there is no optimal treatment regimen for DEX implant therapy for DME (12). In the MEAD study, the protocol allows as-needed (*pro re nata,* PRN) retreatment with DEX implant with a frequency of no more than once every 6 months (13). As the out-of-pocket expense for our patients was about 40,000 NTD (1,370 USD) for each DEX implant during the study, we treated most eyes with one dose of DEX implant, followed by PRN injections when macular edema reoccurred. During the mean follow-up of 7.4 ± 4.6 months, almost 80% of the patients received only one DEX implant, and only two eyes received three injections.

The various available treatments for DME include anti-VEGFs, laser, surgery, and corticosteroids, with each targeting different pathogenic mechanisms of the disease (4). Our study suggests two main explanations for the observed benefit of DEX implant after refractory ranibizumab treatment: the pharmacologic and pharmacokinetic properties of the DEX implant and the possible tachyphylaxis or tolerance to ranibizumab. First, inflammation plays a prominent role in the pathogenesis of DME. Many features of inflammation, such as the leukocyte recruitment and adhesion to vascular endothelium (leukostasis), increased blood flow and vascular permeability, tissue (macular) edema, neovascularization, and upregulation of inflammatory mediators, have been described in both human and animal models of diabetic retinopathy (12, 14–18). Intravitreally administered corticosteroids act to ameliorate DME in multiple ways. As established anti-inflammatory agents, they reduce the production of pro-inflammatory factors, limit

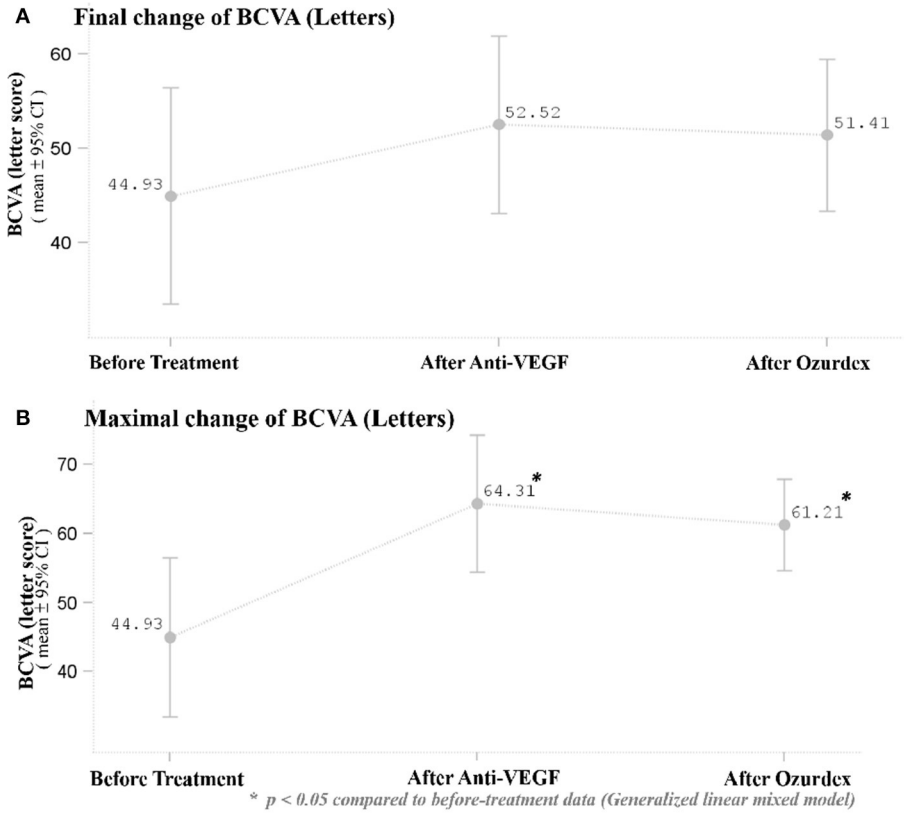

FIGURE 2 | (A) Mean BCVA at baseline and after the respective treatments. There was no significant improvement in BCVA 1 month after the last ranibizumab and after DEX implant treatment. **(B)** Mean maximal BCVA (the highest letter score recorded during follow-up) at baseline and after respective treatments. The mean maximal BCVA after DEX implant treatment was significantly higher than baseline BCVA ($p = 0.0022$). *$p < 0.05$ compared to before-treatment data (Generalized linear mixed model).

TABLE 2 | Clinical parameters of patients with different therapeutic responses.

	ΔCRT ≤ −50 *n* = 12 (41.38%)	**ΔCRT > −50 *n* = 17 (58.62%)**	***p***	**ΔBCVA ≥ 15 *n* = 8 (27.59%)**	**ΔBCVA< 15 *n* = 21 (72.41%)**	***p***
Initial CRT 2	477.17 ± 106.90	319.00 ± 63.61	<0.0001*	420.38 ± 134.10	370.76 ± 106.37	0.305
Initial HbA1c	6.65 ± 0.59	7.99 ± 1.61	0.018*	7.12 ± 1.41	7.60 ± 1.50	0.487
Age	61.17 ± 10.25	61.94 ± 7.82	0.819	57.25 ± 6.09	63.29 ± 9.13	0.097
Gender						
Female	7 (58.33%)	6 (35.29%)	0.274	6 (75.00%)	7 (33.33%)	0.092
Male	5(41.67%)	11 (64.71%)		2 (25.00%)	14 (66.67%)	
Initial BCVA (Letters)	37.42 ± 27.27	50.24 ± 31.89	0.269	18.63 ± 40.19	54.95 ± 18.24	0.002*
Initial IOP	14.67 ± 2.93	15.12 ± 3.33	0.709	14.13 ± 3.00	15.24 ± 3.19	0.402
Anti-VEGF injection times	9.00 ± 4.43	7.53 ± 4.32	0.379	9.88 ± 3.80	7.48 ± 4.45	0.189
Lens status						
Phakic	9 (75.00%)	11 (64.71%)	0.694	7 (87.50%)	13 (61.90%)	
Pseudophakic	3 (25.00%)	6 (35.29%)		1 (12.50%)	8 (38.10%)	

*$p < 0.05$; BCVA, best-corrected visual acuity; CRT, central retina thickness; HbA1c, glycated hemoglobin; IOP, intraocular pressure; VEGF, vascular endothelial growth factor.

vascular permeability, and inhibit the expression of VEGFs (19). The DEX implant, a sustained-release drug delivery system for the potent corticosteroid dexamethasone, was developed to reduce the need for frequent intraocular injections due to the short half-life of intravitreally injected dexamethasone (<4 h) (20). The implant releases DEX into the vitreous for up to 6 months (21). In a previous study, Lazic et al. demonstrated the therapeutic efficacy of DEX implant for DME resistant to

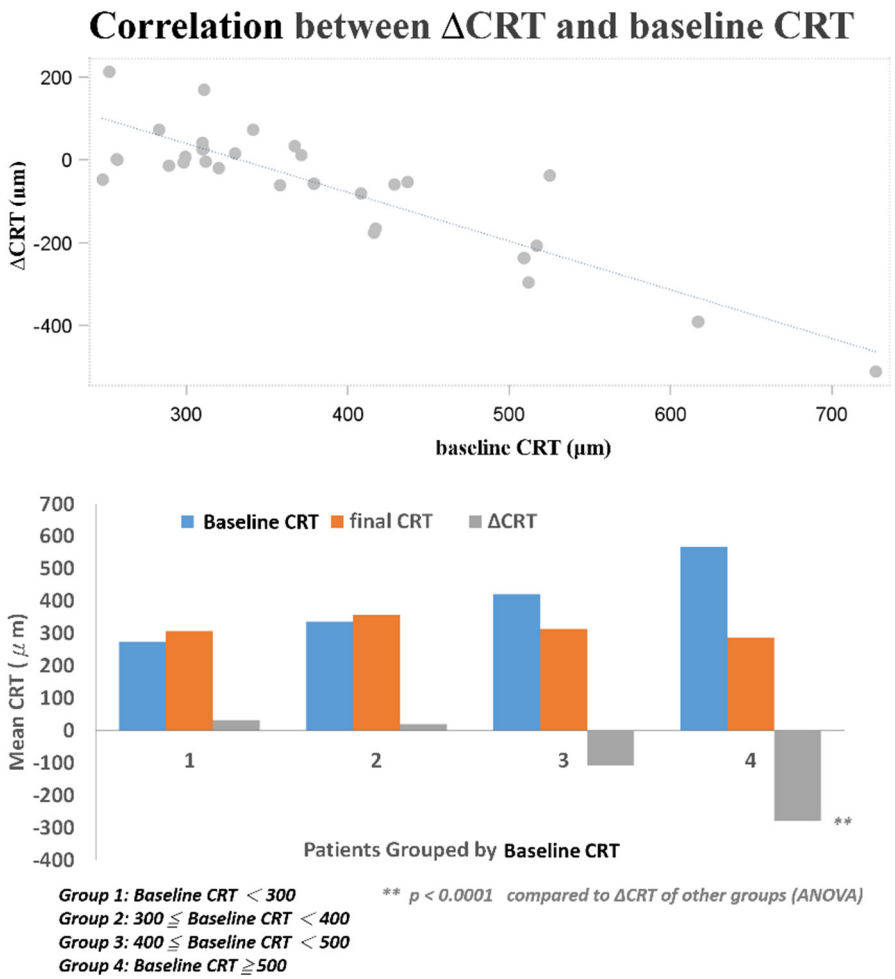

FIGURE 3 | Correlation between changes in CRT and baseline CRT.

the anti-VEGF bevacizumab (22). The use of bevacizumab for DME is off-label, and therefore we examined patients who were initially treated with ranibizumab, which is FDA-approved for DME. Second, the patients' tachyphylaxis/tolerance to the previously administered ranibizumab might be another possible mechanism for the observed therapeutic effect after switching to intravitreal DEX implant. Even though there is a difference between tachyphylaxis and tolerance, both terms have long been presented as phenomena of reduced drug efficacy and are used synonymously in the literature (23). Tachyphylaxis/tolerance in chronic treatment with bevacizumab and ranibizumab was first described in 2007 for age-related macular degeneration (24, 25). Tachyphylaxis/tolerance to ranibizumab might be a result of the neutralization of ranibizumab by the formation of circulating antibodies, the desensitization of the target tissue to the drug, or the reactivation of DME driven by another pathway (26, 27). These effects might be circumvented with the use of pharmaceuticals aiming at other DME-associated pathways.

In our study, DEX implant treatment showed a generally favorable safety profile. Historically, adverse events most commonly associated with corticosteroid therapy include cataracts and steroid-induced glaucoma. Although none of our patients received a cataract surgery after DEX implants, the mean follow-up period was about 7 months, which may not be sufficient for the worsening of cataracts. Some patients in this study experienced transient increase in IOP that were successfully managed with topical medication. There was no case of serious ocular or systemic adverse events such as endophthalmitis, non-infectious endophthalmitis, vitreous hemorrhage, retinal tear, retinal detachment, or sustained IOP elevations.

We found three clinical factors that correlated with the treatment responses. Patients with lower baseline HbA1c had better anatomic improvement after treatment. The importance of glycemic control in the management of diabetic retinopathy was emphasized by previous studies (28, 29). The other two baseline predictive factors were thicker CRT and worse BCVA. Both factors correlated with better responses to DEX treatment in their respective aspects. Campos et al. also found that lower baseline BCVA predicted a higher visual acuity gain (30). It may be

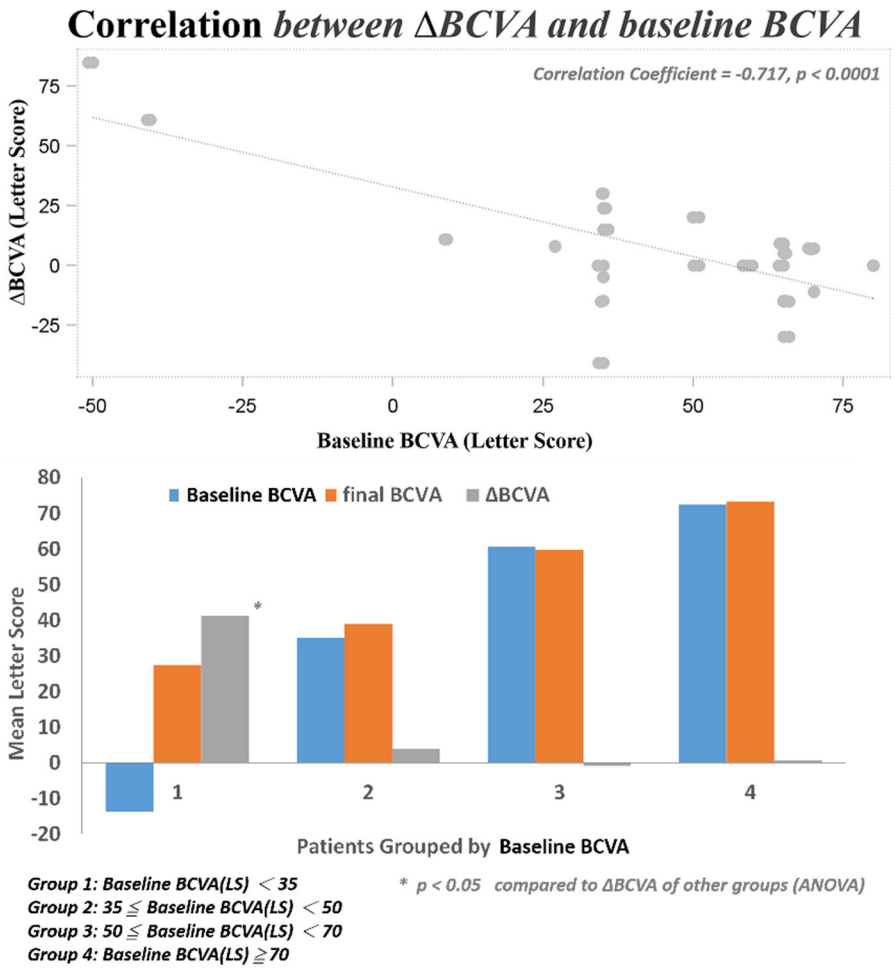

FIGURE 4 | Correlation between changes in BCVA and baseline BCVA.

suggestive of a "ceiling effect" that cannot be ruled out completely in this prediction model; that is, smaller improvements are required to achieve good vision in patients with better starting vision, while those with lower BCVA at baseline have greater capacity to achieved better vision outcome. Another limit of visual acuity improvement was the uncertain optimal timing for DEX switching in patients with DME non-responder to intravitreal ranibizumab. If we can determine patients with DME who are more response to DEX implants, early switch to DEX implant may be performed, which may additional improve their final visual acuity. Limitations of this study include the small sample size and short-term follow-up, the uncontrolled retrospective design of the study, the non-standard treatment protocols, and a lack of consistent performance of fluorescein angiography prior to switching to DEX implant treatment. Nevertheless, this study showed that intravitreal DEX implant treatment was effective immediately after switch and safe in cases of refractory DME resistant to ranibizumab. Switching to DEX implant can be considered in eyes with DME that do not respond to anti-VEGF treatments. Furthermore, higher baseline CRT and worse BCVA were found to be the predictive factors for better therapeutic responses. However, further studies are necessary to determine the optimal timing for DEX switching in patients with DME non-responder to intravitreal ranibizumab and to shed light on the long-term outcomes of this treatment modality.

CONCLUSION

This study demonstrated the feasibility of switching to intravitreal DEX implant in cases of DME that are refractory to intravitreal ranibizumab treatment. Conversion to DEX implant treatment resulted in a significant improvement in CRT. Although BCVA decreased a little after DEX treatment compared with BCVA after anti-VEGF injections, there was no statistical significance. Nevertheless, higher baseline CRT and worse BCVA can predict better therapeutic responses. Further larger-scale or multicenter studies would be conducted to explore different DEX treatment strategies for DME, such as first-line or early switch therapy, for better BCVA improvement.

DATA AVAILABILITY STATEMENT

The original contributions presented in the study are included in the article/supplementary material, further inquiries can be directed to the corresponding author/s.

ETHICS STATEMENT

The studies involving human participants were reviewed and approved by China medical university and hospital research ethics committee-CMUH109-REC3-158. Written informed consent for participation was not required for this study in accordance with the national legislation and the institutional requirements. Written informed consent for publication of his clinical details and clinical images was obtained from the patient.

AUTHOR CONTRIBUTIONS

N-YH, C-JL, H-SC, C-HC, C-TL, J-ML, W-LC, P-TT, and Y-YT were responsible for substantial contributions to the conception or design of the work, and acquisition of data. C-JL, H-SC, and C-HC were responsible for interpretation of results. N-YH, C-JL, and HB participated in the design and was a major contributor in writing the manuscript. N-YH, C-JL, HB, W-LC, and W-CW were responsible for final approval of the version to be published. All authors reviewed and approved the final manuscript.

REFERENCES

1. International Diabetes Federation. *IDF Diabetes Atlas. 8th edn*. Brussels: International Diabetes Federation (2017).
2. Yau JW, Rogers SL, Kawasaki R, Lamoureux EL, Kowalski JW, Bek T et al. Meta-Analysis for eye disease (META-EYE) study group. Global prevalence and major risk factors of diabetic retinopathy. *Diabetes Care.* (2012) 35:556–64. doi: 10.2337/dc11-1909
3. Cebeci Z, Kir N. Role of implants in the treatment of diabetic macular edema: focus on the dexamethasone intravitreal implant. *Diabetes Metab Syndr Obes.* (2015) 8:555–66. doi: 10.2147/DMSO.S73540
4. Das A, McGuire PG, Rangasamy S. Diabetic macular edema: pathophysiology and novel therapeutic targets. *Ophthalmology.* (2015) 122:1375–94. doi: 10.1016/j.ophtha.2015.03.024
5. Wells JA, Glassman AR, Ayala AR, Jampol LM, Bressler NM, Bressler SB, et al. Diabetic retinopathy clinical research network. aflibercept, bevacizumab, or ranibizumab for diabetic macular edema: two-year results from a comparative effectiveness randomized clinical trial. *Ophthalmology*. (2016) 123:1351–9. doi: 10.1016/j.ophtha.2016.02.022
6. Schmidt-Erfurth U, Lang GE, Holz FG, Schlingemann RO, Lanzetta P, Massin P et al. Three-year outcomes of individualized ranibizumab treatment in patients with diabetic macular edema: the RESTORE extension study. *Ophthalmology*. (2014) 121:1045–53. doi: 10.1016/j.ophtha.2013.11.041
7. Totan Y, Guler E. Dexamethasone intravitreal implant for chronic diabetic macular edema resistant to intravitreal bevacizumab treatment. *Curr Eye Res.* (2016) 41:107–13. doi: 10.3109/02713683.2014.1002048
8. Kook D, Wolf A, Kreutzer T, Neubauer A, Strauss R, Ulbig M, et al. Long-term effect of intravitreal bevacizumab (avastin) in patients with chronic diffuse diabetic macular edema. *Retina.* (2008) 28:1053–60. doi: 10.1097/IAE.0b013e318176de48
9. Haller JA, Kuppermann BD, Blumenkranz MS, Williams GA, Weinberg DV, Chou C, et al. Randomized controlled trial of an intravitreous dexamethasone drug delivery system in patients with diabetic macular edema. *Arch Ophthalmol.* (2010) 128:289–96. doi: 10.1001/archophthalmol.2010.21
10. Mehta H, Gillies M, Fraser-Bell S. Perspective on the role of ozurdex (dexamethasone intravitreal implant) in the management of diabetic macular oedema. *Ther Adv Chronic Dis.* (2015) 6:234–45. doi: 10.1177/2040622315590319
11. Pareja-Ríos A, Ruiz-de la Fuente-Rodríguez P, Bonaque-González S, López-Gálvez M, Lozano-López V, Romero-Aroca P. Intravitreal dexamethasone implants for diabetic macular edema. *Int J Ophthalmol.* (2018) 11:77–82. doi: 10.18240/ijo.2018.01.14
12. Yuuki T, Kanda T, Kimura Y, Kotajima N, Tamura J, Kobayashi I, et al. Inflammatory cytokines in vitreous fluid and serum of patients with diabetic vitreoretinopathy. *J Diabetes Complications.* (2001) 15:257–9. doi: 10.1016/S1056-8727(01)00155-6
13. Boyer DS, Yoon YH, Belfort R Jr, Bandello F, Maturi RK, Augustin AJ, et al. Three-year, randomized, sham-controlled trial of dexamethasone intravitreal implant in patients with diabetic macular edema. *Ophthalmology.* (2014) 121:1905–14. doi: 10.1016/j.ophtha.2014.04.024
14. Antonetti DA, Barber AJ, Bronson SK, Freeman WM, Gardner TW, Jefferson LS et al. Diabetic retinopathy: seeing beyond glucose-induced microvascular disease. *Diabetes.* (2006) 55:2401–11. doi: 10.2337/db05-1635
15. Meleth AD, Agrón E, Chan CC, Reed GF, Arora K, Byrnes G, et al. Serum inflammatory markers in diabetic retinopathy. *Invest Ophthalmol Vis Sci.* (2005) 46:4295–301. doi: 10.1167/iovs.04-1057
16. Joussen AM, Poulaki V, Le ML, Koizumi K, Esser C, Janicki H, et al. A central role for inflammation in the pathogenesis of diabetic retinopathy. *FASEB J.* (2004) 18:1450–2. doi: 10.1096/fj.03-1476fje
17. Semeraro F, Cancarini A, dell'Omo R, Rezzola S, Romano MR, Costagliola C. Diabetic retinopathy: vascular and inflammatory disease. *J Diabetes Res.* (2015) 2015:582060. doi: 10.1155/2015/582060
18. Adamis AP, Berman AJ. Immunological mechanisms in the pathogenesis of diabetic retinopathy. *Semin Immunopathol.* (2008) 30:65–84. doi: 10.1007/s00281-008-0111-x
19. Wang K, Wang Y, Gao L, Li X, Li M, Guo J. Dexamethasone inhibits leukocyte accumulation and vascular permeability in retina of streptozotocin-induced diabetic rats via reducing vascular endothelial growth factor and intercellular adhesion molecule-1 expression. *Biol Pharm Bull.* (2008) 31:1541–46. doi: 10.1248/bpb.31.1541
20. Calvo P, Ferreras A, Al Adel F, Dangboon W, Brent MH. Effect of an intravitreal dexamethasone implant on diabetic macular edema after cataract surgery. *Retina*. (2018) 38:490–6. doi: 10.1097/IAE.0000000000001552
21. Chang-Lin JE, Attar M, Acheampong AA, Robinson MR, Whitcup SM, Kuppermann BD, et al. Pharmacokinetics and pharmacodynamics of a sustained-release dexamethasone intravitreal implant. *Invest Ophthalmol Vis Sci.* (2011) 52:80–6. doi: 10.1167/iovs.10-5285
22. Lazic R, Lukic M, Boras I, Draca N, Vlasic M, Gabric N, et al. Treatment of anti-vascular endothelial growth factor-resistant diabetic macular edema with dexamethasone intravitreal implant. *Retina.* (2014) 34:719–24. doi: 10.1097/IAE.0b013e3182a48958
23. Binder S. Loss of reactivity in intravitreal anti-VEGF therapy: tachyphylaxis or tolerance? *Br J Ophthalmol.* (2012) 96:1–2. doi: 10.1136/bjophthalmol-2011-301236
24. Schaal S, Kaplan HJ, Tezel TH. Is there tachyphylaxis to intravitreal antivascular endothelial growth factor pharmacotherapy in age-related macular degeneration? *Ophthalmology.* (2008) 115:2199–205. doi: 10.1016/j.ophtha.2008.07.007
25. Keane PA, Liakopoulos S, Ongchin SC, Heussen FM, Msutta S, Chang KT, et al. Quantitative subanalysis of optical coherence tomography after treatment with ranibizumab for neovascular age-related macular degeneration. *Invest Ophthalmol Vis Sci.* (2008) 49:3115–20. doi: 10.1167/iovs.08-1689

26. Gasperini JL, Fawzi AA, Khondkaryan A, Lam L, Chong LP, Eliott D, et al. Bevacizumab and ranibizumab tachyphylaxis in the treatment of choroidal neovascularisation. *Br J Ophthalmol.* (2012) 96:14–20. doi: 10.1136/bjo.2011.204685
27. Eghøj MS, Sørensen TL. Tachyphylaxis during treatment of exudative age-related macular degeneration with ranibizumab. *Br J Ophthalmol.* (2012) 96:21–3. doi: 10.1136/bjo.2011.203893
28. Matsuda S, Tam T, Singh RP, Kaiser PK, Petkovsek D, Carneiro G, et al. The impact of metabolic parameters on clinical response to VEGF inhibitors for diabetic macular edema. *J Diabetes Complications.* (2014) 28:166–70. doi: 10.1016/j.jdiacomp.2013.11.009
29. Bressler SB, Odia I, Maguire MG, Dhoot DS, Glassman AR, Jampol LM, et al. Factors associated with visual acuity and central subfield thickness changes when treating diabetic macular edema with anti–vascular endothelial growth factor therapy: an exploratory analysis of the protocol t randomized clinical trial. *JAMA Ophthalmol.* (2019) 137:382–9. doi: 10.1001/jamaophthalmol.2018.6786
30. Campos A, Campos EJ, do Carmo A, Caramelo F, Martins J, Sousa JP, et al. Evaluation of markers of outcome in real-world treatment of diabetic macular edema. *Eye Vis.* (2018) 5:27. doi: 10.1186/s40662-018-0119-9

Conflict of Interest: H-SC is employed by company NephroCare Ltd.

The remaining authors declare that the research was conducted in the absence of any commercial or financial relationships that could be construed as a potential conflict of interest.

frontiers in Medicine

ORIGINAL RESEARCH
published: 03 May 2021
doi: 10.3389/fmed.2021.668107

Age, Initial Central Retinal Thickness, and OCT Biomarkers Have an Influence on the Outcome of Diabetic Macular Edema Treated With Ranibizumab– Tri-center 12-Month Treat-and-Extend Study

Chun-Ting Lai[1], Yi-Ting Hsieh[2], Chun-Ju Lin[1,3,4], Jia-Kang Wang[5,6], Chih-Ying Lin[1,3], Ning-Yi Hsia[1,3], Henry Bair[1], Huan-Sheng Chen[7], Chiung-Yi Chiu[5] and Shao-Wei Weng[5]*

[1] Department of Ophthalmology, China Medical University Hospital, China Medical University, Taichung, Taiwan, [2] Department of Ophthalmology, National Taiwan University Hospital, Taipei, Taiwan, [3] School of Medicine, College of Medicine, China Medical University, Taichung, Taiwan, [4] Department of Optometry, Asia University, Taichung, Taiwan, [5] Department of Ophthalmology, Far Eastern Memorial Hospital, Taipei, Taiwan, [6] Department of Electrical Engineering, Yuan Ze University, Taoyuan City, Taiwan, [7] An-Shin Dialysis Center, NephroCare Ltd., Fresenius Medical Care, Taichung, Taiwan

OPEN ACCESS

Edited by:
Dong Ho Park,
Kyungpook National University Hospital, South Korea

Reviewed by:
Yong Koo Kang,
Kyungpook National University, South Korea
Min-Woo Lee,
Konyang University, South Korea

***Correspondence:**
Chun-Ju Lin
doctoraga@gmail.com

Specialty section:
This article was submitted to Ophthalmology, a section of the journal Frontiers in Medicine

Received: 15 February 2021
Accepted: 06 April 2021
Published: 03 May 2021

Citation:
Lai C-T, Hsieh Y-T, Lin C-J, Wang J-K, Lin C-Y, Hsia N-Y, Bair H, Chen H-S, Chiu C-Y and Weng S-W (2021) Age, Initial Central Retinal Thickness, and OCT Biomarkers Have an Influence on the Outcome of Diabetic Macular Edema Treated With Ranibizumab– Tri-center 12-Month Treat-and-Extend Study. Front. Med. 8:668107. doi: 10.3389/fmed.2021.668107

Objective: We report the tri-center 1-year outcomes of a treat-and-extend (T&E) regimen in four-week intervals with ranibizumab for diabetic macular edema (DME).

Methods: In this retrospective study, all eyes received 3 monthly loading injections of 0.5 mg ranibizumab, followed by a T&E regimen for DME. Regression models were used to evaluate the associating factors for visual and anatomical outcomes.

Results: Ninety one eyes from 64 patients were enrolled. Mean LogMAR best-corrected visual acuity (BCVA) improved from 0.58 at baseline to 0.36 at month 12 and mean central retinal thickness (CRT) decreased from 411 μm at baseline to 290 μm at month 12. Younger age and eyes having thinner baseline CRT, with ellipsoid zone disruption (EZD), and without epiretinal membrane (ERM) were associated with better final CRT. Moreover, eyes with thicker baseline CRT tend to receive more injections. Among the parameters, only having ERM or EZD was associated with significant BCVA recovery.

Conclusions: A T&E regimen with ranibizumab by 4-week intervals is effective in improving BCVA and reducing CRT with efficacy notable starting from the third month. Clinical parameters including age, initial CRT, and presence of ERM or EZD significantly influenced therapeutic outcomes. Moreover, the presence of ERM should not preclude DME patients from receiving anti-VEGF therapy. Future studies with larger cohorts are warranted.

Keywords: age, central retinal thickness, diabetic macular edema, OCT biomarkers, ranibizumab, treat-and-extend regimen 5

INTRODUCTION

Diabetic retinopathy (DR) affects an estimated one in three people with diabetes mellitus (DM) (1) and causes severe visual impairment. Diabetic macular edema (DME), a common complication of DR, can present in both non-proliferative diabetic retinopathy (NPDR) and proliferative diabetic retinopathy (PDR) (2).

DME is pathologically linked to the disruption of the blood retinal barrier. In the hypoxic microenvironment of DR, vascular endothelial growth factor (VEGF) increases capillary permeability and breaks down blood retinal barrier (3). Ranibizumab (Lucentis, Genentech Inc., South San Francisco, CA), an anti-angiogenic agent, has revolutionized the treatment of DME. The RISE and RIDE phase II trial showed that 44.8% of patients gain more than 15 letters in vision after monthly injections of 0.3 mg ranibizumab (4). The success of ranibizumab over intravitreal steroid and photocoagulation monotherapy has also been established in the literatures (5, 6).

Nonetheless, monthly injections of ranibizumab is impractical as the cost of anti-VEGF agents and the requirement of frequent clinic visits be barriers to patient compliance to regimen (7). The TREX-DME study demonstrated that treat and extend (T&E) dosing was comparable with monthly dosing and allows for incremental increases in treatment intervals by 2 weeks. This resulted in less frequent injections and less expenditure (8). Therefore, T&E dosing with 4-week intervals may be more practical in terms of reducing treatment burden.

Despite robust findings from clinical trials, around half of eyes do not fully respond to anti-VEGF (9), and further exploration of prognostic factors associated with better visual outcomes is warranted. Age, HbA1c status, central retinal thickness (CRT) have been investigated but to mixed results (10–13). Moreover, little is known regarding how optical coherence tomography (OCT) biomarkers including epiretinal membrane (ERM) and ellipsoid zone disruption (EZD) affect the resolution of macular edema and final vision, and its implication for therapeutic strategy.

This tri-center 12 month study aims to investigate the efficacy of ranibizumab on DME following a regimen of 3 monthly loading injections plus 4-week T&E therapeutic intervals. To understand favorable factors for functional and anatomical visual outcomes, we assessed clinical parameters of patients with different therapeutic responses.

MATERIALS AND METHODS

Subjects

This retrospective study was conducted from 2017 to 2019 at the Department of Ophthalmology of three tertiary centers in Taiwan (China Medical University Hospital, National Taiwan University Hospital, and Far Eastern Memorial Hospital). We reviewed subjects with either type I or type II DM and a concomitant DR diagnosis. DME diagnosis was made according to features of exudates and macular thickening on fundus and OCT exam. CRT was calculated as the average thickness of the central 1,000 μm diameter area (14) with spectral domain OCT (SD-OCT) device (Heidelberg Engineering, Heidelberg, Germany). Among the OCT biomarkers, EZD is defined as having any discontinuity of the second hyper-reflective layer of fovea on OCT. The shadowing effect of cysts and retinal vessels was not regarded as part of the EZD (15).

Inclusion criteria for receiving ranibizumab were as follows: eyes having Snellen best-corrected visual acuity (BCVA) between 20/400 and 20/40, CRT on OCT being >300 μm at the initial presentation, and eyes demonstrating late onset hyperfluorescence typical of macular leakage on fluorescence angiography (FA). Exclusion criteria involves having macular edema of non-diabetic causes, a history of vitrectomy and laser photocoagulation 3 months prior to study entry. Among PDR patients, subjects who were treated with additional laser photocoagulation during the study period were excluded. OCT images of poor quality were excluded as well.

The study protocol was approved by the Institutional Review Board and informed consent was obtained from all participants. The study complies with the tenets of the Declaration of Helsinki.

Study Design and Statistical Analysis

All patients received 3 monthly loading injections of 0.5 mg ranibizumab, followed by a T&E algorithm in which the treatment intervals were increased by 4 weeks after reaching a stable BCVA status and a CRT<300 μm. Ranibizumab injections interval were reduced by 4 weeks if the individual had vision loss due to DME recurrence. DME recurrence was defined as having CRT >300 μm. If there was no recurrence, patients were allowed to extend their clinical visit and injection one more month due to personal reasons (**Figure 1**). All subjects were followed for at least 12 months.

Primary outcomes included variations in BCVA and CRT after 12 months of treatment. Secondary outcomes were the univariate analysis and multivariate logistic regression analysis of the biomarkers that predicted better BCVA outcomes in DME. We applied Chi-square for the univariate analysis of categorical variable and ANOVA for numerical variable. In the multivariate logistic regression analysis, eventual CRT, BCVA changes and injection times were dependent variables. Baseline parameters such as age, DR staging and OCT biomarkers were independent variables. Statistical analysis was conducted with Statistical Package for the Social Sciences (SPSS) version 22.0 for Windows.

RESULTS

Ninety-one eyes of 64 patients with DME were enrolled. Thirty five (54.7%) males and 29 (45.3%) females were included. The baseline HbA1C was 7.44 ± 1.02 %. There were 4 eyes of mild NPDR, 14 of moderate NPDR, 28 of severe NPDR, 6 of PDR, and 39 of eyes with PDR that had received PRP (**Table 1**). The majority of DR staging was severe NPDR and PDR.

The mean injection number was 7.67 ± 2.09 (5–12; 95% confidence interval) with 71.21% eyes received five to eight injections. The majority of cases needed eight injections. The proportion of eyes with BCVA improvement had gradually

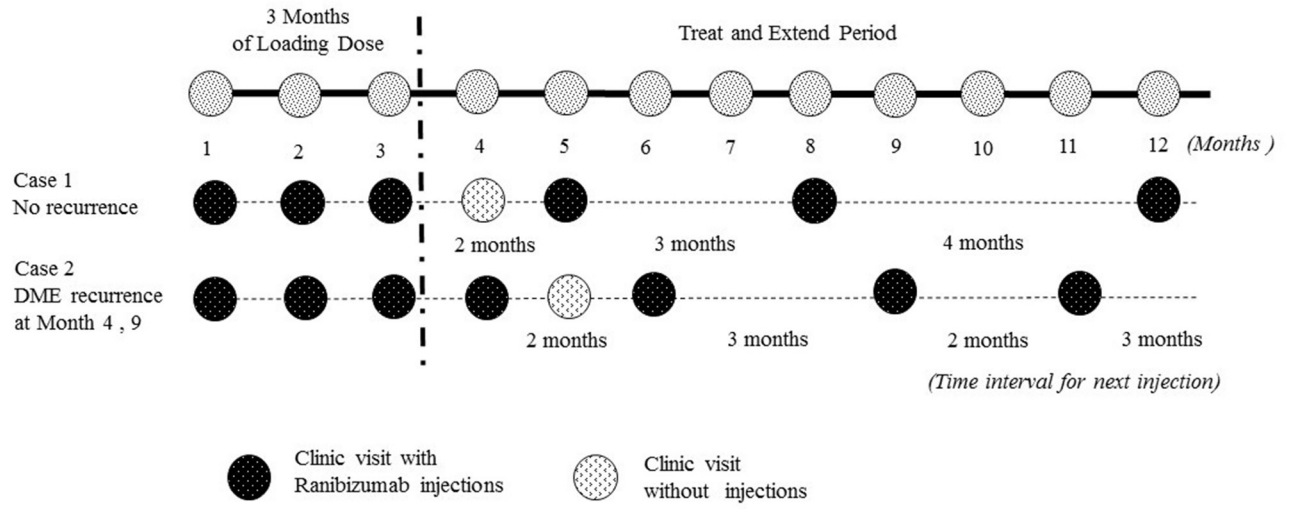

FIGURE 1 | Illustrated the treat and extend (T&E) dosing algorithm in our real world study to determine treatment intervals. In this study, there were 3 monthly injections of ranibizumab, and injection intervals were extended by 4 weeks if there was no DME recurrence. DME recurrence was defined as having central retinal thickness >300 μm. If there was no recurrence, patients were allowed to extend their clinical visit and injection one more month due to personal reasons. BCVA, best-corrected visual acuity; DME, diabetic macular edema.

TABLE 1 | Demographic data.

Baseline characteristics	All patients ($N = 64$), Eyes ($n = 91$)
Age	60.31 ± 10.75
Gender	
Female	29/64 (45.3%)
HbA1C (%)	7.44% ± 1.02%
CRT (μm)	411.30 ±114.61
LogMAR	0.58 ± 0.36
DR staging	
Mild NPDR	4/91 (4.40%)
Moderate NPDR	14/91 (15.4%)
Severe NPDR	28/91 (30.8%)
PDR	6/91 (6.59%)
PDR with PRP	39/91 (42.9%)
IRC	71/91 (78.0%)
HE	70/91 (76.9%)
DRIL	31/91 (34.1%)
EZD	26/91 (28.6%)
ERM	23/91 (25.3%)
SRF	18/91 (19.8%)

N, number; CRT, Central Retinal Thickness; DR, Diabetic Retinopathy; NPDR, Non Proliferative Diabetic Retinopathy; PDR, Proliferative Diabetic Retinopathy; PRP, Panretinal Photocoagulation; IRC, Intra-Retinal Cyst; HE, Hard Exudate; DRIL, Disorganization of Retinal Inner Layers; EZD, Ellipsoid Zone Disruption; ERM, Epiretinal Membrane; SRF, Subretinal Fluid.

increased from 58.2% since Month three and reached 72.5% at month 12. The mean LogMAR BCVA improved significantly from 0.58 at baseline to 0.36 in month 12 (**Figure 2**). The mean CRT decreased significantly from 411.3 μm at baseline to 289.8 m in month 12 (**Figure 3**). In both **Figures 2**, **3**, all the *p*-values shown were compared to the baseline LogMAR and baseline CRT, respectively.

Next, we performed inter-cohort univariate and multivariate analysis. Patients were further classified according to final CRT thickness (> or <300 μm), the final change in BCVA (with or without BCVA improvements) and total injection times (more or fewer than six injections) (**Table 2**). In the inter-cohort analysis of final CRT > or < 300 μm, eyes of younger age and eyes having thinner baseline CRT, with EZD, and without ERM were associated with better final CRT (<300 μm) (**Table 2**). This correlation were also confirmed in multivariate analysis, where older age (odds ratio = 1.094, $p = 0.0115$), thicker CRT at study entry (odds ratio = 1.009, $p = 0.0013$), having ERM (odds ratio = 3.619, $p = 0.0256$) and without EZD (odds ratio = 0.127, $p = 0.0045$) were associated with worse final CRT (**Table 3**).

Comparing the two groups with or without BCVA improvements, we observed that patients having worse baseline BCVA, severe baseline NPDR status, and having ERM or EZD were associated with significant logMAR BCVA improvements in univariate analysis. Subjects with mild NPDR status were not associated with significant BCVA recovery (**Table 2**). However, in multivariate analysis, only having ERM (ERM with no final BCVA recovery, odds ratio = 0.160, $p = 0.0219$) or EZD (EZD with no final BCVA recovery, odds ratio = 0.134, $p = 0.0111$) was associated with significant final BCVA recovery.

Searching for factors predictive of frequent injections, we discovered that eyes with thicker CRT and worse BCVA at study entry were associated with more Ranibizumab injections in the univariate analysis (**Table 2**). Multivariate analysis confirmed that only thicker baseline CRT was predictive of receiving more than six injections (odd ratio = 1.006, $p = 0.011$) (**Table 3**).

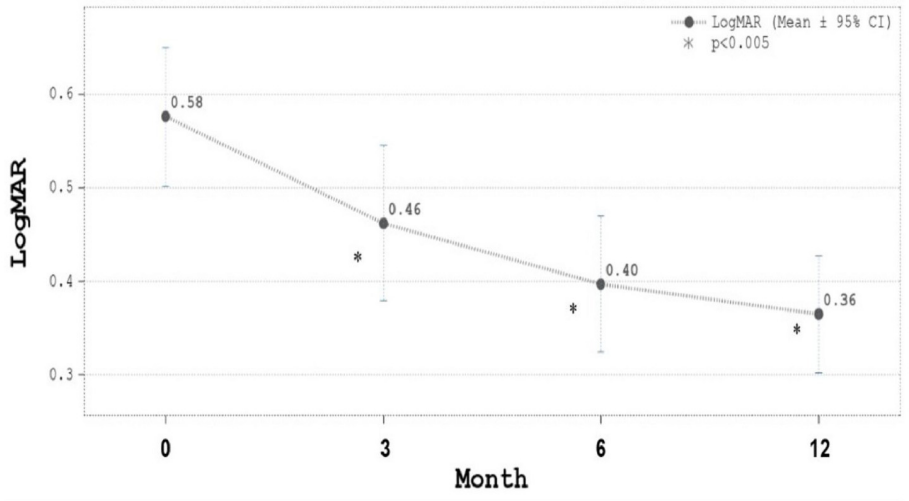

FIGURE 2 | Best-corrected visual acuity (BCVA) in LogMAR during ranibizumab treatment. LogMAR was 0.58 ± 0.36 (mean ± SD) at baseline, 0.46 ± 0.40 μm at Month 3, 0.40 ± 0.35 at Month 6, and 0.36 ± 0.30 at Month 12. Mean LogMAR BCVA improved significantly from 0.58 at baseline to 0.36 in month 12.

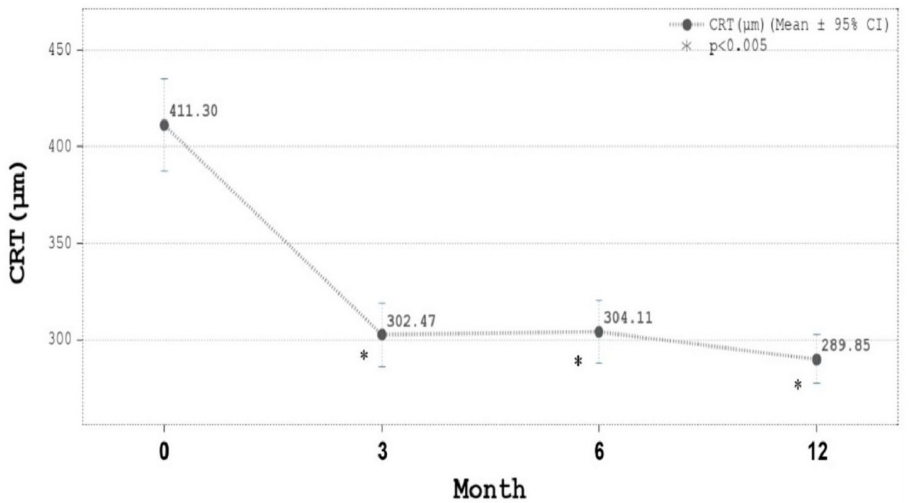

FIGURE 3 | Central retinal thickness (CRT, μm) during ranibizumab treatment. CRT was 411.30 ± 114.61 μm (mean ± SD) at baseline, 302.47 ± 79.22 μm at Month 3, 304.11 ± 78.59 at Month 6, and 289.85 ± 60.71 μm at Month 12. Mean CRT decreased significantly from 411 μm at baseline to 289 μm in month 12.

Among the OCT biomarkers, only the presence of EZD and ERM significantly influenced the final BCVA improvements and final CRT (**Tables 2**, **3**). No OCT biomarkers statistically significantly influenced the total injection times in both univariate and multivariate analysis (**Tables 2**, **3**).

DISCUSSION

We have demonstrated the efficacy of T&E regimen with 0.5 mg ranibizumab by 4-week intervals. On average, the BCVA gain was 10 letters after 12 months. These results were concordant with the clinical trials that adopt extended 2-week treatment intervals. For instance, in the TREX-DME 1-year study, a standard interval of 2 weeks was adopted and BCVA gains were 9.6 and 9.5 letters for the respective T&E and T&E plus laser arms (16). Our study, though adopting an interval twice as long as the standard interval, attained similar BCVA gains as in the TREX-DME 1-year study. Moreover, on average, only eight injections per year were required to reach efficacy, whereas the TREX-DME 1-year study required 10.7 injections (16). Hence, we demonstrated that a longer 4-week T&E interval is feasible and economical for achieving adequate control of DME.

In the present analysis, ranibizumab reduced the average CRT by 121 μm at month 12 (**Figure 3**). Similarly, in the TREX-DME trial, CRT was reduced by 123 and 146 μm, respectively, for monthly and T&E regimens. No statistical significance were

TABLE 2 | Intercohort univariate analysis.

Baseline	Grouped By final CRT			Grouped By final VA change			Grouped By injection times		
Clinical data	**< 300 μm**	**≥ 300 μm**		**Improved**	**Not improved**		**≤ 6 shots**	**> 6 shots**	
Age (years)	**57.64 ± 11.66**	**64.48 ± 7.63**	$p < 0.05^{\dagger}$	60.85 ± 9.19	58.82 ± 14.45	NS	59.30 ± 13.14	61.05 ± 8.71	NS
Gender (Female)	20/39 (51.3%)	9/25 (36.0%)	NS	21/47 (44.7%)	8/17 (47.1%)	NS	12/27 (44.4%)	17/37 (45.9%)	NS
HbA1c (%)	7.47 ± 1.03	7.40 ± 1.02	NS	7.47 ± 0.92	7.37 ±1.29	NS	7.24 ± 0.98	7.59 ± 1.04	NS
CRT (μm)	**392.76 ± 108.58**	**445.47 ± 119.24**	$p < 0.05^{\dagger}$	421.36 ± 118.39	384.72 ± 101.42	NS	**366.58 ± 86.84**	**434.40 ± 120.87**	$p < 0.05^{\dagger}$
LogMAR	0.59 ± 0.37	0.55 ± 0.33	NS	**0.63 ± 0.36**	**0.42 ± 0.29**	$p < 0.05$	**0.47 ± 0.30**	**0.63 ± 0.37**	$p < 0.05^{\dagger}$
DR staging/OCT Biomarkers									
Mild NPDR	3/59 (5.08%)	1/32 (3.13%)	NS	**1/66 (1.52%)**	**3/25 (12.0%)**	$p < 0.05$	3/31 (9.68%)	1/60 (1.67%)	NS
Moderate NPDR	9/59 (15.3%)	5/32 (15.6%)	NS	11/66 (16.7%)	3/25 (12.0%)	NS	5/31 (16.1%)	9/60 (15.0%)	NS
Severe NPDR	16/59 (27.1%)	12/32 (37.5%)	NS	**25/66 (37.9%)**	**3/25 (12.0%)**	$p < 0.05$	7/31 (22.6%)	21/60 (35.0%)	NS
PDR	3/59 (5.08%)	3/32 (9.38%)	NS	4/66 (6.06%)	2/25 (8.00%)	NS	2/31 (6.45%)	4/60 (6.67%)	NS
PDR s/p PRP	28/59 (47.5%)	11/32 (34.4%)	NS	25/66 (37.9%)	14/25 (56.0%)	NS	14/31 (45.2%)	25/60 (41.7%)	NS
SRF (+)	14/59 (23.7%)	4/32 (12.5%)	NS	13/66 (19.7%)	5/25 (20.0%)	NS	4/31 (12.9%)	14/60 (23.3%)	NS
IRC (+)	45/59 (76.3%)	26/32 (81.3%)	NS	54/66 (81.8%)	17/25 (68.0%)	NS	25/31 (80.6%)	46/60 (76.7%)	NS
ERM (+)	**10/59 (16.9%)**	**13/32 (40.6%)**	$p < 0.05^{\dagger}$	**21/66 (31.8%)**	**2/25 (8.00%)**	$p < 0.05^{\dagger}$	5/31 (16.1%)	18/60 (30.0%)	NS
EZD (+)	**21/59 (35.6%)**	**5/32 (15.6%)**	$p < 0.05^{\dagger}$	**24/66 (36.4%)**	**2/25 (8.00%)**	$p < 0.05^{\dagger}$	7/31 (22.6%)	19/60 (31.7%)	NS
DRIL (+)	20/59 (33.9%)	11/32 (34.4%)	NS	23/66 (34.8%)	8/25 (32.0%)	NS	9/31 (29.0%)	22/60 (36.7%)	NS
HE (+)	45/59 (76.3%)	25/32 (78.1%)	NS	53/66 (80.3%)	17/25 (68.0%)	NS	23/31 (74.2%)	47/60 (78.3%)	NS

CRT, Central Retinal Thickness; DR, Diabetic Retinopathy; NPDR, Non Proliferative Diabetic Retinopathy; PDR, Proliferative Diabetic Retinopathy; PRP, Panretinal Photocoagulation; SRF, Subretinal Fluid; IRC, Intra-Retinal Cyst; ERM, Epiretinal Membrane; EZD, Ellipsoid Zone Disruption; DRIL, Disorganization of Retinal Inner Layers; HE, Hard Exudate. N: Indicates a non-statistically significant. †Indicates that statistical significance in this univariate analysis was also confirmed in multivariate analysis in ***Table 3****. The bold values indicate $p < 0.05$.*

TABLE 3 | Multiple logistic regression.

Parameter	DF	Estimate	Standard Error	Wald Chi-Square	*P*-value	Odds ratio	95% Wald
Dependent variable: Final CRT ≥ 300 μm (event) vs. Final CRT < 300 μm							
Intercept	1	−10.0342	2.8891	12.0624	0.0005		
Age	1	0.0897	0.0355	6.3803	0.0115	1.094	1.020–1.173
ERM (+)	1	0.6431	0.2882	4.9807	0.0256	3.619	1.170–11.20
EZD (+)	1	−1.0323	0.3638	8.0525	0.0045	0.127	0.030–0.528
Initial CRT	1	0.00873	0.00272	10.2745	0.0013	1.009	1.003–1.014
Dependent variable: Final VA not improved (event, ΔLogMAR ≥ 0) vs. Final VA improved							
Intercept	1	−2.1631	0.5133	17.7602	<.0001		
ERM (+)	1	−0.9148	0.3991	5.2546	0.0219	0.160	0.034–0.767
EZD (+)	1	−1.0054	0.3960	6.4451	0.0111	0.134	0.028–0.632
Dependent variable: Injections > 6 shots (event) vs. Injection times ≤ 6 shots							
Intercept	1	−1.9051	0.9950	3.666	0.056		
Initial CRT	1	0.0065	0.0025	6.507	0.011	1.006	1.002–1.012

Other Variables included before model selection were as following: gender, age, HbA1C, initial LogMAR, initial CRT, DR staging and initial OCT data. CRT, Central Retinal Thickness; DR, Diabetic Retinopathy; EZD, Ellipsoid Zone Disruption; ERM, Epiretinal Membrane.

observed between the two protocols in that trial (8). Interestingly, we demonstrated that the improvements of BCVA and CRT were parallel and significant starting from month 3 and until month 12 (**Figures 2**, **3**). Moreover, the greatest increases in both BCVA and CRT were observed after 3 monthly loading injections. Protocol I from Diabetic Retinopathy Clinical Research (DRCR) and research by Lai et al. had similar results in demonstrating that BCVA restoration after the 3 monthly injections was predictive of long-term visual benefits (12, 17).

Even though we have established the efficacy of ranibizumab in DME as in other clinical trials, 35.6 and 27.5% of our patients, respectively, failed to response in CRT and BCVA under the study protocol. In both univariate and multivariate analysis, we discovered that younger age, initial CRT, and the presence of ERM or EZD were significant clinical parameters that influenced final CRT outcomes. Younger ages were, in previous studies, correlated with better vision recovery but its relation to final CRT outcomes had not been established (10, 18). However, the age was not significantly associated with BCVA recovery in our study. Instead, we found that age was only predictive of thinner final CRT.

Aside from age, we found that thinner baseline CRT was predictive of better final CRT while thicker baseline CRT is predictive of worse final CRT outcome. Bressler et al. proposed that a thicker baseline CRT may result in a failure to achieve the ideal final CRT of <250 μm, but may still attain greater reduction of macular edema in the end (10). Hence, eyes having more severe DME with thicker CRT at the beginning may still benefit from anti-VEGF injections.

Whether baseline CRT predicts better BCVA recovery is controversial. While eyes with thinner retinal thickness is expected to have lesser capacity for BCVA improvements, baseline CRT in our study did not make a difference in final vision recovery. Contrary to our present analysis, the RESTORE trial reported that eyes with thicker initial CRT experienced greater VA gains (6). Of note, in this trial baseline BCVA of the thicker retina was not adjusted and may be a confounding factor to vision gain analysis. In later literature, Well et al. and others have demonstrated that baseline BCVA is a stronger predictor of visual improvement than retinal thickness (19, 20). Also, it has been observed that visual acuity may not be compatible with a given degree of macular edema. That is, one may have better gain in vision but develop a paradoxical increase in retinal thickness (21). Therefore, though it is possible that retinal thickness is modestly related to functional vision outcome, its impact may not be as essential as initial BCVA status.

Since factors other than CRT reductions relate to vision improvement, researchers have explored the microstructure of the retina in search of other co-variables (13, 22). The presence of photoreceptor integrity and the co-existence of vitreoretinal interface (VRI) abnormality may affect visual outcome (23). In our study, eyes with EZD had thinner final CRT compared with eyes without EZD. We hypothesized that the reduction of CRT is related to external limiting membrane (ELM) defect. ELM is considered as the organized layer that comprised of the cellular attachment between Muller glial cells and contact between Muller cells and photoreceptors (24, 25). In addition to the anatomical location of the ELM, the presence of tight junction proteins such as occludins on it, further support the notion that, the ELM serves as a retinal barrier between the inner retinal layer and outer photoreceptor segments. In eyes with DME, there are ELM defect due to swollen Muller glial cells and further loss of occludin proteins (24, 25). Though our study did not measure the continuity of the ELM on OCT, ELM disruption has frequently been associated with EZD (26). Under this premise, final CRT reduction in eyes with EZD may be related to ELM defects, which facilitate the pumping function of RPE and lead to the reduction of intra-retinal fluid. Hence, under the effect of ranibizumab, eyes with EZD would have better CRT outcome than those without EZD.

One may propose that CRT reductions in EZD are related to fovea atrophy instead of true therapeutic effects seen in DME

patients. However, in reviewing our data, we found that the final average CRT thickness in EZD group was 289.85 ± 60.71 μm at 1 year, and only one eye with EZD had a CRT thickness of <200 μm. Our CRT data of EZD group was far thicker than the criteria set for fovea atrophy, which was as either <200 or 150 μm (27, 28). Hence, fovea atrophy was unlikely the contributing factor in our study. We suppose it was the therapeutic effect of ranibizumab and ELM disruption that led to thinner final CRT in the EZD group.

Vitreoretinal interface abnormality encompasses disorders such as ERM, vitreomacular adhesion (VMA), and vitreomacular traction (VMT), and affects the vision outcome of DME patients. Kulikov et al. revealed that the presence of ERM, VMT, and VMA were associated with less CRT reduction after anti-VEGF injections. However, this study did not analyze BCVA gains and was involved a 1 month period, long term outcomes uncertain (29). Others have found that anti-VEGF is still beneficial for eyes with VMA (30), while some have observed no difference in vision recovery and CRT reduction in VMA and ERM group (13, 31). VMT was, however, mostly indicative of poor visual outcome (29, 31). The traction from partial posterior vitreous detachment in VMT might lead to the distortion of inner retinal layer and thus adverse outcomes.

On the other hand, whether ERM precludes better BCVA gain is controversial. Intriguingly, we found that eyes with ERM have greater BCVA improvements than eyes without ERM. Other parameters such as initial CRT or the presence of DRIL, IRC, and SRF did not affect BCVA improvement. Similar to our observation, other studies had also found better vision recovery in eyes with ERM under anti-VEGF therapy; however, the mechanism is not well-known (32). Some proposed that in the absence of VMT and fibrovascular proliferation, ERM did not contribute to the difference to final BCVA (12). From our data, we conclude that the presence of ERM leads to at least non-inferior BCVA recovery. It is difficult to ascertain whether having ERM lead to superior visual outcome, so further study with larger cohort is warranted. Therefore, in our study the presence of ERM should not preclude treatment with anti-VEGF since the presence of ERM does not hinder BCVA improvements.

Our study is limited as it is retrospective in nature. We acknowledge that there are no matching controls and confounding factors may exist in inter-cohort analysis. In inter-cohort analysis, parameters such as age, gender, and HbA1c were analyzed by individuals. For DR staging and OCT parameters, the data were analyzed by eyes. This difference did not influence the univariate analysis, but may lead to some bias in multivariable analysis. Analyzing only one eye from one person will resolve this problem but will also decrease the available data. For the current study, consideration of sample size still outweighs the existence of possible bias. Second, this study is of a relatively small sample size with short follow-up period. This might affect the statistical power in regression model analysis. However, most factors identified as significant in univariate analysis were also confirmed in multivariate regression.

Notwithstanding its limitations, our study bears significance in identifying that the presence of ERM should not preclude the individual from receiving anti-VEGF therapy. Additionally, we demonstrate how ranibizumab therapy affects retinal microstructure both anatomically and functionally.

In conclusion, the T&E regimen in a 4-week interval with ranibizumab was a feasible and economical option for patients with DME. Parameters including age, initial CRT, and presence of ERM significantly influenced the outcome of T&E regimen. Moreover, the presence ERM should not preclude patients from receiving anti-VEGF therapy. Further study with larger cohorts is warranted.

DATA AVAILABILITY STATEMENT

The raw data supporting the conclusions of this article will be made available by the authors, without undue reservation.

ETHICS STATEMENT

The studies involving human participants were reviewed and approved by China Medical University Hospital Institutional Review Board. The patients/participants provided their written informed consent to participate in this study.

AUTHOR CONTRIBUTIONS

C-JL, C-TL, Y-TH, and J-KW contributes to conception and design of the study. C-JL, C-TL, Y-TH, J-KW, N-YH, H-SC, C-YC, and S-WW participated in data acquisition. C-JL, C-TL, C-YL, HB, N-YH, H-SC, C-YC, and S-WW analyzed and interpreted the data set. C-JL, C-TL, C-YL, HB, and N-YH drafted the manuscript. C-JL and C-TL supervised and revised the manuscript to meet academic standards. All authors had approved the integrity of the manuscript.

REFERENCES

1. Sheu SJ, Lin WL, Kao Yang YH, Hwu CM, Cheng CL. Pay for performance program reduces treatment needed diabetic retinopathy - a nationwide matched cohort study in Taiwan. *BMC Health Serv Res.* (2018) 18:638. doi: 10.1186/s12913-018-3454-6
2. Massin P, Bandello F, Garweg JG, Hansen LL, Harding SP, Larsen M, et al. Safety and efficacy of ranibizumab in diabetic macular edema (RESOLVE Study): a 12-month, randomized, controlled, double-masked, multicenter phase II study. *Diabetes Care.* (2010) 33:2399–405. doi: 10.2337/dc10-0493
3. Dervenis N, Mikropoulou AM, Tranos P, Dervenis P. Ranibizumab in the treatment of diabetic macular edema: a review of the current status, unmet needs, and emerging challenges. *Adv Therapy.* (2017) 34:1270–82. doi: 10.1007/s12325-017-0548-1
4. Nguyen QD, Brown DM, Marcus DM, Boyer DS, Patel S, Feiner L, et al. Ranibizumab for diabetic macular edema: results from 2 phase III randomized trials: RISE and RIDE. *Ophthalmology.* (2012) 119:789–801. doi: 10.1016/j.ophtha.2011.12.039
5. Elman MJ, Bressler NM, Qin H, Beck RW, Ferris FL, 3rd, Friedman SM, et al. Expanded 2-year follow-up of ranibizumab plus prompt or deferred laser or

triamcinolone plus prompt laser for diabetic macular edema. *Ophthalmology.* (2011) 118:609–14. doi: 10.1016/j.ophtha.2010.12.033
6. Mitchell P, Bandello F, Schmidt-Erfurth U, Lang GE, Massin P, Schlingemann RO, et al. The RESTORE study: ranibizumab monotherapy or combined with laser versus laser monotherapy for diabetic macular edema. *Ophthalmology.* (2011) 118:615–25. doi: 10.1016/j.ophtha.2011.01.031
7. Shea AM, Curtis LH, Hammill BG, Kowalski JW, Ravelo A, Lee PP, et al. Resource use and costs associated with diabetic macular edema in elderly persons. *Arch Ophthalmol.* (2008) 126:1748–54. doi: 10.1001/archopht.126.12.1748
8. Payne JF, Wykoff CC, Clark WL, Bruce BB, Boyer DS, Brown DM. Randomized trial of treat and extend ranibizumab with and without navigated laser versus monthly dosing for diabetic macular edema: TREX-DME 2-year outcomes. *Am J Ophthalmol.* (2019) 202:91–9. doi: 10.1016/j.ajo.2019.02.005
9. Sun JK, Jampol LM. The diabetic retinopathy clinical research network (DRCR.net) and its contributions to the treatment of diabetic retinopathy. *Ophthalmic Re.* (2019) 62:225–30. doi: 10.1159/000502779
10. Bressler SB, Qin H, Beck RW, Chalam KV, Kim JE, Melia M, et al. Factors associated with changes in visual acuity and central subfield thickness at 1 year after treatment for diabetic macular edema with ranibizumab. *Arch Ophthalmol.* (2012) 130:1153–61. doi: 10.1001/archophthalmol.2012.1107
11. Sophie R, Lu N, Campochiaro PA. Predictors of functional and anatomic outcomes in patients with diabetic macular edema treated with ranibizumab. *Ophthalmology.* (2015) 122:1395–401. doi: 10.1016/j.ophtha.2015.02.036
12. Lai TT, Yang CM, Yang CH, Ho TC, Hsieh YT. Treatment outcomes and predicting factors for diabetic macular edema treated with ranibizumab - One-year real-life results in Taiwan. *J Formosan Med Association.* (2019) 118(1 Pt 1):194–202. doi: 10.1016/j.jfma.2018.03.009
13. Fickweiler W, Schauwvlieghe AME, Schlingemann RO, Maria Hooymans JM, Los LI, Verbraak FD. Predictive value of optical coherence tomographic features in the bevacizumab and ranibizumab in patients with diabetic macular edema (BRDME) study. *Retina.* (2018) 38:812–9. doi: 10.1097/IAE.0000000000001626
14. Chan A, Duker JS, Ko TH, Fujimoto JG, Schuman JS. Normal macular thickness measurements in healthy eyes using Stratus optical coherence tomography. *Arch Ophthalmol.* (2006) 124:193–8. doi: 10.1001/archopht.124.2.193
15. Campos A, Campos EJ, do Carmo A, Caramelo F, Martins J, Sousa JP, et al. Evaluation of markers of outcome in real-world treatment of diabetic macular edema. *Eye Vision.* (2018) 5:27. doi: 10.1186/s40662-018-0119-9
16. Payne JF, Wykoff CC, Clark WL, Bruce BB, Boyer DS, Brown DM. Randomized trial of treat and extend ranibizumab with and without navigated laser for diabetic macular edema: TREX-DME 1 year outcomes. *Ophthalmology.* (2017) 124:74–81. doi: 10.1016/j.ophtha.2016.09.021
17. Gonzalez VH, Campbell J, Holekamp NM, Kiss S, Loewenstein A, Augustin AJ, et al. Early and long-term responses to anti-vascular endothelial growth factor therapy in diabetic macular edema: analysis of protocol i data. *Am J Ophthalmol.* (2016) 172:72–9. doi: 10.1016/j.ajo.2016.09.012
18. Singh RP, Habbu K, Ehlers JP, Lansang MC, Hill L, Stoilov I. The impact of systemic factors on clinical response to ranibizumab for diabetic macular edema. *Ophthalmology.* (2016) 123:1581–7. doi: 10.1016/j.ophtha.2016.03.038
19. Wells JA, Glassman AR, Jampol LM, Aiello LP, Antoszyk AN, Baker CW, et al. Association of baseline visual acuity and retinal thickness with 1-year efficacy of aflibercept, bevacizumab, and ranibizumab for diabetic macular edema. *JAMA Ophthalmol.* (2016) 134:127–34. doi: 10.1001/jamaophthalmol.2015.4599
20. Dugel PU, Hillenkamp J, Sivaprasad S, Vogeler J, Mousseau MC, Wenzel A, et al. Baseline visual acuity strongly predicts visual acuity gain in patients with diabetic macular edema following anti-vascular endothelial growth factor treatment across trials. *Clin Ophthalmol.* (2016) 10:1103–10. doi: 10.2147/OPTH.S100764
21. Browning DJ, Glassman AR, Aiello LP, Beck RW, Brown DM, Fong DS, et al. Relationship between optical coherence tomography-measured central retinal thickness and visual acuity in diabetic macular edema. *Ophthalmology.* (2007) 114:525–36. doi: 10.1016/j.ophtha.2006.06.052
22. Al Faran A, Mousa A, Al Shamsi H, Al Gaeed A, Ghazi NG. Spectral domain optical coherence tomography predictors of visual outcome in diabetic cystoid macular edema after bevacizumab injection. *Retina.* (2014) 34:1208–15. doi: 10.1097/IAE.0000000000000059
23. Shin HJ, Lee SH, Chung H, Kim HC. Association between photoreceptor integrity and visual outcome in diabetic macular edema. *Graefes Arch Clin Exp Ophthalmol..* (2012) 250:61–70. doi: 10.1007/s00417-011-1774-x
24. Saxena S, Akduman L, Meyer CH. External limiting membrane: retinal structural barrier in diabetic macular edema. *Int J Retina Vitreous.* (2021) 7:16. doi: 10.1186/s40942-021-00284-x
25. Omri S, Omri B, Savoldelli M, Jonet L, Thillaye-Goldenberg B, Thuret G, et al. The outer limiting membrane (OLM) revisited: clinical implications. *Clin Ophthalmol.* (2010) 4:183–95. doi: 10.2147/OPTH.S5901
26. Mohamed EHES, Nabil K, Gomaa AR, Haddad OHE, editors. External limiting membrane and ellipsoid zone integrity and presenting visual acuity in treatment-naive center involved diabetic macular edema. *EC Ophthalmology.* (2018) 2018:408–21.
27. Karst SG, Schuster M, Mitsch C, Meyer EL, Kundi M, Scholda C, et al. Atrophy of the central neuroretina in patients treated for diabetic macular edema. *Acta Ophthalmol.* (2019) 97:e1054–61. doi: 10.1111/aos.14173
28. Forooghian F, Yeh S, Faia LJ, Nussenblatt RB. Uveitic foveal atrophy: clinical features and associations. *Archi Ophthalmol.* (2009) 127:179–86. doi: 10.1001/archophthalmol.2008.564
29. Kulikov AN, Sosnovskii SV, Berezin RD, Maltsev DS, Oskanov DH, Gribanov NA. Vitreoretinal interface abnormalities in diabetic macular edema and effectiveness of anti-VEGF therapy: an optical coherence tomography study. *Clin Ophthalmol.* (2017) 11:1995–2002. doi: 10.2147/OPTH.S146019
30. Chang CK, Cheng CK, Peng CH. The incidence and risk factors for the development of vitreomacular interface abnormality in diabetic macular edema treated with intravitreal injection of anti-VEGF. *Eye.* (2017) 31:762–70. doi: 10.1038/eye.2016.317
31. Eski Yucel O, Birinci H, Sullu Y. Outcome and Predictors for 2-Year Visual Acuity in Eyes with Diabetic Macular Edema Treated with Ranibizumab. *J Ocular Pharmacol Therapeutics.* (2019) 35:229–34. doi: 10.1089/jop.2018.0082
32. Maryam AK, Tafgeh M, Mahmoud M, Pasha A, Ahad S, Khalil GF. Short term effect of intravitreal bevacizumab for diabetic macular edema associated with epiretinal membrane. *Rom J Ophthalmol.* (2018) 62:212–6. doi: 10.22336/rjo.2018.32

Conflict of Interest: The authors declare that the research was conducted in the absence of any commercial or financial relationships that could be construed as a potential conflict of interest.

frontiers in Medicine

ORIGINAL RESEARCH
published: 17 June 2021
doi: 10.3389/fmed.2021.685032

Sulforaphane Alleviates Particulate Matter-Induced Oxidative Stress in Human Retinal Pigment Epithelial Cells

Hyunchae Sim[1†], Wonhwa Lee[1†], Samyeol Choo[1], Eui Kyun Park[2], Moon-Chang Baek[3], In-Kyu Lee[4,5,6], Dong Ho Park[4,7] and Jong-Sup Bae[1*]*

[1] College of Pharmacy, Kyungpook National University, Daegu, South Korea, [2] Department of Pathology and Regenerative Medicine, School of Dentistry, Kyungpook National University, Daegu, South Korea, [3] Department of Molecular Medicine, School of Medicine, Kyungpook National University, Daegu, South Korea, [4] Leading-Edge Research Center for Drug Discovery and Development for Diabetes and Metabolic Disease, Kyungpook National University Hospital, Daegu, South Korea, [5] Department of Internal Medicine, School of Medicine, Kyungpook National University, Kyungpook National University Hospital, Daegu, South Korea, [6] Research Institute of Aging and Metabolism, Kyungpook National University, Daegu, South Korea, [7] Department of Ophthalmology, School of Medicine, Kyungpook National University, Kyungpook National University Hospital, Daegu, South Korea

OPEN ACCESS

Edited by:
Ravirajsinh Jadeja, Augusta University, United States

Reviewed by:
Agustina Alaimo, Consejo Nacional de Investigaciones Científicas y Técnicas (CONICET), Argentina
Ryo Mukai, Gunma University, Japan

***Correspondence:**
Dong Ho Park
DongHo_Park@knu.ac.kr
Jong-Sup Bae
baejs@knu.ac.kr

[†]These authors have contributed equally to this work

Specialty section:
This article was submitted to Ophthalmology, a section of the journal Frontiers in Medicine

Received: *24 March 2021*
Accepted: *26 May 2021*
Published: *17 June 2021*

Citation:
Sim H, Lee W, Choo S, Park EK, Baek M-C, Lee I-K, Park DH and Bae J-S (2021) Sulforaphane Alleviates Particulate Matter-Induced Oxidative Stress in Human Retinal Pigment Epithelial Cells. Front. Med. 8:685032. doi: 10.3389/fmed.2021.685032

Age-related macular degeneration (AMD) is a leading cause of blindness in the elderly, and oxidative damage to retinal pigment epithelial (RPE) cells plays a major role in the pathogenesis of AMD. Exposure to high levels of atmospheric particulate matter (PM) with an aerodynamic diameter of $<2.5\,\mu m$ ($PM_{2.5}$) causes respiratory injury, primarily due to oxidative stress. Recently, a large community-based cohort study in the UK reported a positive correlation between $PM_{2.5}$ exposure and AMD. Sulforaphane (SFN), a natural isothiocyanate found in cruciferous vegetables, has known antioxidant effects. However, the protective effects of SNF in the eye, especially in the context of AMD, have not been evaluated. In the present study, we evaluated the effect of SFN against $PM_{2.5}$-induced toxicity in human RPE cells (ARPE-19) and elucidated the molecular mechanism of action. Exposure to $PM_{2.5}$ decreased cell viability in ARPE-19 cells in a time- and dose-dependent manner, potentially due to elevated intracellular reactive oxygen species (ROS). SFN treatment increased ARPE-19 cell viability and decreased $PM_{2.5}$-induced oxidative stress in a dose-dependent manner. $PM_{2.5}$-induced downregulation of serum- and glucocorticoid-inducible kinase 1 (SGK1), a cell survival factor, was recovered by SFN. $PM_{2.5}$ treatment decreased the enzymatic activities of the antioxidant enzymes including superoxide dismutase and catalase, which were restored by SFN treatment. Taken together, these findings suggest that SFN effectively alleviates $PM_{2.5}$-induced oxidative damage in human ARPE-19 cells via its antioxidant effects, and that SFN can potentially be used as a therapeutic agent for AMD, particularly in cases related to $PM_{2.5}$ exposure.

Keywords: age-related macular degeneration, retinal pigment epithelium, oxidative stress, retina, choroid

INTRODUCTION

Age-related macular degeneration (AMD) is the most devastating chorioretinal disease, and is a leading cause of blindness in the elderly population (1). The retinal pigment epithelium (RPE) is a monolayer of cells located between the retinal photoreceptors and choroid vascular bed. RPE cells support photoreceptors, which are both postmitotic and highly sensitive to environmental insults, and therefore subject to irreversible degeneration. RPE cells are continuously exposed to reactive oxygen species (ROS) due to light exposure, high retinal oxygen consumption, and abundant polyunsaturated fatty acids and photosensitizers in photoreceptors and the RPE (2). Chronic excessive ROS production and accumulation cause oxidative dysfunction in the RPE, which leads to photoreceptor loss in the advanced form of AMD, geographic atrophy (3).

Increased exposure to particulate matter (PM), especially ultrafine particles with an average aerodynamic diameter of $<2.5\,\mu m$ ($PM_{2.5}$), has been linked to adverse health effects, such as increased risk of cardiovascular and respiratory death (4–6). $PM_{2.5}$ accumulation causes oxidative stress in the body (7), which is considered to be an important molecular mechanism of $PM_{2.5}$-mediated toxicity (8).

Sulforaphane (SFN) (**Figure 1A**) is an organosulfur compound found in cruciferous vegetables such as broccoli, Brussels sprouts, and cabbage (9). SFN has attracted particular interest as an indirect antioxidant due to its ability to induce expression of multiple endogenous antioxidant enzymes by activating nuclear factor E2-related factor-2 (Nrf2) (9). Although supplementation of antioxidant agents such as lutein and zeaxanthin has protective effects in AMD (10), the effect of SFN in AMD has not previously been evaluated. In the present study, we aimed to investigate whether SFN could alleviate $PM_{2.5}$-induced oxidative stress in human retinal pigment epithelial cells (ARPE-19), and subsequently to explore the mechanisms underlying the antioxidant effects of SFN in this context.

MATERIALS AND METHODS

Reagents

Diesel PM NIST 1650b (11) was purchased from Sigma-Aldrich (St. Louis, MO, USA), mixed with saline, and sonicated for 30 min to avoid agglomeration of suspended $PM_{2.5}$ particles, as described previously (12). SFN and dexamethasone (DEX), a well-known anti-inflammatory drug (13) used as a positive control, were purchased from Sigma-Aldrich. All other chemicals and reagents were obtained from Sigma-Aldrich unless otherwise stated.

ARPE-19 Culture and $PM_{2.5}$ Treatment

The human RPE cell line ARPE-19 (ATCC, Manassas, VA, USA, CLR-2302) was maintained in DMEM/F12 medium (Thermo Fisher, Waltham, MA, USA) with 10% FBS and 100 U/mL penicillin−100 μg/mL streptomycin (P/S), and passaged at a ratio of 1:2 to 1:4 using trypsin-EDTA (Thermo Fisher). Cells were grown at 37°C and 5% CO_2. Cells were grown for 24 h and subsequently treated for 24 h with different concentrations of $PM_{2.5}$ (25, 50, or 100 μg/mL) in the absence or presence of different concentrations of SFN (2, 5, 10, 20, or 30 μM) or DEX (1 μM).

Cell Viability Assay

A 3-(4,5-dimethylthiazol-2-yl)-2,5-diphenyltetrazolium bromide (MTT) assay was performed to measure cell viability as described previously (12, 14–16). The viability of treated cells was expressed as the percentage of absorbance relative to that of untreated cells, which was assumed to be 100% viability.

Flow Cytometric Analysis of Apoptosis

Apoptosis was examined using an Annexin V-FITC/PI Apoptosis Detection Kit (BD Biosciences, San Jose, CA, USA) according to the manufacturer's protocol. ARPE-19 cells were grown in a 6-well plate (2×10^5 cells/well) and treated with 100 μg/mL $PM_{2.5}$ for 24 h followed by subsequent treatment with SFN for 6 h. Subsequently, cultured cells in all groups were washed twice with ice-cold PBS, resuspended in 300 μL binding buffer, and stained with 10 μL Annexin V-FITC stock and 10 μL PI in dark conditions for 20 min. Stained cells were immediately analyzed with a FACScan Calibur Flow Cytometer (BD Biosciences), and the number of apoptotic cells was calculated using CellQuest software (Becton–Dickinson, CA, USA). The results were expressed as the percentage of Annexin V-stained cells relative to control, and all experiments were performed in triplicate.

Western Blot Analysis

For western blot analysis, cells were first rinsed with ice-cold phosphate-buffered saline and treated with lysis buffer comprising 0.5% sodium dodecyl sulfate, 1% NP-40, 1% sodium deoxycholate, 150 mM NaCl, 50 mM Tris-HCl (pH 7.5), and protease inhibitors, as previously described (17). Protein blots were blocked with 5% bovine serum albumin BSA for 2 h and incubated with the following primary antibodies: anti-Bax (1:2000), anti-Bcl2 (1:2000), anti-SGK1 (1:1000), anti-cytochrome c (1:500), and anti-cleaved caspase-3 (1:500) (Cell Signaling Technology, Inc., Danvers, MA, USA). β-actin was used as a loading control. Subsequently, membranes were washed and incubated with horseradish peroxidase-conjugated secondary antibodies (Cell Signaling Technology, 1:5,000). Densitometry analysis was performed using the ImageJ Gel Analysis tool (NIH, Bethesda, MD, USA).

Lactate Dehydrogenase Assay

To assess the cellular toxicity of $PM_{2.5}$, lactate dehydrogenase (LDH) released from cells after exposure to $PM_{2.5}$ was measured. After 24 h exposure to $PM_{2.5}$ (100 μg/mL), cell-free supernatant aliquots were separated and measured using a commercially available kit (Pointe Scientific, Lincoln Park, MI, USA). All samples were assayed for LDH content in duplicate using a plate reader (Tecan Austria GmbH, Grödig, Austria).

ROS Measurement

ROS production was determined using 2′, 7′-dichlorodihydrofluorescein diacetate (DCFH-DA). Cells were incubated in a 96-well plate at 2×10^5 cells/well and treated for 4, 12, 24, 48 h with different concentrations of $PM_{2.5}$ (25,

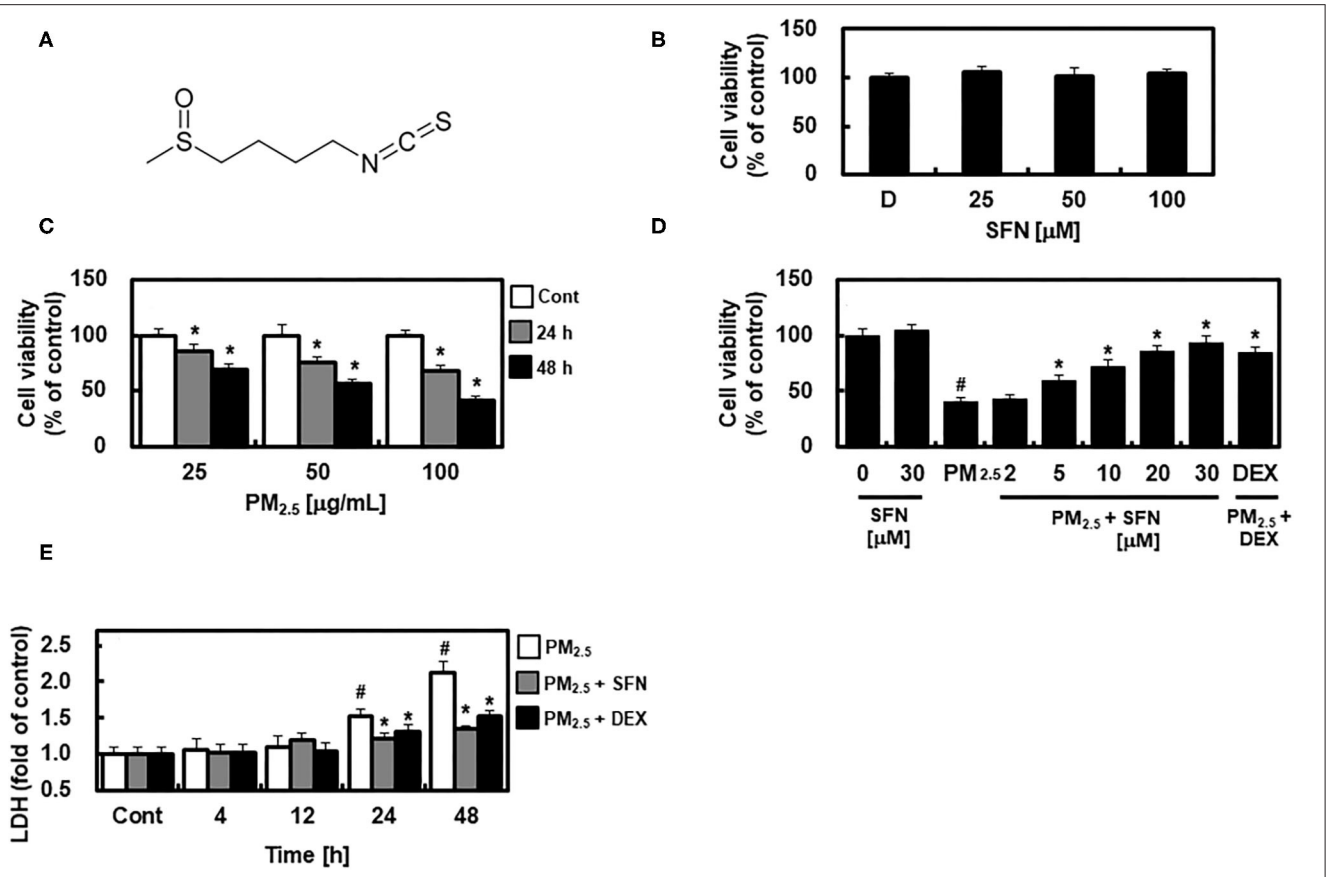

FIGURE 1 | Chemical structure of Sulforaphane (SFN) and effects of SFN on $PM_{2.5}$-induced cell toxicity in ARPE-19 cells. **(A)** Chemical structure of SFN. **(B)** ARPE-19 cells were treated with 0.5% dimethyl sulfoxide as a control indicated as D, and 25, 50, or 100 μM SFN for 24 h, and cell viability was measured using an MTT Assay. **(C)** ARPE-19 cells were treated with 25, 50, or 100 μg/mL $PM_{2.5}$ for 24 or 48 h, and cell viability was measured using an MTT assay. **(D)** ARPE-19 cells were treated with the specified concentrations of SFN or DEX (1 μM) for 6 h after 24 h $PM_{2.5}$ challenge (100 μg/mL). After treatment, cell viability was determined using an MTT assay. **(E)** ARPE-19 cells were treated with SFN (50 μM) or DEX (1 μM) for 6 h after $PM_{2.5}$ challenge (100 μg/mL) for the indicated time periods. Subsequently, LDH levels were determined using an LDH kit. Values represent the mean ± SD of three independent experiments. $^{*}p < 0.01$ relative to control **(C)** or PM-challenged group **(D,E)**, one-way ANOVA. $^{\#}p < 0.01$ relative to control **(D,E)**, one-way ANOVA.

50, or 100 μg/mL). And then, the media were replaced with DCFH-DA (50 μg/mL)-containing media and incubated for 30 min. Intracellular ROS levels were measured by monitoring the fluorescence generated from the oxidation product of DCFH-DA at excitation wavelengths of 485 and 535 nm.

Evaluation of Oxidative Stress Markers

SOD activity was measured using a SOD assay kit (Fluka). CAT activity was measured using a CAT assay kit (Sigma-Aldrich) based on the decomposition rate of the substrate hydrogen peroxide (H_2O_2), which was measured at 240 nm.

Statistical Analyses

All experiments were performed independently at least three times, and results are expressed as mean ± standard deviation (SD). Statistical significance was analyzed using a one-way analysis of variance (ANOVA) followed by Dunnett's test, with a p-value < 0.05 considered statistically significant. SPSS for Windows version 16.0 (SPSS, Chicago, IL, USA) was used to conduct all statistical analyses.

RESULTS

Effects of SFN on $PM_{2.5}$-Induced Cell Death and Cytotoxicity

First, we examined the potential cytotoxic effects of SFN in human ARPE-19 cells using an MTT assay. No change in cell viability occurred in cells treated with 0.5% DMSO as a control and different concentrations of SFN ranging from 25 to 100 μM for 24 h (**Figure 1B**). ARPE-19 cell viability decreased with $PM_{2.5}$ exposure in a dose- and time-dependent manner (**Figure 1C**), and was recovered by post-treatment with SFN for 6 h (**Figure 1D** and **Supplementary Figure 1**). DEX, a well-known anti-inflammatory drug (13, 18), was used as a positive control. Furthermore, cellular LDH release significantly increased after 24 h exposure to $PM_{2.5}$ but decreased after treatment with 30 μM SFN (**Figure 1E**). These results indicated

that the amount of LDH released from cells treated with $PM_{2.5}$ was related to cell viability, and that SFN alleviated $PM_{2.5}$-induced cytotoxicity.

Effects of SFN on $PM_{2.5}$-Induced Apoptosis

To further investigate the effect of SFN against $PM_{2.5}$ in ARPE-19 cells, ARPE-19 cell apoptosis was assessed using flow cytometry. Exposure to 100 μg/mL $PM_{2.5}$ for 24 h significantly increased late apoptosis relative to the control group, but post-treatment of ARPE-19 cells with SFN (10 and 30 μM) after $PM_{2.5}$ exposure significantly decreased the $PM_{2.5}$ -induced late apoptosis (**Figure 2**).

Effects of SFN on $PM_{2.5}$ Induction of Apoptotic Protein Levels

In light of the effects of SFN against $PM_{2.5}$-induced apoptosis in ARPE-19 cells, we further investigated the effects of SFN on the levels and cleavage of apoptotic proteins, including Bax, Bcl-2, cytochrome c, and caspase-3, by western blotting. Exposure to 100 μg/mL $PM_{2.5}$ (24 h) decreased Bcl-2 and increased Bax, cytochrome c, and cleaved caspase-3 (**Figure 3A**), which was consistent with the flow cytometry findings. However, post-treatment of ARPE-19 cells with SFN (10 and 30 μM) for 6 h dose-dependently reversed this interaction, as demonstrated by decreased Bax, cytochrome c, and cleaved caspase-3 levels and increased Bcl-2 levels (**Figure 3B**). Protein levels of SGK1, known as an anti-apoptotic factor (19), were also downregulated by $PM_{2.5}$ treatment and recovered by SFN treatment, suggesting that SGK1 could be relevant to cell survival following $PM_{2.5}$ exposure.

Effects of SFN on $PM_{2.5}$-Induced ROS Increase

Subsequently, we determined the effects of SFN on $PM_{2.5}$ induction of ROS by measuring DCFH-DA fluorescence intensity in ARPE-19 cells after exposure to 25, 50, or 100 μg/mL $PM_{2.5}$ for 4, 12, 24, or 48 h. PM_{25} exposure increased intracellular ROS levels in a dose-dependent manner (**Figure 4A**). DCFH-DA fluorescence intensity peaked after 4 h exposure and then dropped to baseline levels after 24 h. Post-treatment with SFN for 6 h after 24 h $PM_{2.5}$ exposure suppressed $PM_{2.5}$-induced ROS in a dose-dependent manner (**Figure 4B**). DEX decreased ROS levels in $PM_{2.5}$-treated cells (**Figure 4B**).

Effects of $PM_{2.5}$ and SFN on Antioxidant Enzyme Activity

The activities of SOD and CAT in ARPE-19 cells were decreased in a dose-dependent manner after 48 h exposure to $PM_{2.5}$, and were recovered by post-treatment with SFN, also in a dose-dependent manner (**Figure 5**). These results suggested that SFN decreased $PM_{2.5}$-induced oxidative stress by increasing intracellular antioxidant enzyme activity. DEX increased SOD and CAT activities under $PM_{2.5}$ challenge (**Figure 5**).

DISCUSSION

A growing body of evidence supports that ROS-induced oxidative stress damages the RPE, which can eventually lead to geographic atrophy and subsequent development of AMD (20, 21). Oxidative stress results primarily from an imbalance between ROS generation and antioxidant defenses, and especially in the context of the RPE, oxidative stress increases with age, leading to photoreceptor impairment and loss (22). Thus, a balanced redox state is crucial for preventing or delaying progression of AMD and vision loss. Consistent with this hypothesis, clinical and basic research studies have demonstrated that daily dietary supplementation of natural antioxidants, such as b-carotenoid, lutein, zeaxanthin, and anthocyanins, inhibits development and progression of AMD (23, 24).

Epidemiological evidence indicates that the greatest health risks posed by environmental PM are associated with ultrafine PM (25). The PM used in the present study was <2.5 μm in diameter, which is known to exert cellular damage in the alveolar regions of the lung (25). Further, a recent study identified that $PM_{2.5}$ promotes epithelial-mesenchymal transition of human RPE, which is mediated by upregulation of TGF-β-dependent nuclear transcription factors (26).

Interestingly, the relationship between air pollution and retinal structure was reported in large community-based cohort studies, collectively referred to as the UK Biobank. Higher concentrations of $PM_{2.5}$ were associated decreased thickness of the ganglion cell-inner plexiform, inner nuclear, and outer plexiform + outer nuclear layers (27). Furthermore, greater exposure to $PM_{2.5}$ was associated with increased incidence of self-reported AMD and decreased thickness of the RPE layer (28).

Despite evidence supporting the association between $PM_{2.5}$ exposure and AMD, $PM_{2.5}$ -mediated oxidative responses and the anti-oxidant effect of SFN, especially in the context of AMD, have not been thoroughly investigated. The purpose of the present study was therefore to examine the potential therapeutic effects of SFN against $PM_{2.5}$-induced RPE cytotoxicity.

The cell viability assay is important in determining the cellular response to toxins, and provides information on cell death, cell survival, and metabolic activities (29). $PM_{2.5}$ is believed to cause genotoxicity and cytotoxicity and suppress cell proliferation (30). The present study demonstrated that $PM_{2.5}$ increased LDH released from ARPE-19 cells, suggesting that PM_{25} exposure decreased cell viability in a time- and dose-dependent manner.

Particles from gasoline engine exhausts filtered by a pore size of 19 μm decrease cell viability in human bronchia epithelium airway cells (31). In addition, exposure to particle suspensions significantly increases LDH levels in rat macrophages (32), which is consistent with our data. In many previous studies, the effect of improving $PM_{2.5}$-caused damage such as pulmonary injury, airway inflammation, and oxidative stress was analyzed in comparison with DEX. Thus, we have scrutinized the efficacy of SFN compared to DEX (33–36). In the present study, SFN reversed $PM_{2.5}$-induced cellular toxicity. Because ROS-triggered apoptosis plays a crucial role in the pathogenesis of AMD (37). Bcl-2 family proteins, including anti-apoptotic proteins, such as Bcl-2 and pro-apoptotic proteins such as Bax, are well-known regulators of apoptosis (38). Prior studies have demonstrated that increases in the Bax/Bcl-2 ratio increase the permeability of the mitochondrial membranes, which results in cytochrome c release

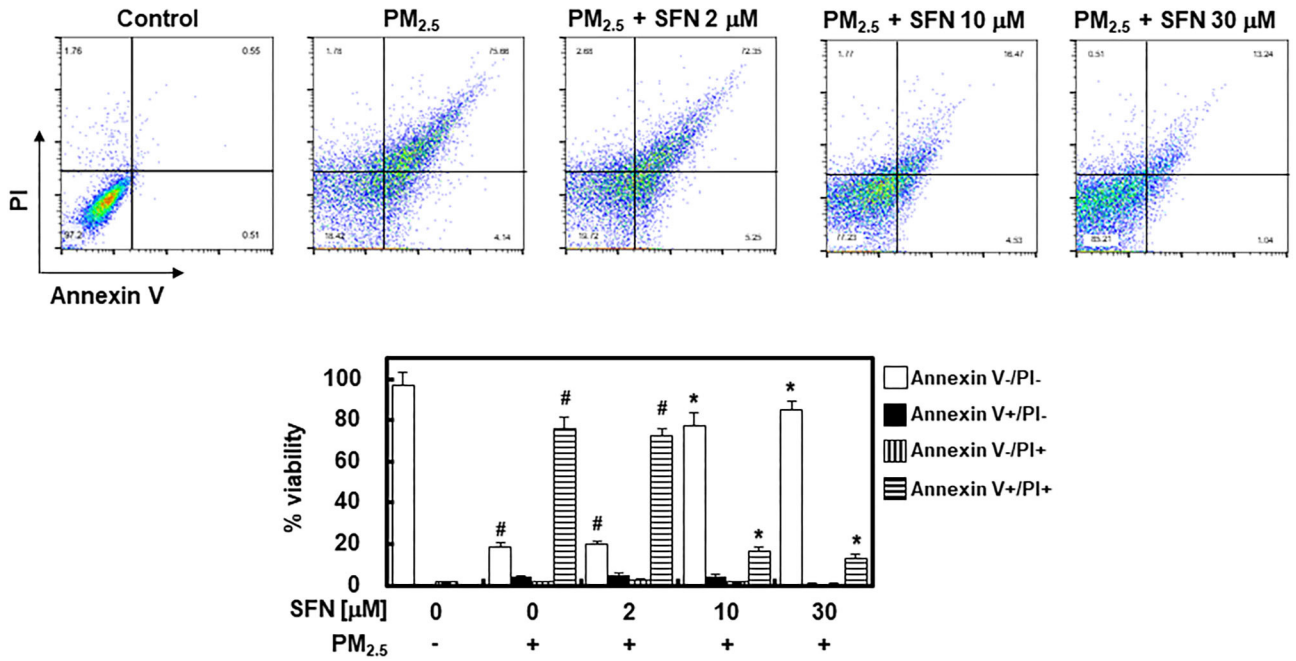

FIGURE 2 | Effects of Sulforaphane (SFN) on $PM_{2.5}$-induced apoptosis in ARPE-19 cells. ARPE-19 cells were treated with $PM_{2.5}$ (100 μg/mL) for 24 h and subsequently treated with the specified concentrations of SFN (0–30 μM) for 6 h. Apoptosis was measured by Annexin V flow cytometry analysis. Values represent the mean ± SD of three independent experiments. $^{*}p < 0.01$ relative to PM-challenged group, one-way ANOVA. $^{\#}p < 0.01$ relative to control, one-way ANOVA.

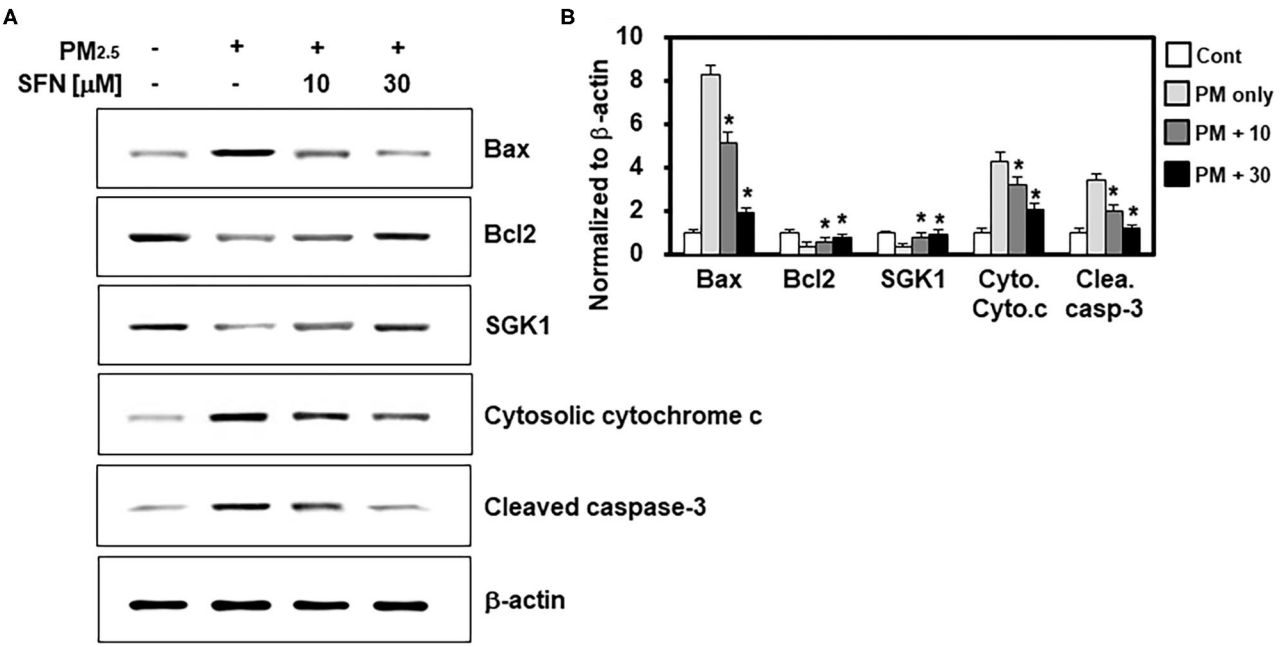

FIGURE 3 | Effects of Sulforaphane (SFN) on $PM_{2.5}$-induced changes in apoptosis-related protein levels. **(A)** ARPE-19 cells were treated with the indicated concentrations of SFN or DEX (1 μM) 24 h after $PM_{2.5}$ challenge (100 μg/mL). Subsequently, western blot analysis was conducted to measure Bax, Bcl-2, SGK1, cytochrome c, and cleaved caspase-3. β-actin was used as a loading control. Representative images from each group are shown ($n = 3$). **(B)** The graphs show the densitometric intensities of each gene normalized to β-actin. $n = 3$ blots. $^{*}p < 0.01$ relative to the control group, one-way ANOVA.

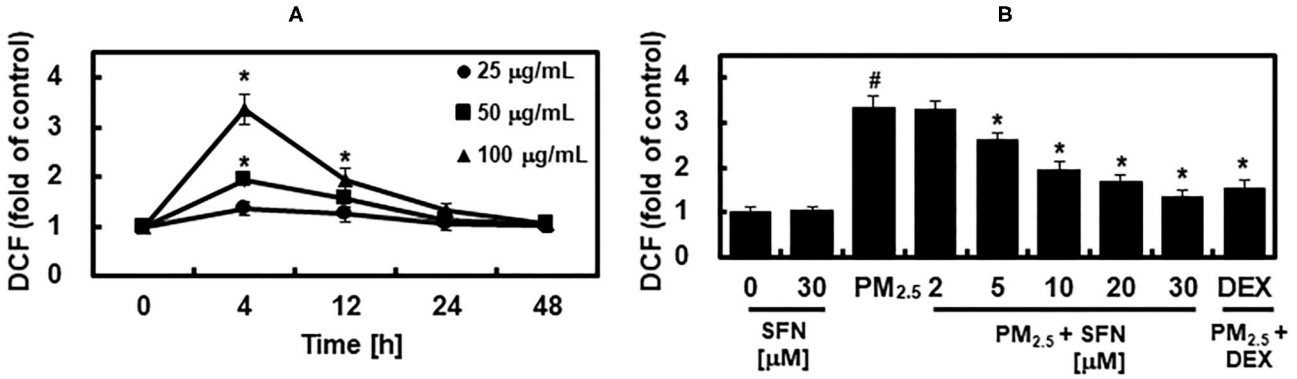

FIGURE 4 | Effects of Sulforaphane (SFN) on $PM_{2.5}$-induced ROS generation. **(A)** ARPE-19 cells were treated for the indicated times with the following concentrations of $PM_{2.5}$: 25 μg/mL (closed circle), 50 μg/mL (closed square), or 100 μg/mL (closed triangle). Intracellular ROS levels were determined using DCFH-DA. DCFH-DA fluorescence values are expressed as the fluorescence ratio (fold) between $PM_{2.5}$-treated cells and untreated control cells. **(B)** ARPE-19 cells were treated with the indicated concentrations of SFN or DEX (1 μM) 24 h after being challenged with $PM_{2.5}$ (100 μg/mL). After treatment, ROS levels were measured. Values represent the mean ± SD of three independent experiments. $^{*}p < 0.01$ relative to 0 h group **(A)** or PM-challenged group **(B)**, one-way ANOVA. $^{\#}p < 0.01$ relative to control **(B)**, one-way ANOVA.

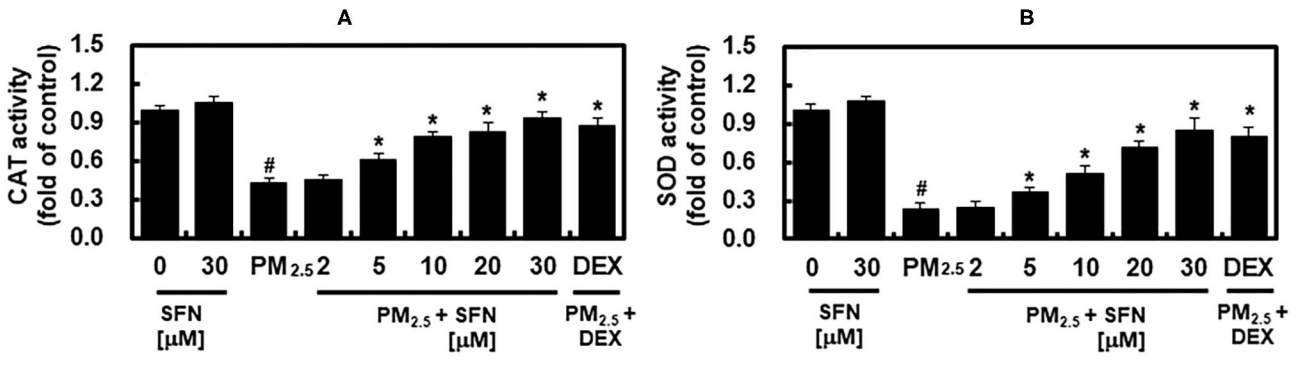

FIGURE 5 | Effects of Sulforaphane (SFN) and $PM_{2.5}$ on antioxidant enzyme activities. ARPE-19 cells were treated with the indicated concentrations of SFN or DEX (1 μM) for 6 after 24 h $PM_{2.5}$ challenge (100 μg/mL). After treatment, the activities of **(A)** catalase (CAT) and **(B)** superoxide dismutase (SOD) were measured. Values represent mean ± SD of three independent experiments. $^{*}p < 0.01$ relative to PM-challenged group, one-way ANOVA. $^{\#}p < 0.01$ relative to control, one-way ANOVA.

and subsequent caspase activation (39, 40). Among activated caspases, cleaved caspase-3 serves as the central executioner in cell death in receptor- or mitochondrial-mediated apoptosis (41). The present study demonstrated that $PM_{2.5}$ exposure increased Bax, cytosolic cytochrome c, and cleaved caspase-3 protein levels and decreased Bcl-2 protein levels. However, post-treatment with SNF after $PM_{2.5}$ exposure effectively reversed these pro-apoptotic changes, including decreased protein levels of Bax, cytosolic cytochrome c, and cleaved caspase-3, and increased Bcl-2 levels. This suggested that elevated intracellular ROS was related to $PM_{2.5}$-induced apoptosis in ARPE-19 cells. Furthermore, previous studies reported that SGK1 promotes cell survival and inhibits cell apoptosis including cardiomyocytes (42). Interestingly, expression of SGK1 was decreased in $PM_{2.5}$-treated human lung alveolar epithelial cells, and overexpression of SGK1 significantly attenuated apoptosis with reduced ROS generation (19). These results were similarly shown in the present study by the SFN treatment. Thus, SFN has a therapeutic effect against $PM_{2.5}$-induced apoptosis in RPE cells by regulating mechanisms upstream of caspase-3, such as antioxidant defense mechanisms.

$PM_{2.5}$ is known to cause oxidative damage (43, 44). Although it is difficult to determine the contribution of $PM_{2.5}$ pollutants to total oxidative burden, many studies have shown that $PM_{2.5}$, metals, carbonaceous materials, and polycyclic aromatic hydrocarbons increase ROS levels (25, 45). $PM_{2.5}$-induced oxidative stress and cytotoxicity are due in part to adsorption of particle transition metals and their oxidation products, which are associated with polycyclic aromatic hydrocarbons (25, 45).

Oxidative stress occurs due to an imbalance between ROS levels and the antioxidant defense mechanisms that quench ROS (46). Antioxidant defense mechanisms, which involve antioxidant enzymes such as SOD, CAT, GSH, and GPx, prevent generation of the most reactive forms of ROS, for example hydroxyl radical, preventing oxidative damage to cellular macromolecules, including DNA, proteins, and lipids (46). SOD catalyzes the dismutation of O_2^- to H_2O_2, and CAT quenches H_2O_2 (47). The present study demonstrated that $PM_{2.5}$

decreased SOD and CAT antioxidant enzyme activities at high concentrations (**Figure 5**), which is consistent with a prior report that PM impaired the antioxidant enzymatic activities of SOD, GR, CAT, and glutathione-S-transferase in human epithelial cells (48). The results of the present study demonstrated that enzymatic activities of SOD and CAT were decreased by PM exposure, and that these effects were reversed by SFN post-treatment. These results suggest that SFN has antioxidant activity against RPE exposure to $PM_{2.5,}$ which was recently identified as a risk factor for AMD (28).

There are several limitations in this study. First, the main limitation is the inability to determine the precise molecular mechanisms of the SFN. Intriguingly, BAK and BAX may not always be required for pro-apoptotic stimuli to promote cytochrome c release and the consequent caspase activation (49). Second, because a wide range of retinal and choroidal pathologies are also involved in AMD such as RPE-Bruch membrane thickening, drusen accumulation, reduced blood flow, photoreceptor degeneration, cofactor accumulation, and inflammatory cytokines and chemokines, our model was not able to explain all of them. Instead, our study focused on the findings that SFN alleviated $PM_{2.5}$-induced RPE cell death in the aspect of oxidative stress suggesting a potential therapeutic for AMD. We will expand our study to focus on other mechanisms such as the complemental pathway (50) and to elucidate the precise molecular mechanism.

Taken together, our findings suggested that $PM_{2.5}$ treatment induced oxidative stress in RPE cells, possibly by elevated intracellular ROS and/or decreasing antioxidant enzyme activity, leading to ARPE-19 cell death. Our findings suggest that $PM_{2.5}$-induced oxidative stress likely exacerbates RPE dysfunction in the context of RPE, and that SFN alleviates $PM_{2.5}$-induced cell death by regulating mechanisms upstream of caspase-3, such as antioxidant defense mechanisms. These findings suggest that SFN is a potential therapeutic for AMD, which is characterized in part by RPE atrophy.

DATA AVAILABILITY STATEMENT

The data that support the findings of this study are available from the corresponding authors upon reasonable request.

ETHICS STATEMENT

The animal study was reviewed and approved by Animal Care Committee of Kyungpook National University (2019-0104-01).

AUTHOR CONTRIBUTIONS

HS, WL, DP, and J-SB: design and conduct of the study, analysis and interpretation of data, writing the manuscript, and critical revision of the manuscript. All authors: collection of data and final approval of the manuscript, contributed to the article, and approved the submitted version.

FUNDING

J-SB was supported by a grant from the Korea Health Technology R&D Project through the Korea Health Industry Development Institute (KHIDI), funded by the Ministry of Health & Welfare, Republic of Korea (grant number: HI15C0001) and by a National Research Foundation of Korea (NRF) grant funded by the Korean government (2020R1A2C1004131, 2017M3A9G8083382, 2017R1A5A2015391). DP was financially supported by the Basic Science Research Program of the National Research Foundation of Korea (NRF), funded by the Korean government (Ministry of Science and ICT) (2019R1A2C1084371). DP was also supported by the Ministry of Science and ICT (MSIT), Korea, under the Information Technology Research Center (ITRC) support program (IITP-2021-2020-0-01808) supervised by the Institute of Information & Communications Technology Planning & Evaluation (IITP). I-KL and DP were supported by a grant of the Korea Health technology R&D Project through the Korea Health Industry Development Institute (KHIDI), funded by the Ministry of Health & Welfare, Republic of Korea (HI16C1501).

SUPPLEMENTARY MATERIAL

The Supplementary Material for this article can be found online at: https://www.frontiersin.org/articles/10.3389/fmed.2021.685032/full#supplementary-material

REFERENCES

1. Gehrs KM, Anderson DH, Johnson LV, Hageman GS. Age-related macular degeneration–emerging pathogenetic and therapeutic concepts. *Ann Med.* (2006) 38:450–71. doi: 10.1080/07853890600946724
2. Tokarz P, Kaarniranta K, Blasiak J. Role of antioxidant enzymes and small molecular weight antioxidants in the pathogenesis of age-related macular degeneration (AMD). *Biogerontology.* (2013) 14:461–82. doi: 10.1007/s10522-013-9463-2
3. Mao H, Seo SJ, Biswal MR, Li H, Conners M, Nandyala A, et al. Mitochondrial oxidative stress in the retinal pigment epithelium leads to localized retinal degeneration. *Invest Ophthalmol Vis Sci.* (2014) 55:4613–27. doi: 10.1167/iovs.14-14633
4. Maier KL, Alessandrini F, Beck-Speier I, Hofer TP, Diabate S, Bitterle E, et al. Health effects of ambient particulate matter–biological mechanisms and inflammatory responses to *in vitro* and *in vivo* particle exposures. *Inhal Toxicol.* (2008) 20:319–37. doi: 10.1080/08958370701866313
5. Kim KH, Kabir E, Kabir S. A review on the human health impact of airborne particulate matter. *Environ Int.* (2015) 74:136–43. doi: 10.1016/j.envint.2014.10.005
6. Lee W, Ku SK, Kim JE, Cho SH, Song GY, Bae JS. Inhibitory effects of black ginseng on particulate matter-induced pulmonary injury. *Am J Chin Med.* (2019) 47:1237–51. doi: 10.1142/S0192415X19500630
7. Brunekreef B, Holgate ST. Air pollution and health. *Lancet.* (2002) 360:1233–42. doi: 10.1016/S0140-6736(02)11274-8
8. Liu CW, Lee TL, Chen YC, Liang CJ, Wang SH, Lue JH, et al. PM2.5-induced oxidative stress increases intercellular adhesion molecule-1 expression in lung epithelial cells through the IL-6/AKT/STAT3/NF-kappaB-dependent pathway. *Part Fibre Toxicol.* (2018) 15:4. doi: 10.1186/s12989-018-0240-x

9. Fahey JW, Talalay P. Antioxidant functions of sulforaphane: a potent inducer of Phase II detoxication enzymes. *Food Chem Toxicol.* (1999) 37:973–9. doi: 10.1016/S0278-6915(99)00082-4
10. Pintea A, Rugin,ă DO, Pop R, Bunea A, Socaciu C. Xanthophylls protect against induced oxidation in cultured human retinal pigment epithelial cells. *J Food Comp Anal.* (2011) 24:830–6. doi: 10.1016/j.jfca.2011.03.007
11. Bergvall C, Westerholm R. Determination of dibenzopyrenes in standard reference materials (SRM) 1649a, 1650, and 2975 using ultrasonically assisted extraction and LC-GC-MS. *Anal Bioanal Chem.* (2006) 384:438–47. doi: 10.1007/s00216-005-0192-5
12. Lee W, Ku SK, Kim JE, Cho GE, Song GY, Bae JS. Pulmonary protective functions of rare ginsenoside Rg4 on particulate matter-induced inflammatory responses. *Biotechnol Bioprocess Eng.* (2019) 24:445–53. doi: 10.1007/s12257-019-0096-4
13. Mikolka P, Kosutova P, Kolomaznik M, Topercerova J, Kopincova J, Calkovska A, et al. Effect of different dosages of dexamethasone therapy on lung function and inflammation in an early phase of acute respiratory distress syndrome model. *Physiol Res.* (2019) 68(Suppl 3):S253–63. doi: 10.33549/physiolres.934364
14. Lee BS, Lee C, Yang S, Ku SK, Bae JS. Renal protective effects of zingerone in a mouse model of sepsis. *BMB Rep*. (2019) 52:271–6. doi: 10.5483/BMBRep.2019.52.4.175
15. Jeong SY, Kim M, Park EK, Kim J-S, Hahn D, Bae J-S. Inhibitory functions of novel compounds from dioscorea batatas decne peel on HMGB1-mediated septic responses. *Biotechnol Bioprocess Eng.* (2020) 25:1–8. doi: 10.1007/s12257-019-0382-1
16. Lee W, Lee H, Lee T, Park EK, Bae JS. Inhibitory functions of maslinic acid, a natural triterpene, on HMGB1-mediated septic responses. *Phytomedicine*. (2020) 69:153200. doi: 10.1016/j.phymed.2020.153200
17. Ma YH, Karunakaran T, Veeraraghavan VP, Mohan SK, Li SL. Sesame inhibits cell proliferation and induces apoptosis through inhibition of STAT-3 translocation in thyroid cancer cell lines (FTC-133). *Biotechnol Bioprocess Eng.* (2019) 24:646–52. doi: 10.1007/s12257-019-0151-1
18. Zhang YY, Liu MC, Fan RP, Zhou QL, Yang JP, Yang SJ, et al. Walnut protein isolates attenuate particulate matter-induced lung and cardiac injury in mice and zebra fish. *Rsc Adv.* (2019) 9:40736–44. doi: 10.1039/C9RA06002B
19. Li J, Zhou Q, Yang T, Li Y, Zhang Y, Wang J, et al. SGK1 inhibits PM2.5-induced apoptosis and oxidative stress in human lung alveolar epithelial A549cells. *Biochem Biophys Res Commun.* (2018) 496:1291–5. doi: 10.1016/j.bbrc.2018.02.002
20. Winkler BS, Boulton ME, Gottsch JD, Sternberg P. Oxidative damage and age-related macular degeneration. *Mol Vis.* (1999) 5:32.
21. Plafker SM, O'Mealey GB, Szweda LI. Mechanisms for countering oxidative stress and damage in retinal pigment epithelium. *Int Rev Cell Mol Biol.* (2012) 298:135–77. doi: 10.1016/B978-0-12-394309-5.00004-3
22. Halliwell B. Role of free radicals in the neurodegenerative diseases: therapeutic implications for antioxidant treatment. *Drugs Aging.* (2001) 18:685–716. doi: 10.2165/00002512-200118090-00004
23. Liu Y, Liu M, Zhang X, Chen Q, Chen H, Sun L, et al. Protective effect of fucoxanthin isolated from laminaria japonica against visible light-induced retinal damage both *in vitro* and *in vivo*. *J Agric Food Chem.* (2016) 64:416–24. doi: 10.1021/acs.jafc.5b05436
24. Huang WY, Wu H, Li DJ, Song JF, Xiao YD, Liu CQ, et al. Protective effects of blueberry anthocyanins against H2O2-induced oxidative injuries in human retinal pigment epithelial cells. *J Agric Food Chem.* (2018) 66:1638–48. doi: 10.1021/acs.jafc.7b06135
25. Jia YY, Wang Q, Liu T. Toxicity research of PM2.5 compositions *in vitro*. *Int J Environ Res Public Health*. (2017) 14:232. doi: 10.3390/ijerph14030232
26. Lee H, Hwang-Bo H, Ji SY, Kim MY, Kim SY, Park C, et al. Diesel particulate matter2.5 promotes epithelial-mesenchymal transition of human retinal pigment epithelial cells via generation of reactive oxygen species. *Environ Pollut*. (2020) 262:114301. doi: 10.1016/j.envpol.2020.114301
27. Chua SYL, Khawaja AP, Dick AD, Morgan J, Dhillon B, Lotery AJ, et al. Ambient air pollution associations with retinal morphology in the UK Biobank. *Invest Ophthalmol Vis Sci.* (2020) 61:32. doi: 10.1167/iovs.61.5.32
28. Chua SYL, Warwick A, Peto T, Balaskas K, Moore AT, Reisman C, et al. Association of ambient air pollution with age-related macular degeneration and retinal thickness in UK Biobank. *Br J Ophthalmol.* (2021). doi: 10.1136/bjophthalmol-2020-316218. [Epub ahead of print].
29. Zwolak I. Comparison of three different cell viability assays for evaluation of vanadyl sulphate cytotoxicity in a Chinese hamster ovary K1 cell line. *Toxicol Indus Health.* (2016) 32:1013–25. doi: 10.1177/0748233714544190
30. Dumax-Vorzet AF, Tate M, Walmsley R, Elder RH, Povey AC. Cytotoxicity and genotoxicity of urban particulate matter in mammalian cells. *Mutagenesis.* (2015) 30:621–33. doi: 10.1093/mutage/gev025
31. Bisig C, Steiner S, Comte P, Czerwinski J, Mayer A, Petri-Fink A, et al. Biological effects in lung cells *in vitro* of exhaust aerosols from a gasoline passenger car with and without particle filter. *Emission Control Sci Technol.* (2015) 1:237–46. doi: 10.1007/s40825-015-0019-6
32. Geng H, Meng Z, Zhang Q. *In vitro* responses of rat alveolar macrophages to particle suspensions and water-soluble components of dust storm PM(2.5). *Toxicol In Vitro.* (2006) 20:575–84. doi: 10.1016/j.tiv.2005.09.015
33. Pang L, Zou S, Shi Y, Mao Q, Chen Y. Apigenin attenuates PM2.5-induced airway hyperresponsiveness and inflammation by down-regulating NF-kappaB in murine model of asthma. *Int J Clin Exp Pathol.* (2019) 12:3700–9.
34. Lee W, Baek MC, Kim KM, Bae JS. Biapenem as a novel insight into drug repositioning against particulate matter-induced lung injury. *Int J Mol Sci.* (2020) 21:1462. doi: 10.3390/ijms21041462
35. Nguyen LTH, Ahn SH, Nguyen UT, Yang IJ, Shin HM. Geniposide, a principal component of gardeniae fructus, protects skin from diesel exhaust particulate matter-induced oxidative damage. *Evid Based Complement Alternat Med.* (2021) 2021:8847358. doi: 10.1155/2021/8847358
36. Wang YW, Wu YH, Zhang JZ, Tang JH, Fan RP, Li F, et al. Ruscogenin attenuates particulate matter-induced acute lung injury in mice via protecting pulmonary endothelial barrier and inhibiting TLR4 signaling pathway. *Acta Pharmacol Sin.* (2021) 42:726–34. doi: 10.1038/s41401-020-00502-6
37. Musat O, Ochinciuc U, Gutu T, Cristescu TR, Coman C. Pathophysiology and treatment of ARMD. *Oftalmologia.* (2012) 56:45–50.
38. Jurgensmeier JM, Xie Z, Deveraux Q, Ellerby L, Bredesen D, Reed JC. Bax directly induces release of cytochrome c from isolated mitochondria. *Proc Natl Acad Sci U S A.* (1998) 95:4997–5002. doi: 10.1073/pnas.95.9.4997
39. Brentnall M, Rodriguez-Menocal L, De Guevara RL, Cepero E, Boise LH. Caspase-9, caspase-3 and caspase-7 have distinct roles during intrinsic apoptosis. *BMC Cell Biol.* (2013) 14:32. doi: 10.1186/1471-2121-14-32
40. Lin L, Cheng K, Xie Z, Chen C, Chen L, Huang Y, et al. Purification and characterization a polysaccharide from Hedyotis diffusa and its apoptosis inducing activity toward human lung cancer cell line A549. *Int J Biol Macromol.* (2019) 122:64–71. doi: 10.1016/j.ijbiomac.2018.10.077
41. Yang B, Ye D, Wang Y. Caspase-3 as a therapeutic target for heart failure. *Expert Opin Ther Targets.* (2013) 17:255–63. doi: 10.1517/14728222.2013.745513
42. Sun N, Meng F, Xue N, Pang G, Wang Q, Ma H. Inducible miR-145 expression by HIF-1a protects cardiomyocytes against apoptosis via regulating SGK1 in simulated myocardial infarction hypoxic microenvironment. *Cardiol J.* (2018) 25:268–78. doi: 10.5603/CJ.a2017.0105
43. Lodovici M, Bigagli E. Oxidative stress and air pollution exposure. *J Toxicol.* (2011) 2011:487074. doi: 10.1155/2011/487074
44. Valavanidis A, Vlachogianni T, Fiotakis K, Loridas S. Pulmonary oxidative stress, inflammation and cancer: respirable particulate matter, fibrous dusts and ozone as major causes of lung carcinogenesis through reactive oxygen species mechanisms. *Int J Environ Res Public Health.* (2013) 10:3886–3907. doi: 10.3390/ijerph10093886
45. Valavanidis A, Fiotakis K, Vlachogianni T. Airborne particulate matter and human health: toxicological assessment and importance of size and composition of particles for oxidative damage and carcinogenic mechanisms. *J Environ Sci Health C Environ Carcinog Ecotoxicol Rev.* (2008) 26:339–62. doi: 10.1080/10590500802494538
46. Birben E, Sahiner UM, Sackesen C, Erzurum S, Kalayci O. Oxidative stress and antioxidant defense. *World Allergy Organ J.* (2012) 5:9–19. doi: 10.1097/WOX.0b013e3182439613
47. Ighodaro OM, Akinloye OA. First line defence antioxidants-superoxide dismutase (SOD), catalase (CAT) and glutathione peroxidase (GPX): their fundamental role in the entire antioxidant defence grid. *Alex J Med.* (2018) 54:287–93. doi: 10.1016/j.ajme.2017.09.001

48. Chirino YI, Sanchez-Perez Y, Osornio-Vargas AR, Morales-Barcenas R, Gutierrez-Ruiz MC, Segura-Garcia Y, et al. PM(10) impairs the antioxidant defense system and exacerbates oxidative stress driven cell death. *Toxicol Lett.* (2010) 193:209–16. doi: 10.1016/j.toxlet.2010.01.009
49. Galluzzi L, Vitale I, Aaronson SA, Abrams JM, Adam D, Agostinis P, et al. Molecular mechanisms of cell death: recommendations of the Nomenclature Committee on Cell Death 2018. *Cell Death Differ.* (2018) 25:486–541. doi: 10.1038/s41418-017-0012-4
50. Amadi-Obi A, Yu CR, Dambuza I, Kim SH, Marrero B, Egwuagu CE. Interleukin 27 induces the expression of complement factor H (CFH) in the retina. *PLoS ONE.* (2012) 7:e45801. doi: 10.1371/journal.pone.0045801

Conflict of Interest: The authors declare that the research was conducted in the absence of any commercial or financial relationships that could be construed as a potential conflict of interest.

frontiers in Medicine

CLINICAL TRIAL
published: 27 August 2021
doi: 10.3389/fmed.2021.700793

Comparison Between Nylon and Polyglactin Sutures in Pediatric Cataract Surgery: A Randomized Controlled Clinical Trial

Mathias V. Melega[1], Roberto dos Reis[1], Rodrigo Pessoa Cavalcanti Lira[2], Denise Fornazari de Oliveira[1], Carlos Eduardo Leite Arieta[1] and Monica Alves[1]*

[1] School of Medical Sciences, University of Campinas, São Paulo, Brazil, [2] School of Medical Sciences, Federal University of Pernambuco (UFPE), Recife, Brazil

OPEN ACCESS

Edited by:
Dong Ho Park, Kyungpook National University Hospital, South Korea

Reviewed by:
Rahul Bhargava, GS Medical College and Hospital, India
Savleen Kaur, Post Graduate Institute of Medical Education and Research (PGIMER), India

***Correspondence:**
Mathias V. Melega
mvmelega@hotmail.com

Specialty section:
This article was submitted to Ophthalmology, a section of the journal Frontiers in Medicine

Received: *26 April 2021*
Accepted: *09 August 2021*
Published: *27 August 2021*

Citation:
Melega MV, dos Reis R, Lira RPC, de Oliveira DF, Arieta CEL and Alves M (2021) Comparison Between Nylon and Polyglactin Sutures in Pediatric Cataract Surgery: A Randomized Controlled Clinical Trial. Front. Med. 8:700793. doi: 10.3389/fmed.2021.700793

Purpose: To compare the performance of nylon sutures to that of polyglactin sutures in pediatric patients undergoing cataract surgery.

Setting: University of Campinas (UNICAMP), Campinas, São Paulo, Brazil

Design: A prospective, randomized, partially masked, single-site clinical trial. (https://clinicaltrials.gov/ct2/show/NCT03812640).

Methods: A total of 80 eyes from 80 patients who underwent pediatric cataract surgery were randomized into two groups in block sizes of four. Group A consisted of 41 patients whose surgical incisions were sutured with polyglactin 10-0 material. Group B consisted of 39 patients whose surgical incisions were sutured with nylon 10-0 material. The primary outcome was frequency of suture-related complications in each group. Secondary outcomes were the frequency with which suture removal was necessary.

Results: The incidence of suture-related complications within 6 months of follow up was 0 out of 41 eyes (0.00%) in the polyglactin group and 17 out of 39 eyes (43.59%) in the nylon control group ($p < 0.001$). In all of the eyes with suture-related complications, the sutures were promptly removed. The most frequent complications were vascularization near the suture (17.95%) and loose sutures (17.95%). No ocular or systemic study-related adverse events were observed.

Conclusions: Polyglactin sutures were found to be safe and effective for pediatric patients undergoing cataract surgery. Their lower rate of complications and reduced likelihood of removal (and the subsequent need for general anesthesia) make their use preferrable to that of nylon sutures. This study represents the first controlled randomized clinical trial to compare nylon sutures to polyglactin sutures in pediatric patients undergoing cataract surgery.

Clinical Trial Registration: URL: https://clinicaltrials.gov/ct2/show/, Identifier: NCT03812640.

Keywords: pediatric cataract, suture, nylon, polyglactin, suture-related complications

INTRODUCTION

Though rare, pediatric cataracts are a major cause of childhood blindness. Children deprived of adequate treatment experience worsened quality of life, and the socioeconomic costs are higher overall. The prevalence of pediatric cataracts is estimated to range from 1:10,000 to 4:10,000 in industrialized nations and from 5:10,000 to 15:10,000 in developing countries. Pediatric cataracts generate ∼200,000 cases of blindness in children around the world each year as a result of unoperated cataracts, surgical complications, or consequences of diseases such as glaucoma and amblyopia (1–4).

Pediatric cataracts must be diagnosed as early as possible; a late diagnosis worsens the visual prognosis. Because the patients are children, trauma or eye rubbing in the postoperative period cannot be fully avoided. In addition, children's sclera exhibits limited rigidity, resulting in poor integrity of the surgical incision if no sutures are made. This situation requires surgeons to systematically suture the surgical incision in order to guarantee the perfect closure of the eyeball and prevent complications such as leakage of the aqueous humor with postoperative hypotonia, iris prolapse, or anterior synechiae formation, as well as to prevent intraocular infection caused by the entrance of microorganisms into the incision. In Brazil, this suture has been performed using 10-0 nylon for decades. Because nylon is a non-absorbable material, it can remain in the patient's cornea for years, predisposing the patient to suture loosening with the accumulation of mucus, corneal erosion, corneal neovascularization, infectious keratitis, (5–7) endophthalmitis, (8, 9) and giant papillary conjunctivitis (10). Because of the risk of complications associated with suturing, the removal of these sutures is essentially obligatory, though they must be removed under sedation in a surgical facility (11, 12). Due to the need for nylon suture removal, other materials are being considered.

In 1998, a randomized clinical trial comparing polyglactin 10-0 to nylon 10-0 in adult cataract surgeries with a 5.2 mm incision demonstrated safety in incision closure and a low rate of complications associated with the use of polyglactin; because polyglactin can be absorbed by the body within 56–70 days, additional interventions to remove it are not necessary (13, 14). In 2007, a retrospective study on pediatric patients comparing absorbable polyglactin sutures to non-absorbable polyester sutures demonstrated a lower rate of complications in the patients who received the polyglactin sutures (15). This study found that the polyglactin sutures produced no complications and that their removal was not necessary; meanwhile, the polyester sutures were associated with complications in 18% of the cases in which they were used, and their removal was required. However, the study was retrospective and used vastly different group sizes.

To our knowledge, no controlled randomized clinical trials have been performed to compare sutures performed using nylon to those performed using polyglactin in pediatric patients. We performed the current study in an attempt to establish evidence-based conclusions regarding the prevention of suture-related complications.

Our study is the first randomized clinical trial to compare nylon sutures to polyglactin sutures in terms of rates of complications and the frequency with which suture removal is necessary in pediatric patients undergoing cataract surgery.

MATERIALS AND METHODS

This study was a single-site, prospective, parallel-group, randomized, partially masked, phase 3 clinical trial. It was performed after approval from the University of Campinas research ethics committee and was conducted in accordance with the tenets of the Declaration of Helsinki and current legislation on clinical research. Written informed consent was obtained from all subjects after the explanation of the procedures and study requirements. The trial was registered and began in January 2019 (Comparison Between Nylon and Polyglactin Corneal Suture in Pediatric Cataract Surgery: A Randomized and Controlled Clinical Trial; ClinicalTrials.gov identifier: NCT03812640; https://clinicaltrials.gov/ct2/show/NCT03812640). The inclusion criteria were patients 14 years of age or younger for whom pediatric cataract surgery was clinically indicated. The exclusion criteria were traumatic cataract with ocular perforation, cataract surgery associated with other procedures (such as glaucoma filtering surgery, vitreoretinal surgery, or corneal surgery), signs of ocular or periocular infection, advanced glaucoma, and severe ocular surface disease.

Data were collected from patients undergoing cataract surgery at the University of Campinas (UNICAMP) Clinical Hospital. Medical records, routine preoperative clinical exam data, data from intraoperative evaluations, and data from the 1st, 7th, 30th, 90th, 120th, and 180th postoperative days were collected on each patient.

Patients were randomly divided into one of two groups approximately equal in size and stratified by age (0–6 months, 6–12 months, 1–3 years, 3–6 years, and older than 6 years of age). Group A had their surgical incisions sutured with polyglactin 10-0 material (Vicryl®, composed of polyglactin 910, 10-0 diameter, absorbable, a 0.62 cm, 3/8 circle needle) at the end of cataract surgery. Patients in Group B had their surgical incisions sutured with nylon 10-0 material (composed of nylon monofilament, 10-0 diameter, absorbable, a 0.55 cm, 1/2 circle needle) at the end of cataract surgery.

All cataract surgeries were performed by the same surgeon (M.V.M.) in accordance with the protocols used in the Department of Ophthalmology of the University of Campinas (UNICAMP). Preoperative antibiotics were not used. Briefly, the surgery protocol consisted of skin antisepsis with 10% povidone-iodine, placement of a sterile surgical drape to isolate lid margin and eyelashes, the application of four drops of 5% povidone-iodine into the conjunctival sac, and subsequent irrigation using a balanced salt solution. In cases of povidone-iodine allergy, an aqueous solution consisting of 0.05% chlorhexidine was used. Phacoaspiration using the Infiniti® phacoemulsifier (Alcon Laboratories Inc., Fort Worth, Texas, USA) was performed, and an AcrySof® MA60AC intraocular foldable lens (Alcon Laboratories Inc, Fort Worth, Texas, USA) was implanted in

patients 6 months of age and older. Ultrasound energy was not used.

The Pediatric Cataract Department of the University of Campinas does not indicate intraocular lens implantation in patients younger than 6 months of age, and these patients remain aphakic. Intraocular lens implants are always recommended for patients 6 months of age and older. We chose to perform an a YAG laser posterior capsulotomy as an outpatient procedure; when patients were too young or otherwise unable to undergo the YAG procedure, we chose to perform a primary posterior capsulotomy (PPC) combined with an anterior vitrectomy (AV). With a few exceptions, patients 5 years of age and older exhibited the level of cooperation necessary to receive a YAG laser posterior capsulotomy.

We therefore performed one of three surgical combinations on each patient: on children younger than 6 months of age, we performed phacoaspiration combined with a PPC and an AV with no intraocular lens implant. In children 6 months of age and older who could not tolerate a YAG laser posterior capsulotomy, we performed phacoaspiration with an intraocular lens implant, as well as a PPC and an AV at the time of the cataract surgery. In children who were able to tolerate an outpatient YAG laser posterior capsulotomy, we performed phacoaspiration with an intraocular lens implant.

Clear corneal incision was used. Only one side port was made in all cases, and both incisions were sutured with the knots buried into the corneal side. The topical postoperative regimen consisted of 0.5% moxifloxacin combined with 0.1% dexamethasone every 3 h for 7 days only during waking hours. On the seventh postoperative day, this regimen was changed to only 0.1% dexamethasone, which was tapered over the course of 3 weeks.

The primary outcome was incidence of complications associated with sutures in each group. The suture-related complications were defined as corneal neovascularization close to the suture, loosening of the suture, accumulation of mucus on the suture, early suture rupture (within 2 weeks), aqueous humor leakage through the incision (as determined by the Seidel test), prolapse of the iris through the incision site, infectious or traumatic keratitis, endophthalmitis, and giant papillary conjunctivitis. In eyes with suture-related complications, the sutures were promptly removed. Secondary outcome was the need for suture removal under sedation in each group.

Sample size was calculated based on the frequency of suture-related complications described in the literature (15, 16) and using a two-tailed 95% confidence interval, 80% power, an exposed/unexposed radius of 1, and a null frequency of complications in the polyglactin suture group, which resulted in approximately 40 subjects per group. The trial would have been suspended if a difference between the two groups lower than a type I error (α) of 4% had been found in the pre-analysis of 50, 75, and 100% of the patients included. Eligible patients were randomly assigned at a 1:1 ratio. Randomization was stratified by age in block sizes of four. One nurse generated the random allocation sequence using a computer randomization list, and another nurse enrolled and assigned the subjects to the interventions in a masked fashion. Sealed opaque envelopes were used for allocation and were opened immediately before surgery.

After the attribution of the interventions, the patients and their guardians were masked to the type of intervention. The surgeons were not masked because the type of suture used can easily be identified during surgery and in the biomicroscopy exam in the postoperative period.

STATISTICAL ANALYSIS

Continuous data have been expressed as the mean ± standard deviation and range. Medians and interquartile ranges were used for variables with non-normal distribution. Between-group differences of continuous variables were compared using the Wilcoxon signed-rank test, and categorical variables were compared using the x^2 test or Fisher's exact test when appropriate. Multiple Firth logistic regressions were used to assess the effect of covariates on the studied outcomes. Analyses were performed using STATA 14.0 (StataCorp LP, College Station, TX, USA). Statistical significance was established when $p \leq 0.05$.

RESULTS

This study enrolled 80 patients between January 2019, and August 2020. These subjects were randomized into group A (polyglactin suture) or group B (nylon suture). In total, 41 patients in the polyglactin group and 39 patients in the nylon group completed the 6 months of follow-up care; no subjects were lost to follow up (**Figure 1**). Demographic data demonstrate homogeneity between the groups, as displayed in **Table 1**.

Table 2 shows the surgical options applied to each group.

Multiple logistic regression analysis was employed to determine the factors most closely associated with intraoperative complications, and the results are shown in **Table 3**.

Table 4 shows the results of the multiple logistic regression employed to assess the factors associated with suture complications and the need for suture removal.

DISCUSSION

Unlike in adult cataract surgery, pediatric cataract extraction surgery requires that the surgical incision be systematically sutured. In Brazil, the most commonly used suture material is currently nylon 10-0. Nylon is a monofilament and non-absorbable material composed of polyamides that enables increased suture tension time and induces minimal cellular reactions. Vicryl is an absorbable synthetic compound made of polyglactin (a copolymer of glycolide and lactide) (14). Suture absorption occurs as a result of hydrolysis, which itself is generated by glycolic and lactic acids. Many nylon sutures must be removed from patients during the postoperative period. Because the patients in these cases are children, this normally simple removal procedure requires sedation. As was demonstrated in our patient groups (**Table 1**), there is a major association between pediatric cataract and systemic

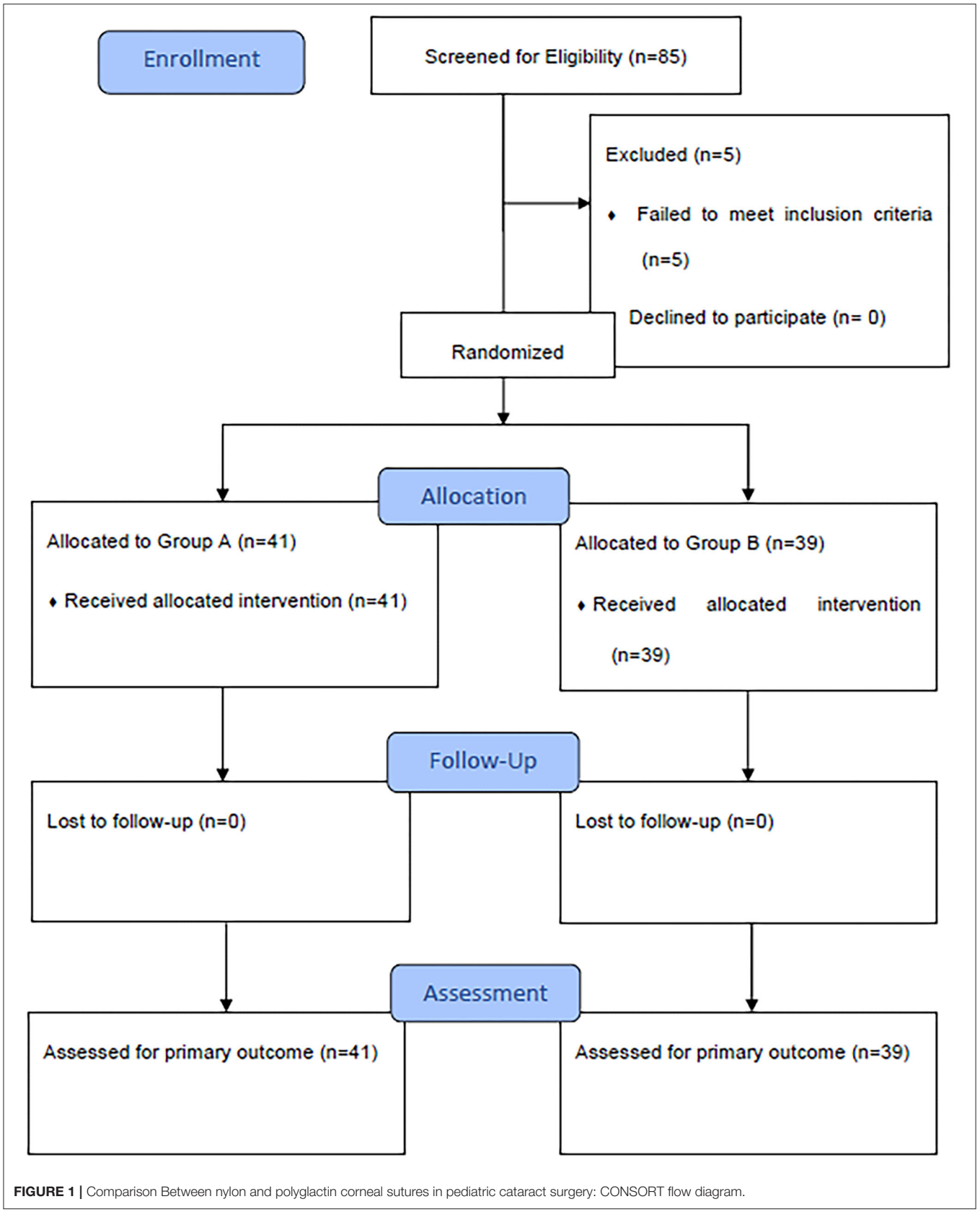

FIGURE 1 | Comparison Between nylon and polyglactin corneal sutures in pediatric cataract surgery: CONSORT flow diagram.

TABLE 1 | Demographic characteristics of pediatric cataract patients in the polyglactin suture group and the nylon suture group.

	Polyglactin group	Nylon group	*p*-Value
Sex, *N* (%) **Male**	21 (51.22)	26 (66.67)	0.161*
Age (months), mean ± SD (median; 25% percentile; 75% percentile)	45.76 ± 50.24 (16.00; 7.00; 72.00)	42.49 ± 46.41 (24.00; 5.00; 72.00)	0.780†
Operated eye, *N*(%) OD	18 (43.90)	25 (64.10)	0.070*
Systemic comorbidities, *N* (%)			0.151*
Marfan syndrome	3 (7.32)	7 (17.95)	
Toxoplasmosis	1 (2.44)	1 (2.56)	
Ichthyosis	1 (2.44)	1 (2.56)	
Galactosemia	0 (0.00)	3 (7.69)	
Down syndrome	1 (2.44)	2 (5.13)	
Cockayne syndrome	0 (0.00)	1 (2.56)	
No comorbidities	35 (85.37)	24 (61.54)	
Ocular comorbidities, *N* (%)			0.548#
Chorioretinitis scarring	1 (2.44)	0 (0.00)	
Persistent fetal vasculature	1 (2.44)	0 (0.00)	
Congenital glaucoma	1 (2.44)	1 (2.56)	
Strabismus	1 (2.44)	0 (0.00)	
Traumatic cataracts	0 (0.00)	1 (2.56)	
Aniridia	1 (2.44)	0 (0.00)	
No comorbidities	36 (87.80)	37 (94.87)	

SD, Standard Deviation; OD, Right Eye.
**Chi-Squared test.*
†Wilcoxon signed-rank test.
#Fisher's exact test.

TABLE 2 | Pediatric cataract surgery outcomes organized by suture material used (polyglactin vs. nylon sutures).

	Polyglactin group ***N*** (%)	Nylon group ***N*** (%)	*p*-Value
Surgery type			0.776*
Phaco + PPC + AV	23 (56.10)	25 (64.10)	
Phaco + PPC + AV + IOL	7 (17.07)	6 (15.38)	
Phaco + IOL	11 (26.83)	8 (20.51)	
Intraoperative complications			0.999#
PCR	1 (2.44)	1 (2.56)	
Iris damage	1 (2.44)	1 (2.56)	
None	39 (95.12)	37 (94.87)	
Suture-related complications			<0.001#
Vascularized suture	0 (0.00)	7 (17.95)	
Suture loosening	0 (0.00)	7 (17.95)	
Suture with mucus	0 (0.00)	1 (2.56)	
Suture rupture	0 (0.00)	2 (5.13)	
No complications	41 (100.00)	22 (56.41)	

PPC, primary posterior capsulotomy; AV, anterior vitrectomy; IOL, intraocular lens; Phaco, phacoaspiration; PCR, posterior capsule rupture.
**Chi-Squared test.*
#Fisher's exact test.

TABLE 3 | Multiple logistic regression analysis applied to data on intraoperative complications in pediatric cataract surgeries in which either nylon or polyglactin sutures were used.

	Odds ratio (95% CI)	*p*-Value
Sex		0.178
Male	Reference	
Female	7.43 (0.40–137.25)	
Age (months)	1.02 (0.99–1.04)	0.062
Systemic comorbidities		0.232
No	Reference	
Yes	0.21 (0.02–2.69)	
Ocular comorbidities		0.820
No	Reference	
Yes	1.44 (0.06–32.22)	
Surgery type		-
Phaco + PPC + AV	Reference	
Phaco + PPC + AV + IOL	0.43 (0.02–10.86)	0.606
Phaco + IOL	0.55 (0.07–4.54)	0.578
Type of suture material		-
Nylon	Reference	
Polyglactin	2.04 (0.25–16.63)	0.504

PPC, primary posterior capsulotomy; AV, anterior vitrectomy; IOL, intraocular lens; Phaco, phacoaspiration; CI, confidence interval.

diseases (Marfan syndrome, Down syndrome, congenital cardiac abnormalities, ichthyosis, inborn errors of metabolism, toxoplasmosis, rubella, syphilis, and other congenital infections). These comorbidities may increase the rate of complications in cases requiring general anesthesia in a group of patients whose age already makes them more vulnerable in this procedure (17, 18).

In addition to the risks associated with general anesthesia, suture removal itself also increases the risk of endophthalmitis in that it makes it easier for microorganisms to enter the eye as the string is being pulled (8). Certain measures must be taken to prevent this complication, including the use of 5% povidone-iodine before the procedure, cutting the suture at one end to prevent the external portion of the string from entering the eye, postoperative topical antibiotics, and outpatient follow-up care to catch and treat any infections as early as possible.

Other researchers have also compared different suture materials for use in pediatric cataract surgery. Bar-sela et al. (15). performed a retrospective study to compare polyester 10-0 (Mersilene®) to polyglactin 10-0 (Vicryl®) over 6 months of follow up and, similar to our results, found no suture-related complications in the polyglactin 10-0 group. Matalia et al. performed a non-randomized prospective study to compare the same suture materials considered herein in pediatric cataract surgeries and obtained similar results (16). As in the surgeries performed herein, these researchers found the polyglactin string to be more difficult to work with and bury. In Matalia et al.

TABLE 4 | Multiple logistic regression analysis applied to suture complications and the need for suture removal in cases of pediatric cataract surgeries with either nylon or polyglactin sutures.

	Coefficient (95% CI)	*p*-Value
Sex		
Male	Reference	
Female	1.61 (0.38–6.86)	0.519
Age (months)	1.01 (0.99–1.03)	0.334
Systemic comorbidities		
No	Reference	
Yes	1.08 (0.23–5.17)	0.922
Ocular comorbidities		
No	Reference	
Yes	4.85 (0.29–81.94)	0.273
Surgery type		
Phaco + PPC + AV	Reference	
Phaco + PPC + AV + IOL	0.43 (0.05–3.54)	0.437
Phaco + IOL	0.13 (0.01–1.90)	0.136
Intraoperative complications		
No	Reference	
Yes	1.64 (0.21–12.86)	0.636
Type of suture material		
Nylon	Reference	
Polyglactin	61.69 (3.43–1110.93)	0.005

PPC, primary posterior capsulotomy; AV, anterior vitrectomy; IOL, intraocular lens; Phaco, phacoaspiration; CI, confidence interval.

and in our study, this finding is merely anecdotal and was not measured quantitatively.

Sukhija and Kaur (20) performed a non-randomized prospective study to compare the efficacy and outcome of viscosealing the incisions using 1.4% sodium hyaluronate with polyglactin sutures in children <5 years. They concluded viscosealing is comparable to suturing of incisions in children undergoing cataract surgery.

Bartholomew et al. (19) also performed a prospective randomized study to compare polyglactin 8-0, nylon 10-0, and silk 8-0, but they reported a greater risk of complications in the polyglactin group within the first month after surgery relative to their other study groups. This finding differs from more recent studies because, according to the authors, they experienced difficulty in knotting the polyglactin string, which resulted in ineffective incision closure. It is important to note that their study was performed in 1976, before the advent of phacoemulsification; therefore, the number of sutures required to close the incision was considerably higher than is required today. This large number of sutures predisposed patients to experiencing suture-related complications. Furthermore, this study was performed on adult patients.

As in other well-known studies on pediatric patients (15, 16), this study concluded that polyglactin 10-0 (Vicryl®) sutures were associated with fewer complications than polyester 10-0 (Mersilene®) sutures; the results therefore demonstrate the benefits of this polyglactin product. Our study seems to be the first to compare different suture materials in prospective and randomized groups of children. We found that the only factor associated with suture-related complications in and following pediatric cataract surgery was the type of material used: subjects who received the nylon sutures were 61.7 times more likely to experience suture-related complications and to require suture removal relative to subjects who received polyglactin sutures (OR = 61.69; 95% CI: 3.43–1110.93; $p = 0.005$). The most frequent complications were vascularization near the suture (17.95%) and suture loosening (17.95%). In the nylon group, the mean time for suture removal was 88.23 ± 59.50 days (median = 60 days). It is important to note that there were no significant differences between the groups in terms of types of surgery ($p = 0.776$) or intraoperative complications ($p = 0.776$).

This study presents some limitations. The degree of astigmatism induced was not assessed due to the lack of adequate methods available for measurement in children, who are unable to undergo in-office keratometry. The exact amount of time required for polyglactin absorption was not determined; however, at the end of the 6-month follow-up period, the biomicroscope exams performed on the polyglactin group revealed no evidence of any suture remains. Our study would have been improved by data comparing the average amount of time spent on suturing in each of the groups, since, as mentioned previously, we experienced greater difficulty and required more time to suture with polyglactin string than with nylon. In a future study, we plan to assess the cost-effectiveness of the use of polyglactin string: though this material is more expensive than nylon, it clearly reduces the need for both additional procedures and the use of general anesthesia for suture removal.

Our study is the first randomized clinical trial to demonstrate that absorbable polyglactin 10-0 sutures are safe for use in pediatric cataract surgery and result in fewer postoperative complications than non-absorbable nylon 10-0 sutures. None of the patients who received polyglactin sutures required suture removal under sedation; these patients were therefore spared the risks associated with general anesthesia and with suture removal itself.

DATA AVAILABILITY STATEMENT

The raw data supporting the conclusions of this article will be made available by the authors, without undue reservation.

ETHICS STATEMENT

The studies involving human participants were reviewed and approved by Ethics committee of the School of Medical Sciences, University of Campinas (UNICAMP). Written informed consent to participate in this study was provided by the participants' legal guardian/next of kin.

AUTHOR CONTRIBUTIONS

MM, RL, CA, and MA contributed to conception and design of the study. MM and RR organized the database. MM, RR,

DO, and MA performed the statistical analysis. MM and MA wrote the first draft of the manuscript. MM, RR, RL, DO, CA, and MA wrote sections of the manuscript. All authors contributed to manuscript revision, read, and approved the submitted version.

FUNDING

Financial support: São Paulo Research Foundation (FAPESP) Grant No. 2014/19138-5 and School of Medical Sciences, University of Campinas (UNICAMP).

ACKNOWLEDGMENTS

We would like to thank our colleagues who greatly assisted in this research: Fabrício Ferreira do Santos provided assistance with statistics. Arthur Fernandes provided assistance with statistics. Danielle Deremo Cosimo provided English-language editing.

SUPPLEMENTARY MATERIAL

The Supplementary Material for this article can be found online at: https://www.frontiersin.org/articles/10.3389/fmed.2021.700793/full#supplementary-material

REFERENCES

1. Foster A, Gilbert C, Rahi J. Epidemiology of cataract in childhood: a global perspective. *J Cataract Refract Surg [Internet]*. (1997) 23:601–4. doi: 10.1016/S0886-3350(97)80040-5
2. Gilbert CE, Wood M, Waddel K, Foster A. Causes of childhood blindness in east Africa: results in 491 pupils attending 17 schools for the blind in Malawi. Kenya and Uganda. *Ophthalmic Epidemiol [Internet]*. (1995) 2:77–84. doi: 10.3109/09286589509057086
3. Haargaard B, Wohlfahrt J, Fledelius HC, Rosenberg T, Melbye M. Incidence and Cumulative Risk of Childhood Cataract in a Cohort of 2.6 Million Danish Children. *Invest Ophthalmol Vis Sci [Internet]*. (2004) 45:1316–20. doi: 10.1167/iovs.03-0635
4. WHO | Priority eye diseases [Internet]. WHO. World Health Organization. (2018). Available online at: http://www.who.int/blindness/causes/priority/en/index1.html
5. Wilson BME. *Pediatric Cataracts : Overview Classification (Categorization)*. (2016). Available online at: https://www.aao.org/disease-review/pediatric-cataracts-overview
6. Heaven CJ, Boase DL. Suppurative keratitis with endophthalmitis due to biodegraded full thickness monofilament nylon corneal sutures. *Eur J Implant Refract Surg [Internet]*. (1993) 5:164–8. doi: 10.1016/S0955-3681(13)80436-4
7. Lee BJ, Smith SD, Jeng BH. Suture-related corneal infections after clear corneal cataract surgery. *J Cataract Refract Surg [Internet]*. (2009) 35:939–42. doi: 10.1016/j.jcrs.2008.10.061
8. Culbert RB, Devenyi RG. Bacterial endophthalmitis after suture removal. *J Cataract Refract Surg*. (1999) 25:725–7. doi: 10.1016/S0886-3350(99)00020-6
9. Khurshid GS, Fahy GT. Endophthalmitis secondary to corneal sutures: Series of delayed-onset keratitis requiring intravitreal antibiotics. *J Cataract Refract Surg*. (2003) 29:1370–2. doi: 10.1016/S0886-3350(03)00404-8
10. Acheson CF, London L. Ocular Morbidity Due to Monofilament Nylon Corneal *Sutures. Eye [Internet]*. (1991) 5:106–12. doi: 10.1038/eye.1991.20
11. Danjoux JP, Reck AC. Corneal sutures: Is Routine Removal Really Necessary? Eye (Lond). 8:339–42. doi: 10.1038/eye.1994.70
12. Jackson H, Bosanquet R. Should nylon corneal sutures be routinely removed? *Br J Ophthalmol*. (1991) 75:663–4. doi: 10.1136/bjo.75.11.663
13. Bainbridge JWB, Teimory M, Kirwan JF, Rostron CK, A. prospective controlled study of a 10/0 absorbablepolyglactin suture for corneal incision phacoemulsification. *Eye*. (1998) 12:399–402. doi: 10.1038/eye.1998.94
14. Ethicon. Ethicon product catalog. (2014) p. 208–30. Available online at: http://www.ecatalog.ethicon.com/sites/default/files/ethicon-catalog.pdf
15. Bar-Sela SM, Spierer O, Spierer A. Suture-related complications after congenital cataract surgery: Vicryl versus Mersilene sutures. *J Cataract Refract Surg*. (2007) 33:301–4. doi: 10.1016/j.jcrs.2006.10.039
16. Matalia J, Panmand P, Ghalla P. Original article comparative analysis of non-absorbable 10 - 0 nylon sutures with absorbable 10 - 0 Vicryl sutures in pediatric cataract surgery. (2018) 661–4. doi: 10.4103/ijo.IJO_654_17
17. Thomas FA. Complications following general anesthesia. *Curr Res Anesth Analg*. (1940) 19:94–6.
18. Benezra D. The surgical approaches to paediatric cataract. Eur J Implant Refract Surg [Internet]. (1990) 2:241–4. doi: 10.1016/S0955-3681(13)80091-3
19. Bartholomew RS, Phillips CI, Munton CG. Vicryl (polyglactin 910) in cataract surgery. A controlled trial. *Br J Ophthalmol*. (1976) 60:536–8. doi: 10.1136/bjo.60.7.536
20. Sukhija J, Kaur S. Comparison of two methods of wound closure in paediatric cataract surgery. *J Clin Exp Ophthalmol*. (2018) 9:766. doi: 10.4172/2155-9570.1000766

Conflict of Interest: The authors declare that the research was conducted in the absence of any commercial or financial relationships that could be construed as a potential conflict of interest.

Publisher's Note: All claims expressed in this article are solely those of the authors and do not necessarily represent those of their affiliated organizations, or those of the publisher, the editors and the reviewers. Any product that may be evaluated in this article, or claim that may be made by its manufacturer, is not guaranteed or endorsed by the publisher.

frontiers in Medicine

ORIGINAL RESEARCH
published: 03 September 2021
doi: 10.3389/fmed.2021.717602

ROCK1 Mediates Retinal Glial Cell Migration Promoted by Acrolein

Kanae Fukutsu, Miyuki Murata, Kasumi Kikuchi, Shiho Yoshida, Kousuke Noda and Susumu Ishida*

Laboratory of Ocular Cell Biology and Visual Science, Department of Ophthalmology, Faculty of Medicine and Graduate School of Medicine, Hokkaido University, Sapporo, Japan

Objective: Acrolein is a highly reactive aldehyde that covalently binds to cellular macromolecules and subsequently modulates cellular function. Our previous study demonstrated that acrolein induces glial cell migration, a pathological hallmark of diabetic retinopathy; however, the detailed cellular mechanism remains unclear. The purpose of this study was to investigate the role of acrolein in retinal glial cell migration by focusing on rho-associated coiled-coil-containing protein kinases (ROCKs).

Methods: Immunofluorescence staining for ROCK isoforms was performed using sections of fibrovascular tissue obtained from the eyes of patients with proliferative diabetic retinopathy (PDR). Rat retinal Müller glial cell line, TR-MUL5, was stimulated with acrolein and the levels of ROCK1 were evaluated using real-time PCR and western blotting. Phosphorylation of the myosin-binding subunit of myosin light chain phosphatase [myosin phosphatase target subunit 1, (MYPT1)] and myosin light chain 2 (MLC2) was assessed. The cell migration rate of TR-MUL5 cells exposed to acrolein and/or ripasudil, a non-selective ROCK inhibitor, was measured using the Oris cell migration assay.

Results: ROCK isoforms, ROCK1 and ROCK2, were positively stained in the cytosol of glial cells in fibrovascular tissues. In TR-MUL5 cells, the mRNA expression level of *Rock1*, but not *Rock2,* was increased following acrolein stimulation. In line with the PCR data, western blotting showed increase in ROCK1 and cleaved ROCK1 protein in TR-MUL5 cells stimulated with acrolein. N-acetylcysteine (NAC) suppressed acrolein-associated *Rock1* upregulation in TR-MUL5 cells. Acrolein augmented the phosphorylation of MYPT1 and MLC2 and increased the cell migration rate of TR-MUL5 cells, both of which were abrogated by ripasudil.

Conclusions: Our study demonstrated that ROCK1 mediates the migration of retinal glial cells promoted by the unsaturated aldehyde acrolein.

Keywords: rho-associated coiled-coil-containing protein kinase 1, acrolein, retinal glial cells, cell migration, diabetic retinopathy

OPEN ACCESS

Edited by:
Ryoji Yanai,
Yamaguchi University, Japan

Reviewed by:
Audrey N. Chang,
University of Texas Southwestern Medical Center, United States
Takayuki Kamiya,
Asahikawa Medical University, Japan

****Correspondence:***
Kousuke Noda
nodako@med.hokudai.ac.jp

Specialty section:
This article was submitted to Ophthalmology, a section of the journal Frontiers in Medicine

Received: *31 May 2021*
Accepted: *10 August 2021*
Published: *03 September 2021*

Citation:
Fukutsu K, Murata M, Kikuchi K, Yoshida S, Noda K and Ishida S (2021) ROCK1 Mediates Retinal Glial Cell Migration Promoted by Acrolein. Front. Med. 8:717602. doi: 10.3389/fmed.2021.717602

INTRODUCTION

Diabetic retinopathy (DR) is one of the leading causes of blindness worldwide (1). During its advanced stage, pathological neovascularization due to retinal ischemia causes the formation of fibrovascular tissues at the vitreoretinal surface, which is a hallmark of proliferative diabetic retinopathy (PDR). Vitreous traction against fibrovascular tissues subsequently leads to severe

complications such as vitreous hemorrhage and tractional retinal detachment in PDR, both of which, without adequate treatment, eventually result in severe visual impairment. Therefore, the mechanisms implicated in the development of fibrovascular tissue are of great significance to both clinicians and researchers.

Fibrovascular tissue consists of small new vessels, extracellular matrix, and cellular components, such as inflammatory cells, fibroblasts, and glial cells (2). In the eye, there are two basic types of macroglial cells: Müller glial cells and astrocytes (3). Of these, Müller glial cells, which provide homeostatic, metabolic, and functional support to neurons, can become activated upon pathogenic stimuli (3) and migrate toward the vitreoretinal surface in the diabetic retina (4). Since activated Müller glial cells produce a variety of inflammatory cytokines including vascular endothelial growth factor (VEGF) (5, 6), it has been presumed that migrated Müller glial cells are one of the major participants in the formation of fibrovascular tissue. We previously investigated the triggers that facilitate the migratory response of Müller glial cells and found that acrolein, an unsaturated aldehyde, was one of the causative factors (7). Acrolein is a highly reactive aldehyde distributed in air pollutants such as cigarette smoke (8) and is associated with the increase in oxidative stress by reducing the antioxidant glutathione (GSH) in retinal capillary endothelial cells (9). In Müller glial cells, acrolein is generated through polyamine metabolism under hypoxic conditions (10) and accelerates cellular motility by inducing chemokine (CXC motif) ligand 1 (CXCL1) in an autocrine fashion (7). Therefore, a growing body of evidence explicitly suggests that acrolein is one of the trigger stimuli for glial cell migration in the diabetic retina and therefore, plays a role in the cell motility mechanism.

Rho-associated coiled-coil-containing protein kinases (ROCKs) are ubiquitously expressed serine-threonine kinases, which represent the main effector proteins of the RhoA and RhoC pathways (11). In humans, ROCKs exist in two isoforms, i.e., ROCK1 and ROCK2, and these enzymes mainly regulate the organization of the actin cytoskeleton and associated dynamic events such as cell contraction and migration (12). Among more than 30 common ROCK substrates, one of the most described targets is the myosin phosphatase target subunit 1 (MYPT1) of the myosin light chain phosphatase (MLCP) (12). ROCK-mediated phosphorylation of MYPT1 hampers the catalytic activity of MLCP, in turn resulting in an increase in myosin light chain (MLC) phosphorylation and subsequent cell contraction. Previously, it was reported that cigarette smoking induces barrier dysfunction through the ROCK pathway in lung microvascular cells, indicating that the acrolein found in cigarette smoke acts upstream of the ROCK cascade. In addition, it was demonstrated that ROCK is involved in leukocyte-induced diabetic retinal endothelial injury (13) and inflammatory microvascular damage (14). Lines of evidence indicate that ROCK participates particularly in the vascular injury and plays a role in the pathogenesis of PDR. By contrast, the role of ROCKs and its associated pathways in retinal glial cells, which also participate in the progression of DR, remains uninvestigated.

In this study, we explored the regulatory mechanisms responsible for Müller glial cell migration induced by the unsaturated aldehyde acrolein, especially focusing on ROCKs.

MATERIALS AND METHODS

Specimens and Materials

Fibrovascular tissues surgically removed from patients with PDR were used for immunofluorescence microscopy. All experiments were conducted in accordance with the tenets of the Declaration of Helsinki, following approval from the Institutional Review Committee of Hokkaido University Hospital (IRB #014-0293). Written informed consent was obtained from all the patients after explaining the purpose and procedures of this study. Ripasudil, a ROCK inhibitor, was provided by Kowa Company, Ltd. (Tokyo, Japan).

Cell Culture

Conditionally immortalized rat retinal Müller cell line TR-MUL5 from transgenic rats harboring the temperature-sensitive SV 40 large T-antigen gene was provided by Fact Inc. (Sendai, Japan) (15). TR-MUL5 cells were cultured at 33°C in Dulbecco's modified Eagle's medium (Fuji Film Wako Pure Chemicals, Osaka, Japan), supplemented with 10% fetal bovine serum (Thermo Fisher Scientific, Waltham, MA, USA) in an atmosphere of 95% air and 5% CO_2.

Immunofluorescence Microscopy

Paraffin sections of fibrovascular tissues were deparaffinized and hydrated *via* exposure to xylene and graded alcohols, followed by water. After microwave-based antigen retrieval in 10 mM citrate buffer (pH 6.0), the paraffin sections were incubated in 10% normal goat serum (Thermo Fisher Scientific) for 30 min and then incubated overnight with a primary rabbit monoclonal antibody against ROCK1 (1:50, EP786Y, Abcam, Cambridge, MA, USA) and mouse monoclonal antibody against GFAP (1:50, NCL-L-GFAP-GA5, Leica Biosystems, Wetzlar, Germany), or mouse monoclonal antibody against ROCK2 (1:100, 610623, BD, Franklin Lakes, NJ, USA) and rabbit polyclonal antibody against GFAP (1:200, Z033429, Agilent Technologies, Inc., Santa Clara, CA, USA) at 4°C, prior to exposure to Alexa Fluor 546 goat anti-rabbit IgG and Alexa Fluor 488 goat anti-mouse IgG, or Alexa Fluor 488 goat anti-rabbit IgG and Alexa Fluor 546 goat anti-mouse IgG (1:500, Thermo Fisher Scientific) for 1 h at room temperature. Serial sections were incubated with normal rabbit IgG (Abcam) and normal mouse IgG (Agilent) as negative controls.

For immunocytochemistry, TR-MUL5 cells were seeded into a 6-well plate with a cover glass and incubated for 24 h. The cells were serum-starved for 17 h and stimulated with acrolein for 23 h, followed by addition of ripasudil (2 μM) and incubation for 1 h. The cells were fixed with 4% paraformaldehyde for 15 min and permeabilized with 0.1% Triton X-100 for 10 min. Cells were incubated in 10% normal goat serum for 30 min and then incubated with a primary mouse monoclonal antibody against phosphorylated MLC2 (p-MLC2, 1:100, #3675, Cell Signaling, Danvers, MA, USA) at 4°C overnight, prior to exposure to Alexa Fluor 546 goat anti-mouse IgG (1:400) and

phalloidin (1:143, Cytoskeleton, Inc. Denver, CO, USA) for 1 h at room temperature.

Nuclei were counterstained with 4′,6-diamidino-2-phenylindole (DAPI; Roche Applied Science, Indianapolis, IN, USA), and photomicrographs were taken with a fluorescence microscope (BIOREVO BZ-9000, Keyence, Osaka, Japan).

Quantitative Real-Time PCR

The expression levels of *Rock1, Rock2*, *Mypt1*, and *Mlc2* mRNA were examined with quantitative real-time PCR. TR-MUL5 cells were seeded into a 6-well plate at a density of 4×10^5 cells per well and incubated for 24 h. The cells were serum-starved for 17 h and stimulated with acrolein for 6 h with or without N-acetylcysteine (NAC) pre-treatment for 30 min. Another set of the cells were also serum-starved for 17 h and stimulated with H_2O_2 (100 μM) for 6 h as a positive control. Total RNA was extracted from cells using TRI reagent (Molecular Research Center, Inc., Cincinnati, OH, USA) and reverse transcribed to cDNA using GoScript reverse transcriptase (Promega, Madison, WI, USA), according to the manufacturer's protocol. Analysis of mRNA levels was performed on a StepOnePlus Real-Time PCR system (Thermo Fisher Scientific) using GoTaq qPCR Master Mix (Promega). The primer sequences used for real-time PCR and the expected size of the amplified products were as follows: 5′-ATGAACTTCAAATGCAGTTGGCT-3′ (forward) and 5′-AATAAGGAATGCAGGCAGAACCA-3′ (reverse) for

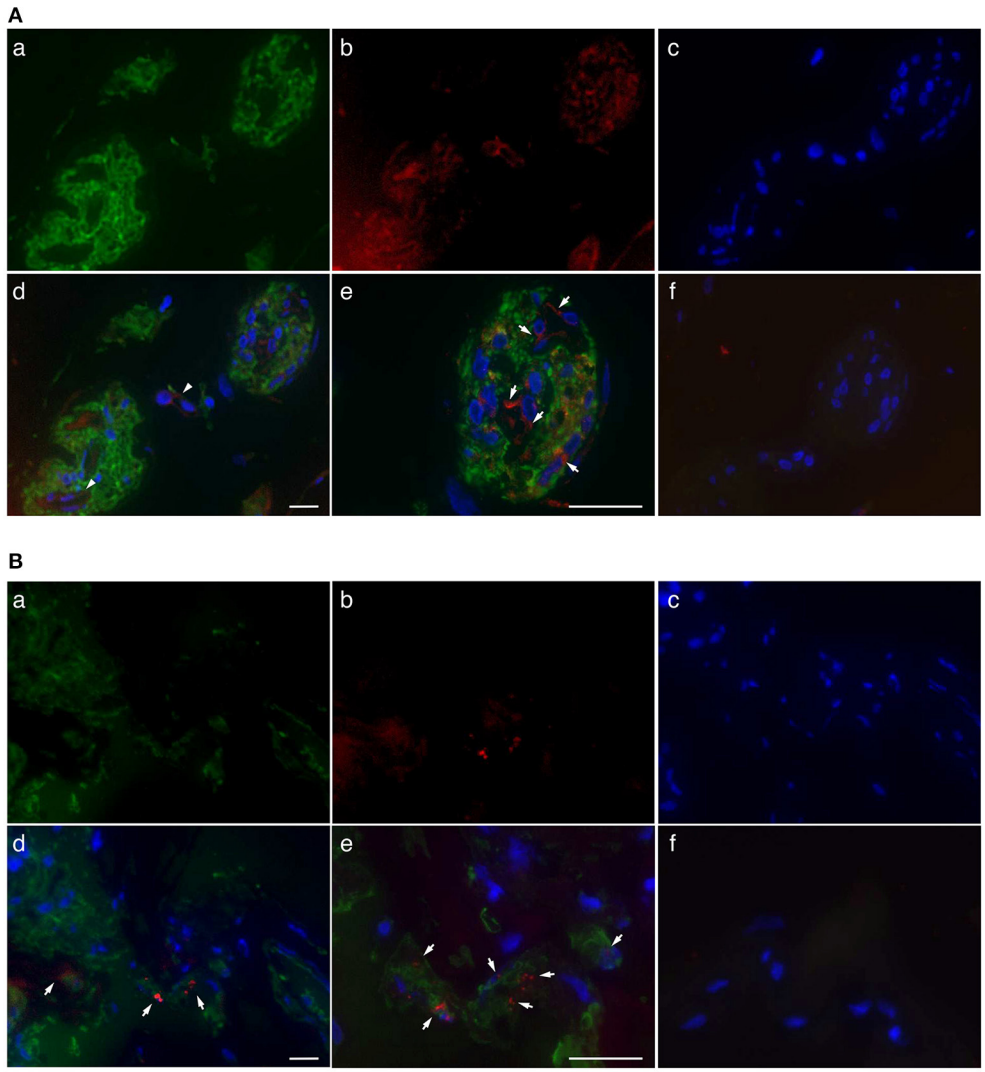

FIGURE 1 | Localization of ROCKs in GFAP-positive cells in fibrovascular tissues of patients with PDR. **(A)** Representative fluorescent micrographs of ROCK1 immunofluorescence in fibrovascular tissues. (a) Green, GFAP (Alexa Fluor® 488). (b) Red, ROCK1 (Alexa Fluor® 546). (c) Blue, nuclei counterstained with DAPI. (d) Merged image. Arrows indicate the co-localization of ROCK1 with GFAP in the fibrovascular tissue. (e) High-magnification image. (f) Negative control (mouse and rabbit IgG) in sequential sections. **(B)** Representative fluorescence micrographs of ROCK2 immunofluorescence in fibrovascular tissues. (a) Green, GFAP (Alexa Fluor® 488). (b) Red, ROCK2 (Alexa Fluor® 546). (c) Blue, nuclei counterstained with DAPI. (d) Merged image. Arrows indicate co-localization of ROCK-2 with GFAP in fibrovascular tissue. (e) High-magnification image. (f) Negative control (mouse and rabbit IgG) in sequential sections. Scale bars, 25 μm.

rat *Rock1* (NM_001389239.1), 156 bp; 5′-CTGCTGACTGAGCGAACACT-3′ (forward) and 5′- ACCACGCTTGACAGGTTCTT-3′ (reverse) for rat *Rock2* (NM_013022.2), 84 bp; 5′-GCCTTGCCCTCAGAGGATCTA-3′ (forward) and 5′-CATTGGAGCTCCCTTCTGCTG-3′ (reverse) for rat *Mlc2* (*Myl2,* NM_001035252.2), 77 bp; 5′-GTCAGCTCAACAGGCCAAAC-3′ (forward) and 5′-TCGCCGTCGTTCTCTGATTG-3′ (reverse) for rat *Mypt1* (*Ppp1r12a,* NM_053890.2), 152 bp; 5′-GGGAAATCGTGCGTGACATT-3′ (forward) and 5′-GCGGCAGTGGCCATCTC-3′ (reverse) for rat *Actb* (NM_031144), 76 bp. The PCR conditions used were 95°C for 2 min, followed by 95°C for 15 s and 40 cycles of 60°C for 1 min. All data were calculated using the ΔΔCt method, with the level of *Actb* mRNA as a normalization control.

Western Blotting

TR-MUL5 cells were seeded into a 6-cm dish at a density of 8×10^5 cells per dish and incubated for 24 h. The cells were serum-starved for 17 h and stimulated with acrolein for 24 h. For MYPT1 and MLC2 western blotting, ripasudil (0.08, 0.4, or 2 μM) was added 1 h before cell collection. TR-MUL5 cells were lysed in 1x SDS sample buffer [62.5 mM Tris-HCl (pH 6.8), 2%SDS, 10% glycerol, phosphatase inhibitor cocktail (PhosSTOP, Merck, Burlington, MA, USA) and protease inhibitor cocktail (Complete mini, Merck)]. The cell lysates were sonicated thrice for 5 s each on ice and centrifuged at 15,000 × *g* at 4°C for 10 min. Protein concentration was measured using a BCA protein assay kit (Thermo Fisher Scientific) and adjusted to 2 mg/mL with 0.01% bromophenol blue and 5% 2-mercaptoethanol. The samples were boiled at 95°C for 3 min, separated using SDS-PAGE, and electroblotted onto polyvinylidene fluoride membranes (Merck). Membranes were incubated with 5% skim milk for 1 h and then incubated with primary antibodies against ROCK1 (1:5000, EP786Y, Abcam), MLC2 (1:1000, #8505, Cell Signaling), p-MLC2 (1:1000, #3675, Cell Signaling), MYPT1 (1:1000, #2634, Cell Signaling), pMYPT1 (1:1000, #5163, Cell Signaling), and cleaved ROCK1 (1:1000, 154C1465, Novus biologicals, Centennial, CO, USA) at 4°C overnight, followed by incubation with goat anti-mouse IgG (H+L) horseradish peroxidase conjugate (1:4000, Jackson ImmunoResearch Laboratories, Inc., West Grove, PA, USA) or goat anti-rabbit IgG (H+L) horseradish peroxidase conjugate

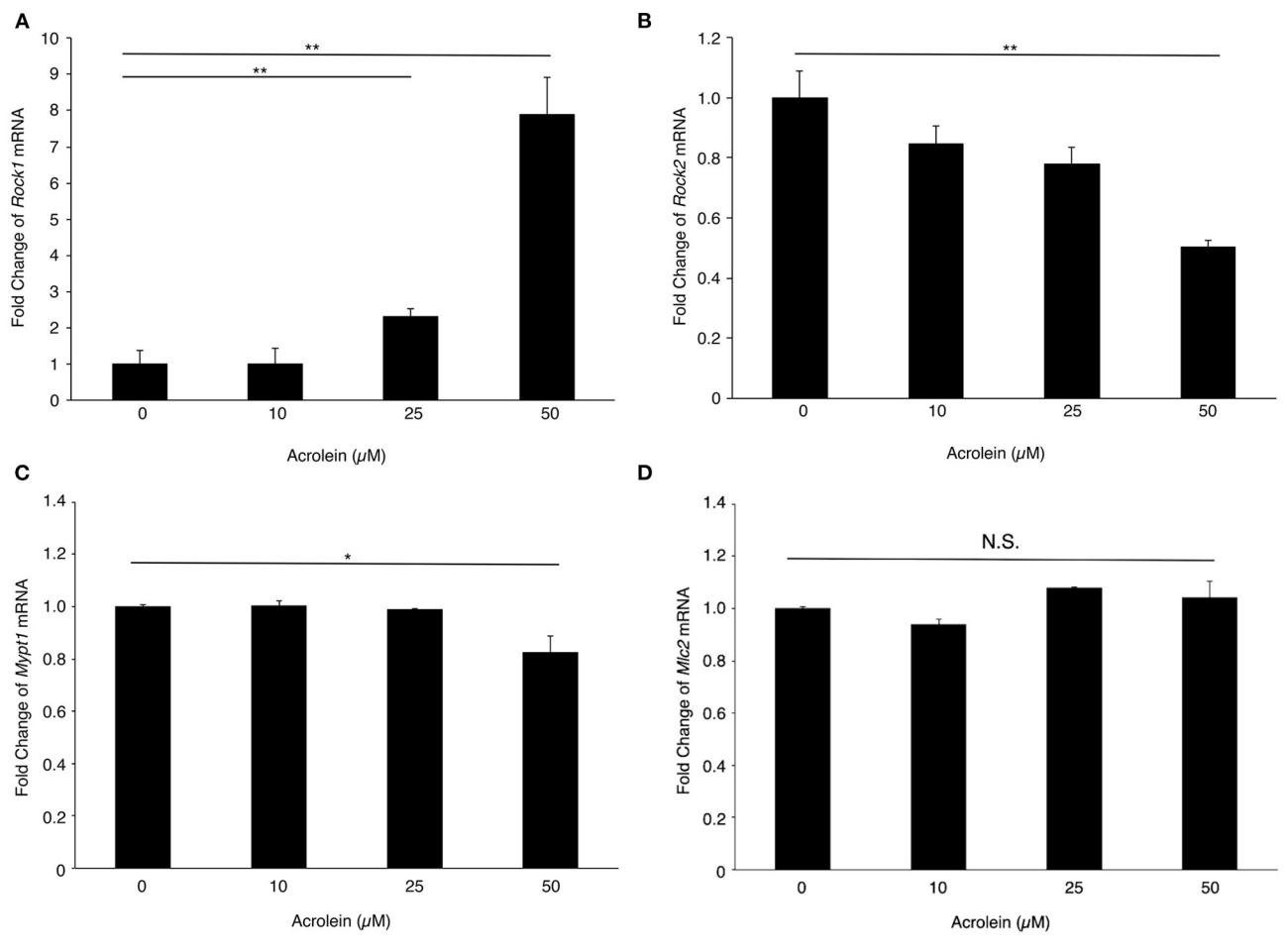

FIGURE 2 | Effect of acrolein on transcriptional levels of *Rocks*, *Mypt1*, and *Mlc2* in TR-MUL5 cells. The mRNA expression levels of **(A)** *Rock1*, **(B)** *Rock2*, **(C)** *Mypt1*, and **(D)** *Mlc2* when TR-MUL5 cells were incubated with acrolein (0–50 μM, $n = 6$ each). Values represent mean ± SEM; $^*P < 0.05$; $^{**}P < 0.01$; N.S., not significant.

(1:4000, Jackson Immunoresearch) at room temperature for 1 h. Signals were visualized using a SuperSignal West Pico Chemiluminescent Substrate (Thermo Fisher Scientific).

GSH Assay

TR-MUL5 cells were seeded into a 24-well plate at a density of 1×10^5 cells per well and incubated for 24 h. The cells were serum-starved for 17 h and stimulated with 10–50 μM acrolein for 3 h. Total GSH levels were measured using a total GSH assay kit (Nikken Seil Co., Ltd., Shizuoka, Japan), according to the manufacturer's protocol.

Migration Assay

Migration capacity was assessed using the Oris™ Cell Migration Assay kit (Platypus Technologies, Madison, WI, USA) according to the manufacturer's protocol. Briefly, TR-MUL5 cells were seeded into a collagen I-coated 96-well Oris™ plate at a density of 1×10^5 cells per well and incubated for 24 h at 33°C in an atmosphere of 95% air and 5% CO_2. The cells were starved for 17 h and stimulated with 25 μM acrolein for 24 h. Ripasudil (0.08, 0.4, or 2 μM) and the DNA synthesis inhibitor aphidicolin (10 μg/mL) were added to the cells 1 h prior to the start of migration. Silicone stoppers were then removed to allow cell migration to the central detection zone for 24 h at 33°C in an atmosphere of 95% air and 5% CO_2. The cell migration area was evaluated using BIOREVO BZ-9000 (Keyence) and analyzed with a BZ-II analyzer (Keyence).

Statistical Analysis

All results are presented as the mean ± SEM. Student's *t*-test was used for pairwise statistical comparisons between groups, and one-way ANOVA, followed by the *post-hoc* Tukey-Kramer test, if appropriate, was used for multiple comparisons. Differences in the means were considered statistically significant at $P < 0.05$.

RESULTS

Tissue Localization of ROCKs in Fibrovascular Tissues of PDR

Immunofluorescence staining was performed to determine the localization of ROCKs in fibrovascular tissues obtained from patients with PDR. ROCK1 staining was observed in clusters of GFAP-positive cells and vascular structures in fibrovascular tissues (**Figure 1A**). Similarly, ROCK2 signals

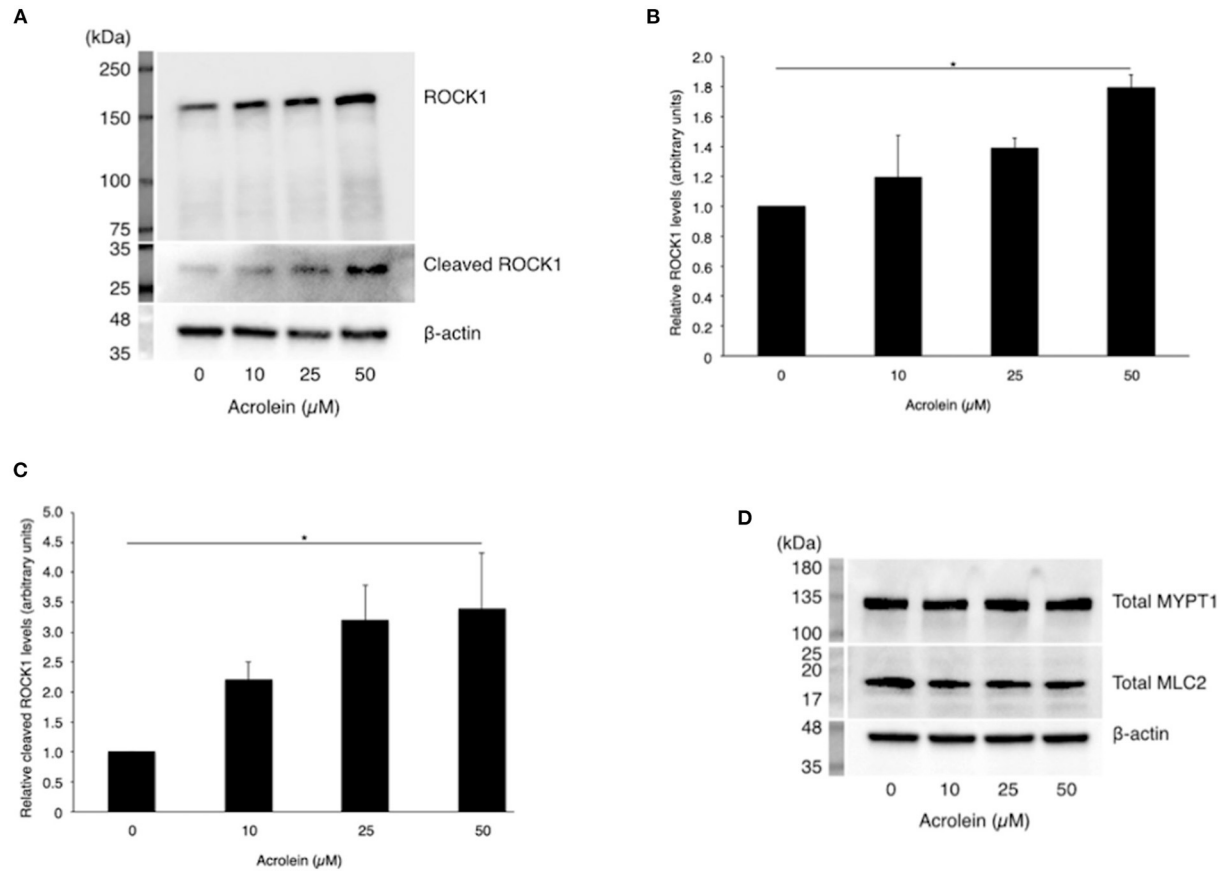

FIGURE 3 | Effect of acrolein on protein levels of ROCK1, MYPT1, and MLC2 in TR-MUL5 cells. **(A)** Western blotting of total and cleaved forms of ROCK1 protein when TR-MUL5 cells were incubated with acrolein (0–50 μM). **(B,C)** Densitometric analysis of the bands. **(B)** Total forms of ROCK1 protein (0–50 μM, $n = 3$ each). **(C)** Relative cleaved forms of ROCK1 protein (0–50 μM, $n = 4$ each). **(D)** Total protein of MYPT1 and MLC2 in TR-MUL5 cells exposed to acrolein (0–50 μM). Values represent mean ± SEM; $^*P < 0.05$.

were found in clusters of GFAP-positive cells; however, its fluorescence staining intensity was relatively faint (**Figure 1B**). High-magnification images revealed that immunoreactivity of ROCK1 and ROCK2 was the most abundant in the areas surrounding the nuclei (**Figures 1A,B**). These data indicate that ROCKs are predominantly localized in the cytoplasm of glial cells in fibrovascular tissues.

Acrolein Induces ROCK1 Production in Retinal Glial Cells

To evaluate the changes in expression of ROCKs and its associated molecules in Müller glial cells stimulated with acrolein, the mRNA levels of *Rock1*, *Rock2, Mypt1*, and *Mlc2* mRNA were assessed. *Rock1* mRNA expression was significantly increased by acrolein stimulation in a dose-dependent manner ($n = 3$ each, $P < 0.01$, **Figure 2A**), whereas *Rock2* mRNA expression decreased in response to acrolein exposure (**Figure 2B**). In addition, the mRNA levels of *Mypt1* and *Mlc2* were not changed after acrolein stimulation (**Figures 2C,D**).

In accordance with real-time PCR data, western blotting (**Figure 3A**) revealed an increase in ROCK1 production in TR-MUL5 cells stimulated with acrolein ($n = 3$ each, $P < 0.05$, **Figure 3B**). Furthermore, acrolein increased cleaved form of ROCK1 in a dose-dependent manner ($n = 4$ each, $P < 0.05$, **Figures 3A,C**). The protein levels of MYPT1 and MLC2 showed no increase with acrolein stimulation (**Figure 3D**).

Oxidative Stress Mediates ROCK1 Production in Retinal Müller Glial Cells Under Acrolein Stimulation

Based on the real-time PCR results, we focused on ROCK1 and examined whether oxidative stress is involved in acrolein-induced ROCK1 production in Müller glial cells. Total GSH levels were reduced from 4.19 nmol/mg to 1.56 nmol/mg in

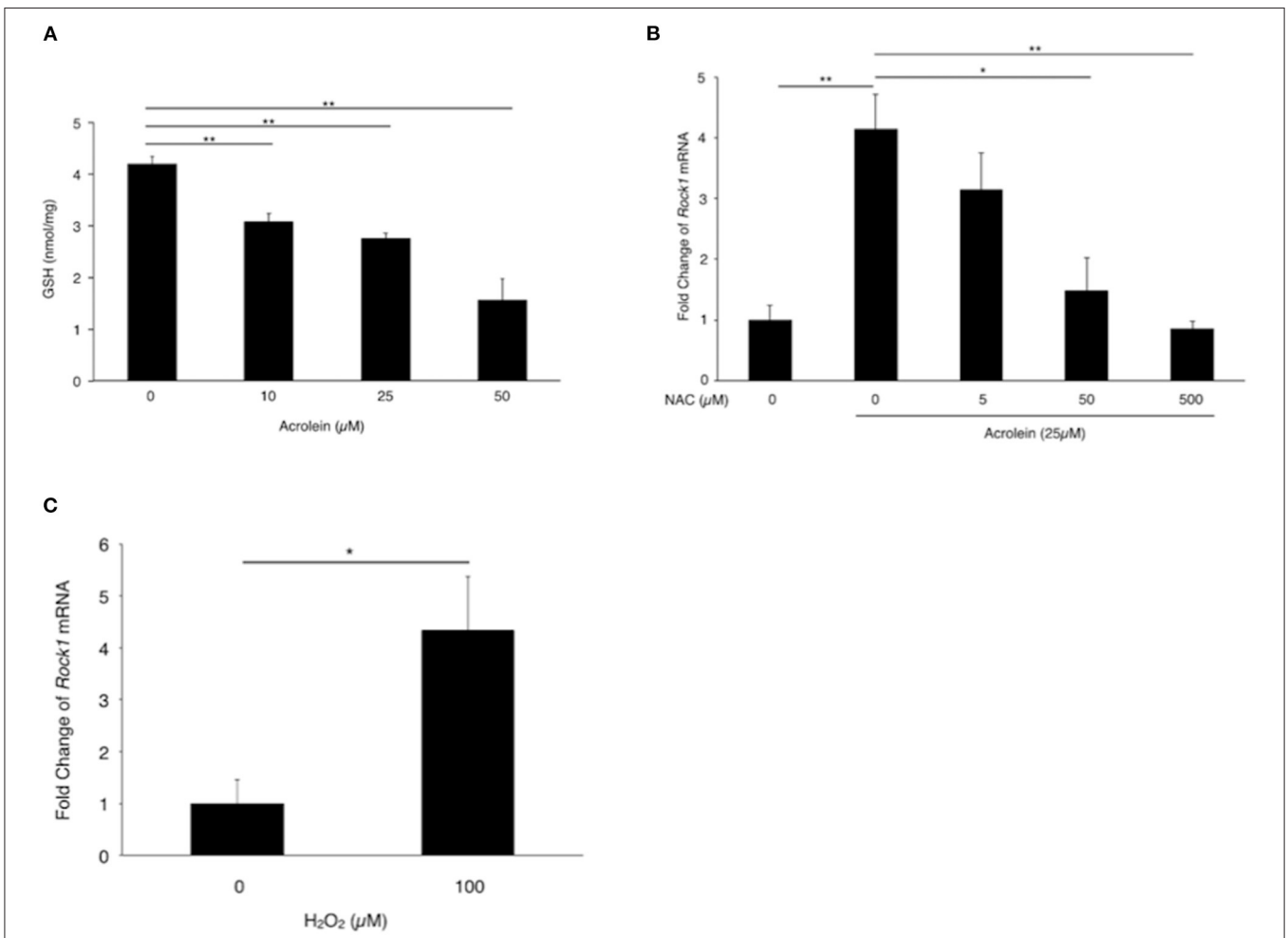

FIGURE 4 | Impact of acrolein stimulation on antioxidant defense systems in TR-MUL5 cells. **(A)** Total GSH levels when TR-MUL5 cells were exposed to acrolein for 3 h. **(B)** *Rock1* mRNA levels in acrolein-stimulated TR-MUL5 cells with or without treatment of N-acetylcysteine (NAC) ($n = 3$ each). **(C)** *Rock1* mRNA levels in TR-MUL5 cells treated with or without hydrogen peroxide ($n = 3$ each). Values represent mean ± SEM; $^{*}P < 0.05$; $^{**}P < 0.01$.

TR-MUL5 cells after acrolein stimulation ($n = 4$, $P < 0.05$, **Figure 4A**). Furthermore, ROCK1 expression showed an ∼4-fold increase in TR-MUL5 cells stimulated with acrolein compared to the control cells, while the increase was abolished by NAC in a dose-dependent manner ($n = 3$, $P < 0.01$, **Figure 4B**). In response to hydrogen peroxide, ROCK1 expression showed an ∼4-fold increase in TR-MUL5 cells compared with the control ($n = 3$, $P < 0.05$, **Figure 4C**).

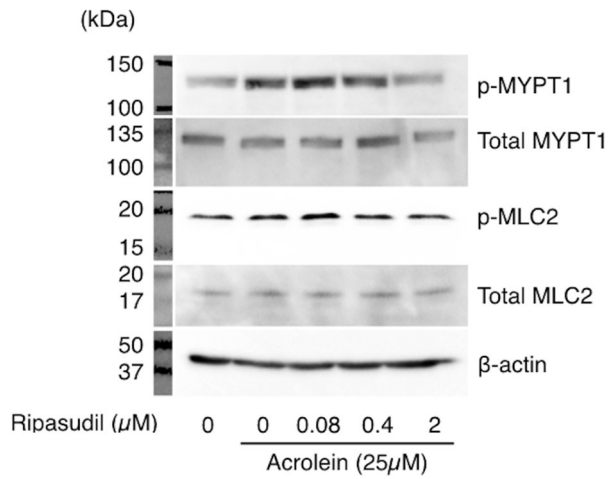

FIGURE 5 | Changes in phosphorylation of MYPT1 and MLC2 in TR-MUL5 cells treated with acrolein and ripasudil. Phosphorylation levels of MYPT1 and MLC2 in TR-MUL5 cells after acrolein stimulation. Ripasudil suppressed the increase of phosphorylated forms of MYPT1 and MLC2 induced by acrolein stimulation in TR-MUL5 cells.

ROCK1-pMYPT1-pMLC Pathway Is Activated by Acrolein

To examine the impact of acrolein and ripasudil on ROCK activity, phosphorylation of MYPT1 and MLC2 was assessed in TR-MUL5 cells. As shown in **Figure 5**, phosphorylation of both MYPT1 and MLC2 showed increase in TR-MUL5 cells when stimulated with acrolein, while the total protein levels of MYPT1 and MLC2 were unchanged (**Figure 3D**). In addition, ripasudil reduced the acrolein-induced phosphorylation of MYPT1 and MLC2 (**Figure 5**).

As shown in **Figure 6**, immunofluorescence microscopy revealed that acrolein stimulation increased organization of actin stress fibers in TR-MUL5 cells, whereas actin depolymerization was observed in the cells treated with ripasudil. The staining signal of p-MLC2 increased with acrolein stimulation along with actin fibers, and it was attenuated in the presence of ripasudil. Additionally, ripasudil administration caused cell body shrinkage in TR-MUL5 cells.

Ripasudil Attenuates Glial Cell Migration Induced by Acrolein

To evaluate the association between ROCK1 and the migration of Müller glial cells, we performed a migration assay of TR-MUL5 cells after acrolein stimulation with or without ripasudil. Acrolein accelerated the migration of TR-MUL5 cells compared to the control ($n = 4$, $P < 0.01$), and ripasudil (0.4 μM, 2 μM) attenuated this increase in migration ($n = 4$, $P < 0.05$, **Figure 7**).

DISCUSSION

In the present study, we demonstrated that: (1) ROCK proteins are present in the cytosol of glial cells in the

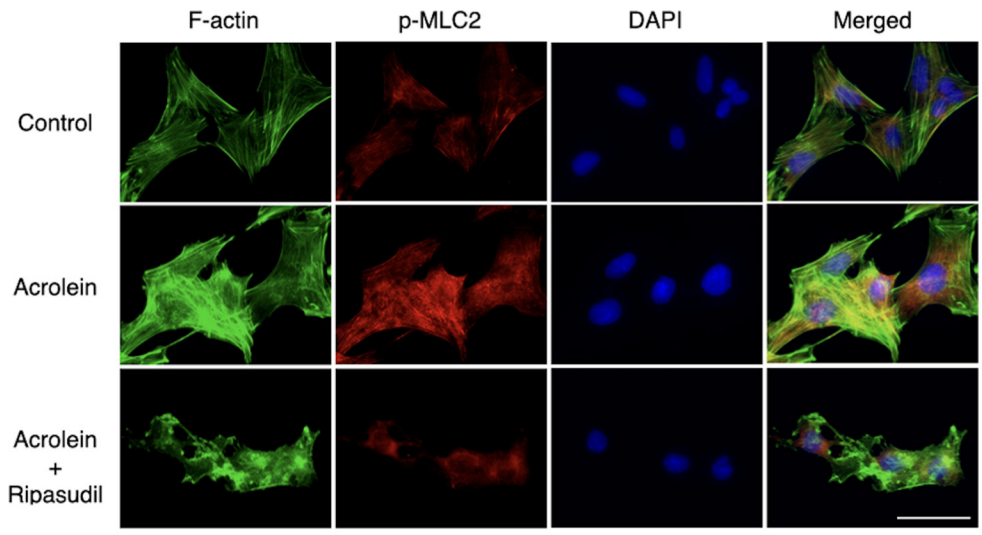

FIGURE 6 | Changes in cellular morphology and stress fiber formation in TR-MUL5 cells treated with acrolein and ripasudil. Representative fluorescent staining patterns of F-actin (green, Acti-stain™ 488) and p-MLC2 (red, Alexa Fluor® 546) in TR-MUL5 cells treated with acrolein (25 μM) and/or ripasudil (2 μM). Blue, nuclei counterstained with DAPI. Scale bar, 50 μm.

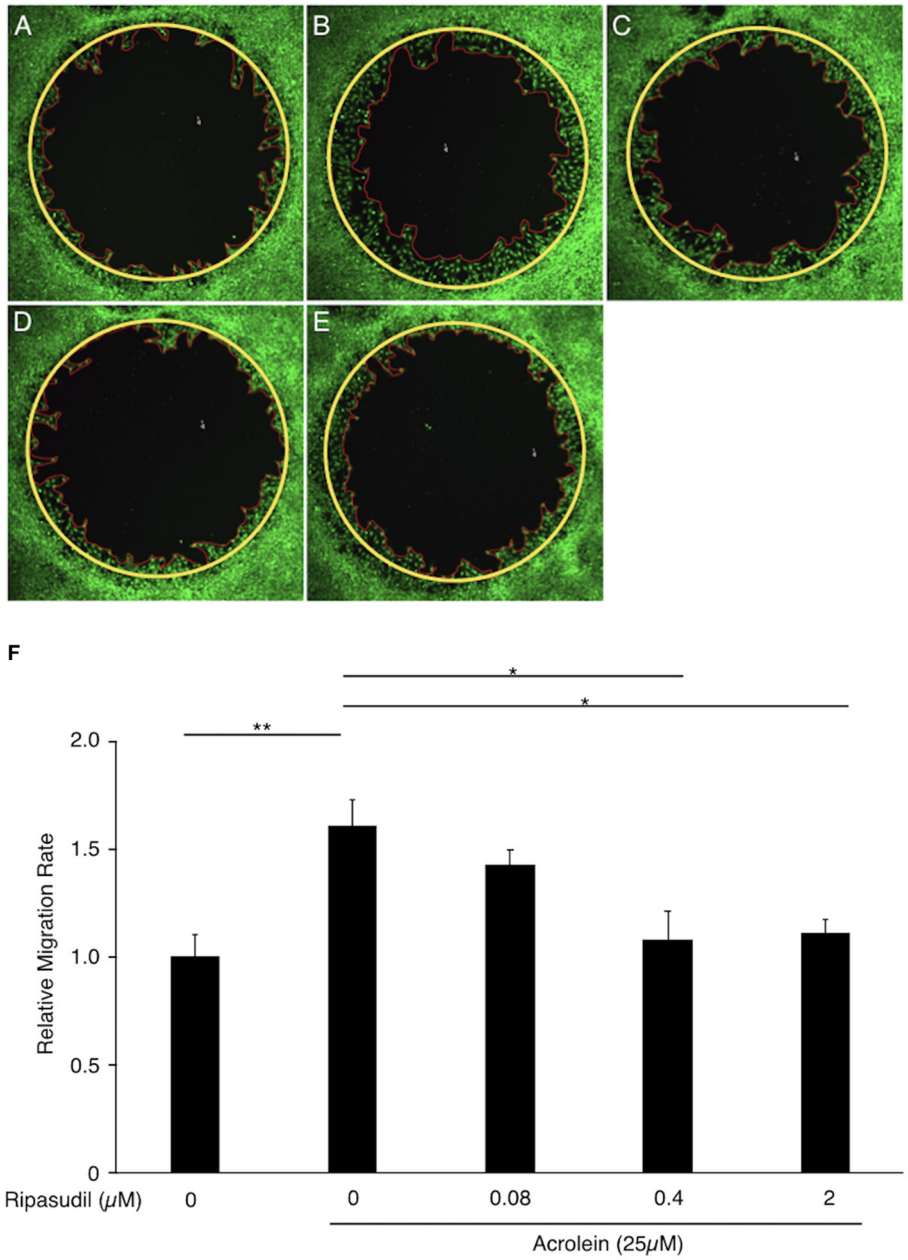

FIGURE 7 | Impact of ripasudil administration on acrolein-induced migration of TR-MUL5 cells. Representative micrographs of TR-MUL5 cell migration after acrolein stimulation with or without ripasudil treatment. **(A)** Control. **(B)** Acrolein stimulation (25 μM). **(C)** Acrolein stimulation (25 μM) with ripasudil (0.08 μM). **(D)** Acrolein stimulation (25 μM) with ripasudil (0.4 μM). **(E)** Acrolein stimulation (25 μM) with ripasudil (2 μM). **(F)** Cell migration analysis in TR-MUL5 cells after acrolein stimulation with or without ripasudil ($n = 4$ each). Values represent the mean ± SEM; $^{*}P < 0.05$, $^{**}P < 0.01$.

fibrovascular tissues of patients with PDR; (2) the unsaturated aldehyde acrolein increases the production of ROCK1, but not ROCK2, in cultured Müller glial cells; (3) acrolein enhances phosphorylation of MYPT1 and MLC2 through the ROCK1 cascade induced by oxidative stress; and (4) ripasudil, a specific inhibitor of ROCKs, hampers formation and migration of stress fibers in Müller glial cells. The current data provide new insights into the mechanisms of glial cell migration, a significant process in fibrovascular formation in eyes afflicted with PDR.

Glial cells have increasingly gained attention as one of the major participants in the progression of DR. While the activation of glial cells represents some of the earliest events in the pathogenesis of DR (16), macroglial cells are also implicated in promoting proliferative changes through VEGF secretion and internal limiting membrane degradation during the late stage of

DR (17–19). Hence, elucidating the cellular behaviors of glial cells in advanced stages of DR contributes to further understanding of the pathological mechanisms underlying vision-threatening disease. We previously demonstrated that acrolein-conjugated proteins are localized in glial cells in the fibrovascular tissues of PDR patients (20). The current data further demonstrated that ROCK proteins are ubiquitously present in glial cells in fibrovascular tissues and that acrolein stimulation increased the production of ROCK1 in cultured Müller glial cells. Intriguingly, acrolein stimulation decreased the expression levels of ROCK2. In addition, the expression levels of ROCK-associated molecules including MYPT1 and MLC2 were not changed by acrolein stimulation. Whereas, our group previously showed that acrolein stimulation increases cell viability in cultured retinal glial cells (7), the current data clearly demonstrated that increase of ROCK1 protein is not simply attributed to the effect of acrolein to the cell viability in cultured retinal glial cells.

In ROCK proteins, ROCK2 is known as the predominant form of in ocular tissues (11). Since ROCK1 and ROCK2 exhibit a high degree of sequence homology, both kinases essentially share not only a wide variety of downstream substrates but also consequent cellular functions. In fact, the ROCK isoforms promote the rearrangement of actin-myosin cytoskeleton organization mediated by phosphorylation of downstream target proteins, including MYPT1 and MLC2 (21). However, using mouse embryonic fibroblast cells derived from ROCK1$^{-/-}$ and ROCK2$^{-/-}$ mice, it was elucidated that the roles of ROCK1 and ROCK2 are not strictly equal; i.e., ROCK1 is involved in destabilizing the actin cytoskeleton by regulating MLC2 phosphorylation and peripheral actomyosin contraction, whereas ROCK2 is required for stabilizing the actin cytoskeleton by regulating cofilin phosphorylation (21). Therefore, selective upregulation of ROCK1 by acrolein, which was demonstrated in the present study, indicates that acrolein facilitates a transition in the ROCK system to rearrange actin cytoskeleton and generate contractile force in Müller glial cells, eventually leading to glial cell migration.

Cigarette smoking is known to produce an estimated 10^{17} oxidant molecules per puff (22). Previous studies revealed that acrolein, a major cytotoxic factor in cigarette smoke extract, rapidly binds to GSH (23) and induces oxidative stress in the body (24–26). In line with these findings and our previous data (7), the current data also showed that acrolein reduces intracellular GSH levels in cultured Müller glial cells. In addition, acrolein-induced *Rock1* mRNA synthesis was remarkably suppressed by NAC, a thiol-containing antioxidant and precursor of GSH, in a dose-dependent manner. Furthermore, hydrogen peroxide, one of the representative reactive oxygen species, increased *de novo* synthesis of *Rock1*. The present data convincingly demonstrates that depletion of GSH by acrolein increases intracellular oxidative stress, thereby enhancing ROCK1 production in retinal glial cells.

Furthermore, although not quantified, acrolein appears to augment phosphorylation of MYPT1 and MLC2, both of which appears to be suppressed by ripasudil in cultured Müller glial cells. In line with the western blotting data, immunofluorescence microscopy also suggested that acrolein increased MLC2 phosphorylation and F-actin bundling, which are characteristics of stress fiber formation, in cultured Müller glial cells. Whereas, immunofluorescent staining of total MLC2 protein was not conducted in the present study, western blotting showed no significant change in the expression of total MLC2, indicating that the increased signal of p-MLC2 along with actin fibers in the TR-MUL5 cells exposed to acrolein, at least in part, due to the increase of MLC2 phosphorylation. In addition, since the possible increase in MLC2 phosphorylation and F-actin bundling was diminished by ripasudil, the present study demonstrated that ROCKs are the downstream effectors of acrolein.

Notably, the current study exhibited that glial cell migration induced by acrolein was suppressed by the non-selective ROCK inhibitor ripasudil. We previously reported that acrolein induces the production of the pro-inflammatory chemokine CXCL1 and promotes glial cell migration in an autocrine fashion (7). Enriching the previous findings, the present study revealed that ROCKs are involved in acrolein-induced glial cell migration. Furthermore, given the selective upregulation of ROCK1 by acrolein, ROCK1 might be the focus of future studies investigating the mechanism of glial cell migration regulated by acrolein.

There are several limitations to this study. First, there was a tendency toward decreasing migration rate in the acrolein-stimulated glial cells treated with 0.08 μM ripasudil administration, while identical concentration of ripasudil showed no inhibitory effect to the phosphorylation of MYPT1 and MLC2. Second, the decrease of *Rock2* in retinal glial cells stimulated with acrolein was intriguing; however, the physiological and/or pathological significance was not studied in the current study. Further investigation is warranted to obtain further mechanistic insights into non-muscle myosin phosphorylation regulation through ROCK1 signaling in glial cells.

In summary, our data shed light on the regulatory mechanism of Müller glial cell migration. The current results suggest that acrolein and its downstream molecule ROCK1 are attractive molecular targets for the prevention of fibrovascular tissue formation in PDR.

DATA AVAILABILITY STATEMENT

The raw data supporting the conclusions of this article will be made available by the authors, without undue reservation.

ETHICS STATEMENT

The studies involving human participants were reviewed and approved by Institutional Review Committee of Hokkaido University Hospital. The patients/participants provided their written informed consent to participate in this study.

AUTHOR CONTRIBUTIONS

KN contributed to conception and design of the study. KF, MM, KK, and SY conducted the experiments. KF, MM, and KN wrote sections of the manuscript. SI revised the first draft of the

manuscript. All authors contributed to manuscript revision, read, and approved the submitted version.

FUNDING

This work was supported by Kowa Company, Ltd (Tokyo, Japan), Grant-in-Aid for Scientific Research (C) (21K09667), and Grant-in-Aid for Scientific Research (B) (20H03837, 21H03091) from the Japan Society for the Promotion of Science.

ACKNOWLEDGMENTS

The authors thank Ikuyo Hirose (Hokkaido University) for her skillful technical assistance.

REFERENCES

1. Lee R, Wong TY, Sabanayagam C. Epidemiology of diabetic retinopathy, diabetic macular edema and related vision loss. *Eye Vis.* (2015) 2:17. doi: 10.1186/s40662-015-0026-2
2. Yanoff M, Sassani JW. *Ocular Pathology*. 7th ed. London: Elsevier Health Sciences (2015).
3. Reichenbach A, Bringmann A. Glia of the human retina. *Glia.* (2020) 68:768–96. doi: 10.1002/glia.23727
4. Nork TM, Wallow IH, Sramek SJ, Anderson G. Muller's cell involvement in proliferative diabetic retinopathy. *Arch Ophthalmol.* (1987) 105:1424–9. doi: 10.1001/archopht.1987.01060100126042
5. Amin RH, Frank RN, Kennedy A, Eliott D, Puklin JE, Abrams GW. Vascular endothelial growth factor is present in glial cells of the retina and optic nerve of human subjects with nonproliferative diabetic retinopathy. *Invest Ophthalmol Vis Sci.* (1997) 38:36–47.
6. Coughlin BA, Feenstra DJ, Mohr S. Muller cells and diabetic retinopathy. *Vision Res.* (2017) 139:93–100. doi: 10.1016/j.visres.2017.03.013
7. Murata M, Noda K, Yoshida S, Saito M, Fujiya A, Kanda A, et al. Unsaturated aldehyde acrolein promotes retinal glial cell migration. *Invest Ophthalmol Vis Sci.* (2019) 60:4425–35. doi: 10.1167/iovs.19-27346
8. Feng Z, Hu W, Hu Y, Tang MS. Acrolein is a major cigarette-related lung cancer agent: preferential binding at p53 mutational hotspots and inhibition of DNA repair. *Proc Natl Acad Sci USA.* (2006) 103:15404–9. doi: 10.1073/pnas.0607031103
9. Murata M, Noda K, Kawasaki A, Yoshida S, Dong Y, Saito M, et al. Soluble vascular adhesion protein-1 mediates spermine oxidation as semicarbazide-sensitive amine oxidase: possible role in proliferative diabetic retinopathy. *Curr Eye Res.* (2017) 42:1674–83. doi: 10.1080/02713683.2017.1359847
10. Wu D, Noda K, Murata M, Liu Y, Kanda A, Ishida S. Regulation of spermine oxidase through hypoxia-inducible factor-1alpha signaling in retinal glial cells under hypoxic conditions. *Invest Ophthalmol Vis Sci.* (2020) 61:52. doi: 10.1167/iovs.61.6.52
11. Julian L, Olson MF. Rho-associated coiled-coil containing kinases (ROCK): structure, regulation, and functions. *Small GTPases.* (2014) 5:e29846. doi: 10.4161/sgtp.29846
12. Loirand G. Rho kinases in health and disease: from basic science to translational research. *Pharmacol Rev.* (2015) 67:1074–95. doi: 10.1124/pr.115.010595
13. Arita R, Hata Y, Nakao S, Kita T, Miura M, Kawahara S, et al. Rho kinase inhibition by fasudil ameliorates diabetes-induced microvascular damage. *Diabetes.* (2009) 58:215–26. doi: 10.2337/db08-0762
14. Arita R, Nakao S, Kita T, Kawahara S, Asato R, Yoshida S, et al. A key role for ROCK in TNF-alpha-mediated diabetic microvascular damage. *Invest Ophthalmol Vis Sci.* (2013) 54:2373–83. doi: 10.1167/iovs.12-10757
15. Tomi M, Funaki T, Abukawa H, Katayama K, Kondo T, Ohtsuki S, et al. Expression and regulation of L-cystine transporter, system xc-, in the newly developed rat retinal Muller cell line (TR-MUL). *Glia.* (2003) 43:208–17. doi: 10.1002/glia.10253
16. Rolev KD, Shu XS, Ying Y. Targeted pharmacotherapy against neurodegeneration and neuroinflammation in early diabetic retinopathy. *Neuropharmacology.* (2021) 187:108498. doi: 10.1016/j.neuropharm.2021.108498
17. Ishida S, Shinoda K, Kawashima S, Oguchi Y, Okada Y, Ikeda E. Coexpression of VEGF receptors VEGF-R2 and neuropilin-1 in proliferative diabetic retinopathy. *Invest Ophthalmol Vis Sci.* (2000) 41:1649–56.
18. Noda K, Ishida S, Inoue M, Obata K, Oguchi Y, Okada Y, et al. Production and activation of matrix metalloproteinase-2 in proliferative diabetic retinopathy. *Invest Ophthalmol Vis Sci.* (2003) 44:2163–70. doi: 10.1167/iovs.02-0662
19. Noda K, Ishida S, Shinoda H, Koto T, Aoki T, Tsubota K, et al. Hypoxia induces the expression of membrane-type 1 matrix metalloproteinase in retinal glial cells. *Invest Ophthalmol Vis Sci.* (2005) 46:3817–24. doi: 10.1167/iovs.04-1528
20. Dong Y, Noda K, Murata M, Yoshida S, Saito W, Kanda A, et al. Localization of acrolein-lysine adduct in fibrovascular tissues of proliferative diabetic retinopathy. *Curr Eye Res.* (2017) 42:111–7. doi: 10.3109/02713683.2016.1150491
21. Shi J, Wu X, Surma M, Vemula S, Zhang L, Yang Y, et al. Distinct roles for ROCK1 and ROCK2 in the regulation of cell detachment. *Cell Death Dis.* (2013) 4:e483. doi: 10.1038/cddis.2013.10
22. Church DF, Pryor WA. Free-radical chemistry of cigarette smoke and its toxicological implications. *Environ Health Perspect.* (1985) 64:111–26. doi: 10.1289/ehp.8564111
23. Kehrer JP, Biswal SS. The molecular effects of acrolein. *Toxicol Sci.* (2000) 57:6–15. doi: 10.1093/toxsci/57.1.6
24. Luo J, Shi R. Acrolein induces oxidative stress in brain mitochondria. *Neurochem Int.* (2005) 46:243–52. doi: 10.1016/j.neuint.2004.09.001
25. Jia L, Liu Z, Sun L, Miller SS, Ames BN, Cotman CW, et al. Acrolein, a toxicant in cigarette smoke, causes oxidative damage and mitochondrial dysfunction in RPE cells: protection by (R)-alpha-lipoic acid. *Invest Ophthalmol Vis Sci.* (2007) 48:339–48. doi: 10.1167/iovs.06-0248
26. Sun Y, Ito S, Nishio N, Tanaka Y, Chen N, Liu L, et al. Enhancement of the acrolein-induced production of reactive oxygen species and lung injury by GADD34. *Oxid Med Cell Longev.* (2015) 2015:170309. doi: 10.1155/2015/170309

Conflict of Interest: The authors declare that the research was conducted in the absence of any commercial or financial relationships that could be construed as a potential conflict of interest.

Publisher's Note: All claims expressed in this article are solely those of the authors and do not necessarily represent those of their affiliated organizations, or those of the publisher, the editors and the reviewers. Any product that may be evaluated in this article, or claim that may be made by its manufacturer, is not guaranteed or endorsed by the publisher.

frontiers in Medicine

ORIGINAL RESEARCH
published: 08 September 2021
doi: 10.3389/fmed.2021.699254

Comparison of Inflammatory and Angiogenic Factors in the Aqueous Humor of Vitrectomized and Non-Vitrectomized Eyes in Diabetic Macular Edema Patients

*Youling Liang[1], Bin Yan[1], Zhishang Meng[1], Manyun Xie[1], Zhou Liang[1], Ziyi Zhu[1], Yongan Meng[1], Jiayue Ma[1], Bosheng Ma[1], Xiaoxi Yao[2] and Jing Luo[1]**

[1] Department of Ophthalmology, The Second Xiangya Hospital, Central South University, Changsha, China, [2] Shenzhen College of International Education, Shenzhen, China

OPEN ACCESS

Edited by:
Dong Ho Park,
Kyungpook National University Hospital, South Korea

Reviewed by:
Francesco Maria D'Alterio,
Imperial College Healthcare NHS Trust, United Kingdom
Yong Koo Kang,
Kyungpook National University, South Korea

***Correspondence:**
Jing Luo
luojing001@csu.edu.cn

Specialty section:
This article was submitted to Ophthalmology, a section of the journal Frontiers in Medicine

Received: 23 April 2021
Accepted: 09 August 2021
Published: 08 September 2021

Citation:
Liang Y, Yan B, Meng Z, Xie M, Liang Z, Zhu Z, Meng Y, Ma J, Ma B, Yao X and Luo J (2021) Comparison of Inflammatory and Angiogenic Factors in the Aqueous Humor of Vitrectomized and Non-Vitrectomized Eyes in Diabetic Macular Edema Patients. Front. Med. 8:699254. doi: 10.3389/fmed.2021.699254

Objectives: To compare the aqueous concentrations of inflammatory and angiogenetic factors in vitrectomized vs. non-vitrectomized eyes with diabetic macular edema (DME).

Methods: Aqueous samples were obtained from 107 eyes with DME before intravitreal injection of anti-VEGF, 36 eyes with previous pars plana vitrectomy (PPV) combined with pan-retinal endolaser photocoagulation (PRP), and 71 treatment-naïve. Interleukin (IL)-6, IL-8, interferon-induced protein (IP)-10, monocyte chemoattractant protein (MCP)-1, and vascular endothelial growth factor (VEGF) were measured by cytometric bead array (CBA). Optical coherence tomography (OCT) was used for measuring central retinal thickness (CRT).

Results: IL-6, IL-8, IP-10, and MCP-1 in aqueous humor of DME vitrectomized eyes were significantly higher than in non-vitrectomized DME eyes, while VEGF was lower than in non-vitrectomized DME eyes. VEGF in aqueous humor significantly correlated with CRT for DME in non-vitrectomized DME eyes. IL-6, IL-8, IP-10, and MCP-1 in aqueous humor were not significantly associated with VEGF for DME in vitrectomized eyes.

Conclusions: Inflammation might play an important role in the pathogenesis of DME in vitrectomized eyes. Moreover, inflammation might play a central role in the development of DME *via* the VEGF-independent pathway. Thus, anti-inflammatory therapy might be a strategy for DME in vitrectomized eyes.

Keywords: central retinal thickness, diabetic macula edema, inflammation, post-operative DME, VEGF

INTRODUCTION

Anti-VEGF intravitreous injection is emerging as first-line therapy for diabetic macular edema (DME) (1). Still, the effectiveness of anti-VEGF therapy in eyes after pars plana vitrectomy (PPV) remains uncertain. PPV is a treatment for advanced proliferative diabetic retinopathy (PDR) (2), but many patients still suffer from DME post-PPV, and no consensus has been reached regarding the optimal treatment for those patients.

The study by Yanyali et al. (3) demonstrated that anti-VEGF therapy in vitrectomized eyes with DME had no effect on visual acuity or foveal thickness, which indicated that the mechanism of DME post-PPV might be different from DME without surgery due to the changes in the microenvironment. Inflammation is also an important contributor to DME pathogenesis (4), especially when the blood–retina barrier is broken by the surgery. Thus, inflammation might be an important reason for post-operative DME. Interleukin (IL)-6 is a pro-inflammatory cytokine associated with the blood-ocular barrier; therefore, increased IL-6 might increase endothelial permeability by rearranging actin filaments and changing the shape of the endothelial cells (5), leading to the leakage of fluorescein in the macula (6). In addition, IL-6 levels are associated with the recurrence of DME after anti-VEGF treatment (7). IL-8 is believed to be involved in inflammation-mediated angiogenesis and serves as a fundamental factor in the inflammatory basis of diabetic retinopathy (DR) (8). The vitreous levels of IL-8 are elevated in DME compared with non-DME eyes (7, 9). Interferon-induced protein (IP)-10 is known to inhibit neovascularizations (10). IP-10 can prevent IL-8-mediated angiogenesis and prevent the progression of PDR (11, 12). MCP-1 is a chemotactic chemokine that induces monocyte and macrophage infiltration into tissue (13) and might have a tight relationship with the process of fibroproliferation (14). Aqueous MCP-1 levels are elevated in DME eyes (15).

In order to investigate and analyze the role of inflammatory factors in post-operative DME, we compared the levels of the inflammatory cytokines mentioned above and VEGF in the aqueous humor of vitrectomized vs. non-vitrectomized DME eyes. The purpose of this study was to determine the optimal treatment for post-operative DME patients. Steroids, including slow-release steroids, might be an option for DME in vitrectomized eyes if the inflammation factors are proven to be an important factor in DME after PPV.

METHODS

Patients

This study was approved by the Ethical Committee of The Second Xiangya Hospital (LYZ2020009), and all enrolled patients were treated in accordance with the Declaration of Helsinki. All patients provided informed consent before inclusion in the study. To reduce selection bias, all patients were recruited consecutively.

We obtained undiluted aqueous humor samples from 109 DR patients (109 eyes) prior to receiving an anti-VEGF intravitreal injection, including 38 eyes that had previously undergone PPV combined with pan-retinal endolaser photocoagulation (PRP) due to vitreous hemorrhage (referred to as the vitrectomized group), and 71 treatment-naïve eyes (referred to as the non-vitrectomized group). The PPV-combined PRP in the vitrectomized group was performed at The Second Xiangya Hospital of Central South University (Hunan province, China) by the same surgeon.

The inclusion criteria were:

- patients aged 18–80 years with type 2 DM
- diagnosed with PDR
- best correct visual acuity <20/40
- DME involving macular
- vitrectomized group: PPV was performed at least 4 weeks before enrollment
- non-vitrectomized group: all patients were treatment-naïve

The exclusion criteria were:

- vitrectomized group: intravitreous injection after PPV
- non-vitrectomized group: prior ocular surgery, including intravitreous injection
- any history of ocular inflammation
- an abnormal vitreoretinal interface
- history of renal and hematologic diseases, uremia, prior chemotherapy, and chronic diseases other than diabetes (renal disease and hematological disease).

Sampling Procedure

Aqueous humor samples (50–100 μl) from patients with DME were obtained by anterior chamber paracentesis at the beginning of the vitreous injection. The specimens were manually aspirated using a 30-gauge needle and then transferred immediately into sterile tubes. The scheduled vitreous injections were subsequently performed. All samples were stored at −80°C until assayed.

Testing of Macular Edema

Central retinal thickness (CRT) was measured using spectral-domain optical coherence tomography (OCT; RTVue XR Avanti, Optovue, Inc., Fremont, CA, USA) in all included eyes before the collection of aqueous humor samples. A macular profile of the central 6-mm zone was obtained using the fast macular scan protocol. CRT was calculated by extrapolating radial measurements as an average value within a circle with a 500-μm radius centered on the fovea. In the presence of vitreoretinal traction or epiretinal membrane, an OCT signal strength <4, or the OCT featured retinal border detection algorithm artifacts, the OCT result was excluded from the analysis.

Cytokine Detection

The quantitative determination of IL-6, IL-8, IP-10, MCP-1, and VEGF levels in the aqueous humor samples was performed using the CBA Human Cytokine kit (BD Biosciences; San Diego, CA, USA), according to the manufacturer's protocol. A sample volume of 10 μl (either the standards or the patient samples) was added to 50 μl of a cocktail consisting of capture beads and detector antibodies, and the mixture was incubated for 18 h at room temperature in the dark. Before data acquisition, the excess unbound detector antibody was washed off. For statistical analyses, a measured value below the threshold of detection was conservatively omitted from the analysis.

Statistical Analysis

Statistical analysis was performed using SPSS 24.0 (IBM, Armonk, NY, USA). The results are presented as the mean ± SD. The mean cytokine levels, as detected by CBA, were compared between groups using the Mann–Whitney *U*-test. Spearman's correlation analysis was used to examine the correlations between

TABLE 1 | Clinical and laboratory characteristics of the patients.

	Vitrectomized group	Non-vitrectomized group	*p*-value
Age (years)	53.6 ± 6.4	56.7 ± 8.2	0.051
Sex (*n*)			0.740
Male	15	32	
Female	21	39	
Duration of diabetes (years)	11.7 ± 6.6	9.1 ± 6.9	0.059
Glycosylated hemoglobin (%)	7.26 ± 0.89	7.78 ± 1.49	0.056

TABLE 2 | Levels of inflammatory cytokines and VEGF in the aqueous humor of vitrectomized and non-vitrectomized groups.

	Vitrectomized group	Non-vitrectomized group	*p*-value
IL-6	288.60 ± 392.28	44.43 ± 83.88	<0.001*
IL-8	50.08 ± 34.30	18.27 ± 17.37	<0.001*
IP-10	154.99 ± 162.15	50.59 ± 69.17	<0.001*
MCP-1	1650.45 ± 911.02	712.07 ± 429.57	<0.001*
VEGF	36.18 ± 28.95	72.44 ± 62.67	0.001*

**Statistical significance: p < 0.01 determined by Mann–Whitney U test.*
IL-6, interleukin-6; IL-8, interleukin-8; IP-10, interferon-induced protein-10; MCP-1, monocyte chemotactic protein-1; VEGF, vascular endothelial growth factor.

TABLE 3 | Correlations between factor levels in the aqueous humor and CRT in vitrectomized group.

	ρ	*p*
IL-6	0.352	0.035
IL-8	0.068	0.695
IP-10	0.248	0.145
MCP-1	0.171	0.319
VEGF	−0.004	0.983

ρ = correlation coefficient.
P = probability value.
CRT, central retinal thickness; IL-6, interleukin-6; IL-8, interleukin-8; IP-10, interferon-induced protein-10; MCP-1, monocyte chemotactic protein-1; VEGF, vascular endothelial growth factor.

TABLE 4 | Correlations between factor levels in the aqueous humor and CRT in the non-vitrectomized group.

	ρ	*p*
IL-6	0.231	0.053
IL-8	0.216	0.070
IP-10	0.194	0.105
MCP-1	0.147	0.222
VEGF	0.333	0.005*

ρ = correlation coefficient.
p = probability value.
**Statistical significance: p < 0.007 after Ryan–Holm step-down Bonferroni correction.*
CRT, central retinal thickness; IL-6, interleukin-6; IL-8, interleukin-8; IP-10, interferon-induced protein-10; MCP-1, monocyte chemotactic protein-1; VEGF, vascular endothelial growth factor.

cytokine concentrations and CRT values. *p*-values <0.01 were considered significant when comparing data between two groups, and Bonferroni-corrected alphas were used for the evaluation of the results. There were two groups, and five pairwise tests were performed. The resulting *p*-values were evaluated at an alpha = 0.01 and with a *p*-value < 0.01 which was judged significant. When doing correlation analysis, we will find a significant *p*-value after Ryan–Holm step-down Bonferroni correction.

RESULTS

The clinical characteristics of all patients are shown in **Table 1**. Two samples fell below the detection threshold; therefore, all data associated with these two eyes were omitted from the study. The number of enrolled eyes in the vitrectomized group was 36 (15 men and 21 women), and the number of enrolled eyes in the non-vitrectomized group was 71 (32 men and 39 women). The mean duration of DM in the vitrectomized group was 11.7 ± 6.6 years compared with 9.1 ± 6.9 years in the non-vitrectomized group. In addition, the mean glycosylated hemoglobin (HbA1c) levels were similar in the two groups.

The mean concentrations of IL-6, IL-8, IP-10, and MCP-1 were significantly higher in the vitrectomized group than those in the non-vitrectomized group ($p < 0.001$). However, the levels of VEGF were significantly lower in the vitrectomized group than in the non-vitrectomized group ($p = 0.001$; **Table 2**).

Non-significant correlations were identified between any factors' levels in the aqueous humor and the CRT value in the vitrectomized group (**Table 3**). In the non-vitrectomized group, the aqueous humor levels of VEGF were significantly correlated with the CRT values, whereas IL-6, IL-8, IP-10, and MCP-1 in the aqueous humor were not significantly correlated with the CRT values (**Table 4**).

In the vitrectomized group, the aqueous humor levels of IL-6 were significantly correlated with the aqueous humor levels of IL-8, IP-10, and MCP-1. The levels of IL-8 in the aqueous humor were significantly correlated with the levels of IP-10 and MCP-1 in the aqueous humor. However, the levels of VEGF were not significantly correlated with any of the measured inflammatory factors (**Table 5**). In the non-vitrectomized group, the aqueous humor levels of IL-6 were significantly correlated with the aqueous humor levels of IL-8, IP-10, MCP-1, and VEGF. The levels of IL-8 in the aqueous humor were significantly correlated with the levels of IP-10, MCP-1, and VEGF in the aqueous humor. The aqueous humor levels of IP-10 were significantly correlated with the aqueous humor levels of MCP-1 (**Table 6**).

The mean interval between vitrectomy and the anti-VEGF intravitreal injection in the vitrectomized group was 17.8 weeks (range 4–78 weeks), and none of the inflammatory or VEGF levels were associated with the days after PPV ($p > 0.05$).

DISCUSSION

It was the first study to investigate the inflammatory and angiogenic factors in vitrectomized DME eyes. The duration

TABLE 5 | Correlation matrix for aqueous humor factors in the vitrectomized group.

Variable	IL-6	IL-8	IP-10	MCP-1	VEGF
	ρ	*ρ*	*ρ*	*ρ*	*ρ*
	p	***p***	***p***	***p***	***p***
IL-6	–	0.662	0.537	0.775	0.155
		<0.001*	0.001*	<0.001*	0.365
IL-8	–	–	0.564	0.729	0.075
			<0.001*	<0.001*	0.665
IP-10	–	–	–	0.551	−0.020
				<0.001*	0.909
MCP-1	–	–	–	–	0.104
					0.545

ρ = correlation coefficient.
p = probability value.
**Statistical significance: p < 0.005 after Ryan–Holm step-down Bonferroni correction.*
IL-6, interleukin-6; IL-8, interleukin-8; IP-10, interferon-induced protein-10; MCP-1, monocyte chemotactic protein-1; VEGF, vascular endothelial growth factor.

TABLE 6 | Correlation matrix for aqueous humor factors in the non-vitrectomized group.

Variable	IL-6	IL-8	IP-10	MCP-1	VEGF
	ρ	*ρ*	*ρ*	*ρ*	*ρ*
	p	***p***	***p***	***p***	***p***
IL-6	–	0.647	0.581	0.718	0.479
		<0.001*	<0.001*	<0.001*	<0.001*
IL-8	–	–	0.522	0.676	0.583
			<0.001*	<0.001*	<0.001*
IP-10	–	–	–	0.631	0.233
				<0.001*	0.05
MCP-1	–	–	–	–	0.238
					0.046

ρ = correlation coefficient.
P = probability value.
**Statistical significance: p< 0.007 after Ryan–Holm step-down Bonferroni correction.*
IL-6, interleukin-6; IL-8, interleukin-8; IP-10, interferon-induced protein-10; MCP-1, monocyte chemotactic protein-1; VEGF, vascular endothelial growth factor.

of diabetes in the vitrectomized group was longer than that in the non-vitrectomized group. A longer duration of diabetes might induce severe PDR, resulting in the vitrectomized patients receiving PPV prior to this study. Still, the HbA1c levels were lower in the vitrectomized group than in the non-vitrectomized group, which might be due to the strict control of blood glucose among patients who underwent surgery.

The ocular microenvironment is likely to change after PPV, resulting in a different effect for anti-VEGF treatment in vitrectomized DME eyes. We found that the inflammatory factors including IL-6, IL-8, IP-10, and MCP-1 levels were higher in vitrectomized DME eyes than in non-vitrectomized DME eyes. In contrast, the levels of VEGF were lower in vitrectomized DME eyes than in non-vitrectomized DME eyes.

VEGF is vital to vascular leakage, leading to macular edema (16). In patients with DME, the aqueous humor levels of VEGF are associated with the severity of macular edema (17). In treatment-naïve DME eyes, the levels of VEGF in the aqueous humor were high and were significantly correlated with the CRT, consistent with previous studies (12, 17). The levels of VEGF were lower in vitrectomized DME eyes than in non-vitrectomized DME eyes, which might be due to the removal of VEGF by the PPV procedure. Yanyali et al. (3) showed that anti-VEGF therapy did not affect visual acuity or foveal thickness in vitrectomized eyes with DME. This phenomenon might be due to the reduced contribution of VEGF to DME in vitrectomized eyes. Inflammation might play a more important role in vitrectomized DME eyes than VEGF.

Various cytokines, especially inflammatory factors, form a network that might influence the development and exacerbation of macular edema. We found that the inflammatory factors including IL-6, IL-8, IP-10, and MCP-1 levels were higher in vitrectomized DME eyes than in non-vitrectomized DME eyes.

In this study, the levels of IL-6 in the aqueous humor were higher in the vitrectomized group than in the non-vitrectomized group. This indicates that IL-6 is probably important to the pathogenesis of DME. Indeed, elevated levels of IL-6 in the aqueous humor were associated with macular fluorescein leakage (6), and the recurrence of DME after anti-VEGF treatment has been associated with elevated aqueous humor levels of IL-6 but not with VEGF levels (7).

Our results showed that the levels of IL-8 in the aqueous humor were significantly higher in the vitrectomized group than in the non-vitrectomized group, indicating that DME in vitrectomized eyes might also be associated with IL-8. Previous studies showed that IL-8 enhances inflammation and stimulates angiogenesis by binding its receptor and inducing downstream signaling. Some studies have demonstrated that the levels of IL-8 in the aqueous humor are elevated in DME patients compared with patients without DM (7, 9), supporting a role of IL-8 in the development of DME and supporting the results of the present study.

In this study, the IP-10 levels in the aqueous humor were significantly higher in the vitrectomized group than in the non-vitrectomized group, which might be due to the relationship with IL-8 and the reaction to PRP. Indeed, the levels of IP-10 in the aqueous humor have been significantly correlated with the levels of IL-8 (12), and IP-10 can prevent IL-8-induced neovascularization in a corneal pocket model of angiogenesis (11). These studies indicated that IP-10 might at least partially antagonize the function of IL-8. The levels of IP-10 in the aqueous humor were significantly higher in PDR patients who underwent PRP than who did not receive PRP, indicating that IP-10 might play a role in the inhibition of PDR progression (12).

Our results suggested that the levels of MCP-1 were significantly higher in the vitrectomized group than in the non-vitrectomized group, indicating that MCP-1 might be an important modulator after PPV, especially in DME eyes. MCP-1 levels in the aqueous humor were elevated in DME patients (15),

and mean vitreous levels of MCP-1 were significantly higher in vitrectomized eyes with DME than in eyes without DME (18), supporting the present study. Even though clinical examinations showed no inflammatory responses in the eye, MCP-1 levels were still elevated (19).

The high concentrations of inflammatory factors in vitrectomized eyes may be related to the disruptions of the blood–aqueous barrier by surgery (20). Still, a study showed no differences in IL-6, IL-8, MCP-1, and VEGF levels in aqueous humor between PDR patients with and without PRP (12). Another study also found that some inflammatory factors (IL-8 and IP-10) were increased in the aqueous humor of post-vitrectomy eyes in rhegmatogenous retinal detachment patients, whereas other factors (IL-6 and MCP-1) remained unchanged (21). This phenomenon might indicate that some inflammatory factors originate from intraocular cells or tissues. In addition, several studies have found that IL-6, IL-8, IP-10, and MCP-1 are associated with DME; therefore, the elevation of these inflammatory factors might not simply be due to intraocular surgery but also be the result of DME pathology in vitrectomized eyes.

In non-vitrectomized DME eyes, the levels of IL-6, IL-8, and VEGF were significantly correlated with each other, likely because these cytokines are essential to DME pathogenesis and interact among themselves. In vitrectomized DME eyes, IL-6, IL-8, IP-10, and MCP-1 levels were significantly associated; however, VEGF levels in the aqueous humor were not correlated with any inflammatory factors. These findings indicated that inflammation might influence macular edema along with VEGF in non-vitrectomized DME eyes, whereas inflammation might play a more important role in the pathogenesis of DME in vitrectomized eyes *via* the VEGF-independent pathway. Thus, anti-VEGF treatment might not represent an effective treatment for some vitrectomized DME eyes (3).

The evidence shows that DR is mediated by inflammatory responses, including leukostasis (22). The inflammatory cascade appears to be crucial for the occurrence and development of DME. The treatment of DME using intravitreal injections of corticosteroids has been reported to be safe and effective (23). Corticosteroids inhibit the synthesis of multiple inflammatory proteins that might be responsible for the development of vascular leakage (24). The effects of corticosteroid injections for DME in vitrectomized eyes are worth considering.

In this study, non-vitrectomized eyes received intravitreal injections before PRP, while vitrectomized eyes received PRP during PPV. Oh et al. (12) showed that in PDR patients the levels of IL-6, IL-8, MCP-1, and VEGF had no significant differences between eyes that underwent PRP or not, except for IP-10.

The mean interval between PPV and intravitreal injection (17.8 weeks) did not have a significant relationship with any of the cytokines measured in this study. Therefore, the interval after vitrectomy in this study did not influence the results.

One limitation of our study is that we did not examine all cytokines, and the ultimate effects of these cytokines in vitrectomized DME eyes remain to be explored. Moreover, the number of samples in our study was limited.

CONCLUSION

In conclusion, this study showed that the levels of inflammatory factors in the aqueous humor were higher, whereas the VEGF levels were lower in vitrectomized DME eyes than in non-vitrectomized DME eyes. In addition, inflammatory factor levels had no relationship with VEGF levels in vitrectomized DME eyes. These findings indicate that inflammation might play an important role in the pathogenesis of DME in vitrectomized eyes. Anti-inflammatory therapies might represent another strategy for the treatment of DME in vitrectomized eyes. Further studies are needed to investigate the mechanism and treatment strategy of DME in vitrectomized eyes.

DATA AVAILABILITY STATEMENT

The raw data supporting the conclusions of this article will be made available by the authors, without undue reservation.

ETHICS STATEMENT

Our study was approved by the Ethical Committee of The Second Xiangya Hospital (LYZ2020009), and all enrolled patients were treated in accordance with the Declaration of Helsinki. All patients provided informed consent before inclusion in the study. To reduce selection bias, all patients were recruited in a consecutive manner.

AUTHOR CONTRIBUTIONS

YL was responsible for designing the study, conducting the search, screening potentially eligible studies, extracting and analyzing the data, interpreting the results, and writing the paper. BY was responsible for extracting data. ZM, MX, ZL, ZZ, YM, JM, and BM were responsible for extracting data. XY was responsible for the data collection and modifying the language. JL was responsible for designing the study. All authors contributed to the article and approved the submitted version.

FUNDING

This work was supported by the National Natural Science Foundation of China (81570847), Natural Science Foundation of Hunan Province (2020JJ4800).

REFERENCES

1. Cai S, Bressler NM. Aflibercept, bevacizumab or ranibizumab for diabetic macular oedema: recent clinically relevant findings from drcr.Net protocol t. *Curr Opin Ophthalmol*. (2017) 28:636–43. doi: 10.1097/ICU.0000000000000424
2. Rush RB, Del Valle Penella A, Reinauer RM, Rush SW, Bastar PG. Internal limiting membrane peeling during vitrectomy for diabetic

vitreous hemorrhage: a randomized clinical trial. *Retina*. (2020) 41: 1118–26. doi: 10.1097/IAE.0000000000002976
3. Yanyali A, Aytug B, Horozoglu F, Nohutcu AF. Bevacizumab (avastin) for diabetic macular edema in previously vitrectomized eyes. *Am J Ophthalmol*. (2007) 144:124–6. doi: 10.1016/j.ajo.2007.02.048
4. Vujosevic S, Micera A, Bini S, Berton M, Esposito G, Midena E. Proteome analysis of retinal glia cells-related inflammatory cytokines in the aqueous humour of diabetic patients. *Acta Ophthalmol*. (2016) 94:56–64. doi: 10.1111/aos.12812
5. Yang X, Yan H, Jiang N, Yu Z, Yuan J, Ni Z, et al. Il-6 trans-signaling drives a stat3-dependent pathway that leads to structural alterations of the peritoneal membrane. *Am J Physiol Renal Physiol*. (2020) 318:F338–53. doi: 10.1152/ajprenal.00319.2019
6. Funatsu H, Yamashita H, Noma H, Shimizu E, Mimura T, Hori S. Prediction of macular edema exacerbation after phacoemulsification in patients with nonproliferative diabetic retinopathy. *J Cataract Refract Surg*. (2002) 28:1355. doi: 10.1016/S0886-3350(02)01243-9
7. Roh MI, Kim HS, Song JH, Lim JB, Kwon OW. Effect of intravitreal bevacizumab injection on aqueous humor cytokine levels in clinically significant macular edema. *Ophthalmology*. (2009) 116:80–6. doi: 10.1016/j.ophtha.2008.09.036
8. Sprague AH, Khalil RA. Inflammatory cytokines in vascular dysfunction and vascular disease. *Biochem Pharmacol*. (2009) 78:539–52. doi: 10.1016/j.bcp.2009.04.029
9. Funk M, Schmidinger G, Maar N, Bolz M, Benesch T, Zlabinger GJ, et al. Angiogenic and inflammatory markers in the intraocular fluid of eyes with diabetic macular edema and influence of therapy with bevacizumab. *Retina*. (2010) 30:1412–9. doi: 10.1097/IAE.0b013e3181e095c0
10. Ruffilli I, Ferrari SM, Colaci M, Ferri C, Fallahi P, Antonelli A. Ip-10 in autoimmune thyroiditis. *Horm Metab Res*. (2014) 46:597–602. doi: 10.1055/s-0034-1382053
11. Strieter RM, Kunkel SL, Arenberg DA, Burdick MD, Polverini PJ. Interferon gamma-inducible protein 10 (ip-10), a member of the c-x-c chemokine family, is an inhibitor of angiogenesis. *Biochem Biophys Res Commun*. (1995) 210:51–7. doi: 10.1006/bbrc.1995.1626
12. Oh IK, Kim SW, Oh J, Lee TS, Huh K. Inflammatory and angiogenic factors in the aqueous humor and the relationship to diabetic retinopathy. *Curr Eye Res*. (2010) 35:1116–27. doi: 10.3109/02713683.2010.510257
13. Yoshimura T. The chemokine mcp-1 (ccl2) in the host interaction with cancer: a foe or ally? *Cell Mol Immunol*. (2018) 15:335–45. doi: 10.1038/cmi.2017.135
14. Hoerster R, Fauser S, Cursiefen C, Kirchhof B, Heindl LM. The influence of systemic renin-angiotensin-inhibition on ocular cytokines related to proliferative vitreoretinopathy. *Graefes Arch Clin Exp Ophthalmol*. (2017) 255:1721–5. doi: 10.1007/s00417-017-3707-9
15. Funatsu H, Noma H, Mimura T, Eguchi S, Hori S. Association of vitreous inflammatory factors with diabetic macular edema. *Ophthalmology*. (2009) 116:73–9. doi: 10.1016/j.ophtha.2008.09.037
16. Arima M, Nakao S, Yamaguchi M, Feng H, Fujii Y, Shibata K, et al. Claudin-5 redistribution induced by inflammation leads to anti-vegf-resistant diabetic macular edema. *Diabetes*. (2020) 69:981–99. doi: 10.2337/db19-1121
17. Funatsu H, Yamashita H, Noma H, Mimura T, Yamashita T, Hori S. Increased levels of vascular endothelial growth factor and interleukin-6 in the aqueous humor of diabetics with macular edema. *Am J Ophthalmol*. (2002) 133:70–7. doi: 10.1016/S0002-9394(01)01269-7
18. Yoshida S, Kubo Y, Kobayashi Y, Zhou Y, Nakama T, Yamaguchi M, et al. Increased vitreous concentrations of mcp-1 and il-6 after vitrectomy in patients with proliferative diabetic retinopathy: possible association with postoperative macular oedema. *Br J Ophthalmol*. (2015) 99:960–6. doi: 10.1136/bjophthalmol-2014-306366
19. Kawai M, Inoue T, Inatani M, Tsuboi N, Shobayashi K, Matsukawa A, et al. Elevated levels of monocyte chemoattractant protein-1 in the aqueous humor after phacoemulsification. *Invest Ophthalmol Vis Sci*. (2012) 53:7951–60. doi: 10.1167/iovs.12-10231
20. Inoue Y, Kadonosono K, Yamakawa T, Uchio E, Watanabe Y, Yanagi Y, et al. Surgically-induced inflammation with 20-, 23-, and 25-gauge vitrectomy systems: an experimental study. *Retina*. (2009) 29:477–80. doi: 10.1097/IAE.0b013e31819a6004
21. Gu R, Zhou M, Jiang C, Yu J, Xu G. Elevated concentration of cytokines in aqueous in post-vitrectomy eyes. *Clin Exp Ophthalmol*. (2016) 44:128–34. doi: 10.1111/ceo.12638
22. Meleth AD, Agron E, Chan CC, Reed GF, Arora K, Byrnes G, et al. Serum inflammatory markers in diabetic retinopathy. *Invest Ophthalmol Vis Sci*. (2005) 46:4295–301. doi: 10.1167/iovs.04-1057
23. Gillies MC, Lim LL, Campain A, Quin GJ, Salem W, Li J, et al. A randomized clinical trial of intravitreal bevacizumab versus intravitreal dexamethasone for diabetic macular edema: the bevordex study. *Ophthalmology*. (2014) 121:2473–81. doi: 10.1016/j.ophtha.2014.07.002
24. Luis ME, Sampaio F, Costa J, Cabral D, Teixeira C, Ferreira JT. Dril influences short-term visual outcome after intravitreal corticosteroid injection for refractory diabetic macular edema. *Curr Eye Res*. (2021) 46:1378–86. doi: 10.1080/02713683.2021.1878540

Conflict of Interest: The authors declare that the research was conducted in the absence of any commercial or financial relationships that could be construed as a potential conflict of interest.

Publisher's Note: All claims expressed in this article are solely those of the authors and do not necessarily represent those of their affiliated organizations, or those of the publisher, the editors and the reviewers. Any product that may be evaluated in this article, or claim that may be made by its manufacturer, is not guaranteed or endorsed by the publisher.

frontiers in Medicine

ORIGINAL RESEARCH
published: 21 September 2021
doi: 10.3389/fmed.2021.710079

Reduced Expression of Erythropoietin After Intravitreal Ranibizumab in Proliferative Diabetic Retinopathy Patients—Retrospective Interventional Study

Li Chen†, Jing Feng†, Yanhong Shi, Fuxiao Luan, Fang Ma, Yingjie Wang, Weiqiang Yang and Yong Tao**

Department of Ophthalmology, Beijing Chaoyang Hospital, Capital Medical University, Beijing, China

OPEN ACCESS

Edited by:
Ryoji Yanai,
Yamaguchi University, Japan

Reviewed by:
Yujing Bai,
Peking University People's Hospital, China
Makoto Hatano,
Yamaguchi University, Japan

***Correspondence:**
Jing Feng
drfengj@gmail.com
Yong Tao
taoyong@bjcyh.com

†These authors have contributed equally to this work and share first authorship

Specialty section:
This article was submitted to Ophthalmology, a section of the journal Frontiers in Medicine

Received: *15 May 2021*
Accepted: *24 August 2021*
Published: *21 September 2021*

Citation:
Chen L, Feng J, Shi Y, Luan F, Ma F, Wang Y, Yang W and Tao Y (2021) Reduced Expression of Erythropoietin After Intravitreal Ranibizumab in Proliferative Diabetic Retinopathy Patients—Retrospective Interventional Study. Front. Med. 8:710079. doi: 10.3389/fmed.2021.710079

Purpose: To evaluate the expressions of erythropoietin (EPO) and vascular endothelial growth factor (VEGF) in the vitreous and fibrovascular membranes (FVMs) of proliferative diabetic retinopathy (PDR) after the intravitreal injection of ranibizumab (IVR) and further explore the relationship between EPO and VEGF.

Method: The concentrations of EPO and VEGF levels in the vitreous fluid were measured in 35 patients (24 PDR and 11 non-diabetic patients) using enzyme-linked immunosorbent assay. The patients were divided into three groups: PDR with IVR (IVR group) before par plana vitrectomy ($n = 10$), PDR without IVR (Non-IVR group) ($n = 14$) and a control group [macular holes (MHs) or epiretinal membranes (ERM), $n = 11$]. Fluorescence immunostaining was performed to examine the expressions of VEGF, EPO and CD 105 in the excised epiretinal membranes.

Result: The PDR eyes of Non-IVR group had the highest vitreous VEGF and EPO levels (836.30 ± 899.50 pg/ml, 99.29 ± 27.77 mIU/ml, respectively) compared to the control group (10.98 ± 0.98 pg/ml and 18.96 ± 13.30 mIU/ml/ml). Both the VEGF and EPO levels in the IVR group (13.22 ± 2.72 pg/ml and 68.57 ± 41.47 mIU/ml) were significantly lower than the Non-IVR group ($P = 0.004$ and $P = 0.04$, respectively). Furthermore, no significant difference was observed for VEGF levels between the control and IVR groups (10.9 ± 0.98 pg/ml and 13.22 ± 2.72 pg/ml, respectively, $P = 0.9$). Yet the EPO level in the IVR group was significantly higher than that in the Non-diabetic group (68.57 ± 41.47 pg/ml and 18.96 ± 13.30 pg/ml, respectively, $P = 0.001$). The expressions of EPO, VEGF, and CD105 were significantly reduced in fluorescence immunostaining of FVMs in the IVR group compared with the Non-IVR group. The receiver operating characteristic (ROC) curve of the EPO and VEGF levels were 0.951 and 0.938 in the PDR group.

Conclusion: Both of the VEGF and EPO level were significantly increased in PDR patients, which have equal diagnostic value in the prediction of PDR. IVR could reduce the EPO level, but not enough to the normal level.

Keywords: erythropoietin, intraocular fluid, intravitreal ranibizumab, proliferative diabetic retinopathy (PDR), vascular endothelial growth factor (VEGF)

INTRODUCTION

Proliferative diabetic retinopathy (PDR) is advanced diabetic retinopathy (DR), characterised by the pathologic growth of new blood vessels, which is driven by the release of local angiogenic factors in ischemic and hypoxic retina (1). Vascular endothelial growth factor (VEGF) is a potent mediator that controls angiogenesis and vascular permeability in both pathological and physiological ocular conditions (2). The current evidence indicates that VEGF plays a central role in the development of DR (3–5). Although the inhibition of VEGF reduces retinal neovascularization, it does not completely inhibit ischemia-driven retinal neovascularization (6). Thus, the angiogenic process is likely to involve numerous growth factors and cytokines (7).

Erythropoietin (EPO) is a pleiotropic cytokine, with the function of a circulatory growth factor (8). Higher levels of EPO in the vitreous and serum samples of PDR patients than in a control group were recently demonstrated (9–12). Furthermore, the evidence shows that EPO is a potent retinal angiogenic factor independent of VEGF and is capable of stimulating ischemia-induced retinal angiogenesis in PDR (13). Evidences have proved that EPO has an angiogenic potential equal to VEGF. There is no information available regarding the influence of anti-VEGF for the EPO level.

The purpose of the present study was to evaluate the changes of VEGF and EPO vitreous concentrations after intravitreal ranibizumab injection and to detect the expressions of VEGF and EPO on epiretinal fibrovascular membranes (FVMs) obtained during vitrectomy in eyes with PDR.

PATIENTS AND METHODS

Subjects and Enrolment Criteria

This was a retrospective, interventional study. The study was conducted in accordance with the Declaration of Helsinki, and we received approval from the Investigational Review Board of the Beijing Chaoyang Hospital (2018-4-3-3). Informed consent for all examinations and procedures was obtained from the patients, who provided their written informed consent to participate. This study enrolled patients with vitreous haemorrhage or tractional retinal detachment (TRD) as the PDR groups and non-diabetic patients with idiopathic macular hole (MH) or macular epiretinal membranes (ERM) as the control group. All the patients underwent pars plana vitrectomies (PPV) between January 2019 and June 2020. The inclusion criteria for the PDR group were type 2 diabetes, age $>$ 18 years and PDR. The exclusion criteria were as follows: (1) any anti-VEGF therapy or pan-retinal photocoagulation within 6 months prior to the study; (2) any history of ocular diseases other than DR; (3) a history of ocular surgery on the study eye; and (4) a history of systemic thromboembolic events, including myocardial infarction and stroke. The exclusion criteria for the non-diabetic control group were uveitis, a previous intraocular surgery, diabetes mellitus, a malignant tumour and the use of immunosuppressive drugs.

Thirty-five patients (35 eyes) fulfilled the inclusion criteria and were divided into three groups: (1) 14 PDR patients underwent PPV without intravitreal ranibizumab (IVR) treatment (Non-IVR group); (2) 10 PDR patients underwent PPV with IVR treatment (0.5 mg/0.05 ml of intravitreal ranibizumab injected 7–10 days before surgery) (IVR group); and (3) 11 patients with MH or macular ERM as the control group.

Physical and Ocular Examinations

Each patient's demographic, clinical, and ocular data were recorded. Each patient (diabetics and controls) underwent complete ophthalmological examinations, including visual acuity, slit lamp, tonometry, fluorescein retinal angiography, and optical coherence tomography. Diabetic retinopathy was evaluated using standardised fundus colour photographs and fluorescein angiograms. If a vitreous haemorrhage or lens opacity prevented an ophthalmoscopic examination of the ocular fundus, an ocular ultrasound was the auxiliary examination.

Intravitreal Ranibizumab Injection

A 30-gauge needle was inserted through the corneal limbus to withdraw 0.05 mL of aqueous humour and to soften the globe. Subsequently, 0.5 mg (0.05 mL) of ranibizumab was injected into the vitreous fluid as preoperative adjunctive therapy 7 days before vitrectomy. Topical antibiotics were applied as postoperative medications.

Surgical Procedures and Vitreous Sampling

All the surgeries were performed by the same surgeon at the Beijing Chaoyang Hospital. All the patients underwent a 23-gauge standardised technique pars plana vitrectomies. At the beginning of surgery, 0.5 mL of undiluted vitreous sample was aspirated through the vitreous cutter under simultaneous inflation of the vitreous cavity with air through the infusion cannula. For ethical and technical reasons, it was impossible to obtain paired samples of vitreous humour in the same eye (with and without IVR). Therefore, the vitreous samples of eyes with and without IVR were unpaired. Fibrovascular membranes from seven PDR patients were surgically retrieved during vitrectomy.

Vitreous samples were taken during the surgery and immediately centrifuged for 5 min at 4°C at 3,000 rotations per minute (rpm). The liquid component without sediment was immediately stored at −80°C until analysis. Fibrovascular membranes were immediately frozen at −80°C.

ELISA Analysis

The concentrations of VEGF (Quantikine VEGF ELISA Kit; R&D Systems, Inc., Minneapolis, MN, USA) and EPO (Quantikine VEGF ELISA Kit; R&D Systems, Inc., Minneapolis, MN, USA) in the vitreous fluid were measured using enzyme-linked immunosorbent assay kits. Each assay was performed in accordance with the instructions of the user manual of the kit. Standard curves for each cytokine were generated using the reference cytokine concentrations supplied with the kit.

Immunofluorescence Staining

Immunofluorescence staining was performed on the frozen sections of the FVMs by staining with the following antibodies:

rabbit anti-EPO polyclonal IgG (1:150 dilution; No. ab126876 Abcam, Cambridge, MA, USA), mouse anti-CD105 monoclonal IgG (1:150 dilution; No. ab69772 Abcam, Cambridge, MA, USA), rabbit anti-VEGF polyclonal IgG (1:200 dilution; No. ab39250 Abcam, Cambridge, MA, USA), tetramethylrhodamine isothiocyanate- conjugated goat anti-mouse IgG (1: 200 dilution; Zhongshan Goldenbridge Biotechnology Co. Ltd., Beijing, China), and/or fluorescein isothiocyanate- conjugated goat anti-rabbit IgG (1: 200 dilution; Zhongshan Goldenbridge Biotechnology Co. Ltd.). The samples were counterstained with 4′,6′-diamino- 2-phenylindole (DAPI) (1: 1,000 dilution, No. D9542; Sigma-Aldrich, St. Louis, MO, USA). All the sections were examined using a fluorescence microscope (DS-Ril-U2; Nikon, Tokyo, Japan) and photographed (DS-U2; Nikon).

Statistical Analysis

A statistical analysis was performed using GraphPad Prism 8 software. The data were presented as the mean ± standard deviation. T Differences between the study group and the control group were estimated with a non-parametric Mann-Whitney rank sum test and *t*-test when appropriate. Parameters were used Kruskal-Wallis *H*-test and ANOVA test to compare variables among various groups when appropriate. Chi-squared test or Fisher's exact test were used to compare non-continuous variables. Correlation coefficients were determined by using the Pearson correlation test on the transformed data of a decadic logarithm scale. Two-tailed probabilities of <0.05 were considered to indicate statistical significance.

RESULT

Demographic Data of Patients

The main characteristic of the 24 patients with PDR and 11 non-diabetic control patients enrolled in the study are shown in **Table 1**. The PDR group and control group showed no significant difference in gender. The mean age of 65.64 ± 5.14 in the control group was significantly older than that for the PDR without and with IVR group (54.71 ± 6.94, and 53.90 ± 7.95, respectively, $P < 0.01$).

The duration of diabetes mellitus in Non-IVR group was 12.86 ± 4.43 years, and it was 16 ± 3.23 years in the IVR group. No statistically significant difference was noted in the duration of diabetes mellitus between the PDR groups ($P = 0.076$). As for hypertension history, the ration of the control group was 36.36%, which was lower than that for the PDR without (57.14%) and with IVR group (40%) ($P = 0.54$).

A statistically significant difference in the mean visual acuity (Log Mar) values were found among the three groups for both preoperative and postoperative vision. Before vitrectomy, the visual acuity values in the control group (0.82 ± 0.57) were significantly superior to the other two PDR groups (1.97 ± 0.58 and 1.60 ± 0.86, respectively, $P < 0.01$). After vitrectomy, visual acuity improved in all three groups. Similarly, visual acuity in the control group was better than that in the PDR group ($P < 0.01$).

The mean intraocular pressure (IOP) value before vitrectomy, measured using applanation tonometry in this study, was 13.27 mmHg in the MH+ERM group of subjects, 13.21 mmHg in the Non-IVR group and 14.20 mmHg in the IVR group. No statistically significant difference was found in the average IOP values among the three groups ($P = 0.72$). After vitrectomy, the IOP value in the PDR groups (17.00 ± 2.71 mmHg in without IVR group, 16.40 ± 4.19 mmHg in with IVR group) was higher than that in the control group (12.27 ± 1.90 mmHg) ($P = 0.001$).

EPO and VEGF Levels in Vitreous

Samples of undiluted vitreous fluid were collected from the eyes of 24 patients with PDR and from 11 patients in the control group. **Table 2** presents the concentrations (medians and 95% CI) of EPO and VEGF in the vitreous fluid among the three groups. The median EPO level was 99.29 mIU per millilitre (95% CI: 83.25–115.3) in the patients with Non-IVR group and 68.57 mIU per millilitre (95% CI: 38.91–98.24) in the patients with IVR group and 18.96 mIU per millilitre (95% CI, 10.02–27.90) in the patients with Non-diabetic ocular diseases ($p < 0.001$).

TABLE 1 | General clinical information of the patients.

Variables	MH and ERM	PDR		*P-value*	P1	P2	P3
	(control group)	Non-IVR	IVR		#	§	&
Patients, *n*	11	14	10	–			
Age (years)	65.64 ± 5.14	54.71 ± 6.94	53.90 ± 7.95	**0.0003**	0.001	0.001	0.95
Female/male	7/4	7/7	5/5	0.759	0.79	0.81	0.99
DM duration (y)	/	12.86 ± 4.43	16 ± 3.23	0.076			
Hypertension	4 (36.36%)	8 (57.14%)	4 (40%)	0.543	0.57	0.98	0.70
Visual acuity (LogMar)							
Before surgery	0.82 ± 0.57	1.97 ± 0.58	1.60 ± 0.86	**<0.001**	**<0.001**	**0.001**	0.577
After surgery	0.60 ± 0.29	1.27+0.39	1.49 ± 0.38	**<0.001**	**<0.001**	**<0.001**	0.327
Intraocular pressure							
Before surgery	13.27 ± 2.14	13.21 ± 3.49	14.20 ± 3.67	0.72	0.99	0.77	0.74
After surgery	12.27+1.90	17.00 ± 2.71	16.40 ± 4.19	**0.001**	**0.001**	**0.01**	0.88

MH, macular hole; ERM, epiretinal membrane; DM, diabetes mellitus; PDR, proliferative diabetic retinopathy; #Control vs. Non-IVR; §Control vs. IVR; &Non-IVR vs. IVR.
Bold value indicates p < 0.05, which are statistically significant.

The median VEGF level was 836.3 pg/ml (95% CI: 316.90–1,356) in the patients with Non-IVR group and 13.22 pg/ml (95% CI: 11.27–15.17) in the patients with IVR group and 10.98 pg/ml (95% CI, 10.32–11.64) in the control group ($p < 0.001$). The vitreous EPO and VEGF levels were significantly higher in the patients with PDR than in the control group (**Figure 1**).

A scatter plot of the log-transformed levels of EPO and VEGF in the patients with PDR indicated a positive correlation (**Figure 2A**). However, the Pearson correlation coefficient was 0.18, and no significant difference was seen ($P = 0.22$).

For exploratory purposes, we also analysed the receiver operating characteristic (ROC) curve of the EPO and VEGF levels in the PDR group (**Figure 2B**). The AUC values for EPO and VEGF were 0.951 and 0.938, respectively.

Immunofluorescence Staining

The staining of epiretinal fibrovascular membranes (FVMs) showed strong positives for EPO and VEGF and for the marker CD105 of the neovascular endothelial cells in the Non-IVR group (**Figure 3** top row and **Figure 4** top row). After IVR, the positive expressions significantly decreased for EPO, VEGF, and CD105 in the FVMs of PDR patients (**Figure 3** bottom row and **Figure 4** bottom row). **Figure 5** reveals the expression of vimentin for the maker of fibroblastic cells, which was weakly positive in the PDR group and negative in the IVR group (**Figure 5**).

DISCUSSION

The present study indicates that the vitreous levels of EPO and VEGF in PDR patients is strikingly higher than the levels in Non-diabetic patients. These results are consistent with other researchers (11–17). Furthermore, the levels of VEGF and EPO in vitreous fluids and FVMs significantly declined after IVR. Although not significant, the vitreous levels of EPO showed a trend of positive correlation with VEGF in the DR patients. The ROC curve analysis showed that EPO and VEGF had clear specificity and sensitivity in the indication of PDR. Our present study provides a valuable foundation for further study of the relationship between EPO and VEGF in PDR and their potential future use in clinical practise.

VEGF-mediated pathogenic effects are primarily related to vascular permeability and neovascularization (18). VEGF was found to be closely related to the development and progression of PDR (11, 19, 20). Recently, anti-VEGF therapy has led to great advances in ocular neovascular diseases. However, the inhibition of VEGF is not associated with a total regression of retinal

TABLE 2 | Vitreous levels of erythropoietin and vascular endothelial growth factor (VEGF).

Variables	MH and ERM	PDR		*P*-value	P1	P2	P3
	(control group)	Non-IVR	IVR		#	§	&
EPO (mIU/ml)							
Mean ± SD	18.96 ± 13.30	99.29 ± 27.77	68.57 ± 41.47	**<0.001**	**<0.001**	**0.001**	**0.04**
95% CI	10.02–27.90	83.25–115.3	38.91–98.24				
VEGF (pg/ml)							
Mean ± SD	10.98 ± 0.98	836.30 ± 899.5	13.22 ± 2.72	**0.001**	**0.003**	0.99	**0.004**
95% CI	10.32–11.64	316.90–1356	11.27–15.17				

MH, macular hole; ERM, epiretinal membrane; DM, diabetes mellitus; PDR, proliferative diabetic retinopathy; #Control vs. Non-IVR; §Control vs. IVR; &Non-IVR vs. IVR.
Bold value indicates p < 0.05, which are statistically significant.

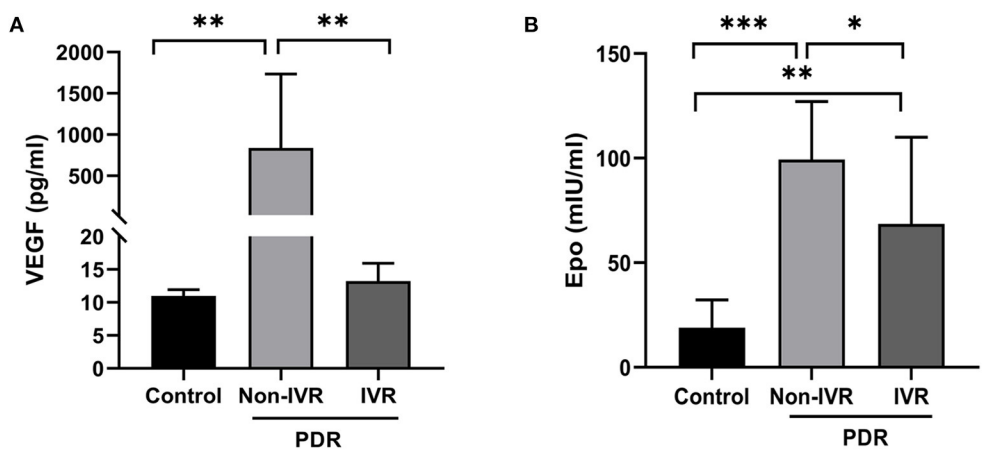

FIGURE 1 | Vitreous concentration of VEGF **(A)** and EPO **(B)** in the control and PDR group. *$P < 0.05$; **$P < 0.01$; ***$P < 0.0001$. PDR, proliferative diabetic retinopathy; IVR, intravitreal ranibizumab.

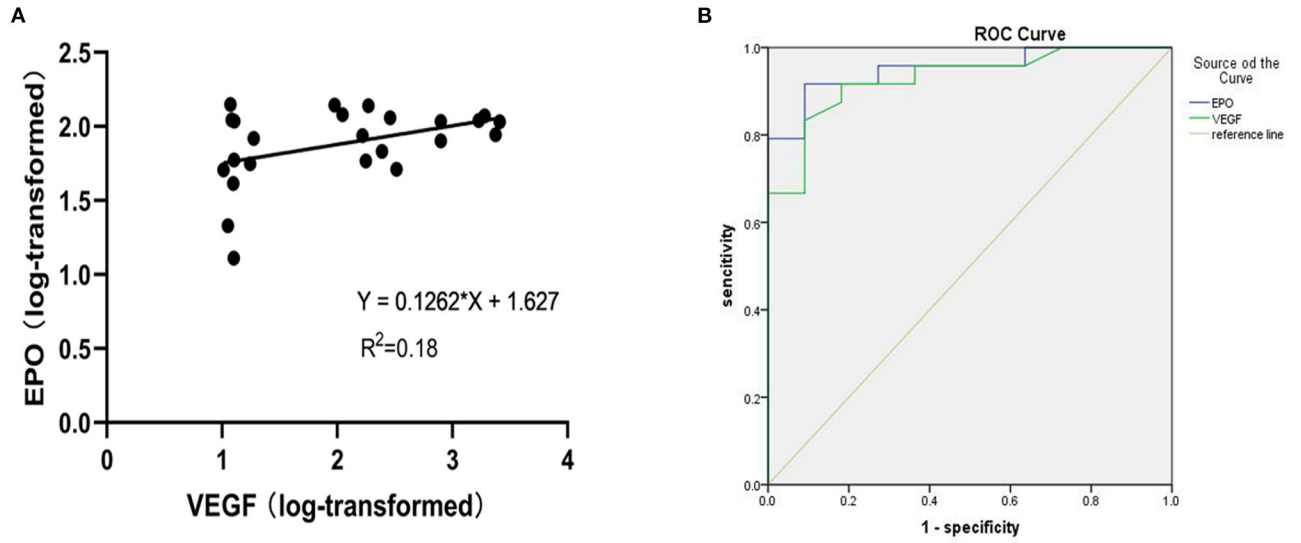

FIGURE 2 | (A) Shows a scatter plot for the correlation between log-transformed vitreous VEGF and EPO levels in patients with PDR. **(B)** Receiver operating characteristic (ROC) curve of EPO and VEGF levels in PDR.

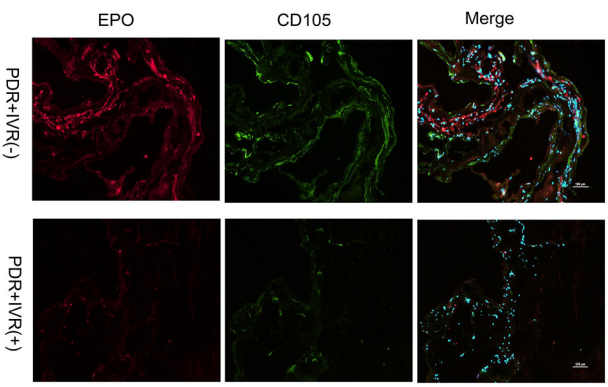

FIGURE 3 | Epiretinal fibrovascular membranes (FVMs) showed strong positive for EPO and the marker CD105 of neovascular endothelial cells in the Non-IVR group. Scale bars: 100 μm.

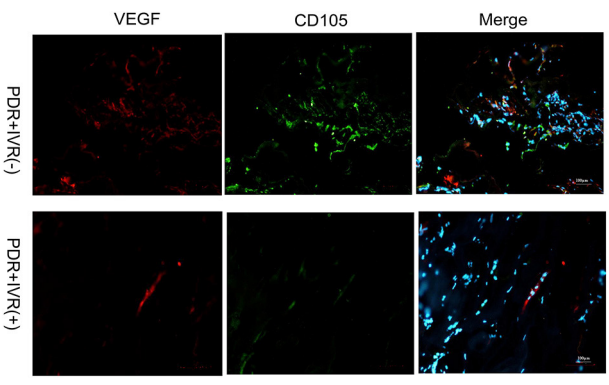

FIGURE 4 | Epiretinal fibrovascular membranes (FVMs) showed strong positive for VEGF and the marker CD105 of neovascular endothelial cells in the Non-IVR group. Scale bars: 100 μm.

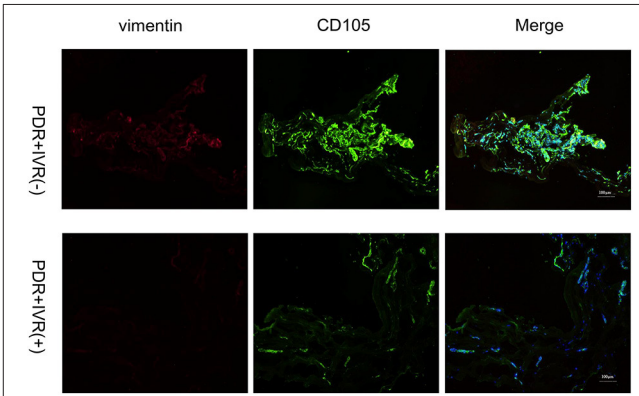

FIGURE 5 | Epiretinal fibrovascular membranes (FVMs) showed negative for Vimentin and positive for the marker CD105 of neovascular endothelial cells in the Non-IVR group. Scale bars: 100 μm.

neovascularization, indicating that other angiogenic factors and inflammation factors may play a role in this process, including TNF-α, IL-6, EPO and the pigment epithelium-derived factor (PEDF) (11).

Many recent studies have shown that EPO has different biological effects *in vivo* and *in vitro* studies (13, 21). EPO was demonstrated to protect against the VEGF-induced permeability of the blood-brain barrier (BBB) through restoring the tight junction proteins and VE-cadherin in experimental diabetic retinopathy and *in vitro* bovine model (22, 23). EPO improved oxygen carriage to retinal tissue and ameliorated diabetic retinopathy. However, some studies have indicated that EPO has an angiogenic potential equivalent to that of VEGF and independently contributes to retinal

neovascularization in the pathogenesis of PDR. Therefore, the precise role of EPO is still of great interest for many researchers. It is yet unclear whether EPO has a protective or aggravating role in DR, considering the contradictive results from various studies.

Our study demonstrated a high level of EPO in vitreous fluids and FVMs in PDR patients, which was consistent with other studies about EPO. However, the source of the locally increasing EPO in PDR was not confirmed in the present study since the serum samples from the PDR patients were not collected due to ethical consideration. Thus, we were unable to explore the possible association between serum EPO and vitreous EPO in PDR patients. In a previous study, Semeraro et al. and Watanabe et al. showed that serum EPO concentrations did not significantly differ between diabetic and non-diabetic patients (11, 13). Furthermore, there was no correlation between haemoglobin and intraocular EPO deposition (in both vitreous and aqueous humours), but positive correlation between EPO and glycated haemoglobin and hyperglycaemia was confirmed. It seems clear that EPO in vitreous fluid is probably not due to the breakdown of the blood retinal barrier and is not serum derived. Hernandez first detected EPO RNA expression in the adult human retina, and its expression was significantly higher in diabetic than in non-diabetic donors. EPO expression was found to be more abundant in RPE than in the neuroretina, which supported the notions that EPO is actually produced in the local microenvironment of the eye and that ischemia and hypoxia caused by hyperglycaemia may be stimulating factors (16).

We further explored the relationship between EPO and VEGF, especially EPO after anti-VEGF treatment. Our result revealed that the levels of EPO and VEGF increased in vitreous fluid in the PDR patients. In addition, the level of EPO showed a trend of positive correlation with the VEGF level, yet no significant correlation was found. This is consistent with the results of other studies, Semeraro et al. found no correlation between the concentrations of EPO and VEGF in the vitreous body (11). Recently, anti-VEGF therapy has become the first-line treatment in PDR-complicated neovascularization and DME. However, EPO changes after anti-VEGF treatment have not been evaluated. Our study, for the first time, demonstrated that the concentration of EPO in vitreous fluid and FMVs significantly decreased after anti-VEGF treatment, indicating a possible interaction between EPO and VEGF in PDR. EPO and VEGF may be involved in similar signalling pathways. However, further studies are needed to verify these hypotheses.

Due to the contradictive results of EPO from various studies, we explored whether EPO has a protective or aggravating role in PDR. It was suggested that serum EPO concentrations increased in direct proportion with the severity of the clinical stage of PDR and that blocking EPO may be beneficial to the treatment of PDR (13). However, in an early diabetes animal model and DME patients, exogenous EPO administration not only protected against the VEGF-induced permeability of the BBB and restored the tight junction proteins, but it also counteracted neurodegeneration (16, 20, 24). Another *in vivo* study confirmed that compared to IVB alone with intravitreal IVB, IVB combined with EPO did not significantly improve visual acuity and reduce retinal thickness in DME patients, nor did any retinopathy progression or neovascularization (25). Therefore, EPO may play different roles in different stages of DR. It is important to find a dynamic balance for EPO between the protection effect on the permeability of the BBB and the risk for retinal vaso-proliferative diseases. Further studies are necessary, including research on the effect of angiogenesis on exogenous EPO and neuronal side effects and the BBB permeability of an EPO blockade.

Furthermore, we analysed the receiver operating characteristic (ROC) curves of EPO and VEGF. The ROC curve is a useful tool for evaluating the performance of diagnostic tests within the range of possible values of predictive variables. The area under the ROC curve (AUC) is an overall measure of a test's ability to determine whether a particular situation exists or not. An AUC of 0.5 indicates a test with no discrimination (i.e., no better than chance), while an AUC of 1.0 indicates a test with perfect discrimination (26, 27). The AUCs of EPO and VEGF were 0.951 and 0.928, respectively, which suggested that EPO and VEGF have equal diagnostic value in the prediction of PDR. Of course, the detection of vitreous body fluid is an invasive examination, which is difficult to pass in an ethics review. But the results of ROC curve in this study indicated that both EPO monitoring and VEGF are of great significance, which may be of certain significance for the treatment of different stages of clinical DR.

Our study has some limitations. First, this was a retrospective comparative study with a limited number of patients enrolled. Second, paired samples of vitreous fluid from the same eye (before and after the injection) were not collected due to ethical considerations. Therefore, only the vitreous fluid of post-injection eyes was examined, based on the comparability of the groups. Third, the grouping of DR was not further refined. In particular, NPDR patients with or without DME were not included in this study. Because vitrectomy is not needed in patients with NPDR and DME, no vitreous and intraocular fluid samples could be collected due to ethical considerations. Finally, further research on the mechanisms of the different effects of EPO in DR is needed.

In summary, we found that both of the VEGF and EPO level were significantly increased in PDR patients, which have equal diagnostic value in the prediction of PDR. IVR could reduce the EPO level, but not enough to the normal level. The interaction between EPO and VEGF still needs to be further explored.

DATA AVAILABILITY STATEMENT

The original contributions presented in the study are included in the article/supplementary material, further inquiries can be directed to the corresponding authors.

ETHICS STATEMENT

The studies involving human participants were reviewed and approved by Ethical Review Committee of Beijing Chaoyang Hospital. The patients/participants provided their written informed consent to participate in this study.

AUTHOR CONTRIBUTIONS

Design and conduct of the study by LC, JF, and YT. Collection, management, analysis, and interpretation of the data by LC, JF, YS, FL, FM, YW, WY, and YT. Preparation of the manuscript by LC and JF. Review and final approval of the manuscript by all the authors.

FUNDING

This study was supported by National Natural Science Foundation of China (Nos. 82070948 and 82101142), Beijing Talent Project (No. 2020027), Shunyi District Beijing Science and technology achievements transformation coordination and service platform construction fund (SYGX202010), and Beijing Hospitals Authority Youth Programme (No. QML20190303).

REFERENCES

1. Frank RN. On the pathogenesis of diabetic retinopathy. A 1990 update. *Ophthalmology.* (1991) 98:586–93. doi: 10.1016/S0161-6420(91)32253-X
2. Witmer AN, Vrensen GF, Van Noorden CJ, Schlingemann RO. Vascular endothelial growth factors and angiogenesis in eye disease. *Prog Retin Eye Res.* (2003) 22:1–29. doi: 10.1016/S1350-9462(02)00043-5
3. Roh MI, Kim HS, Song JH, Lim JB, Kwon OW. Effect of intravitreal bevacizumab injection on aqueous humor cytokine levels in clinically significant macular edema. *Ophthalmology.* (2009) 116:80–6. doi: 10.1016/j.ophtha.2008.09.036
4. Jeon S, Lee WK. Intravitreal bevacizumab increases intraocular interleukin-6 levels at 1 day after injection in patients with proliferative diabetic retinopathy. *Cytokine.* (2012) 60:535–9. doi: 10.1016/j.cyto.2012.07.005
5. Zhou M, Chen S, Wang W, Huang W, Cheng B, Ding X, et al. Levels of erythropoietin and vascular endothelial growth factor in surgery-required advanced neovascular glaucoma eyes before and after intravitreal injection of bevacizumab. *Invest Ophthalmol Vis Sci.* (2013) 54:3874–9. doi: 10.1167/iovs.12-11507
6. Bainbridge JW, Mistry A, De Alwis M, Paleolog E, Baker A, Thrasher AJ, et al. Inhibition of retinal neovascularisation by gene transfer of soluble VEGF receptor sFlt-1. *Gene Ther.* (2002) 9:320–6. doi: 10.1038/sj.gt.3301680
7. Ono M. Molecular links between tumor angiogenesis and inflammation: inflammatory stimuli of macrophages and cancer cells as targets for therapeutic strategy. *Cancer Sci.* (2008) 99:1501–6. doi: 10.1111/j.1349-7006.2008.00853.x
8. Pekas NJ, Newton SS. Computational analysis of ligand-receptor interactions in wild-type and mutant erythropoietin complexes. *Adv Appl Bioinform Chem.* (2018) 11:1–8. doi: 10.2147/AABC.S177206
9. Mohan N, Monickaraj F, Balasubramanyam M, Rema M, Mohan V. Imbalanced levels of angiogenic and angiostatic factors in vitreous, plasma and postmortem retinal tissue of patients with proliferative diabetic retinopathy. *J Diabetes Complications.* (2012) 26:435–41. doi: 10.1016/j.jdiacomp.2012.05.005
10. Loukovaara S, Robciuc A, Holopainen JM, Lehti K, Pessi T, Liinamaa J, et al. Ang-2 upregulation correlates with increased levels of MMP-9, VEGF, EPO and TGFbeta1 in diabetic eyes undergoing vitrectomy. *Acta Ophthalmol.* (2013) 91:531–9. doi: 10.1111/j.1755-3768.2012.02473.x
11. Semeraro F, Cancarini A, Morescalchi F, Romano MR, dell'Omo R, Ruggeri G, et al. Serum and intraocular concentrations of erythropoietin and vascular endothelial growth factor in patients with type 2 diabetes and proliferative retinopathy. *Diabetes Metab.* (2014) 40:445–51. doi: 10.1016/j.diabet.2014.04.005
12. Davidovic S, Babic N, Jovanovic S, Barisic S, Grkovic D, Miljkovic A. Serum erythropoietin concentration and its correlation with stage of diabetic retinopathy. *BMC Ophthalmol.* (2019) 19:227. doi: 10.1186/s12886-019-1240-9
13. Watanabe D, Suzuma K, Matsui S, Kurimoto M, Kiryu J, Kita M, et al. Erythropoietin as a retinal angiogenic factor in proliferative diabetic retinopathy. *N Engl J Med.* (2005) 353:782–92. doi: 10.1056/NEJMoa041773
14. Inomata Y, Hirata A, Takahashi E, Kawaji T, Fukushima M, Tanihara H. Elevated erythropoietin in vitreous with ischemic retinal diseases. *Neuroreport.* (2004) 15:877–9. doi: 10.1097/00001756-200404090-00029
15. Katsura Y, Okano T, Matsuno K, Osako M, Kure M, Watanabe T, et al. Erythropoietin is highly elevated in vitreous fluid of patients with proliferative diabetic retinopathy. *Diabetes Care.* (2005) 28:2252–4. doi: 10.2337/diacare.28.9.2252
16. Hernandez C, Fonollosa A, Garcia-Ramirez M, Higuera M, Catalan R, Miralles A, et al. Erythropoietin is expressed in the human retina and it is highly elevated in the vitreous fluid of patients with diabetic macular edema. *Diabetes Care.* (2006) 29:2028–33. doi: 10.2337/dc06-0556
17. Feng J, Li B, Wen J, Jiang Y. Preoperative timing of intravitreal bevacizumab injection for proliferative diabetic retinopathy patients. *Ophthalmic Res.* (2018) 60:250–7. doi: 10.1159/000493640
18. Thomas AA, Feng B, Chakrabarti S. ANRIL: a regulator of VEGF in diabetic retinopathy. *Invest Ophthalmol Vis Sci.* (2017) 58:470–80. doi: 10.1167/iovs.16-20569
19. Bressler SB, Liu D, Glassman AR, Blodi BA, Castellarin AA, Jampol LM, et al. Change in diabetic retinopathy through 2 years: secondary analysis of a randomized clinical trial comparing aflibercept, bevacizumab, and ranibizumab. *JAMA Ophthalmol.* (2017) 135:558–68. doi: 10.1001/jamaophthalmol.2017.0821
20. Xia JP, Liu SQ, Wang S. Intravitreal conbercept improves outcome of proliferative diabetic retinopathy through inhibiting inflammation and oxidative stress. *Life Sci.* (2021) 265:118795. doi: 10.1016/j.lfs.2020.118795
21. Jelkmann W. Effects of erythropoietin on brain function. *Curr Pharm Biotechnol.* (2005) 6:65–79. doi: 10.2174/1389201053167257
22. Martinez-Estrada OM, Rodriguez-Millan E, Gonzalez-De Vicente E, Reina M, Vilaro S, Fabre M. Erythropoietin protects the in vitro blood-brain barrier against VEGF-induced permeability. *Eur J Neurosci.* (2003) 18:2538–44. doi: 10.1046/j.1460-9568.2003.02987.x
23. Liu D, Xu H, Zhang C, Xie H, Yang Q, Li W, et al. Erythropoietin maintains VE-cadherin expression and barrier function in experimental diabetic retinopathy via inhibiting VEGF/VEGFR2/Src signaling pathway. *Life Sci.* (2020) 259:118273. doi: 10.1016/j.lfs.2020.118273

24. Li W, Sinclair SH, Xu GT. Effects of intravitreal erythropoietin therapy for patients with chronic and progressive diabetic macular edema. *Ophthalmic Surg Lasers Imaging.* (2010) 41:18–25. doi: 10.3928/15428877-20091230-03
25. Entezari M, Flavarjani ZK, Ramezani A, Nikkhah H, Karimi S, Moghadam HF, et al. Combination of intravitreal bevacizumab and erythropoietin versus intravitreal bevacizumab alone for refractory diabetic macular edema: a randomized double-blind clinical trial. *Graefes Arch Clin Exp Ophthalmol.* (2019) 257:2375–80. doi: 10.1007/s00417-019-04383-2
26. Mandrekar JN. Receiver operating characteristic curve in diagnostic test assessment. *J Thorac Oncol.* (2010) 5:1315–1316. doi: 10.1097/JTO.0b013e3181ec173d
27. Hoo ZH, Candlish J, Teare D. What is an ROC curve? *Emerg Med J.* (2017) 34:357–9. doi: 10.1136/emermed-2017-206735

Conflict of Interest: The authors declare that the research was conducted in the absence of any commercial or financial relationships that could be construed as a potential conflict of interest.

Publisher's Note: All claims expressed in this article are solely those of the authors and do not necessarily represent those of their affiliated organizations, or those of the publisher, the editors and the reviewers. Any product that may be evaluated in this article, or claim that may be made by its manufacturer, is not guaranteed or endorsed by the publisher.

frontiers in Medicine

REVIEW
published: 15 October 2021
doi: 10.3389/fmed.2021.750586

Gene Therapy in Inherited Retinal Diseases: An Update on Current State of the Art

Alessia Amato, Alessandro Arrigo, Emanuela Aragona, Maria Pia Manitto, Andrea Saladino, Francesco Bandello and Maurizio Battaglia Parodi*

Department of Ophthalmology, Scientific Institute San Raffaele Hospital, Milan, Italy

Background: Gene therapy cannot be yet considered a far perspective, but a tangible therapeutic option in the field of retinal diseases. Although still confined in experimental settings, the preliminary results are promising and provide an overall scenario suggesting that we are not so far from the application of gene therapy in clinical settings. The main aim of this review is to provide a complete and updated overview of the current state of the art and of the future perspectives of gene therapy applied on retinal diseases.

Methods: We carefully revised the entire literature to report all the relevant findings related to the experimental procedures and the future scenarios of gene therapy applied in retinal diseases. A clinical background and a detailed description of the genetic features of each retinal disease included are also reported.

Results: The current literature strongly support the hope of gene therapy options developed for retinal diseases. Although being considered in advanced stages of investigation for some retinal diseases, such as choroideremia (CHM), retinitis pigmentosa (RP), and Leber's congenital amaurosis (LCA), gene therapy is still quite far from a tangible application in clinical practice for other retinal diseases.

Conclusions: Gene therapy is an extremely promising therapeutic tool for retinal diseases. The experimental data reported in this review offer a strong hope that gene therapy will be effectively available in clinical practice in the next years.

Keywords: inherited retinal dystrophies, gene therapy, Stargardt disease, retinitis pigmentosa, choroideremia, X-linked retinoschisis

OPEN ACCESS

Edited by:
Dong Ho Park,
Kyungpook National University Hospital, South Korea

Reviewed by:
Pradeep Venkatesh,
All India Institute of Medical Sciences, India
Chitra Kannabiran,
L. V. Prasad Eye Institute, India

****Correspondence:***
Alessandro Arrigo
alessandro.arrigo@hotmail.com

Specialty section:
This article was submitted to Ophthalmology, a section of the journal Frontiers in Medicine

Received: *30 July 2021*
Accepted: *20 September 2021*
Published: *15 October 2021*

Citation:
Amato A, Arrigo A, Aragona E, Manitto MP, Saladino A, Bandello F and Battaglia Parodi M (2021) Gene Therapy in Inherited Retinal Diseases: An Update on Current State of the Art. Front. Med. 8:750586. doi: 10.3389/fmed.2021.750586

INTRODUCTION

Inherited retinal diseases (IRDs), also referred to as inherited retinal dystrophies, are a clinically and genetically heterogeneous group of neurodegenerative disorders, primarily involving photoreceptors, retinal pigment epithelium (RPE), and/or the choroid. Taken as a whole, IRDs have an estimated global prevalence of about 1 in 2,000 individuals, affecting more than two million people worldwide, and standing out as the leading cause of blindness in the Western working-age population (1).

Inherited Retinal Diseases are classified according to different criteria, including the primarily diseased retinal cell type (rod-dominated disease, cone-dominated disease, generalized retinal degenerations, and vitreoretinal disorders), the age of onset, the progression of visual impairment

over time (stationary or progressive), and the presence or absence of associated systemic features (isolated or syndromic IRDs).

Since the identification of the first gene responsible for an IRD back in 1988 (2), enormous progress has been made in the field of molecular testing, leading to the identification of over 270 disease-causing genes (https://sph.uth.edu/retnet/sum-dis.htm).

Nevertheless, until very recent times, these major diagnostic advances did not go hand in hand with the development of vision-sparing or vision-restoring therapeutic strategies and IRDs have been long accounted as largely incurable diseases.

Over the last decades, this view has changed, as novel therapeutic options started to be explored in preclinical studies, with some of them transitioning to the clinical setting, including gene therapy, cell therapy (3), retinal prosthetics (4), and even direct brain stimulation (5).

In this context, gene-based therapies stand out as one of the most promising frontiers of IRD treatment and the introduction of voretigene neparvovec-rzyl (Luxturna), the first FDA- and EMA-approved gene therapy treatment, paved the way for further research.

The first section of this review is aimed at making the reader familiar with the basic concepts and nomenclature used in the field in retinal gene therapy, while the second section explores in detail those IRDs for which gene-based therapy approaches have made it to the human trial stage. Both sections adopt a combined descriptive and analytic approach, in order to provide a broad overview of the state of the art of gene therapy in IRDs, including discussion of current obstacles and research gaps, as well as a description of the most promising strategies that are being developed to overcome these obstacles and to fill these gaps.

METHODS

We searched all English language and human subject articles using keywords search of MEDLINE library. The keywords included the following: Inherited retinal dystrophies; gene therapy; Stargardt disease (STGD); Retinitis pigmentosa (RP); chorioderemia; X-linked retinoschisis (XLRS); Leber's congenital amaurosis (LCA). All the references were carefully examined by two expert researchers (Alessandro Arrigo, Alessia Amato) which collected and ordered all the relevant information, considering the main topic of this review as expressed in the manuscript title.

SECTION 1: BASICS CONCEPTS IN RETINAL GENE THERAPY

Gene therapy is the treatment of a disease through genetic material (DNA or RNA), that is transferred into the cells of the patient in order to modify gene expression. Since 1990, when the first gene therapy trial was performed in two children with adenosine deaminase (ADA)-deficient severe combined immunodeficiency (SCID) (6), this approach has been studied for and applied to a variety of inherited and acquired disorders, with more than 20 gene therapies officially approved for clinical uses by the drug regulatory agencies from different countries.

The Eye as an Ideal Target for Gene Therapy

Since the dawn of gene therapy, the human eye has always presented itself as an appealing target for a number of reasons.

First, owing to the presence of the so-called blood-retinal barrier (BRB), made up of the tight junctions between the endothelial cells of retinal microvasculature (i.e., inner BRB) and between RPE cells (i.e., outer BRB), the retina is an immune-privileged site, meaning that the introduction of foreign substances is less likely to cause an inflammatory reaction.

Second, the eye is a relatively small and enclosed compartment, which in turn has two important implications: lower doses of therapeutics are needed and the risk of systemic dissemination of the locally administered vector is generally negligible (which, again, minimizes the risk of immune responses).

Moreover, since they are paired organs, it is possible to treat one eye and use the fellow eye as an ideal control to assess the efficacy and safety of the treatment.

Finally, the eye is an easily accessible district, from both a surgical [via subretinal or intravitreal injections (IVIs)] and a diagnostic standpoint, so that non-invasive studies can be performed to monitor function and structure of the treated retinas.

Gene Delivery Systems

With regards to gene therapy, it is crucial to differentiate between *ex vivo* approaches, where patients' cells are collected, cultured, modified, and transplanted back to the same individual (7), and *in vivo* approaches, where a gene-therapy vector is directly administered to a living organism. Though some attempts are being made in the preclinical setting with transplant of gene corrected cells (8), ocular gene therapy relies on an *in vivo* approach, since the genetic material is administered directly into the patient's eye by means of a subretinal or IVI.

Another important distinction is in the way nucleic acids are delivered to their target cells. DNA and RNA are, in fact, large in size and negatively charged molecules, two features that hinder their ability to cross cell membranes. This obstacle is overcome by employing a variety of gene delivery systems, which can be divided into two main categories: *non-viral* and *viral* systems.

Viral Delivery Systems

Viruses are the most used vectors and the process by which they infect and release their genetic content into target cells is termed transduction. Several different recombinant viruses, that are replication deficient, can be used to deliver therapeutic nucleic acids, with differences in terms of cargo limits, integration capabilities, transduction efficiency, cellular tropism, and risk of immune responses.

Adenoviruses (Ads) are a family of DNA viruses that can infect quiescent and dividing cells and replicate in the host nucleus without integrating their genome. Adenoviruses have been largely tested as gene therapy vectors, mainly due to their cargo capacity (approximately 8–36 kb) and ability to transduce many cell types. As far as IRDs are concerned, however, conventional Adenoviral vectors (AVs), constructed

by substituting the E1 region with the transgene cassette of interest (9), had limited success, owing to the expression of some viral genes in the infected target cells, which enhanced immunogenicity and undermined treatment longevity, even in the immune-privileged environment of the human eye. These issues have been partially addressed with second- and third-generation vectors, characterized by progressive stripping of all viral coding sequences and implementation of helper-dependent AVs. However, problems with contaminating helper viruses, vector instability, and replication-competent AVs have been reported (10, 11).

Adeno-Associated Viruses (AAVs) are defective single-strand (ss) DNA parvoviruses with more than 20 integration sites in the human genome. Recombinant AAVs (rAAVs) vectors are by far the most frequently used ones in gene therapy approaches for IRDs, because of their lack of pathogenicity, favorable immunologic profile (since, unlike AVs, they do not carry any virus open reading frame), non-integrating nature in the absence of rep protein (which minimizes the risk of insertional mutagenesis, unlike LVs), ability to provide a stable transgene expression and extended retinal tropism. To date, 13 naturally occurring serotypes of AAV have been isolated from primates (AAV1–AAV13): different serotypes have a different capsid conformation and different properties, especially as far as tropism is concerned. Moreover, AAVs can be modified in several ways, for example by packaging the viral genome bordering the transgene into the capsid of a different AAV serotype, process known as pseudotyping or cross-packaging (e.g., an AAV2/8 vector is a pseudotype in which the genome of AAV2 serotype is packaged into an AAV8 capsid) (12). Both serotype and pseudotype choice are important to optimize vector design for the target disease. To date, the serotypes and pseudotypes that have been used in clinical trials for IRDs include AAV2/5, AAV2/8, and AAV8. The major disadvantage of rAAV vectors is their limited cargo capacity, which cannot exceed 4.7 kb. Although with an apparently reduced photoreceptor transduction efficiency, dual AAV vectors—each of which contains half of a large transgene expression cassette—have been shown to improve retinal phenotype in murine models of IRDs (13–15).

Lentiviruses (LVs) are retroviruses with a larger packing capacity (8 kb), which makes them a compelling alternative to AAV vectors for those IRDs whose causative gene coding sequence exceeds the 4.7 kb limit, such as ABCA4-related Stargardt's disease and MYO7A-related Usher's syndrome type 1B. So far, the retroviral variant of human immunodeficiency virus type 1 (HIV-1) and the equine infectious anemia virus (EIAV) have been studied for IRDs. Lentivirus vectors have two main drawbacks. First, LVs are integrating in nature and genomic integration, if on the one hand leads to a sustained expression of the foreign DNA, on the other hand carries a risk of insertional mutagenesis (16, 17). Such risk may not be justified in the case of IRDs, since in post-mitotic tissues, like the retina, a stable transduction can be achieved even by lentiviral episomes. This limitation can be overcome by employing integration-deficient lentiviral vectors (IDLVs), which have been successfully used in a rodent model of retinal degeneration (18). Second, LVs are capable of effectively transducing RPE cells and only to a lesser extent, which is generally insufficient for therapeutic purposes, differentiated photoreceptors (19, 20).

Non-viral Delivery Systems

Non-viral delivery systems have some advantages over viral delivery systems, including potentially unlimited cargo capacity, simultaneous conveyance of multiple therapeutics, low immunogenicity, and inexpensive manufacturing procedures.

Non-viral delivery systems use physicochemical agents to compact the DNA and/or transport it across the membranes.

Physical methods include, for instance, sonoporation (21), and electroporation (22) (i.e., the use of ultrasound or electricity to temporarily increase cell permeability) and direct injection of DNA into target cells (23), respectively, offering no protection from enzymatic degradation of therapeutic nucleic acids.

Chemical agents, which protect the payload from the action of nucleases, include, among others, cationic liposomes, lipopolyplex, and nanoparticles (NPs) (24–27).

Though some preclinical gene therapy studies have successfully used non-viral DNA systems (28–30), these agents are hard to export to an *in vivo* clinical setting, mainly because of transiency of gene expression (31, 32), ultimately resulting in a relatively inefficient delivery (9).

Administration Routes

At least in part, the success of gene therapy approach depends on its administration route. So far, the ongoing clinical trials for IRDs have relied on two injection modalities (i.e., subretinal and intravitreal), both of which have their strengths and weaknesses.

Subretinal injection (SRI) is adopted in most clinical trials, since it allows for the administration of the vector in close proximity to the most common cell target site (i.e., RPE and photoreceptors). Moreover, SRI places the therapeutic material in a closed immune-privileged compartment, thus diminishing the risk of immune reactions. Of course, SRI is a delicate procedure, requiring a vitrectomy, retinotomy, and the development of a transitory iatrogenic neuroretinal displacement and it is potentially associated with a number of complications, including retinal tears, cataract progression, or retinal/choroidal hemorrhages. With respect to SRI, vitreoretinal subspecialists have reported the utility of *in vivo* real-time monitor of the surgical act through integrated optical coherence tomography (OCT) operating microscope (33).

Intravitreal injection is certainly less invasive and technically challenging and can be performed in a clinic setting, thereby extending the accessibility of gene-based therapies to larger populations. However, while adequately transducing inner retinal cells, such as retinal ganglion cells (RGCs), the intravitreally-administered vectors are far less effective on outer retinal layers, due to dilution in the vitreous cavity and to the inner limiting membrane (ILM) barrier, which is particularly thick in primates. Therefore, in order to compensate for these obstacles and observe a significant therapeutic effect on target cells, much higher doses would have to be injected in a non-immune-privileged site. This, in turn, brings about a significant risk of immunogenicity, not only in the form of potential adverse inflammatory reactions, but

also in the form of neutralizing antibodies, accounting for the need of repeated injections in intrinsically frail retinas.

Apart from these two main administration routes, a third one is currently being studied, that is suprachoroidal delivery, whereby therapeutics are conveyed in the space located between the sclera and the choroid. Though preclinical studies and clinical trials showed a good safety, comparable to that of IVIs, spreading of vectors into the systemic circulation is a potential risk (34–37). Finally, preclinical studies have attempted a sub-ILM approach (38).

Gene-Based Therapies in IRDS: the Strategies

Gene-based therapies can rely on different strategies, depending on the features, and molecular pathogenesis of the diseases being addressed, which can be schematically divided into two main categories:

i. Autosomal recessive (AR) or X-linked recessive (XLR) diseases; when a disease-causing mutation abrogates the normal gene function, it is defined as loss-of-function mutation. In this case, the mechanism underlying the associated disorder is caused by a loss of function, whereby a single copy of the gene (in case of AR inheritance) or the absence of functional alleles (in case of XLR inheritance in hemizygous males) is not sufficient to guarantee sufficient levels of the protein. The best way to address recessively inherited retinal dystrophies is by gene augmentation (or gene replacement).
ii. Autosomal dominant (AD) diseases; these diseases are usually caused by gain-of-function mutations, whereby an aberrant protein is formed, resulting in disruption of cellular or tissue activity, or by a dominant negative effect, in which a defective subunit poisons a macromolecular complex. Gene augmentation alone is not enough to address AD IRDs, which require more sophisticated approaches, broadly classified as forms of gene silencing (or knockdown). Gene silencing can be associated with gene replacement, often by means of dual AAV vectors.

Gene Augmentation

Since its initial conceptualization back in the 1960s (39), the idea of gene therapy was based on the straightforward assumption that monogenic recessive disorders could be cured by replacing a faulty gene with a normal copy of it delivered through therapeutic vectors. This approach is called gene augmentation (or gene replacement) because the synthesis of the protein is augmented and its function, at least partially, restored. The gene of interest can be delivered as DNA or mRNA. Though having the advantage of not requiring delivery into the nucleus, thereby reducing the risk of integration into the host genome, the mRNA platform is far more immunogenic and less stable than the DNA platform, which is therefore the preferred one for ocular gene therapy (40). Most clinical gene therapy trials, as well as the first, and currently only, FDA- and EMA-approved treatment for an IRD, voretigene neparvovec-rzyl (Luxturna), rely on gene replacement, that does not require modification of native DNA and therefore is particularly compelling, owing to its simple design and relative ease of investigation.

Gene Silencing

Gene augmentation is an established approach for recessive monogenic disorders, but it is not suited to AD diseases resulting from pathological gain-of function mutations. In these cases, the therapeutic goal is to prevent the altered gene from expressing and encoding an aberrant protein that would interfere with normal cell function. To do so, it is possible to adopt several different approaches, which, schematically, can act at three levels: DNA, mRNA, and the intermediate process in between them (i.e., transcription).

In all of these cases, the host nucleic acids can be targeted in two ways, that is in a mutation-dependent fashion, whereby specific allele inhibition is sought in order to allow the expression of the wild-type copy of the gene, or in a mutation-independent fashion, in which a combined approach with gene augmentation is mandatory, since both copies of the gene (the mutated and the functional one) are silenced and replaced by a non-silenced wild-type form of it. Although allele-specific strategies do not disrupt the endogenous wild-type genome, allele-independent approaches are more far more practical since they don't have to be customized for specific disease-causing mutations. Allele-independent strategies, however, require the expression of both nucleic acid molecules in the same vector and are therefore limited by packaging issues.

DNA-Based Therapies (Genome Editing)

To date, the CRISPR/Cas9 system is considered the most advanced genome editing tool. This system consists of the Cas9 endonuclease, delivered into target cells in conjunction with a guide RNA (gRNA), which is able to cut the genome at any desired genomic location. The double-strand breaks (DSBs) created by the enzyme subsequently activate one of the DNA repair pathways: non-homologous end joining (NHEJ), homology-directed repair (HDR), or microhomology-mediated and joining (40). The development of the homology-independent targeted integration (HITI) strategy, that relies on NHEJ rather than HDR, enabled gene editing in the retina, since post-mitotic cells lack HDR, and was first used in a rat model of MERTK-related RP, with structural and functional improvements (41).

Other than for strict genome editing, the CRISPR/Cas9 can also be used as part of a gene silencing strategy to inactivate mutant alleles causing a toxic gain-of-function, or as part of a splicing modulation approach to prevent the inclusion of pseudoexons (i.e., deep-intronic sequences erroneously recognized as exons due to DNA mutations) that would result in the synthesis of an aberrant protein. The CRISPR/Cas9-based transcript degradation approach has been successfully used in studies on autosomal dominant retinitis pigmentosa (adRP) associated with rhodopsin mutations (RHO-adRP) (42–45), while the latter strategy of restoring splice defects has been applied to a deep intronic mutation of CEP290 in preclinical models (46).

mRNA Silencing

mRNA silencing strategies rely on a variety of antisense inhibitors (i.e., nucleic acid molecules that are complementary to and hybridize with protein-coding mRNAs) and function either by clearing mRNA molecules or by repressing their translation. mRNA silencing strategies include:

Ribozymes. Ribozymes are RNA molecules able to catalyze a chemical reaction in the absence of proteins, which can be used to promote site-specific cleavage of a target phosphodiester bond in order to inhibit gene expression (47). Ribozymes have been the first RNA-based therapeutic strategy investigated in IRDs (48). This approach, however, has been largely abandoned and replaced by newer RNA-based technologies, mainly because the recognition sequence of these molecules are highly represented in the human genome, with a consequent risk of off-target effects, and because of the computational complexity of identifying mRNA cleavage sites (49).

Small Interfering RNAs. RNA interference (RNAi) is another post-transcriptional gene silencing technology based on an evolutionary conserved pathway (50, 51). The effectors of RNAi, called small interfering RNAs (siRNAs), are 21–23 nucleotide-long double-stranded (ds) RNA molecules able to inhibit gene expression by binding to specific mRNAs. These siRNAs can be either naturally obtained in the presence of long pieces of dsRNA, which—for gene therapy purposes—are delivered by DNA vectors and cleaved by an RNase III enzyme called Dicer (52), or can be synthetically produced and directly introduced into the cells (51), the latter approach being less immunogenic, since long ds-RNAs can trigger an innate immune response (53). Unlike ribozymes, whose nucleolytic activity is independent of proteins, siRNAs do not directly take part to complementary mRNA degradation. Instead, siRNAs, once in the cytoplasm of the target cell, are incorporated in the so-called RNAi-induced silencing complex (RISC), which contains both the helicase that unwinds the ds-siRNA into its sense and antisense strands and the endonuclease Argonaute-2. The latter enzyme is in charge of clearing the sense strand of the siRNA molecule and the target mRNA sequence, the access to which is guided by the complementarity to the antisense strand (54). Just like with ribozymes, off-target effects are a major obstacle in the translation to the human clinics, since they can induce a toxic phenotype in target cells, especially in the presence of specific motifs (55); new computational methods able to screen candidate siRNAs can help overcome such obstacles (56). Another possible side effect is the elicitation of immune responses, which is more likely to occur when certain sequences are present (57). Both the above-described post-transcriptional silencing strategies (i.e., ribozymes and RNAi) have been successfully used in animal models of IRDs, with particular reference to adRP associated with rhodopsin mutations (58–61), providing proof-of-concept for RNA-based retinal gene therapies.

Antisense Oligonucleotides. Antisense oligonucleotides (AONs) are small DNA or RNA molecules that can be designed complementary to their target mRNAs (62). Over the last years, AONs have been the object of increasing interest among retinal gene therapists, since they represent the only approach, other than gene augmentation, that has made it to the clinical setting (see section 2: Gene therapy in IRDS).

Depending on their chemical properties, AONs can display two distinct mechanisms.

First, they can act as authentic gene silencers, by mediating, similarly to siRNAs, degradation of target transcripts in a RNase H1-dependent fashion (63). This mechanism has been studied *in vitro* for a NR2E3 variant underlying adRP (64) and *in vivo* for RHO-adRP, both in the preclinical and clinical settings (65).

Other than for knockdown purposes, AONs can also be used as pre-mRNA splicing modulators, an interesting application in the field of IRDs, since up to 15% of all retinal degeneration-causing mutations affect the splicing machinery (66). In this context, AONs generally promote exon skipping, meaning that they bind to target pre-mRNA sequences, and block the recruitment of splicing factors. This approach proves particularly useful when exclusion of pseudoexons is sought, as in the case of CEP290-related LCA (see section 2: Gene therapy in IRDS), which at present stands out as the most advanced application of this technology, having reached phase III of clinical evaluation (NCT03913143). Though promising proof-of-concept studies have been developed for many other genes, such as OPA1, CHM and ABCA4 (67–72), the only other IRD-causing gene whereby the AON-based approach has been translated to the clinics is USH2A (73), for which—following the success of the phase 1/2 trial (NCT03913143)—two final stage registration trials are planned to start by the end of 2021.

Despite the unquestionable advantages of RNA therapeutics over other gene-based strategies, such as the titratability and affordability of the employed molecules, the reversibility of their effects, and the non-genome altering approach, some major challenges still lie ahead of this field. One of such challenges is related to the instability of naked nucleic acids, which are promptly degraded by endonucleases (74), resulting in a time-limited effect. To avoid enzymatic clearance of antisense molecules, two strategies can be adopted. The first strategy is chemical modification of the nucleic acids, in order to make them endonuclease-resistant, as it has been done with both siRNAs and with first-, second-, and third-AONs (75–80). The second approach is to package these therapeutic molecules inside vectors, either viral (81), thus requiring a SRI, or non-viral (82), allowing for repeated, though sufficiently long-lasting, IVIs. As a matter of fact, in a recent study on a mouse model of CEP290-LCA, IVI injection of second-generation AONs compared to SRI of AAV-packaged AONs, while exhibiting comparable duration of effect (approximately 1 month), turned out to be more effective (81). This is probably due to the fact that chemically modified AONs are more efficiently taken up by cells compared to AAVs, further underscoring the importance of developing IVI-based approaches.

Transcriptional Silencing

Therapeutic strategies for gain-of-function mutations mainly rely on DNA-based technologies, such as the CRISPR/Cas system, and

on RNA silencing, thereby acting upstream and downstream of the transcription process.

Over the last decade, efforts have been made to target the intermediate step between DNA and RNA, that is the process by which genetic sequences are used as templates to assembly pre-mRNA transcripts.

In the field of IRDs, three different mutation-independent transcriptional repression strategies have been developed and successfully applied to preclinical models of RHO-adRP.

The first of these strategies employed zinc finger-based artificial transcription factors (ZF-ATFs) targeting the human rhodopsin promoter to achieve, in a mouse model of adRP, transcriptional silencing of both wild-type and mutated RHO alleles in a mutation-independent fashion, which was followed by gene replacement of the endogenous RHO copies (83).

The same group showed that *in vivo* AAV-mediated delivery of a modified version of a synthetic transcription factor (TF), uncoupled from its repressor domain and designed to bind a 20-bp DNA sequence motif (ZF6-cis sequence), could block RHO expression in living porcine retina without significant genome-wide transcript perturbations (84).

Based on these results, the authors went on to further unveil the potential of TF-based transcription silencing, this time by delivering to rods an ectopic TF (i.e., a TF which is normally not expressed by rods) with a DNA-binding preference for the ZF6-cis sequence photoreceptors of pigs, resulting in suppression of RHO with limited off-target effects in a mouse and porcine retinas (85).

Taken together, these data support the role of transcriptional silencing as a promising novel mode to treat gain-of-function mutations in autosomal dominantly inherited IRDs.

Non-targeted Gene Therapies

With over 270 genes associated with IRDs, developing mutation-specific or even gene-specific approaches becomes challenging. In this context, the role of non-targeted gene therapy is to provide alternative strategies, aimed at improving vision independently of the causative gene (86). Attempts have been made by delivering via AAV vectors molecules capable of prolonging photoreceptor cell survival, including neurotrophic factors, such as ciliary neurotrophic factor (CNTF), glial cell line-derived neurotrophic factor, basic fibroblast growth factor and rod-derived con viability factor, and anti-apoptotic agents, such as X-linked inhibitor of apoptosis (87–92). Other than CNF, whose efficacy was rather modest (93), none of these approaches have been tested in humans so far.

As an alternative mutation-independent strategy, optogenetics delivered as non-targeted gene therapy for advanced RP is also being tested. In this case, the assumption is that inducing expression of light sensitive opsins in bipolar or RGCs could activate the visual pathway even in the absence of viable photoreceptors (94–97). There are three ongoing clinical trials using optogenetics in RP patients, RST-001 (NCT02556736), GS030 (NCT03326336), and BS01 (NCT04278131), while one phase 1/2 clinical trial, vMCO-I, has been recently completed (NCT04919473).

SECTION 2: GENE THERAPY IN IRDS

Gene Therapy in Leber Congenital Amaurosis

Leber congenital amaurosis represents a group of IRDs, with an estimated prevalence of 2–3/100,000, characterized by four clinical milestones: severe and early visual impairment (usually occurring by the 6th week of life), sensory nystagmus (an indirect manifestation of the low fixation ability), amaurotic pupils (an expression of the poor retinal sensitivity from the retina to the brainstem), and non-recordable electroretinography (ERG) responses (98). Other frequent phenotypic features include high refractive errors, photophobia, nyctalopia, and the so-called oculodigital sign of Franceschetti, consisting of a repetitive, deep rubbing of the eyes. Association between LCA and keratoconus and cataracts, as well as with a wide range of systemic manifestations, including intellectual disability, olfactory dysfunction, stereotypical movements, and behaviors has also been reported (98–102). From a clinical standpoint, LCA exhibits an extremely heterogeneous phenotype, ranging from an essentially normal retina to variable degree of vessel attenuation, bone spicule pigmentation, pseudopapilledema, macular coloboma, salt and pepper pigmentation, yellow confluent peripheral spots, white retinal spots, preserved para-arteriolar RPE (PPRPE) and Coats reaction, with some gene-specific features (98–105).

A milder form of the same disease spectrum has been described using several different expressions, including early-onset severe retinal dystrophy (EOSRD), severe early childhood-onset retinal dystrophy (SECORD) and early-onset RP (106). Unlike LCA, which is present at birth or within the first weeks of life and is associated with nystagmus, poor pupillary responses and abolished ERGs, EOSRD/SECORD has a slightly later onset (after infancy but before 5 years of age) and is characterized by a better residual visual function and ERG responses (106). Nevertheless, large genotypic overlap exists between these two disease entities, though certain genes are more frequently associated with LCA and others with EOSRD/SECORD (106).

Genetic Features

Leber congenital amaurosis is mostly inherited in an AR fashion, though for some genes, like CRX, AD patterns have been reported (107). So far, more than 25 genes, overall accounting for at least 80% of all LCA cases, have been described, the most common of which are listed in **Table 1** (106–126). Accordingly with the current literature, the most common LCA-causing genes are, in descending order, *GUCY2D, CEP290, CRB1, RDH12,* and *RPE65* (1, 3, 4). LCA-associated genes encode proteins, whose functions can be divided into four main categories: phototransduction (e.g., *GUCY2D*), photoreceptor morphogenesis (e.g., *CRB1* and *CRX*), retinoid cycle (e.g., *RDH12* and *RPE65*), and ciliary transport processes (e.g., *CEP290*) (98).

Gene Therapy in RPE65-LCA

The *RPE65* gene product plays a critical role in the retinoid cycle, so that *RPE65* mutations affect visual function before photoreceptor structure. Therefore, in contrast with many

TABLE 1 | Main genes associated with the onset of LCA.

Gene	Protein	Function	Molecular weight (kDa)	Reference
IMPDH1	Inosine 5′-monophosphate dehydrogenase 1	Guanine synthesis	∼55	(5)
CRX	Cone–rod homeobox	Photoreceptor morphogenesis	∼32	(6)
CRB1	Crumbs homolog 1	Photoreceptor morphogenesis	∼154	(7)
GDF6	Growth differentiation factor 6	Photoreceptor morphogenesis	∼14	(8)
SPATA7	Spermatogenesis-associated protein 7	Photoreceptor ciliary transport	∼68	(9)
LCA5	Libercilin	Photoreceptor ciliary transport	∼80	(10)
RPGRIP1	Retinitis pigmentosa GTPase regulator-interacting protein 1	Photoreceptor ciliary transport	∼147	(11)
CEP290	Tubby-like protein	Photoreceptor ciliary transport	∼290	(12)
TULP1	Tubby-like protein	Photoreceptor ciliary transport	∼70	(13)
CLUAP1	Clusterin associated protein 1	Photoreceptor ciliary transport	∼48	(14)
IQCB1	Intraflagellar transport 140 chlamydomonas homolog protein	Photoreceptor ciliary transport	∼69	(15)
IFT140	Intraflagellar transport 140 chlamydomonas homolog protein	Photoreceptor ciliary transport	∼165	(16)
ALMS1	ALMS Protein	Photoreceptor ciliary transport	∼460	(17)
GUCY2D	Guanylate cyclase-1	Phototransduction	∼120	(18)
AIPL1	Aryl-hydrocarbon-interacting-protein-like 1	Phototransduction/protein biosynthesis	∼43	(19)
RD3	Protein RD3	Protein trafficking	∼70	(20)
RPE65	Retinoid isomerase	Retinoid cycle	∼65	(21)
RDH12	Retinol dehydrogenase 12	Retinoid cycle	∼38	(22)
LRAT	Lecithin:retinol acyl transferase	Retinoid cycle	∼25	(23)

other IRDs in which visual dysfunction results from rods and cones death, RPE65-LCA patients retain viable cells for years before significant degeneration becomes evident. This structure-function dissociation makes RPE65-related retinal dystrophies a particularly compelling target for gene replacement strategies.

Proof of principle for retinal gene therapy came from the pioneering studies conducted in the early 2000's on a peculiar canine model (127, 128). These preclinical studies employed a subset of Briard dogs with a homozygous 4-bp deletion in the *RPE65* gene resulting in a premature stop codon, thereby appearing to be an excellent spontaneous model for human RPE65-related LCA (129). These studies reported, after a single SRI of AAV-mediated *RE65*, an improvement in blue light stimulated dark-adapted ERGs and cone flicker, pupillometry, and VEP in the injected eyes and in qualitative behavioral assessments in the treated dogs, which were stable 3 years after the procedure (127, 128). Further evidence of the efficacy of this approach came from the naturally *Rpe65*-mutated rd12 murine model and from the genetically built $Rpe65^{-/-}$ knockout mouse (130, 131). Following the success of animal studies, clinical trials were initiated in 2007 by groups from the UK and the US (132–134), culminating in the first FDA- and EMA-approved AAV-based retinal gene therapy drug, voretigene neparvovec-rzyl (Luxturna) (135). Follow-up studies revealed stable improvements in most patients, peaking at 6–12 months after injection (136–138), but observational trials aimed at evaluating the long-term effects of Luxturna are still ongoing (NCT03602820, NCT01208389).

Gene Therapy in CEP290-LCA

The protein encoded by the *CEP290* gene localizes to the photoreceptor connecting cilium and, besides microtubule-associated transport across the cilium, is required for outer segment (OS) regeneration and phototranducsion. The most common *CEP290* mutation is the so called IVS26 c.2991+1655A>G mutation (p.Cys998X), an adenine to guanine point mutation located within intron 26 creating a novel splice donor site, which results in the inclusion of a pseudoexon in the mRNA and in the consequent creation of a premature codon stop. This mutation has been addressed by means of two innovative approaches.

The first strategy relies on a CRISPR/Cas9 system, called EDIT-101, consisting of an AAV5 vector used to deliver the *Sthaphylococcus aureus* Cas9 and CEP290-specific gRNAs with no identified off-targets. EDIT-101, or a non-human primate (NHP) surrogate vector, were shown to restore normal splicing *in vitro* (in photoreceptor-containing retinal explants) and *in vivo* (in mice and NHPs) with no serious adverse events (139).

The second strategy exploits the AON technology to remove the 128-bp pseudoexon included in the IVS26-mutated CEP290 mRNA transcript. Preclinical evidence of the efficacy of the AON designed to restore IVS26 splicing defects, called QR-110, came from *in vitro* studies on LCA10 fibroblasts (140).

In the wake of these results, IVI of this oligonucleotide was successfully attempted in NHP s (141), finally reaching the clinical setting with a phase I/II trial showing vision improvement at 3 months with no complications in LCA type10 patients treated with multiple doses of intravitreal QR-110 (142). A phase II/III multiple-dose clinical trial is still ongoing and is aimed at evaluating efficacy, safety, tolerability, and systemic exposure of QR-110 administered via IVI in patients with LCA type 10 due to *CEP290* c.2991+1655A>G mutation after 24 months of treatment (NCT03913143).

Gene Therapy in Other Forms of LCA

Although so far only two LCA-associated genes have made it to the human trial stage, for many other disease-causing genes, including *GUCY2D*, *CRB1,* and *RDH12*, preclinical studies are underway, showing promising results (143–148).

Gene Therapy in Retinitis Pigmentosa

The term RP refers to a heterogeneous group of IRDs, with variable phenotypes—ranging from mild nyctalopia to total blindness—and genotypes—with over 100 identified RP-causing genes. All inheritance patterns are possible, including AD, AR, or X-linked disorders, whereas maternal (mitochondrial) inheritance is very rare in RP (149). The estimated prevalence of this multiform condition is 1 in 3,000–7,000 individuals (149, 150). In the initial stages, rod photoreceptors degenerate, resulting in night blindness, with difficulty seeing in dim light and adapting to changes in light sensitivity, and in visual field (VF) constriction, starting from the mid-periphery and extending toward the center, eventually leading to complete loss of peripheral vision, the so-called "tunnel vision" (151). With disease progression, also cones become affected and visual acuity (VA) declines. From a clinical standpoint, the fundus appearance of RP features a typical triad, consisting of attenuated retinal vessels, intraretinal pigment deposits with a bone spicule configuration, and optic disc pallor (**Figure 1**).

Though ERG has been long used to help diagnose and monitor RP, nowadays multimodal imaging is of crucial importance for both initial assessment and follow-up of RP patients. Fundus autofluorescence (FAF), shows a coexistence of hypoautofluorescent regions (correlated to the masking effect of pigment deposits or to the presence of areas of RPE atrophy) and hyperautofluorescent regions (usually in the form of an hyperautofluorescent perifoveal ring) (152, 153). Optical Coherence Tomography shows decreased thickness of the outer nuclear layer (ONL) and loss of external limiting membrane (ELM) and ellipsoid zone (EZ), all of which were shown to correlate well with VF defects (154, 155). More recently, a novel imaging technique, optical coherence tomography angiography (OCTA), has been implemented to explore the existence and potential clinical relevance of different retinal and choroidal vascular patterns in RP patients (156, 157).

Considering the heterogeneity of RP, specific genetic features and currently ongoing clinical trials will be discussed separately for each relevant RP-associated gene.

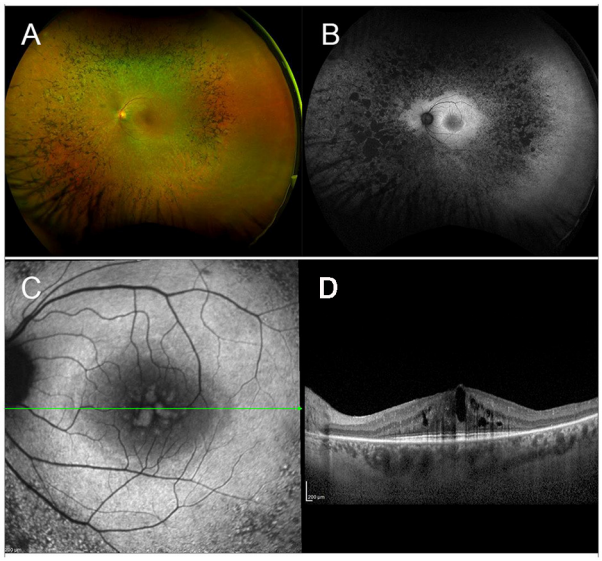

FIGURE 1 | Multimodal imaging in RP. **(A)** Ultra-wide field retinography displays the typical triad: optic disc pallor, vessel attenuation, and bone spicule pigmentation. **(B)** Fundus autofluorescence shows the typical perifoveal ring of hyperautofluorescence and multiple hypoautofluorescent regions, corresponding to the pigment deposits, and to the areas of RPE atrophy. **(C)** Blue fundus autofluorescence shows a petaloid hyperautofluorescent pattern, compatible with a cystoid macular edema. **(D)** Structural OCT confirms the presence of intraretinal cysts.

RHO-RP

Genetic Features

The rhodopsin (RHO) gene was the first identified RP-causing gene (158, 159). Human RHO is a 6.7 kb-long DNA sequence, containing five exons and mapping on the long arm of chromosome 3 (3q22.1). It encodes rhodopsin, a 348-aa light-sensitive G-protein coupled receptor (GPCR) expressed from rod OSs disks. Rhodopsin is the protein that initiates the phototransduction cascade upon absorption of photons by its chromophore, 11-cis retinal. The vast majority of RHO mutations show an AD inheritance pattern (RHO-adRP), accounting for 25% of adRP cases and leading to RP with a toxic gain-of-function or a dominant-negative effect of the mutated protein (160). However, few recessively inherited mutations are described and have been reported to cause a milder phenotype (161).

Gene Therapy

As previously discussed (see Section 1: Basics concepts in retinal gene therapy), IRDs related to a toxic gain-of-function cannot be treated with a gene replacement approach. In these cases, in fact, there is a double therapeutic goal of silencing the mutant allele and increasing the wild type to mutant gene expression ratio. These goals can be achieved in an allele-specific or in a mutation-independent fashion, both of which have their pros and cons (see Section 1: Basics concepts in retinal gene therapy). In Section 1: Basics concepts in retinal gene therapy, we provided an overview of the current gene therapy strategies, and we described the three

main targets of gene silencing approaches, all of which have been investigated in RHO-adRP, as reported in the excellent paper by Meng et al. (162).

As far as DNA-based therapies are concerned, the CRISPR/Cas9 system technology has been successfully applied to animal models and human retinal explants of RHO-adRP, both in an allele-specific (43–45) and in a mutation-independent way (42, 163).

Post-transcriptional RNA-based silencing strategies have perhaps been the most promising for RHO-adRP.

A dual vector short hairpin RNA (shRNA) suppression and replacement therapeutic strategy for RHO-adRP, named RHONova, proved to restore function and preserve morphology in a murine model of the disease independently of the mutation and received orphan drug designation in Europe and in the US, although there has been no publicly available updates on its clinical development (162–166). More recently, another RNAi-based mutation-independent strategy has been attempted, this time by means of a single AAV2/5 vector expressing both a shRNA targeting human RHO and a healthy copy of the gene, modified so as to be shRNA-resistant, with encouraging morpho-functional results (167). Further preclinical studies are currently being conducted on this gene therapy product candidate, now called IC-100, with a phase 1/2 clinical trial expected to begin by the end of 2021.

Antisense oligonucleotides have been used to promote allele-specific knock-down of P23H-mutant mRNA in a murine model of RHO-adRP, without affecting wild-type RHO expression. This approach yielded excellent preclinical results and transitioned to the clinical stage, with a phase 1/2 clinical trial currently ongoing and is scheduled to conclude in October 2021.

Finally, transcriptional repression strategies have also been attempted in the preclinical setting (83–85), as reported in Section 1: Basics concepts in retinal gene therapy of this review.

RPGR-XLRP

Genetic Features

X-linked retinitis pigmentosa (XLRP) is responsible for 5–20% of all RP cases. So far, three disease-causing genes have been identified: RP GTPase Regulator (*RPGR*) at the RP3 locus, retinitis pigmentosa 2 (*RP2*) at the RP2 locus and the oral-facial-digital syndrome type 1 (*OFD1*) (168–170).

The *RPGR* gene, whose mutations account for 70–90% of XLRP cases, encodes *RPGR*, a key protein in photoreceptor ciliary function. *RPGR* transcripts undergo a complex splicing process and generate constitutive variants, expressed by most tissues, and *ORF15* variants, which are highly specific for the retina, by using alternative polyadenylation sites and splicing sites (171, 172). While mutations in the exons unique to the constitutive variant are almost exclusive of XLRP, mutations in the *ORF15* exon, considered a mutational hot spot, are also found in cone dystrophy (COD) and cone-rod dystrophy (CORD) pedigrees (173).

X-linked retinitis pigmentosa is regarded as the most aggressive genetic subtype of RP, with hemizygous males exhibiting a particularly severe phenotype, characterized by early onset and rapid progression, eventually resulting in legal blindness by the end of the third decade of life. Heterozygous female carriers usually show some degree of fundus and FAF alterations, with an associated visual function that can range from 20/20 BCVA to no light perception (174–178). The variable extent of retinal involvement in female carriers could be explained by the dominant nature of some *RPGR* mutations or could be the result of a random skewed X inactivation phenomenon.

Gene Therapy

X-linked retinitis pigmentosa is the IRD with the highest number of ongoing gene therapy clinical trials, all of which rely on a AAV-mediated gene replacement strategy.

Before it was possible to transition to the clinics, *RPGR* canine models of XLRP (XLPRA1 and XLPRA2) treated with subretinal AAV2/5 full-length human RPGRex1-ORF15 provided preclinical evidence of the beneficial effects of this approach (179).

Moving on to the clinical setting, Nightstar Therapeutics/Biogen recently published the initial results at 6 months of its phase 1/2 dose escalation trial (NCT03116113) (180). Eighteen patients divided in six cohorts of three patients received increasing concentrations of AAV8.coRPGR vector (from $5 \times 1{,}010$ to $5 \times 1{,}012$ gp/ml) by means of a SRI. The primary outcome of the study was safety and initial results showed no significant concerns aside from subretinal inflammation in patients at the higher doses, that resolved after steroid treatment. Moreover, some secondary endpoints suggest sustained reversal of VF loss.

Another ongoing phase 1/2 trial, sponsored by MeiraGTx, is employing a SRI of an AAV2/5 vector as part of an open label, non-randomized, dose-escalation intervention followed by randomized dose confirmation against a control arm (NCT03252847). The same company recently initiated a phase 3 trial (NCT04671433).

Applied Genetic Technologies Corp. is sponsoring a phase 1/2 clinical trial (NCT03316560) to evaluate the safety and efficacy of SRI of rAAV2tYF-GRK1-RPGR and a phase 2/3 trial, which is scheduled to begin in the second half of 2021 (NCT04850118).

Finally, 4D Molecular Therapeutics launched the first clinical trial attempting to treat XLRP through a single intravitreal delivery of 4D-125, a drug product developed for gene therapy, which comprises an AAV capsid variant (4D-R100) carrying a codon-optimized human RPGPR transgene (NCT04517149).

PDE6B-RP

Genetic Features

PDE6B encodes the beta-subunit of the rod cGMP-phosphodiesterase, an enzyme that plays a key role during phototransduction. Mutations in *PDE6B* cause 2–5% of autosomal recessive retinitis pigmentosa (arRP) and rarely AD congenital stationary night blindness (CSNB) (181, 182).

Gene Therapy

After preclinical evidence that intraocular administration of the normal *PDE6B* gene preserved retinal morphology and functions in a mouse model of RP, a phase 1/2 clinical trial

for subretinal administration of AAV2/5-hPDE6B was recently initiated (NCT03328130).

PDE6A-RP

Genetic Features

PDE6A encodes the alpha-subunit of the rod cGMP-phosphodiesterase. The loss of this enzyme function leads to chronically elevated cGMP levels, which cause an increased calcium inflow into the cell and thereby the hyperactivation of cell death pathways. Mutations in *PDE6A* cause 2–5% of arRP (183).

Gene Therapy

Patients with biallelic mutations of the *PDE6A* genes usually exhibit a mild to moderate phenotype, with an elevated degree of symmetry between the two eyes and with a relatively slow diseases course, though most patients have constricted VF by their fourth decade of life (184). Considering these features, PDE6A-related RP stands out as a compelling candidate for those gene therapy approaches requiring viable rods.

At the end of 2020, a phase 1/2 clinical trial sponsored by STZ eyetrial was commence and is currently open to enrolment (NCT04611503).

RLBP1-RP

Genetic Features

RLBP1 (also known as *CRALBP*) encodes cellular retinaldehyde-binding protein, which acts primarily as an acceptor of 11-cis retinal during the isomerization step of the visual cycle. Mutations in *RLBP1* can cause three early-onset forms of arRP: retinitis punctata albescens, characterized by round punctate white deposits scattered throughout the entire retina in young patients with progression to more severe phenotypes in older individuals, Newfoundland rod-COD and Bothnia dystrophy, the latter two associated with a more severe prognosis. *RLBP1* mutations can also cause fundus albipunctatus, which is considered as a subtype of CSNB (185–188).

Gene Therapy

Proof of concept of the efficacy of gene replacement in *RLBP1*-related RP came from a study conducted on a mouse model of the disease, in which self-complementary AAV8 vector carrying the gene for human RLBP1 under control of a short RLBP1 promoter (scAAV8-pRLBP1-hRLBP1, or CPK850) was delivered via SRI, resulting in an improved electroretinographic response (189). The success of the preclinical study, followed by the publication of non-clinical safety data by the same group of authors (190), paved the way to clinical trials. To date, there is one ongoing phase 1/2 trial opened for recruiting, aimed at exploring the maximum tolerated dose, safety, and potential efficacy of CPK850 delivered through a single SRI. The trial is scheduled to end in 2026.

MERTK-RP

Genetic Features

MERTK encodes the widely expressed tyrosine-protein kinase Mer, a receptor tyrosine kinase involved in a signal transduction pathway that regulates numerous cellular processes. In the retina, it is expressed in the RPE and it is involved in the phagocytosis of rod OSs. *MERTK* mutations are responsible for arRP, with onset within the second decade of life and progressive decline of VA, which is often reduced to light perception before age 50 (191, 192).

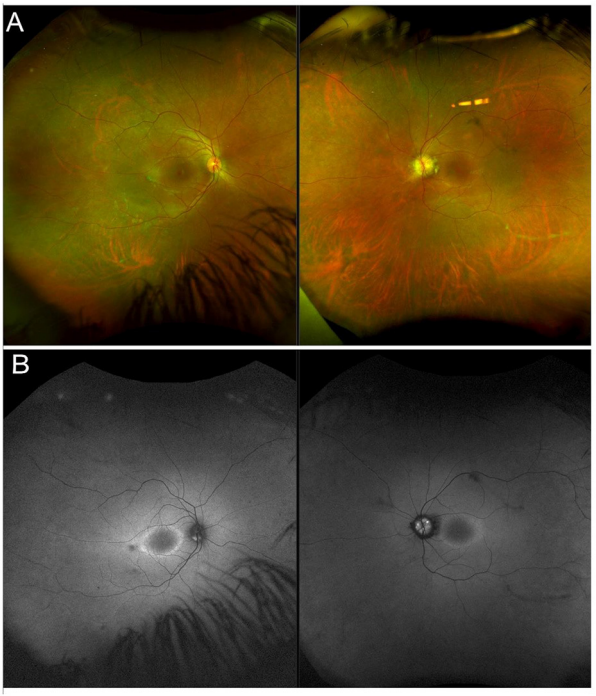

FIGURE 2 | Multimodal imaging in a patient with a non-syndromic USH2A-related form of RP. **(A)** Ultra-wide field retinography shows near complete absence of pigment bone spicules. **(B)** Fundus autofluorescence displays the typical perifoveal ring of hyperautofluorescence.

Gene Therapy

An open-label, dose escalation phase 1 trial of AAV2-mediated gene augmentation therapy for RP caused by *MERTK* mutation was conducted in Saudi Arabia (193). The SRI of the vector was not associated with major side effects, and 50% of patients (three out of six) demonstrated improved VA, though only one of them maintained this improvement after 2 years of follow-up.

Gene Therapy in Usher Syndrome (RP)

Usher syndrome is defined by the association of AR deafness (most commonly congenital) and retinopathy indistinguishable from typical RP (**Figure 2**). Usher syndrome is the most common RP-associated syndrome, accounting for almost 20% of all RP patients. Depending on the severity of the hearing loss, Usher syndrome is divided into three clinical subtypes (194).

Usher syndrome type 1 (the most common form) is characterized by profound, congenital sensorineural deafness (with consequent prelingual deafness or severe speech impairment), vestibular symptoms and childhood onset retinopathy.

Usher syndrome type 2 presents with congenital partial, non-progressive deafness, absence of vestibular symptoms, and milder and later-onset retinopathy.

Finally, Usher syndrome type 3 is characterized by progressive deafness starting in the second to fourth decade, adult-onset retinopathy and hypermetropic astigmatism.

Genetic Features

To date, 16 genes associated to Usher syndrome have been identified, two of which are good candidates for gene therapy and deserve a more detailed description.

The first of such genes is *MYO7A*. *MYO7A* encodes myosin VIIA, involved in in transport of melanosomes and phagosomes along actin filaments in the RPE and of opsin and other phototransduction proteins in photoreceptors (195). Mutations in *MYO7A* are associated with Usher Syndrome type 1B (*USH1B*).

The second relevant gene is *USH2A*, which encodes usherin. Mutations in *USH2A*, besides being the commonest association with type 2 Usher syndrome (80%), are the most frequent cause of AR non-syndromic RP (10–15%) (196–199). Clear genotype-phenotype correlations for *USH2A* mutations are not easy to establish. Generally, however, nonsense mutations, frameshifts mutations, or canonical splice site mutations in *USH2A*, either biallelic or combined with one missense allele, are associated with Usher syndrome type II, whereas the association of two missense mutations tends to result in non-syndromic RP (200). Of note, a peculiar feature of both non-syndromic and syndromic *USH2A*-related retinopathy is the fact that fundoscopy generally shows mild or no pigment deposits.

Gene Therapy

The MYO7A gene has 49 exons and spans approximately 87 kb of genomic sequence on chromosome 11q13.5, therefore significantly exceeding the cargo capacity of AAV vectors. For this reason, attempts have been made to deliver *MYO7A* in the *shaker1* mouse model of Usher syndrome type 1B by means of UshStat, an EIAV lentiviral vector carrying the wild-type gene (EIAV-CMV-MYO7A) (201). Later on, Sanofi sponsored two phase 1/2 clinical trials, one of which is currently ongoing (NCT02065011), while the other has been stopped not for safety reasons (NCT01505062).

As far as *USH2A* is concerned, though being associated with recessive IRDs, a number of factors, including poor understanding of the physiological function of usherin and the *USH2A* gene size (15 kb), stand in the way of gene replacement strategies. Therefore, in order to develop an alternative approach, great interest was focused on a subset of mutations on exon 13 resulting in aberrant pre-mRNA splicing, which leads to the inclusion of a pseudoexon in the mature *USH2A* transcript. Since exon 13 consists of a multiplier of three nucleotides, skipping this exon does not disturb the open reading frame and likely results in the synthesis of a shorter protein with predicted residual function. This is the rationale behind the employment of AONs in an AR IRD. Encouraging results came from preclinical studies (73, 202) and ProQR Therapeutics sponsored the STELLAR phase 1/2 clinical trial (NCT03780257), whose purpose is to evaluate the safety and tolerability of a single intravitreal administration of AONs (QR-421a) in subjects with RP due to mutations in exon 13 of the *USH2A* gene. Enrolled patients receive one single IVT injection of QR-421a or sham-procedure in one eye (subject's worse eye) and are then followed up for 24 months. In March 2021, ProQR announced positive results from clinical trial of QR-421a and planned to start two phase 2/3 trials (SIRIUS and CELESTE).

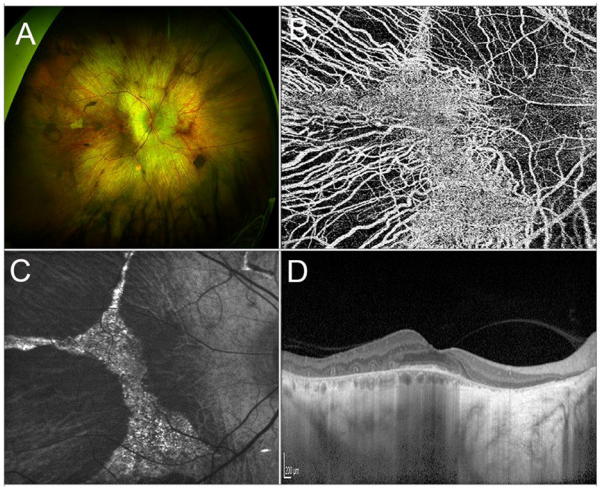

FIGURE 3 | Multimodal imaging in CHM. **(A)** Ultra-wide field retinography shows a widespread chorioretinal atrophy, with a central islet of retinal sparing. **(B)** OCTA detects the sparing of the choriocapillaris vascular layer limited to the central islet. **(C)** Fundus autofluorescence displaying a central hyperautofluorescent region surrounded by hyporeflective atrophic tissue. **(D)** Structural OCT scan passing shows chorioretinal atrophy and outer retinal tubulations in the parafovea and a relative sparing of the photoreceptor layer in the fovea.

Gene Therapy in Choroideremia

Choroideremia (CHM) is a rare XLR IRD, characterized by a progressive, centripetal, retinal degeneration, with a prevalence of 1:50,000 cases (203, 204). Vision loss progresses from nyctalopia in childhood to VF constriction in early adulthood and, ultimately, to legal blindness by the fifth decade of life (205, 206). From a pathogenic standpoint, Müller cells are the site of first damage, which is followed by outer retinal degeneration and, finally, by inner retinal thinning (207). Multimodal imaging findings include extended retinal hypoautofluorescence, with exclusive sparing of a central islet that allows patients to retain a good central vision. Structural OCT outside of this central region usually shows complete outer retinal atrophy (i.e., involving both photoreceptors and RPE cells), outer retinal tubulations and thinning of inner retinal layers and choroid (208, 209). Optical coherence tomography angiography displays an almost preserved superficial capillary plexus and choriocapillaris, with a significantly compromised deep capillary plexus (DCP), in the central islet, surrounded by completely absent choriocapillaris in the rest of the retina (210) (**Figure 3**).

Genetic Features

Choroideremia is caused by mutations in the *CHM* gene, which encodes component A of Rab geranylgeranyl-transferase, referred to as Rab escort protein 1 (REP1), a key mediator of post-translational lipidation (prenylation) and subcellular localization of a family of intracellular protein trafficking regulators, known as the Rab GTPases (211). The *CHM* gene is ubiquitously expressed, but in most tissues, including adrenal gland, brain, and thyroid, the homolog REP2 protein partially counterbalances REP1 deficiency. The reasons why REP2 does not prevent disease manifestation in the eye are yet to be elucidated. In rare instances, CHM may be part of a contiguous gene syndrome involving Xq21. Indeed, males with large interstitial deletions of an additional X-chromosome portion, other than Xq21, may develop CHM together with birth defects (cleft lip and palate and agenesis of the corpus callosum) and severe cognitive deficits (212). Moreover, previous reports described cases of males with a small deletion of Xq21 presenting with CHM, mixed sensorineural and conductive hearing deficits (in case of deletion of *POU3F4*), and varying degrees of cognitive deficits (in case of deletion of *RSK4*) (213). In addition, a previous report described the case of a female patient affected by CHM, sensorineural deafness, and primary ovarian failure secondary to a balanced X-4 translocation (214). A large study, involving more than 70 patients affected by this disease, reported a 94% rate of identification of a *CHM* mutation (204). Mutations of uncertain significance included non-contiguous duplications, insertion, deletion, point mutations, and aberrant splicing (204). It is worth of notice the absence of disease-causing missense mutations, in contrast to the majority of human genetic diseases, which are mainly determined by such mutations (204). To date, no defined genotype–phenotype correlation has been identified for CHM.

Gene Therapy

Choroideremia is a promising candidate for gene therapy since the 1.9 kb CHM cDNA is small enough to fit the size capacity of AAV vectors. Preclinical proof-of-concept studies on the feasibility of CHM gene replacement have been conducted both *in vitro*, by inducing the CHM gene in pluripotent stem cells (iPSCs) from patients with CHM, and *in vivo*, by delivering the AAV2-CHM virus in normal sighted mice and zebrafish, with no evidence of toxicity (215, 216), paving the way to clinical trials on CHM patients. The results of the first-in-human clinical trial date back to 2014, when MacLaren et al. reported phase I safety and efficacy data on six patients treated with low-dose subretinal AAV2-REP administered subfoveally, demonstrating an improvement in BCVA and retinal sensitivity for up to 3.5 years after treatment (217). These findings were confirmed by the 24-month data coming from the phase II trial (218). Less encouraging results came from another phase I clinical trial using the same vector at higher doses in six patients, since one of the six untreated eyes exhibited an improvement of >15 ETDRS letters, prompting the authors to conclude that VA should not be used as a primary outcome measure for future CHM gene therapy trials (219). So far, several clinical trials employing SRI of AAV2.REP1 have been conducted (NCT02671539, NCT02077361, NCT02553135, NCT02341807, NCT03496012). Combining together their results, overall 40 patients have been treated with a median gain of 1.5 ±7.2 SD in ETDRS letters, highly variable between the different trials (220). Although some issues still need to be addresses, such as the identification of proper endpoints and the development of safety enhancements to facilitate subretinal gene delivery, gene therapy for CHM has reached phase III clinical trials, providing real promise for patients. It is worth of notice the launch of the first phase I CHM clinical trial aimed at evaluating safety, tolerability, and preliminary efficacy of a single IVI of a rAAV gene therapy, 4D-110, in male patients with genetically confirmed CHM (NCT04483440).

Gene Therapy in X-Linked Retinoschisis

X-linked retinoschisis is an IRD caused by mutations in the *RS1* gene on Xp22.1. With an estimated prevalence ranging between 1 in 15,000 and 1 in 30,000, it is the most common form of juvenile-onset retinal degeneration in males, whereas heterozygous female carriers usually do not display any symptoms (221, 222). From a clinical standpoint, the typical feature of the disease, present in 98–100% of cases, is the foveal schisis, often seen as a spokewheel pattern of folds radiating out from the fovea, with peripheral retinoschisis being encountered in about 50% of patients (223–225) (**Figure 4**). Visual acuity generally starts declining in the first two decades of life, followed by a very slow progression of macular atrophy until the fifth or sixth decade, with possible evolution to legal blindness (226, 227). However, patients may also have a better prognosis, as long as the most common complications (i.e., retinal detachment and vitreous hemorrhage) do not occur.

Electroretinography is helpful in the diagnosis of XLRS, since there is a typically reduced b-wave amplitude, with a relatively preserved a-wave amplitude (the so-called "negative" waveform) (228).

Multimodal imaging findings include visualization of macular schisis on structural OCT and detection of foveal vascular impairment at the DCP level upon OCTA (229).

Genetic Features

RS1 encodes retinoschisin, a secretory protein exclusively expressed in retinal photoreceptors and bipolar cells, that can however be detected in all neuroretinal layers (230–232). Retinoschisin is found in a homo-oligomeric forms and, more specifically, it is an octamer made up of eight identical discoidin domains joined by intramolecular disulphide bonds (233). Mutations in the *RS1* sequence disrupt subunit assembly, thus interfering with retinoschin's role in retinal cell adhesion and organization of retinal architecture (233, 234).

Gene Therapy

Preclinical studies have shown that IVI administration of AAV8-scRS/IBPhRS vector, as well as SRI of the AAV5-mOPs-RS1 resulted in significant morpho-functional improvement in the retinoschisin knockout (*Rs1-KO*) mouse, with evidence of good tolerability in rabbits (235–238). Building upon these encouraging results, two phase 1/2 trials were initiated with

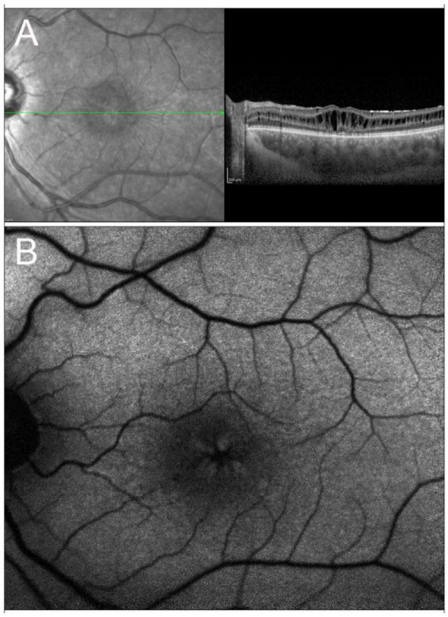

FIGURE 4 | Multimodal imaging in X-linked retinoschisis. **(A)** Combined infrared reflectance imaging and structural OCT. Note the spokewheel pattern of folds radiating out from the fovea, which corresponds to the foveal schitic cavities seen on structural OCT. **(B)** Fundus autofluorescence also shows the spokewheel pattern due to the overlying foveal schisis.

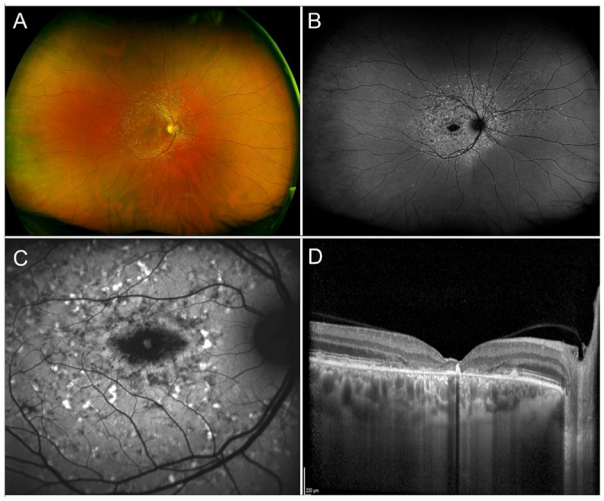

FIGURE 5 | Multimodal imaging in Stargardt disease. **(A)** Ultra-wide field retinography shows numerous flecks inside and outside of the vascular arcades. **(B)** Ultra-wide field fundus autofluorescence displays the flecks as mixed hypo- and hyper-autofluorescent dots and shows an area of central atrophy, better highlighted by 30° fundus autofluorescence **(C)**. **(D)** Structural OCT shows chorioretinal atrophy and clumping of hyperreflective lipofuscin-rich material corresponding to flecks.

different constructs, administered via IVI, since XLRS is an inner retinal pathology. For the first of such trials (NCT02317887), sponsored by the National Eye Institute (NEI), employing AAV8-scRS/IRBPhRS in adults (≥18 years old), promising initial findings have already been reported (239). The second trial (NCT02416622) uses rAAV2tYF-CHhRS1, intravitreally injected in adults (≥18 years old) in the first dose-escalation phase, with subsequent enrolment of individuals ≥6 years of age, after the maximum tolerated dose is identified.

Gene Therapy in Stargardt Disease

Stargardt disease, the most common hereditary macular dystrophy, is characterized by a progressive, centrifugal, macular degeneration, associated with different patterns of peripheral retinal alterations (240). The prevalence is of 1:8,000–10,000 individuals (240). From a clinical standpoint, one of the most typical findings in STGD are flecks, namely debris accumulations resulting from the progressive degeneration of RPE cells. Flecks have been described as hyperautofluorescent, corresponding to lipofuscin accumulations, and hypoautofluorescent, resulting from debris absorption and outer retinal atrophy onset (241). Other fundus findings include complete hypoautofluorescent central atrophy, surrounded by a halo of patchy, mottled hypoautofluorescence (242) (**Figure 5**). More recently, different STGD patterns have been described, characterized by progressively wider involvement of mid and extreme retinal periphery, as assessed by ultrawide field imaging (243). Furthermore, quantitative multimodal imaging and OCTA allowed to categorize STGD eyes accordingly to the amount of involvement of the retinal vascular and choroidal networks, highlighting different morpho-functional features and progression rates (156, 244, 245).

Genetic Features

Stargardt disease can be distinguished in three different forms: (I) STGD1, the most common form, displays an AR homozygous or compound heterozygous transmission and is caused by mutations in the *ABCA4* gene; (II) STGD3, which is determined by AD mutations in the *ELOVL4* gene; (III) STGD4, a rare AD form associated with mutations in the *PROM1* gene.

ABCA4, whose mutations are responsible for STGD1, is a 150 kb gene encoding an ATP-binding cassette transporter localized along the rims of photoreceptor OSs (246). This ATP-dependent flippase importer transports phosphatidylethanolamine (PE) and the all-*trans*-retinal (atRAL)/PE Schiff base (*N*-Ret-PE) into the cytosol, where atRAL is converted to all-*trans*-retinol (atROL) by retinol dehydrogenase RDH8 and RDH12. The absence of ABCA4 results in the accumulation of photo-toxic bisretinoids (A2E) with lipofuscin buildup in the RPE.

STGD3-causing *ELOVL4* gene contains six exons and plays a fundamental role in the synthesis of very long-chain polyunsaturated fatty acids (247).

Finally, the *PROM1* gene contains 23 exons distributed within a genomic sequence of more than 50 kb and encodes a protein

involved in the organization of the plasma membrane and in the biogenesis of photoreceptor disks (248).

Genotype-phenotype correlations are challenging due to the heterogeneous disease manifestations. The most common genotypic classification includes three groups: genotype A (carriers of two or more deleterious variants); genotype B (one deleterious variant and >1 missense or in-frame insertion/deletion variants); genotype C (two or more missense or in-frame insertion or null variants) (249). Previous investigations highlighted how deleterious variants tend to be associated with more aggressive forms of the disease, while missense mutations yield to milder phenotypes (249–252). On the other hand, null alleles result in more severe STGD forms with an earlier onset (253). Other causes of severe phenotypes include truncating and severely misfolding mutations, deletions, stop codons, and insertions (254, 255). Furthermore, hypomorphic and deep intronic variants influencing the splicing process, have been also described (72, 256–258).

Gene Therapy

The main obstacles to the development of gene therapy approaches for STGD regard the dimension of the *ABCA4* gene, whose coding sequence exceeds the cargo capacity of AAV, and the extreme complexity of deleterious variants, as previously described.

In the wake of the success of animal studies using lentiviral gene therapy to deliver the corrected *ABCA4* gene (259), starting from 2011, Sanofi sponsored a phase I/II clinical trial (NCT01367444) to test the efficacy of a SRI of SAR422459, a recombinant lentiviral vector (EIAV) transporting a modified form of the *ABCA4* gene. Notwithstanding the encouraging preliminary findings, in 2020, the sponsor decided to stop development of the product for non-safety reasons.

In 2019, the Applied Genetic Technologies Corporation announced the development of a hybrid AAV dual vector and published preclinical data supporting the potential of this technology in STGD (260).

More recently, promising results have been reported in animal models with a non-viral technique relying on subretinal delivery of self-assembled NPs (261, 262). Compared to viral vectors, non-viral delivery systems have unlimited payload, low immunogenicity, and minimal side effects, features that may allow to circumvent the obstacles which are currently standing in the way of STGD gene therapy (263).

Gene Therapy in Achromatopsia

Achromatopsia (ACHM) is an AR cone dysfunction affecting approximately 1 in 30,000 individuals (264, 265). Achromatopsia is a phenotypically and genotypically heterogeneous disease that can present in a complete or incomplete form. Complete ACHM is characterized by a totally abolished cone function, with a BCVA that is usually no >20/200 and with a total absence of color perception. In incomplete ACHM, residual cone function is present and patients have a higher VA and some degree of color discrimination (266). Prominent features of both complete and incomplete ACHM include photophobia, pendular nystagmus, central scotomata and high refractive (usually hypermetropic) errors (266). Electroretinography shows non-recordable cone-mediated responses with normal o near-normal rod responses (267). Fundus examination is normal or features non-specific alterations, such as central pigment mottling or attenuation of foveal reflex (268). On OCT, ACHM patients may display a variable phenotype, ranging from a normal to disrupted or absent EZ, which can sometimes be replaced by a hyporeflective cavitation, to complete outer retinal atrophy including the RPE (269). Fundus autofluorescence can be normal or show hyperautofluorescence, usually in zones of preserved EZ and likely preceding photoreceptor loss, or hypoautofluorescence, localized to areas of photoreceptor loss or RPE atrophy (270). Interestingly, adaptive optics scanning laser ophthalmoscopy (AOSLO) has shown the presence of cones in all ACHM patients, albeit reduced in number and with a highly variable density, regardless of OCT appearance, including areas of absent EZ reflectivity (271). This has important applications when it comes to patient selection for gene therapy trials.

Genetic Features

Mutations in six genes are responsible for over 90% of all ACHM cases, five of which are involved in the phototransduction process.

CNGA3 and *CNGB3*, encoding for the a- and b-subunit of the cyclic nucleotide-gated (CNG) cation channel 3 found in cones OSs, together account for 70–80% of cases of ACHM worldwide (272).

GNAT2 encodes the catalytic a-subunit of the G-protein transducin and is responsible for an infrequent form (<2%) of ACHM (273).

Equally rare subtypes are those caused by mutations in the *PDE6C* and *PDE6H* gene, encoding for the catalytic a- and inhibitory g-subunits of the photoreceptor-specific phosphodiesterase (274, 275).

Most recently, *ATF6* has been identified as a sixth ACHM-associated gene. ATF6 encodes a transmembrane TFs ubiquitously expressed and involved in endoplasmic reticulum homeostasis (276). The frequent finding of foveal hypoplasia in ATF6-ACHM lead to the suggestion that this gene may be crucial for foveal development (276).

Gene Therapy

Promising preclinical results have been reported for ACHM caused by mutations in the *CNGA3*, *CNB3,* and *GNAT2* genes. Taken together, these studies, which have been conducted on knock-out mouse models and naturally occurring mouse, sheep, and canine models, suggest that gene replacement approaches are effective and durable in ACHM, especially if administered early in life (277–284).

Other than for these encouraging data, ACHM seems particularly suited for gene augmentation for a number of reasons, including the presence of viable cones in all patients,

TABLE 2 | Clinical trials on IRDs.

N	Trial ID	Study title	Disease	Drug	Start date	Stop date	Phase	Status
1	NCT03913143	Double-masked, randomized, controlled, multiple-dose study to evaluate efficacy, safety, tolerability, and syst. exposure of QR-110 in Leber's congenital amaurosis (LCA) due to C.2991+1655A>G mutation (p.Cys998X) in the CEP290 gene	Leber congenital amaurosis	Sepofarsen (QR-110)	2019	Ongoing	Phase I/II	Active, not recruiting
2	NCT02556736	Phase I/IIA, open-label, dose-escalation study of safety, and tolerability of intravitreal RST-001 in patients with advanced retinitis pigmentosa (RP)	Retinitis pigmentosa	RST-001	2015	Ongoing	Phase I/II	Active, not recruiting
3	NCT03326336	A phase 1/2a, open-label, non-randomized, dose-escalation study to evaluate the safety, and tolerability of GS030 in subjects with retinitis pigmentosa	Retinitis pigmentosa	GS030-DP	2017	Ongoing	Phase I/II	Recruiting
4	NCT04278131	Phase 1/2, safety, and efficacy trial of BS01, a recombinant adeno-associated virus vector expressing chronosFP in patients with retinitis pigmentosa	Retinitis pigmentosa	BS01	2020	Ongoing	Phase I/II	Recruiting
5	NCT04919473	A phase I/IIa open label, dose-escalation study to evaluate the safety, and tolerability of intravitreal vMCO-I in patients with advanced retinitis pigmentosa	Retinitis pigmentosa	vMCO-I	2019	2020	Phase I/II	Completed
6	NCT03602820	A long-term follow-up study in subjects who received an adenovirus-associated viral vector serotype 2 containing the human RPE65 gene (AAV2-hRPE65v2, voretigene neparvovec-rzyl) administered via subretinal injection	Leber congenital amaurosis	AAV2-hRPE65v2	2015	Ongoing	N/A	Active, not recruiting
7	NCT01208389	A follow-on study to evaluate the safety of re-administration of adeno-associated viral vector containing the gene for human RPE65 [AAV2-hRPE65v2] to the contralateral eye in subjects with leber congenital amaurosis (LCA) previously enrolled in a phase 1 study	Leber congenital amaurosis	AAV2-hRPE65v2	2010	Ongoing	Phase I/II	Active, not recruiting
8	NCT03913143	Double-masked, randomized, controlled, multiple-dose study to evaluate efficacy, safety, tolerability, and syst. exposure of QR-110 in Leber's congenital amaurosis (LCA) due to c.2991+1655A>G mutation (p.Cys998X) in the CEP290 gene	Leber Congenital Amaurosis	Sepofarsen (QR-110)	2019	Ongoing	Phase II/III	Active, not recruiting
9	NCT03116113	A dose escalation (phase 1), and dose expansion (phase 2/3) clinical trial of retinal gene therapy for X-linked retinitis pigmentosa using an adeno-associated viral vector (AAV8) encoding retinitis pigmentosa GTPase regulator (RPGR)	Retinitis pigmentosa	BIIB112	2017	2020	Phase I/II	Completed
10	NCT03252847	An open label, multi-center, phase I/II dose escalation trial of a recombinant adeno-associated virus vector (AAV2-.RPGR) for gene therapy of adults and children with X-linked retinitis pigmentosa owing to defects in retinitis pigmentosa GTPase regulator (RPGR)	Retinitis pigmentosa	AAV2/5-RPGR	2017	Ongoing	Phase I/II	Active, not recruiting
11	NCT04671433	Phase 3 randomized, controlled study of AAV5-RPGR for the treatment of X-linked retinitis pigmentosa associated with variants in the RPGR gene	Retinitis pigmentosa	AAV5-RPGR	2021	Ongoing	Phase III	Recruiting
12	NCT03316560	A phase 1/2 open-label dose escalation study to evaluate the safety and efficacy of AGTC-501 (rAAV2tYF-GRK1-RPGR) and a phase 2 randomized, controlled, masked, multi-center study comparing two doses of AGTC-501 in male subjects with x-linked retinitis pigmentosa confirmed by a pathogenic variant in the RPGR gene	Retinitis pigmentosa	rAAV2tYF-GRK1-RPGR	2018	Ongoing	Phase I/II	Recruiting

(Continued)

TABLE 2 | Continued

N	Trial ID	Study title	Disease	Drug	Start date	Stop date	Phase	Status
13	NCT04850118	A phase 2/3, randomized, controlled, masked, multi-center study to evaluate the efficacy, safety, and tolerability of two doses of AGTC-501, a Recombinant adeno-associated virus vector expressing RPGR (rAAV2tYF-GRK1-RPGR), compared to an untreated control group in male subjects with X-linked Retinitis pigmentosa confirmed by a pathogenic variant in the RPGR gene	Retinitis pigmentosa	rAAV2tYF-GRK1-hRPGRco	2021	Ongoing	Phase II/III	Not yet recruiting
14	NCT04517149	An open-label, phase 1/2 trial of gene therapy 4D-125 in males with X-linked retinitis pigmentosa (XLRP) caused by mutations in the RPGR gene	Retinitis pigmentosa	4D-125	2020	Ongoing	Phase I/II	Recruiting
15	NCT03328130	Safety and efficacy of a unilateral subretinal administration of HORA-PDE6B in patients with retinitis pigmentosa harboring mutations in the PDE6B gene leading to a defect in PDE6ß expression	Retinitis pigmentosa	AAV2/5-hPDE6B	2017	Ongoing	Phase I/II	Recruiting
16	NCT04611503	PIGMENT—PDE6A gene therapy for retinitis pigmentosa	Retinitis pigmentosa	rAAV.hPDE6A	2019	Ongoing	Phase I/II	Recruiting
17	NCT02065011	An open-label study to determine the long-term safety, tolerability, and biological activity of SAR421869 in patients with usher syndrome type 1B	Retinitis pigmentosa	SAR421869	2013	Ongoing	Phase I/II	Active, not recruiting
18	NCT01505062	A phase I/IIA dose escalation safety study of subretinally injected SAR421869, administered to patients with retinitis pigmentosa associated with usher syndrome type 1B	Retinitis pigmentosa	SAR421869	2012	2019	Phase I/II	Terminated for non-safety reasons
19	NCT03780257	A first-in-human study to evaluate the safety and tolerability of QR-421a in subjects with retinitis pigmentosa (RP) due to mutations in exon 13 of the USH2A gene	Retinitis Pigmentosa	QR-421a	2019	Ongoing	Phase I/II	Active, not recruiting
20	NCT02671539	THOR—tübingen choroideremia gene therapy trial open label phase 2 clinical trial using an adeno-associated viral vector (AAV2) encoding rab-escort protein 1 (REP1)	Choroideremia	rAAV2.REP1	2016	2018	Phase II	Completed
21	NCT02077361	An open label clinical trial of retinal gene therapy for choroideremia using an adeno-associated viral vector (AAV2) encoding Rab-escort protein-1 (REP1)	Choroideremia	rAAV2.REP1	2015	Ongoing	Phase I/II	Active, not recruiting
22	NCT02553135	An open label phase 2 clinical trial of retinal gene therapy for choroideremia using an adeno-associated viral vector (AAV2) encoding Rab-escort protein 1 (REP1)	Choroideremia	AAV2-REP1	2015	2018	Phase II	Completed
23	NCT02341807	A phase 1/2 safety study in subjects with CHM (choroideremia) gene mutations using an adeno-associated virus serotype 2 vector to deliver the normal human CHM gene [AAV2-hCHM] to the retina	Choroideremia	AAV2-hCHM	2015	Ongoing	Phase I/II	Active, not recruiting
24	NCT03496012	A randomized, open label, outcomes-assessor masked, prospective, parallel controlled group, phase 3 clinical trial of retinal gene therapy for choroideremia using an adeno-associated viral vector (AAV2) encoding Rab escort protein 1 (REP1)	Choroideremia	AAV2-REP1	2017	2020	Phase III	Completed
25	NCT04483440	Phase 1 Open-label, dose-escalation study of the safety, tolerability, and preliminary efficacy of intravitreal 4D-110 in patients with choroideremia	Choroideremia	4D-110	2020	Ongoing	Phase I	Recruiting
26	NCT02317887	A phase I/IIa study of RS1 ocular gene transfer for X-linked retinoschisis	X-linked retinoschisis	RS1 AAV	2015	Ongoing	Phase I/II	Recruiting
27	NCT02416622	A multiple-site, phase 1/2, safety, and efficacy trial of a recombinant adeno-associated virus vector expressing retinoschisin (rAAV2tYF-CB-hRS1) in patients with X-linked retinoschisis	X-linked retinoschisis	rAAV2tYF-CB-hRS1	2015	Ongoing	Phase I/II	Active, not recruiting

(Continued)

TABLE 2 | Continued

N	Trial ID	Study title	Disease	Drug	Start date	Stop date	Phase	Status
28	NCT01367444	A phase I/IIA dose escalation safety study of subretinally injected SAR422459, administered to patients with Stargardt's macular degeneration	Stargardt's disease	SAR422459	2011	2019	Phase I/II	Terminated for non-safety reasons
29	NCT02610582	Safety and efficacy of a bilateral single subretinal injection of rAAV.hCNGA3 in adult and minor patients with CNGA3-linked achromatopsia investigated in a randomized, wait list controlled, observer-masked trial	Achromatopsia	rAAV.hCNGA3	2015	Ongoing	Phase I/II	Recruiting
30	NCT02935517	A multiple-site, phase 1/2, safety, and efficacy trial of AGTC 402, a recombinant adeno-associated virus vector expressing CNGA3, in patients with congenital achromatopsia caused by mutations in the CNGA3 gene	Achromatopsia	AGTC-402	2017	Ongoing	Phase I/II	Recruiting
31	NCT03001310	An open label, multi-center, phase I/II dose escalation trial of a recombinant adeno-associated virus vector (AAV2/8-hCARp.hCNGB3) for gene therapy of adults and children with achromatopsia owing to defects in CNGB3	Achromatopsia	AAV-CNGB3	2017	2019	Phase I/II	Completed
32	NCT02599922	A multiple-site, phase 1/2, safety, and efficacy trial of a recombinant adeno-associated virus vector expressing CNGB3 in patients with congenital achromatopsia caused by mutations in the CNGB3 Gene	Achromatopsia	rAAV2tYF-PR1.7-hCNGB3	2016	Ongoing	Phase I/II	Recruiting

The list follows the order of appearance in the manuscript (from https://clinicaltrials.gov/).

as demonstrated by means of AOSLO, and its stationary or slowly progressive nature, which provides a wide window of opportunity.

The first phase I/II clinical trial commenced in November 2015 (NCT02610582) in Germany to assess the safety and efficacy of SRI of rAAV.hCNGA3 in patients with CNGA3-ACHM, using a dose-escalation protocol. Short after, another phase I/II clinical trial for CNGA-related ACHM (NCT02935517) was initiated in the US and in Israel and is still ongoing.

As far as CNGB3-ACHM is concerned, a phase I/II dose-escalation trial has been conducted in the UK (NCT03001310) to test the efficacy and safety of subretinal delivery of AAV2/8-hCARp.hCNGB3 and another similar multicentric phase I/II trial is still ongoing in the US and in Israel (NCT02599922).

Final Remarks

In the present review, we tried to resume all the relevant findings and the present status of gene therapy in IRDs. On the basis of the above-described data (all the quoted clinical trials are listed in **Table 2**), a clinically applicable gene therapy represents a tangible perspective more than a still far target. Some IRDs seem to be closer to an upcoming definitive gene therapy treatment, whereas further studies are warranted for other ones. Overall considering all the techniques and approaches under investigation, the main current limitations include the safety profile of gene therapy, especially regarding the surgically-related risks for the retina, and sometimes the need of repeated treatments. The intravitreal route of administration might provide higher safety and feasibility profiles, although limiting the penetration of the treatment and drug concentrations effectively reaching retinal targets, if compared with subretinal approaches, turning out to be powerful but potentially riskier. Furthermore, it is known that each IRD may be characterized by extremely heterogeneous genotypic-phenotypic relationship. This is quite challenging to be evaluated both in clinical practice and in research contexts. We may assume that the different phenotypic expression of the mutated gene might have an influence not only on the morpho-functional status of the patients, but also on the clinical effect of gene therapy. From this point of view, future prospective studies should be focused on deeper assessments of genotypic-phenotypic features of each IRD, on new classification strategies and on the meanings that these advances in knowledge might have on gene therapy planning.

Conclusions

Inherited retinal diseases are significantly disabling conditions affecting young, working-age populations. Despite the provision of low-vision aids and assistance from specialist services, to date the management of these disorders remains largely suboptimal and the development of definitive therapies should be regarded as a priority. Based on preclinical data and on an ever-growing body of clinical evidence, gene-based strategies can now be looked at with cautious optimism. However, whilst gene therapy holds great hope for the treatment of a wide range of IRDs in the future, there are caveats to be considered, which are mainly related to the careful selection of appropriate target diseases, patients, and outcome measures and to the surgical

challenges of vector delivery. Natural history studies, long term follow-up of treated patients and advances in the field of genetic testing and molecular diagnostics are among the lines of research that can be pursued to address these issues and to expand the spectrum of IRDs that can be treated with this potentially revolutionary approach.

AUTHOR CONTRIBUTIONS

AAr and AAm: review design, data analysis, data interpretation, and manuscript draft. EA, AS, and MM: data acquisition and data analysis. MB and FB: data interpretation, manuscript revision, and study supervision.

REFERENCES

1. Berger W, Kloeckener-Gruissem B, Neidhardt J. The molecular basis of human retinal and vitreoretinal diseases. *Prog Retin Eye Res.* (2010) 29:335–75. doi: 10.1016/j.preteyeres.2010.03.004
2. Mitchell GA, Brody LC, Looney J, Steel G, Suchanek M, Dowling C, et al. An initiator codon mutation in ornithine-delta-aminotransferase causing gyrate atrophy of the choroid and retina. *J Clin Invest.* (1988) 81:630–3. doi: 10.1172/JCI113365
3. Terrell D, Comander J. Current stem-cell approaches for the treatment of inherited retinal degenerations. *Semin Ophthalmol.* (2019) 34:287–92. doi: 10.1080/08820538.2019.1620808
4. Yue L, Weiland JD, Roska B, Humayun MS. Retinal stimulation strategies to restore vision: fundamentals and systems. *Prog Retin Eye Res.* (2016) 53:21–47. doi: 10.1016/j.preteyeres.2016.05.002
5. Bosking WH, Beauchamp MS, Yoshor D. Electrical stimulation of visual cortex: relevance for the development of visual cortical prosthetics. *Annu Rev Vis Sci.* (2017) 3:141–66. doi: 10.1146/annurev-vision-111815-114525
6. Blaese RM, Culver KW, Miller AD, Carter CS, Fleisher T, Clerici M, et al. T lymphocyte-directed gene therapy for ADA-SCID: initial trial results after 4 years. *Science.* (1995) 270:475–80. doi: 10.1126/science.270.5235.475
7. Tang R, Xu Z. Gene therapy: a double-edged sword with great powers. *Mol Cell Biochem.* (2020) 474:73–81. doi: 10.1007/s11010-020-03834-3
8. Bashar AE, Metcalfe AL, Viringipurampeer IA, Yanai A, Gregory-Evans CY, Gregory-Evans K. An *ex vivo* gene therapy approach in X-linked retinoschisis. *Mol Vis.* (2016) 22:718–33.
9. Athanasopoulos T, Munye MM, Yanez-Munoz RJ. Nonintegrating gene therapy vectors. *Hematol Oncol Clin North Am.* (2017) 31:753–70. doi: 10.1016/j.hoc.2017.06.007
10. O'Neal WK, Zhou H, Morral N, Langston C, Parks RJ, Graham FL, et al. Toxicity associated with repeated administration of first-generation adenovirus vectors does not occur with a helper-dependent vector. *Mol Med.* (2000) 6:179–95. doi: 10.1007/BF03402113
11. Steinwaerder DS, Carlson CA, Lieber A. Generation of adenovirus vectors devoid of all viral genes by recombination between inverted repeats. *J Virol.* (1999) 73:9303–13. doi: 10.1128/JVI.73.11.9303-9313.1999
12. Hu ML, Edwards TL, O'Hare F, Hickey DG, Wang JH. Liu Z„ et al. Gene therapy for inherited retinal diseases: progress and possibilities. *Clin Exp Optom.* (2021) 104:444–54. doi: 10.1080/08164622.2021.1880863
13. Ong T, Pennesi ME, Birch DG, Lam BL, Tsang SH. Adeno-associated viral gene therapy for inherited retinal disease. *Pharm Res.* (2019) 36:34. doi: 10.1007/s11095-018-2564-5
14. Trapani I, Colella P, Sommella A, Iodice C, Cesi G, de Simone S, et al. Effective delivery of large genes to the retina by dual AAV vectors. *EMBO Mol Med.* (2014) 6:194–211. doi: 10.1002/emmm.201302948
15. McClements ME, Barnard AR, Singh MS, et al. An AAV Dual vector strategy ameliorates the stargardt phenotype in adult Abca4$^{(-/-)}$ Mice. *Hum Gene Ther.* (2019) 30:590–600. doi: 10.1089/hum.2018.156
16. Trapani I, Puppo A, Auricchio A. Vector platforms for gene therapy of inherited retinopathies. *Prog Retin Eye Res.* (2014) 43:108–28. doi: 10.1016/j.preteyeres.2014.08.001
17. Hacein-Bey-Abina S, von Kalle C, Schmidt M, Le Deist F, Wulffraat N, McIntyre E, et al. A serious adverse event after successful gene therapy for X-linked severe combined immunodeficiency. *N Engl J Med.* (2003) 348:255–6. doi: 10.1056/NEJM200301163480314
18. Yáñez-Muñoz RJ, Balaggan KS, MacNeil A, Howe SJ, Schmidt M, Smith AJ, et al. Effective gene therapy with nonintegrating lentiviral vectors. *Nat Med.* (2006) 12:348–53. doi: 10.1038/nm1365
19. Cashman SM, Sadowski SL, Morris DJ, Frederick J, Kumar-Singh R. Intercellular trafficking of adenovirus-delivered HSV VP22 from the retinal pigment epithelium to the photoreceptors–implications for gene therapy. *Mol Ther.* (2002) 6:813–23. doi: 10.1006/mthe.2002.0806
20. Ziccardi L, Cordeddu V, Gaddini L, Matteucci A, Parravano M, Malchiodi-Albedi F, et al. Gene therapy in retinal dystrophies. *Int J Mol Sci.* (2019) 20:5722. doi: 10.3390/ijms20225722
21. Fechheimer M, Boylan JF, Parker S, Sisken JE, Patel GL, Zimmer SG. Transfection of mammalian cells with plasmid DNA by scrape loading and sonication loading. *Proc Natl Acad Sci USA.* (1987) 84:8463–7. doi: 10.1073/pnas.84.23.8463
22. Neumann E, Schaefer-Ridder M, Wang Y, Hofschneider PH. Gene transfer into mouse lyoma cells by electroporation in high electric fields. *EMBO J.* (1982) 1:841–5. doi: 10.1002/j.1460-2075.1982.tb01257.x
23. Capecchi MR. High efficiency transformation by direct microinjection of DNA into cultured mammalian cells. *Cell.* (1980) 22:479–88. doi: 10.1016/0092-8674(80)90358-X
24. Fraley R, Subramani S, Berg P, Papahadjopoulos D. Introduction of liposome-encapsulated SV40 DNA into cells. *J Biol Chem.* (1980) 255:10431–5. doi: 10.1016/S0021-9258(19)70482-7
25. Gao X, Huang L. Potentiation of cationic liposome-mediated gene delivery by polycations. *Biochemistry.* (1996) 35:1027–36. doi: 10.1021/bi952436a
26. Conley SM, Cai X, Naash MI. Nonviral ocular gene therapy: assessment and future directions. *Curr Opin Mol Ther.* (2008) 10:456–63.
27. Trigueros S, Domenech EB, Toulis V, Marfany G. *In vitro* gene delivery in retinal pigment epithelium cells by plasmid dna-wrapped gold nanoparticles. *Genes (Basel).* (2019) 10:289. doi: 10.3390/genes10040289
28. Farjo R, Skaggs J, Quiambao AB, Cooper MJ, Naash MI. Efficient non-viral ocular gene transfer with compacted DNA nanoparticles. *PLoS ONE.* (2006) 1:e38. doi: 10.1371/journal.pone.0000038
29. Cai X, Nash Z, Conley SM, Fliesler SJ, Cooper MJ, Naash MI, et al. A partial structural and functional rescue of a retinitis pigmentosa model with compacted DNA nanoparticles. *PLoS ONE.* (2009) 4:e5290. doi: 10.1371/journal.pone.0005290
30. Read SP, Cashman SM, Kumar-Singh R. POD nanoparticles expressing GDNF provide structural and functional rescue of light-induced retinal degeneration in an adult mouse. *Mol Ther.* (2010) 18:1917–26. doi: 10.1038/mt.2010.167
31. Dezawa M, Takano M, Negishi H, Mo X, Oshitari T, Sawada H. Gene transfer into retinal ganglion cells by *in vivo* electroporation: a new approach. *Micron.* (2002) 33:1–6. doi: 10.1016/S0968-4328(01)00002-6
32. Matsuda T, Cepko CL. Electroporation and RNA interference in the rodent retina *in vivo* and *in vitro*. *Proc Natl Acad Sci USA.* (2004) 101:16–22. doi: 10.1073/pnas.2235688100
33. Vasconcelos HM Jr, Lujan BJ, Pennesi ME, Yang P, Lauer AK. Intraoperative optical coherence tomographic findings in patients undergoing subretinal gene therapy surgery. *Int J Retina Vitreous.* (2020) 6:13. doi: 10.1186/s40942-020-00216-1
34. Olsen TW, Feng X, Wabner K, Conston SR, Sierra DH, Folden DV, et al. Cannulation of the suprachoroidal space: a novel drug delivery methodology to the posterior segment. *Am J Ophthalmol.* (2006) 142:777–87. doi: 10.1016/j.ajo.2006.05.045
35. Einmahl S, Savoldelli M, D'Hermies F, Tabatabay C, Gurny R, Behar-Cohen F. Evaluation of a novel biomaterial in the suprachoroidal space of the rabbit eye. *Invest Ophthalmol Vis Sci.* (2002) 43:1533–9.
36. Mandelcorn ED, Kitchens JW, Fijalkowski N, Moshfeghi DM. Active aspiration of suprachoroidal hemorrhage using a

guarded needle. *Ophthalmic Surg Lasers Imaging Retina.* (2014) 45:150–2. doi: 10.3928/23258160-20140306-09
37. Goldstein DA, Do D, Noronha G, Kissner JM, Srivastava SK, Nguyen QD. Suprachoroidal corticosteroid administration: a novel route for local treatment of noninfectious uveitis. *Transl Vis Sci Technol.* (2016) 5:14. doi: 10.1167/tvst.5.6.14
38. Gamlin PD, Alexander JJ, Boye SL, Witherspoon CD, Boye SE. SubILM injection of AAV for gene delivery to the retina. *Methods Mol Biol.* (2019) 1950:249–62. doi: 10.1007/978-1-4939-9139-6_14
39. Rogers S, Pfuderer P. Use of viruses as carriers of added genetic information. *Nature.* (1968) 219:749–51. doi: 10.1038/219749a0
40. Vazquez-Dominguez I, Garanto A, Collin RWJ. Molecular therapies for inherited retinal diseases-current standing, opportunities and challenges. *Genes (Basel).* (2019) 10:654. doi: 10.3390/genes10090654
41. Suzuki K, Tsunekawa Y, Hernandez-Benitez R, Wu J, Zhu J, Kim EJ, et al. *In vivo* genome editing via CRISPR/Cas9 mediated homology-independent targeted integration. *Nature.* (2016) 540:144–9. doi: 10.1038/nature20565
42. Tsai YT, Wu WH, Lee TT, Wu WP, Xu CL, Park KS, et al. Clustered regularly interspaced short palindromic repeats-based genome surgery for the treatment of autosomal dominant retinitis pigmentosa. *Ophthalmology.* (2018) 125:1421–30. doi: 10.1016/j.ophtha.2018.04.001
43. Li P, Kleinstiver BP, Leon MY, Prew MS, Navarro-Gomez D, Greenwald SH, et al. Allele-specific CRISPR-Cas9 genome editing of the single-base P23H mutation for rhodopsin-associated dominant retinitis pigmentosa. *CRISPR.* (2018) 1:55–64. doi: 10.1089/crispr.2017.0009
44. Clement K, Rees H, Canver MC, Gehrke JM, Farouni R, Hsu JY, et al. CRISPResso2 provides accurate and rapid genome editing sequence analysis. *Nat Biotechnol.* (2019) 37:224–6. doi: 10.1038/s41587-019-0032-3
45. Bakondi B, Lv W, Lu B, Jones MK, Tsai Y, Kim KJ, et al. *In Vivo* CRISPR/Cas9 gene editing corrects retinal dystrophy in the S334ter-3 rat model of autosomal dominant retinitis pigmentosa. *Mol Ther.* (2016) 24:556–63. doi: 10.1038/mt.2015.220
46. Garanto A, van Beersum SE, Peters TA, Roepman R, Cremers FP, Collin RW. Unexpected CEP290 mRNA splicing in a humanized knock-in mouse model for Leber congenital amaurosis. *PLoS ONE.* (2013) 8:e79369. doi: 10.1371/journal.pone.0079369
47. Lewin AS, Hauswirth WW. Ribozyme gene therapy: applications for molecular medicine. *Trends Mol Med.* (2001) 7:221–8. doi: 10.1016/S1471-4914(01)01965-7
48. Hauswirth WW, Lewin AS. Ribozyme uses in retinal gene therapy. *Prog Retin Eye Res.* (2000) 19:689–710. doi: 10.1016/S1350-9462(00)00007-0
49. Moore SM, Skowronska-Krawczyk D, Chao DL. Emerging concepts for RNA therapeutics for inherited retinal disease. *Adv Exp Med Biol.* (2019) 1185:85–9. doi: 10.1007/978-3-030-27378-1_14
50. Fire A, Xu S, Montgomery MK, Kostas SA, Driver SE, Mello CC. Potent and specific genetic interference by double-stranded RNA in *Caenorhabditis elegans*. *Nature.* (1998) 391:806–11. doi: 10.1038/35888
51. Elbashir SM, Harborth J, Lendeckel W, Yalcin A, Weber K, Tuschl T. Duplexes of 21-nucleotide RNAs mediate RNA interference in cultured mammalian cells. *Nature.* (2001) 411:494–8. doi: 10.1038/35078107
52. Ketting RF, Fischer SE, Bernstein E, Sijen T, Hannon GJ, Plasterk RH. Dicer functions in RNA interference and in synthesis of small RNA involved in developmental timing in *C. elegans*. *Genes Dev.* (2001) 15:2654–9. doi: 10.1101/gad.927801
53. Alexander SP, Mathie A, Peters JA. Guide to receptors and channels (GRAC), 5th edition. *Br J Pharmacol.* (2011) 164(Suppl 1):S1–324. doi: 10.1111/j.1476-5381.2011.01649_1.x
54. Guzman-Aranguez A, Loma P, Pintor J. Small-interfering RNAs (siRNAs) as a promising tool for ocular therapy. *Br J Pharmacol.* (2013) 170:730–47. doi: 10.1111/bph.12330
55. Fedorov Y, Anderson EM, Birmingham A, Reynolds A, Karpilow J, Robinson K, et al. Off-target effects by siRNA can induce toxic phenotype. *RNA.* (2006) 12:1188–96. doi: 10.1261/rna.28106
56. Zhong R, Kim J, Kim HS, Kim M, Lum L, Levine B, et al. Computational detection and suppression of sequence-specific off-target phenotypes from whole genome RNAi screens. *Nucleic Acids Res.* (2014) 42:8214–22. doi: 10.1093/nar/gku306
57. Hornung V, Guenthner-Biller M, Bourquin C, Ablasser A, Schlee M, Uematsu S, et al. Sequence-specific potent induction of IFN-alpha by short interfering RNA in plasmacytoid dendritic cells through TLR7. *Nat Med.* (2005) 11:263–70. doi: 10.1038/nm1191
58. Lewin AS, Drenser KA, Hauswirth WW, Nishikawa S, Yasumura D, Flannery JG, et al. Ribozyme rescue of photoreceptor cells in a transgenic rat model of autosomal dominant retinitis pigmentosa. *Nat Med.* (1998) 4:967–71. doi: 10.1038/nm0898-967
59. Chadderton N, Millington-Ward S, Palfi A, O'Reilly M, Tuohy G, Humphries MM, et al. Improved retinal function in a mouse model of dominant retinitis pigmentosa following AAV-delivered gene therapy. *Mol Ther.* (2009) 17:593–9. doi: 10.1038/mt.2008.301
60. Hernan I, Gamundi MJ, Planas E, Borras E, Maseras M, Carballo M. Cellular expression and siRNA-mediated interference of rhodopsin cis-acting splicing mutants associated with autosomal dominant retinitis pigmentosa. *Invest Ophthalmol Vis Sci.* (2011) 52:3723–9. doi: 10.1167/iovs.10-6933
61. O'Reilly M, Millington-Ward S, Palfi A, Chadderton N, Cronin T, McNally N, et al. A transgenic mouse model for gene therapy of rhodopsin-linked retinitis pigmentosa. *Vision Res.* (2008) 48:386–91. doi: 10.1016/j.visres.2007.08.014
62. Collin RW, Garanto A. Applications of antisense oligonucleotides for the treatment of inherited retinal diseases. *Curr Opin Ophthalmol.* (2017) 28:260–6. doi: 10.1097/ICU.0000000000000363
63. Bennett CF, Swayze EE, RNA. targeting therapeutics: molecular mechanisms of antisense oligonucleotides as a therapeutic platform. *Annu Rev Pharmacol Toxicol.* (2010) 50:259–93. doi: 10.1146/annurev.pharmtox.010909.105654
64. Naessens S, Ruysschaert L, Lefever S, Coppieters F, De Baere E. Antisense oligonucleotide-based downregulation of the G56R pathogenic variant causing NR2E3-associated autosomal dominant retinitis pigmentosa. *Genes (Basel).* (2019) 10:363. doi: 10.3390/genes10050363
65. Murray SF, Jazayeri A, Matthes MT, Yasumura D, Yang H, Peralta R, et al. Allele-specific inhibition of rhodopsin with an antisense oligonucleotide slows photoreceptor cell degeneration. *Invest Ophthalmol Vis Sci.* (2015) 56:6362–75. doi: 10.1167/iovs.15-16400
66. Liu MM, Zack DJ. Alternative splicing and retinal degeneration. *Clin Genet.* (2013) 84:142–9. doi: 10.1111/cge.12181
67. Bonifert T, Gonzalez Menendez I, Battke F, Theurer Y, Synofzik M, Schöls L, et al. Antisense oligonucleotide mediated splice correction of a deep intronic mutation in OPA1. *Mol Ther Nucleic Acids.* (2016) 5:e390. doi: 10.1038/mtna.2016.93
68. Garanto A, van der Velde-Visser SD, Cremers FPM, Collin RWJ. Antisense oligonucleotide-based splice correction of a deep-intronic mutation in CHM underlying choroideremia. *Adv Exp Med Biol.* (2018) 1074:83–9. doi: 10.1007/978-3-319-75402-4_11
69. Albert S, Garanto A, Sangermano R, Khan M, Bax NM, Hoyng CB, et al. Identification and rescue of splice defects caused by two neighboring deep-intronic ABCA4 mutations underlying Stargardt disease. *Am J Hum Genet.* (2018) 102:517–27. doi: 10.1016/j.ajhg.2018.02.008
70. Bauwens M, Garanto A, Sangermano R, Naessens S, Weisschuh N, De Zaeytijd J, et al. ABCA4-associated disease as a model for missing heritability in autosomal recessive disorders: novel noncoding splice, cis-regulatory, structural, and recurrent hypomorphic variants. *Genet Med.* (2019) 21:1761–71. doi: 10.1038/s41436-018-0420-y
71. Garanto A, Duijkers L, Tomkiewicz TZ, Collin RWJ. Antisense oligonucleotide screening to optimize the rescue of the splicing defect caused by the recurrent deep-intronic ABCA4 variant c.4539+2001G>A in Stargardt disease. *Genes (Basel).* (2019) 10:452. doi: 10.3390/genes10060452
72. Sangermano R, Garanto A, Khan M, Runhart EH, Bauwens M, Bax NM, et al. Deep-intronic ABCA4 variants explain missing heritability in Stargardt disease and allow correction of splice defects by antisense oligonucleotides. *Genet Med.* (2019) 21:1751–60. doi: 10.1038/s41436-018-0414-9
73. Slijkerman RW, Vaché C, Dona M, García-García G, Claustres M, Hetterschijt L, et al. Antisense oligonucleotide-based splice correction for USH2A-associated retinal degeneration caused by a frequent deep-intronic mutation. *Mol Ther Nucleic Acids.* (2016) 5:e381. doi: 10.1038/mtna.2016.89
74. Saleh AF, Arzumanov AA, Gait MJ. Overview of alternative oligonucleotide chemistries for exon skipping. *Methods Mol Biol.* (2012) 867:365–78. doi: 10.1007/978-1-61779-767-5_23

75. Hall AH, Wan J, Shaughnessy EE, Ramsay Shaw B, Alexander KA, RNA. interference using boranophosphate siRNAs: structure-activity relationships. *Nucleic Acids Res.* (2004) 32:5991–6000. doi: 10.1093/nar/gkh936
76. Gaglione M, Messere A. Recent progress in chemically modified siRNAs. *Mini Rev Med Chem.* (2010) 10:578–95. doi: 10.2174/138955710791384036
77. Chiu YL, Rana TM. siRNA function in RNAi: a chemical modification analysis. *RNA.* (2003) 9:1034–48. doi: 10.1261/rna.5103703
78. Havens MA, Hastings ML. Splice-switching antisense oligonucleotides as therapeutic drugs. *Nucleic Acids Res.* (2016) 44:6549–63. doi: 10.1093/nar/gkw533
79. Dias N, Stein CA. Antisense oligonucleotides: basic concepts and mechanisms. *Mol Cancer Ther.* (2002) 1:347–55.
80. Devi GR, Beer TM, Corless CL, Arora V, Weller DL, Iversen PL. *In vivo* bioavailability and pharmacokinetics of a c-MYC antisense phosphorodiamidate morpholino oligomer, AVI-4126, in solid tumors. *Clin Cancer Res.* (2005) 11:3930–8. doi: 10.1158/1078-0432.CCR-04-2091
81. Garanto A, Chung DC, Duijkers L, Corral-Serrano JC, Messchaert M, Xiao R, et al. *In vitro* and *in vivo* rescue of aberrant splicing in CEP290-associated LCA by antisense oligonucleotide delivery. *Hum Mol Genet.* (2016) 25:2552–63. doi: 10.1093/hmg/ddw118
82. Turchinovich A, Zoidl G, Dermietzel R. Non-viral siRNA delivery into the mouse retina *in vivo*. *BMC Ophthalmol.* (2010) 10:25. doi: 10.1186/1471-2415-10-25
83. Mussolino C, Sanges D, Marrocco E, Bonetti C, Di Vicino U, Marigo V, et al. Zinc-finger-based transcriptional repression of rhodopsin in a model of dominant retinitis pigmentosa. *EMBO Mol Med.* (2011) 3:118–28. doi: 10.1002/emmm.201000119
84. Botta S, Marrocco E, de Prisco N, Curion F, Renda M, Sofia M, et al. Rhodopsin targeted transcriptional silencing by DNA-binding. *Elife.* (2016) 5:e12242. doi: 10.7554/eLife.12242
85. Botta S, de Prisco N, Marrocco E, Renda M, Sofia M, Curion F, et al. Targeting and silencing of rhodopsin by ectopic expression of the transcription factor KLF15. *JCI Insight.* (2017) 2:e96560. doi: 10.1172/jci.insight.96560
86. Trapani I, Auricchio A. Seeing the light after 25 years of retinal gene therapy. *Trends Mol Med.* (2018) 24:669–81. doi: 10.1016/j.molmed.2018.06.006
87. Liang FQ, Dejneka NS, Cohen DR, Krasnoperova NV, Lem J, Maguire AM, et al. AAV-mediated delivery of ciliary neurotrophic factor prolongs photoreceptor survival in the rhodopsin knockout mouse. *Mol Ther.* (2001) 3:241–8. doi: 10.1006/mthe.2000.0252
88. McGee Sanftner LH, Abel H, Hauswirth WW, Flannery JG. Glial cell line derived neurotrophic factor delays photoreceptor degeneration in a transgenic rat model of retinitis pigmentosa. *Mol Ther.* (2001) 4:622–9. doi: 10.1006/mthe.2001.0498
89. Buch PK, MacLaren RE, Durán Y, Balaggan KS, MacNeil A, Schlichtenbrede FC, et al. In contrast to AAV-mediated Cntf expression, AAV-mediated Gdnf expression enhances gene replacement therapy in rodent models of retinal degeneration. *Mol Ther.* (2006) 14:700–9. doi: 10.1016/j.ymthe.2006.05.019
90. Schuettauf F, Vorwerk C, Naskar R, Orlin A, Quinto K, Zurakowski D, et al. Adeno-associated viruses containing bFGF or BDNF are neuroprotective against excitotoxicity. *Curr Eye Res.* (2004) 29:379–86. doi: 10.1080/02713680490517872
91. Byrne LC, Dalkara D, Luna G, Fisher SK, Clérin E, Sahel JA, et al. Viral-mediated RdCVF and RdCVFL expression protects cone and rod photoreceptors in retinal degeneration. *J Clin Invest.* (2015) 125:105–16. doi: 10.1172/JCI65654
92. Yao J, Feathers KL, Khanna H, Thompson D, Tsilfidis C, Hauswirth WW, et al. XIAP therapy increases survival of transplanted rod precursors in a degenerating host retina. *Invest Ophthalmol Vis Sci.* (2011) 52:1567–72. doi: 10.1167/iovs.10-5998
93. Birch DG, Bennett LD, Duncan JL, Weleber RG, Pennesi ME. Long-term follow-up of patients with retinitis pigmentosa receiving intraocular ciliary neurotrophic factor implants. *Am J Ophthalmol.* (2016) 170:10–4. doi: 10.1016/j.ajo.2016.07.013
94. Bi A, Cui J, Ma YP, Olshevskaya E, Pu M, Dizhoor AM, et al. Ectopic expression of a microbial-type rhodopsin restores visual responses in mice with photoreceptor degeneration. *Neuron.* (2006) 50:23–33. doi: 10.1016/j.neuron.2006.02.026
95. Cehajic-Kapetanovic J, Eleftheriou C, Allen AE, Milosavljevic N, Pienaar A, Bedford R, et al. Restoration of vision with ectopic expression of human rod opsin. *Curr Biol.* (2015) 25:2111–22. doi: 10.1016/j.cub.2015.07.029
96. Lin B, Koizumi A, Tanaka N, Panda S, Masland RH. Restoration of visual function in retinal degeneration mice by ectopic expression of melanopsin. *Proc Natl Acad Sci USA.* (2008) 105:16009–14. doi: 10.1073/pnas.0806114105
97. Tomita H, Sugano E, Yawo H, Ishizuka T, Isago H, Narikawa S, et al. Restoration of visual response in aged dystrophic RCS rats using AAV-mediated channelopsin-2 gene transfer. *Invest Ophthalmol Vis Sci.* (2007) 48:3821–6. doi: 10.1167/iovs.06-1501
98. den Hollander AI, Roepman R, Koenekoop RK, Cremers FP. Leber congenital amaurosis: genes, proteins and disease mechanisms. *Prog Retin Eye Res.* (2008) 27:391–419. doi: 10.1016/j.preteyeres.2008.05.003
99. Heher KL, Traboulsi EI, Maumenee IH. The natural history of Leber's congenital amaurosis. Age-related findings in 35 patients. *Ophthalmology.* (1992) 99:241–5. doi: 10.1016/S0161-6420(92)31985-2
100. Dagi LR, Leys MJ, Hansen RM, Fulton AB. Hyperopia in complicated Leber's congenital amaurosis. *Arch Ophthalmol.* (1990) 108:709–12. doi: 10.1001/archopht.1990.01070070095043
101. Lorenz B, Gyürüs P, Preising M, Bremser D, Gu S, Andrassi M, et al. Early-onset severe rod-cone dystrophy in young children with RPE65 mutations. *Invest Ophthalmol Vis Sci.* (2000) 41:2735–42.
102. Koenekoop RK. An overview of Leber congenital amaurosis: a model to understand human retinal development. *Surv Ophthalmol.* (2004) 49:379–98. doi: 10.1016/j.survophthal.2004.04.003
103. Dharmaraj S, Leroy BP, Sohocki MM, Koenekoop RK, Perrault I, Anwar K, et al. The phenotype of Leber congenital amaurosis in patients with AIPL1 mutations. *Arch Ophthalmol.* (2004) 122:1029–37. doi: 10.1001/archopht.122.7.1029
104. Galvin JA, Fishman GA, Stone EM, Koenekoop RK. Clinical phenotypes in carriers of Leber congenital amaurosis mutations. *Ophthalmology.* (2005) 112:349–56. doi: 10.1016/j.ophtha.2004.08.023
105. Koenekoop RK, Cremers FP, den Hollander AI. Leber congenital amaurosis: ciliary proteins on the move. *Ophthalmic Genet.* (2007) 28:111–2. doi: 10.1080/13816810701537457
106. Kumaran N, Moore AT, Weleber RG, Michaelides M. Leber congenital amaurosis/early-onset severe retinal dystrophy: clinical features, molecular genetics and therapeutic interventions. *Br J Ophthalmol.* (2017) 101:1147–54. doi: 10.1136/bjophthalmol-2016-309975
107. Sohocki MM, Sullivan LS, Mintz-Hittner HA, Birch D, Heckenlively JR, Freund CL, et al. A range of clinical phenotypes associated with mutations in CRX, a photoreceptor transcription-factor gene. *Am J Hum Genet.* (1998) 63:1307–15. doi: 10.1086/302101
108. Xu Y, Guan L, Xiao X, Zhang J, Li S, Jiang H, et al. ALMS1 null mutations: a common cause of Leber congenital amaurosis and early-onset severe cone-rod dystrophy. *Clin Genet.* (2016) 89:442–7. doi: 10.1111/cge.12617
109. Xu M, Yang L, Wang F, Li H, Wang X, Wang W, et al. Mutations in human IFT140 cause non-syndromic retinal degeneration. *Hum Genet.* (2015) 134:1069–78. doi: 10.1007/s00439-015-1586-x
110. Sweeney MO, McGee TL, Berson EL, Dryja TP. Low prevalence of lecithin retinol acyltransferase mutations in patients with Leber congenital amaurosis and autosomal recessive retinitis pigmentosa. *Mol Vis.* (2007) 13:588–93.
111. Sun W, Gerth C, Maeda A, Lodowski DT, Van Der Kraak L, Saperstein DA, et al. Novel RDH12 mutations associated with Leber congenital amaurosis and cone-rod dystrophy: biochemical and clinical evaluations. *Vision Res.* (2007) 47:2055–66. doi: 10.1016/j.visres.2007.04.005
112. Soens ZT Li Y, Zhao L, Eblimit A, Dharmat R, Li Y, et al. Hypomorphic mutations identified in the candidate Leber congenital amaurosis gene CLUAP1. *Genet Med.* (2016) 18:1044–51. doi: 10.1038/gim.2015.205
113. Ramamurthy V, Roberts M, van den Akker F, Niemi G, Reh TA, Hurley JB. AIPL1, a protein implicated in Leber's congenital amaurosis, interacts with and aids in processing of farnesylated proteins. *Proc Natl Acad Sci USA.* (2003) 100:12630–5. doi: 10.1073/pnas.2134194100
114. Perrault I, Hanein S, Gerard X, Delphin N, Fares-Taie L, Gerber S, et al. Spectrum of SPATA7 mutations in Leber congenital amaurosis and delineation of the associated phenotype. *Hum Mutat.* (2010) 31:E1241–50. doi: 10.1002/humu.21203

115. Nichols LL. 2nd, Alur RP, Boobalan E, Sergeev YV, Caruso RC, Stone EM, et al. Two novel CRX mutant proteins causing autosomal dominant Leber congenital amaurosis interact differently with NRL. *Hum Mutat.* (2010) 31:E1472–1483. doi: 10.1002/humu.21268
116. Mataftsi A, Schorderet DF, Chachoua L, Boussalah M, Nouri MT, Barthelmes D, et al. Novel TULP1 mutation causing leber congenital amaurosis or early onset retinal degeneration. *Invest Ophthalmol Vis Sci.* (2007) 48:5160–7. doi: 10.1167/iovs.06-1013
117. Lotery AJ, Jacobson SG, Fishman GA, Weleber RG, Fulton AB, Namperumalsamy P, et al. Mutations in the CRB1 gene cause Leber congenital amaurosis. *Arch Ophthalmol.* (2001) 119:415–20. doi: 10.1001/archopht.119.3.415
118. Li T. Leber congenital amaurosis caused by mutations in RPGRIP1. *Cold Spring Harb Perspect Med.* (2014) 5:a017384. doi: 10.1101/cshperspect.a017384
119. Gerber S, Hanein S, Perrault I, Delphin N, Aboussair N, Leowski C, et al. Mutations in LCA5 are an uncommon cause of Leber congenital amaurosis (LCA) type II. *Hum Mutat.* (2007) 28:1245. doi: 10.1002/humu.9513
120. Estrada-Cuzcano A, Koenekoop RK, Coppieters F, Kohl S, Lopez I, Collin RW, et al. IQCB1 mutations in patients with leber congenital amaurosis. *Invest Ophthalmol Vis Sci.* (2011) 52:834–9. doi: 10.1167/iovs.10-5221
121. Chao DL, Burr A, Pennesi M. RPE65-related leber congenital amaurosis/early-onset severe retinal dystrophy. In: Adam MP, Ardinger HH, Pagon RA, et al., editors. *GeneReviews((R))*. Seattle, WA: University of Washington (1993).
122. Burnight ER, Wiley LA, Drack AV, Braun TA, Anfinson KR, Kaalberg EE, et al. CEP290 gene transfer rescues Leber congenital amaurosis cellular phenotype. *Gene Ther.* (2014) 21:662–72. doi: 10.1038/gt.2014.39
123. Boye SE. Leber congenital amaurosis caused by mutations in GUCY2D. *Cold Spring Harb Perspect Med.* (2014) 5:a017350. doi: 10.1101/cshperspect.a017350
124. Bowne SJ, Sullivan LS, Mortimer SE, Hedstrom L, Zhu J, Spellicy CJ, et al. Spectrum and frequency of mutations in IMPDH1 associated with autosomal dominant retinitis pigmentosa and leber congenital amaurosis. *Invest Ophthalmol Vis Sci.* (2006) 47:34–42. doi: 10.1167/iovs.05-0868
125. Azadi S, Molday LL, Molday RS. RD3, the protein associated with Leber congenital amaurosis type 12, is required for guanylate cyclase trafficking in photoreceptor cells. *Proc Natl Acad Sci USA.* (2010) 107:21158–63. doi: 10.1073/pnas.1010460107
126. Asai-Coakwell M, March L, Dai XH, Duval M, Lopez I, French CR, et al. Contribution of growth differentiation factor 6-dependent cell survival to early-onset retinal dystrophies. *Hum Mol Genet.* (2013) 22:1432–42. doi: 10.1093/hmg/dds560
127. Acland GM, Aguirre GD, Ray J, Zhang Q, Aleman TS, Cideciyan AV, et al. Gene therapy restores vision in a canine model of childhood blindness. *Nat Genet.* (2001) 28:92–5. doi: 10.1038/ng0501-92
128. Acland GM, Aguirre GD, Bennett J, Aleman TS, Cideciyan AV, Bennicelli J, et al. Long-term restoration of rod and cone vision by single dose rAAV-mediated gene transfer to the retina in a canine model of childhood blindness. *Mol Ther.* (2005) 12:1072–82. doi: 10.1016/j.ymthe.2005.08.008
129. Aguirre GD, Baldwin V, Pearce-Kelling S, Narfstrom K, Ray K. Acland GM. Congenital stationary night blindness in the dog: common mutation in the RPE65 gene indicates founder effect. *Mol Vis.* (1998) 4:23.
130. Pang JJ, Chang B, Hawes NL, Hurd RE, Davisson MT Li J, et al. Retinal degeneration 12 (rd12): a new, spontaneously arising mouse model for human Leber congenital amaurosis (LCA). *Mol Vis.* (2005) 11:152–62.
131. Rohrer B, Goletz P, Znoiko S, Ablonczy Z, Ma JX, Redmond TM, et al. Correlation of regenerable opsin with rod ERG signal in Rpe65$^{-/-}$ mice during development and aging. *Invest Ophthalmol Vis Sci.* (2003) 44:310–5. doi: 10.1167/iovs.02-0567
132. Bainbridge JW, Mehat MS, Sundaram V, Robbie SJ, Barker SE, Ripamonti C, et al. Effect of gene therapy on visual function in Leber's congenital amaurosis. *N Engl J Med.* (2008) 358:2231–9. doi: 10.1056/NEJMoa0802268
133. Hauswirth WW, Aleman TS, Kaushal S, Cideciyan AV, Schwartz SB, Wang L, et al. Treatment of leber congenital amaurosis due to RPE65 mutations by ocular subretinal injection of adeno-associated virus gene vector: short-term results of a phase I trial. *Hum Gene Ther.* (2008) 19:979–90. doi: 10.1089/hum.2008.107
134. Maguire AM, Simonelli F, Pierce EA, Pugh EN Jr, Mingozzi F, Bennicelli J, et al. Safety and efficacy of gene transfer for Leber's congenital amaurosis. *N Engl J Med.* (2008) 358:2240–8. doi: 10.1056/NEJMoa0802315
135. Patel U, Boucher M, de Leseleuc L, Visintini S. Voretigene neparvovec: an emerging gene therapy for the treatment of inherited blindness. In: *CADTH Issues in Emerging Health Technologies*. Ottawa, ON: Canadian Agency for Drugs and Technologies in Health (2016). p. 1–11.
136. Drack AV, Bennett J, Russell S, High KA, Yu Z-F, Tillman A, et al. How long does gene therapy last? 4-year follow-up phase 3 voretigene neparvovec trial in RPE65-associated LCA/inherited retinal disease. *J AAPOS.* (2019) 23:e7. doi: 10.1016/j.jaapos.2019.08.018
137. Testa F, Maguire AM, Rossi S, Pierce EA, Melillo P, Marshall K, et al. Three-year follow-up after unilateral subretinal delivery of adeno-associated virus in patients with Leber congenital Amaurosis type 2. *Ophthalmology.* (2013) 120:1283–91. doi: 10.1016/j.ophtha.2012.11.048
138. Bainbridge JW, Mehat MS, Sundaram V, Robbie SJ, Barker SE, Ripamonti C, et al. Long-term effect of gene therapy on Leber's congenital amaurosis. *N Engl J Med.* (2015) 372:1887–97. doi: 10.1056/NEJMoa1414221
139. Maeder ML, Stefanidakis M, Wilson CJ, Baral R, Barrera LA, Bounoutas GS, et al. Development of a gene-editing approach to restore vision loss in Leber congenital amaurosis type 10. *Nat Med.* (2019) 25:229–33. doi: 10.1038/s41591-018-0327-9
140. Biasutto P, Dulla K, Adamson P, Schulkens I, Schmidt I, Lane A, et al. QR-110 treatment for leber's congenital amaurosis type 10: restoration of CEP290 mRNA levels and ciliation in LCA10 iPSC-derived optic cups. *Invest Ophthalmol.* (2017) 58:249.
141. Dulla K, Aguila M, Lane A, Jovanovic K, Parfitt DA, Schulkens I, et al. Splice-modulating oligonucleotide QR-110 restores CEP290 mRNA and function in human c.2991+1655A>G LCA10 models. *Mol Ther Nucleic Acids.* (2018) 12:730–40. doi: 10.1016/j.omtn.2018.07.010
142. Cideciyan AV, Jacobson SG, Drack AV, Ho AC, Charng J, Garafalo AV, et al. Effect of an intravitreal antisense oligonucleotide on vision in Leber congenital amaurosis due to a photoreceptor cilium defect. *Nat Med.* (2019) 25:225–8. doi: 10.1038/s41591-018-0295-0
143. Mihelec M, Pearson RA, Robbie SJ, Buch PK, Azam SA, Bainbridge JW, et al. Long-term preservation of cones and improvement in visual function following gene therapy in a mouse model of leber congenital amaurosis caused by guanylate cyclase-1 deficiency. *Hum Gene Ther.* (2011) 22:1179–90. doi: 10.1089/hum.2011.069
144. Haire SE, Pang J, Boye SL, Sokal I, Craft CM, Palczewski K, et al. Light-driven cone arrestin translocation in cones of postnatal guanylate cyclase-1 knockout mouse retina treated with AAV-GC1. *Invest Ophthalmol Vis Sci.* (2006) 47:3745–53. doi: 10.1167/iovs.06-0086
145. Boye SE, Boye SL, Pang J, Ryals R, Everhart D, Umino Y, et al. Functional and behavioral restoration of vision by gene therapy in the guanylate cyclase-1 (GC1) knockout mouse. *PLoS ONE.* (2010) 5:e11306. doi: 10.1371/journal.pone.0011306
146. Boon N, Wijnholds J, Pellissier LP. Research models and gene augmentation therapy for CRB1 retinal dystrophies. *Front Neurosci.* (2020) 14:860. doi: 10.3389/fnins.2020.00860
147. Alves CH, Wijnholds J, AAV. Gene augmentation therapy for CRB1-associated retinitis pigmentosa. *Methods Mol Biol.* (2018) 1715:135–51. doi: 10.1007/978-1-4939-7522-8_10
148. Feathers KL, Jia L, Perera ND, Chen A, Presswalla FK, Khan NW, et al. Development of a gene therapy vector for RDH12-associated retinal dystrophy. *Hum Gene Ther.* (2019) 30:1325–35. doi: 10.1089/hum.2019.017
149. Tsang SH, Sharma T. Retinitis pigmentosa (non-syndromic). *Adv Exp Med Biol.* (2018) 1085:125–30. doi: 10.1007/978-3-319-95046-4_25
150. Verbakel SK, van Huet RAC, Boon CJF, den Hollander AI, Collin RWJ, Klaver CCW, et al. Non-syndromic retinitis pigmentosa. *Prog Retin Eye Res.* (2018) 66:157–86. doi: 10.1016/j.preteyeres.2018.03.005
151. Hamel C. Retinitis pigmentosa. *Orphanet J Rare Dis.* (2006) 1:40. doi: 10.1186/1750-1172-1-40
152. Popovic P, Jarc-Vidmar M, Hawlina M. Abnormal fundus autofluorescence in relation to retinal function in patients with retinitis pigmentosa. *Graefes Arch Clin Exp Ophthalmol.* (2005) 243:1018–27. doi: 10.1007/s00417-005-1186-x

153. Robson AG, Saihan Z, Jenkins SA, Fitzke FW, Bird AC, Webster AR, et al. Functional characterisation and serial imaging of abnormal fundus autofluorescence in patients with retinitis pigmentosa and normal visual acuity. *Br J Ophthalmol.* (2006) 90:472–9. doi: 10.1136/bjo.2005.082487
154. Fischer MD, Fleischhauer JC, Gillies MC, Sutter FK, Helbig H, Barthelmes D, et al. new method to monitor visual field defects caused by photoreceptor degeneration by quantitative optical coherence tomography. *Invest Ophthalmol Vis Sci.* (2008) 49:3617–21. doi: 10.1167/iovs.08-2003
155. Lupo S, Grenga PL, Vingolo EM. Fourier-domain optical coherence tomography and microperimetry findings in retinitis pigmentosa. *Am J Ophthalmol.* (2011) 151:106–11. doi: 10.1016/j.ajo.2010.07.026
156. Arrigo A, Bordato A, Romano F, Aragona E, Grazioli A, Bandello F, et al. Choroidal patterns in retinitis pigmentosa: correlation with visual acuity and disease progression. *Transl Vis Sci Technol.* (2020) 9:17. doi: 10.3390/jcm8091388
157. Arrigo A, Romano F, Albertini G, Aragona E, Bandello F, Battaglia Parodi M. Vascular patterns in retinitis pigmentosa on swept-source optical coherence tomography angiography. *J Clin Med.* (2019) 8:1425. doi: 10.3390/jcm8091425
158. Dryja TP, McGee TL, Reichel E, Hahn LB, Cowley GS, Yandell DW, et al. A point mutation of the rhodopsin gene in one form of retinitis pigmentosa. *Nature.* (1990) 343:364–6. doi: 10.1038/343364a0
159. Dryja TP, McGee TL, Hahn LB, Cowley GS, Olsson JE, Reichel E, et al. Mutations within the rhodopsin gene in patients with autosomal dominant retinitis pigmentosa. *N Engl J Med.* (1990) 323:1302–7. doi: 10.1056/NEJM199011083231903
160. Mendes HF, van der Spuy J, Chapple JP, Cheetham ME. Mechanisms of cell death in rhodopsin retinitis pigmentosa: implications for therapy. *Trends Mol Med.* (2005) 11:177–85. doi: 10.1016/j.molmed.2005.02.007
161. Kumaramanickavel G, Maw M, Denton MJ, John S, Srikumari CR, Orth U, et al. Missense rhodopsin mutation in a family with recessive RP. *Nat Genet.* (1994) 8:10–1. doi: 10.1038/ng0994-10
162. Meng D, Ragi SD, Tsang SH. Therapy in rhodopsin-mediated autosomal dominant retinitis pigmentosa. *Mol Ther.* (2020) 28:2139–49. doi: 10.1016/j.ymthe.2020.08.012
163. Diner BA, Das A, Nayak R, Flinkstrom Z, Tallo T, DaSilva J, et al. Dual AAV-based "Knock-out-and-replace" of RHO as a therapeutic approach to treat RHO-associated autosomal dominant retinitis pigmentosa (RHO adRP). *Mol Ther.* (2020) 28:108–9.
164. O'Reilly M, Palfi A, Chadderton N, Millington-Ward S, Ader M, Cronin T, et al. RNA interference-mediated suppression and replacement of human rhodopsin *in vivo*. *Am J Hum Genet.* (2007) 81:127–35. doi: 10.1086/519025
165. Millington-Ward S, Chadderton N, O'Reilly M, Palfi A, Goldmann T, Kilty C, et al. Suppression and replacement gene therapy for autosomal dominant disease in a murine model of dominant retinitis pigmentosa. *Mol Ther.* (2011) 19:642–9. doi: 10.1038/mt.2010.293
166. Kiang AS, Palfi A, Ader M, Kenna PF, Millington-Ward S, Clark G, et al. Toward a gene therapy for dominant disease: validation of an RNA interference-based mutation-independent approach. *Mol Ther.* (2005) 12:555–61. doi: 10.1016/j.ymthe.2005.03.028
167. Cideciyan AV, Sudharsan R, Dufour VL, Massengill MT, Iwabe S, Swider M, et al. Mutation-independent rhodopsin gene therapy by knockdown and replacement with a single AAV vector. *Proc Natl Acad Sci USA.* (2018) 115:E8547–56. doi: 10.1073/pnas.1805055115
168. Meindl A, Dry K, Herrmann K, Manson F, Ciccodicola A, Edgar A, et al. A gene (RPGR) with homology to the RCC1 guanine nucleotide exchange factor is mutated in X-linked retinitis pigmentosa (RP3). *Nat Genet.* (1996) 13:35–42. doi: 10.1038/ng0596-35
169. Schwahn U, Lenzner S, Dong J, Feil S, Hinzmann B, van Duijnhoven G, et al. Positional cloning of the gene for X-linked retinitis pigmentosa 2. *Nat Genet.* (1998) 19:327–32. doi: 10.1038/1214
170. Webb TR, Parfitt DA, Gardner JC, Martinez A, Bevilacqua D, Davidson AE, et al. Deep intronic mutation in OFD1, identified by targeted genomic next-generation sequencing, causes a severe form of X-linked retinitis pigmentosa (RP23). *Hum Mol Genet.* (2012) 21:3647–54. doi: 10.1093/hmg/dds194
171. Kirschner R, Rosenberg T, Schultz-Heienbrok R, Lenzner S, Feil S, Roepman R, et al. RPGR transcription studies in mouse and human tissues reveal a retina-specific isoform that is disrupted in a patient with X-linked retinitis pigmentosa. *Hum Mol Genet.* (1999) 8:1571–8. doi: 10.1093/hmg/8.8.1571
172. Vervoort R, Lennon A, Bird AC, Tulloch B, Axton R, Miano MG, et al. Mutational hot spot within a new RPGR exon in X-linked retinitis pigmentosa. *Nat Genet.* (2000) 25:462–6. doi: 10.1038/78182
173. Pelletier V, Jambou M, Delphin N, Zinovieva E, Stum M, Gigarel N, et al. Comprehensive survey of mutations in RP2 and RPGR in patients affected with distinct retinal dystrophies: genotype-phenotype correlations and impact on genetic counseling. *Hum Mutat.* (2007) 28:81–91. doi: 10.1002/humu.20417
174. Grover S, Fishman GA, Anderson RJ, Lindeman M, A. longitudinal study of visual function in carriers of X-linked recessive retinitis pigmentosa. *Ophthalmology.* (2000) 107:386–96. doi: 10.1016/S0161-6420(99)00045-7
175. Talib M, van Schooneveld MJ, Van Cauwenbergh C, Wijnholds J, Ten Brink JB, Florijn RJ, et al. The spectrum of structural and functional abnormalities in female carriers of pathogenic variants in the RPGR gene. *Invest Ophthalmol Vis Sci.* (2018) 59:4123–33. doi: 10.1167/iovs.17-23453
176. Ogino K, Oishi M, Oishi A, Morooka S, Sugahara M, Gotoh N, et al. Radial fundus autofluorescence in the periphery in patients with X-linked retinitis pigmentosa. *Clin Ophthalmol.* (2015) 9:1467–74. doi: 10.2147/OPTH.S89371
177. Comander J, Weigel-DiFranco C, Sandberg MA, Berson EL. Visual function in carriers of X-linked retinitis pigmentosa. *Ophthalmology.* (2015) 122:1899–906. doi: 10.1016/j.ophtha.2015.05.039
178. Salvetti AP, Nanda A, MacLaren RE. RPGR-related X-linked retinitis pigmentosa carriers with a severe "male pattern." *Ophthalmologica.* (2021) 244:60–7. doi: 10.1159/000503687
179. Beltran WA, Cideciyan AV, Lewin AS, Iwabe S, Khanna H, Sumaroka A, et al. Gene therapy rescues photoreceptor blindness in dogs and paves the way for treating human X-linked retinitis pigmentosa. *Proc Natl Acad Sci USA.* (2012) 109:2132–7. doi: 10.1073/pnas.1118847109
180. Cehajic-Kapetanovic J, Xue K, Martinez-Fernandez de la Camara C, Nanda A, Davies A, Wood LJ, et al. Initial results from a first-in-human gene therapy trial on X-linked retinitis pigmentosa caused by mutations in RPGR. *Nat Med.* (2020) 26:354–9. doi: 10.1038/s41591-020-0763-1
181. McLaughlin ME, Sandberg MA, Berson EL, Dryja TP. Recessive mutations in the gene encoding the beta-subunit of rod phosphodiesterase in patients with retinitis pigmentosa. *Nat Genet.* (1993) 4:130–4. doi: 10.1038/ng0693-130
182. Gal A, Orth U, Baehr W, Schwinger E, Rosenberg T. Heterozygous missense mutation in the rod cGMP phosphodiesterase beta-subunit gene in autosomal dominant stationary night blindness. *Nat Genet.* (1994) 7:551. doi: 10.1038/ng0894-551c
183. Huang SH, Pittler SJ, Huang X, Oliveira L, Berson EL, Dryja TP. Autosomal recessive retinitis pigmentosa caused by mutations in the alpha subunit of rod cGMP phosphodiesterase. *Nat Genet.* (1995) 11:468–71. doi: 10.1038/ng1295-468
184. Kuehlewein L, Zobor D, Andreasson SO, Ayuso C, Banfi S, Bocquet B, et al. Clinical phenotype and course of PDE6A-associated retinitis pigmentosa disease, characterized in preparation for a gene supplementation trial. *JAMA Ophthalmol.* (2020) 138:1241–50. doi: 10.1001/jamaophthalmol.2020.4206
185. Fishman GA, Roberts MF, Derlacki DJ, Grimsby JL, Yamamoto H, Sharon D, et al. Novel mutations in the cellular retinaldehyde-binding protein gene (RLBP1) associated with retinitis punctata albescens: evidence of interfamilial genetic heterogeneity and fundus changes in heterozygotes. *Arch Ophthalmol.* (2004) 122:70–5. doi: 10.1001/archopht.122.1.70
186. Eichers ER, Green JS, Stockton DW, Jackman CS, Whelan J, McNamara JA, et al. Newfoundland rod-cone dystrophy, an early-onset retinal dystrophy, is caused by splice-junction mutations in RLBP1. *Am J Hum Genet.* (2002) 70:955–64. doi: 10.1086/339688
187. Burstedt MS, Sandgren O, Holmgren G, Forsman-Semb K. Bothnia dystrophy caused by mutations in the cellular retinaldehyde-binding protein gene (RLBP1) on chromosome 15q26. *Invest Ophthalmol Vis Sci.* (1999) 40:995–1000.
188. Naz S, Ali S, Riazuddin SA, Farooq T, Butt NH, Zafar AU, et al. Mutations in RLBP1 associated with fundus albipunctatus in consanguineous Pakistani families. *Br J Ophthalmol.* (2011) 95:1019–24. doi: 10.1136/bjo.2010.189076
189. Choi VW, Bigelow CE, McGee TL, Gujar AN Li H, Hanks SM, et al. AAV-mediated RLBP1 gene therapy improves the rate of dark

adaptation in Rlbp1 knockout mice. *Mol Ther Methods Clin Dev.* (2015) 2:15022. doi: 10.1038/mtm.2015.22
190. MacLachlan TK, Milton MN, Turner O, Tukov F, Choi VW, Penraat J, et al. Nonclinical safety evaluation of scAAV8-RLBP1 for treatment of RLBP1 retinitis pigmentosa. *Mol Ther Methods Clin Dev.* (2018) 8:105–20. doi: 10.1016/j.omtm.2017.12.001
191. Gal A, Li Y, Thompson DA, Weir J, Orth U, Jacobson SG, et al. Mutations in MERTK, the human orthologue of the RCS rat retinal dystrophy gene, cause retinitis pigmentosa. *Nat Genet.* (2000) 26:270–1. doi: 10.1038/81555
192. Tschernutter M, Jenkins SA, Waseem NH, Saihan Z, Holder GE, Bird AC, et al. Clinical characterisation of a family with retinal dystrophy caused by mutation in the Mertk gene. *Br J Ophthalmol.* (2006) 90:718–23. doi: 10.1136/bjo.2005.084897
193. Ghazi NG, Abboud EB, Nowilaty SR, Alkuraya H, Alhommadi A, Cai H, et al. Treatment of retinitis pigmentosa due to MERTK mutations by ocular subretinal injection of adeno-associated virus gene vector: results of a phase I trial. *Hum Genet.* (2016) 135:327–43. doi: 10.1007/s00439-016-1637-y
194. Fishman GA, Kumar A, Joseph ME, Torok N, Anderson RJ. Usher's syndrome. Ophthalmic and neuro-otologic findings suggesting genetic heterogeneity. *Arch Ophthalmol.* (1983) 101:1367–74. doi: 10.1001/archopht.1983.01040020369005
195. Lopes VS, Gibbs D, Libby RT, Aleman TS, Welch DL, Lillo C, et al. The Usher 1B protein, MYO7A, is required for normal localization and function of the visual retinoid cycle enzyme, RPE65. *Hum Mol Genet.* (2011) 20:2560–70. doi: 10.1093/hmg/ddr155
196. Eudy JD, Weston MD, Yao S, Hoover DM, Rehm HL, Ma-Edmonds M, et al. Mutation of a gene encoding a protein with extracellular matrix motifs in Usher syndrome type IIa. *Science.* (1998) 280:1753–7. doi: 10.1126/science.280.5370.1753
197. Weston MD, Eudy JD, Fujita S, Yao S, Usami S, Cremers C, et al. Genomic structure and identification of novel mutations in usherin, the gene responsible for Usher syndrome type IIa. *Am J Hum Genet.* (2000) 66:1199–210. doi: 10.1086/302855
198. Rivolta C, Berson EL, Dryja TP. Paternal uniparental heterodisomy with partial isodisomy of chromosome 1 in a patient with retinitis pigmentosa without hearing loss and a missense mutation in the Usher syndrome type II gene USH2A. *Arch Ophthalmol.* (2002) 120:1566–71. doi: 10.1001/archopht.120.11.1566
199. Seyedahmadi BJ, Rivolta C, Keene JA, Berson EL, Dryja TP. Comprehensive screening of the USH2A gene in Usher syndrome type II and non-syndromic recessive retinitis pigmentosa. *Exp Eye Res.* (2004) 79:167–73. doi: 10.1016/j.exer.2004.03.005
200. Hartel BP, Löfgren M, Huygen PL, Guchelaar I. Lo-A-Njoe Kort N, Sadeghi AM, et al. A combination of two truncating mutations in USH2A causes more severe and progressive hearing impairment in Usher syndrome type IIa. *Hear Res.* (2016) 339:60–8. doi: 10.1016/j.heares.2016.06.008
201. Zallocchi M, Binley K, Lad Y, Ellis S, Widdowson P, Iqball S, et al. EIAV-based retinal gene therapy in the shaker1 mouse model for usher syndrome type 1B: development of UshStat. *PLoS ONE.* (2014) 9:e94272. doi: 10.1371/journal.pone.0094272
202. Dulla K, Slijkerman R, van Diepen HC, Albert S, Dona M, Beumer W, et al. Antisense oligonucleotide-based treatment of retinitis pigmentosa caused by USH2A exon 13 mutations. *Mol Ther.* (2021) 29:2441s.o. doi: 10.1101/2020.10.06.320499
203. Moosajee M, Ramsden SC, Black GC, Seabra MC, Webster AR. Clinical utility gene card for: choroideremia. *Eur J Hum Genet.* (2014) 22:4. doi: 10.1038/ejhg.2013.183
204. Simunovic MP, Jolly JK, Xue K, Edwards TL, Groppe M, Downes SM, et al. The spectrum of CHM gene mutations in choroideremia and their relationship to clinical phenotype. *Invest Ophthalmol Vis Sci.* (2016) 57:6033–9. doi: 10.1167/iovs.16-20230
205. MacDonald IM, Hume S, Zhai Y, Xu M. Choroideremia. In: Adam MP, Ardinger HH, Pagon RA, et al., editors. *GeneReviews((R))*. Seattle, WA: University of Washington (1993).
206. Roberts MF, Fishman GA, Roberts DK, Heckenlively JR, Weleber RG, Anderson RJ, et al. Retrospective, longitudinal, and cross sectional study of visual acuity impairment in choroideraemia. *Br J Ophthalmol.* (2002) 86:658–62. doi: 10.1136/bjo.86.6.658
207. Jacobson SG, Cideciyan AV, Sumaroka A, Aleman TS, Schwartz SB, Windsor EA, et al. Remodeling of the human retina in choroideremia: rab escort protein 1 (REP-1) mutations. *Invest Ophthalmol Vis Sci.* (2006) 47:4113–20. doi: 10.1167/iovs.06-0424
208. Romano F, Arrigo A, MacLaren RE, Charbel Issa P, Birtel J, Bandello F, et al. Hyperreflective foci as a pathogenetic biomarker in choroideremia. *Retina.* (2020) 40:1634–40. doi: 10.1097/IAE.0000000000002645
209. Arrigo A, Romano F, Parodi MB, Charbel Issa P, Birtel J, Bandello F, et al. Reduced vessel density in deep capillary plexus correlates with retinal layer thickness in choroideremia. *Br J Ophthalmol.* (2021) 105:687–93. doi: 10.1136/bjophthalmol-2020-316528
210. Battaglia Parodi M, Arrigo A, MacLaren RE, Aragona E, Toto L, Mastropasqua R, et al. Vascular alterations revealed with optical coherence tomography angiography in patients with choroideremia. *Retina.* (2019) 39:1200–5. doi: 10.1097/IAE.0000000000002118
211. Seabra MC, Brown MS, Goldstein JL. Retinal degeneration in choroideremia: deficiency of rab geranylgeranyl transferase. *Science.* (1993) 259:377–81. doi: 10.1126/science.8380507
212. Schwartz M, Rosenberg T. Prenatal diagnosis of choroideremia. *Acta Ophthalmol Scand Suppl.* (1996) (219):33–6. doi: 10.1111/j.1600-0420.1996.tb00381.x
213. Yntema HG, van den Helm B, Kissing J, van Duijnhoven G, Poppelaars F, Chelly J, et al. A novel ribosomal S6-kinase (RSK4; RPS6KA6) is commonly deleted in patients with complex X-linked mental retardation. *Genomics.* (1999) 62:332–43. doi: 10.1006/geno.1999.6004
214. Lorda-Sanchez IJ, Ibañez AJ, Sanz RJ, Trujillo MJ, Anabitarte ME, Querejeta ME, et al. Choroideremia, sensorineural deafness, and primary ovarian failure in a woman with a balanced X-4 translocation. *Ophthalmic Genet.* (2000) 21:185–9. doi: 10.1076/1381-6810(200009)2131-ZFT185
215. Vasireddy V, Mills JA, Gaddameedi R, Basner-Tschakarjan E, Kohnke M, Black AD, et al. AAV-mediated gene therapy for choroideremia: preclinical studies in personalized models. *PLoS ONE.* (2013) 8:e61396. doi: 10.1371/journal.pone.0061396
216. Moosajee M, Tracey-White D, Smart M, Weetall M, Torriano S, Kalatzis V, et al. Functional rescue of REP1 following treatment with PTC124 and novel derivative PTC-414 in human choroideremia fibroblasts and the nonsense-mediated zebrafish model. *Hum Mol Genet.* (2016) 25:3416–31. doi: 10.1093/hmg/ddw184
217. MacLaren RE, Groppe M, Barnard AR, Cottriall CL, Tolmachova T, Seymour L, et al. Retinal gene therapy in patients with choroideremia: initial findings from a phase 1/2 clinical trial. *Lancet.* (2014) 383:1129–37. doi: 10.1016/S0140-6736(13)62117-0
218. Lam BL, Davis JL, Gregori NZ, MacLaren RE, Girach A, Verriotto JD, et al. Choroideremia gene therapy phase 2 clinical trial: 24-month results. *Am J Ophthalmol.* (2019) 197:65–73. doi: 10.1016/j.ajo.2018.09.012
219. Dimopoulos IS, Hoang SC, Radziwon A, Binczyk NM, Seabra MC, MacLaren RE, et al. Two-year results after AAV2-mediated gene therapy for choroideremia: the alberta experience. *Am J Ophthalmol.* (2018) 193:130–42. doi: 10.1016/j.ajo.2018.06.011
220. Abbouda A, Avogaro F, Moosajee M, Vingolo EM. Update on gene therapy clinical trials for choroideremia and potential experimental therapies. Medicina (Kaunas) (2021) 57:64. doi: 10.3390/medicina57010064
221. Sikkink SK, Biswas S, Parry NR, Stanga PE, Trump D. X-linked retinoschisis: an update. *J Med Genet.* (2007) 44:225–32. doi: 10.1136/jmg.2006.047340
222. Vainio-Mattila B, Eriksson AW, Forsius H. X-chromosomal recessive retinoschisis in the Region of Pori. An ophthalmo-genetical analysis of 103 cases. *Acta Ophthalmol (Copenh).* (1969) 47:1135–48. doi: 10.1111/j.1755-3768.1969.tb02513.x
223. Kellner U, Brummer S, Foerster MH, Wessing A. X-linked congenital retinoschisis. *Graefes Arch Clin Exp Ophthalmol.* (1990) 228:432–7. doi: 10.1007/BF00927256
224. Mitamura Y, Miyanishi K, Shizukawa N, Tashimo A, Nakamura Y, Tagawa H, et al. A case of X-linked retinoschisis diagnosed in an infant. *Retina.* (2003) 23:731–2. doi: 10.1097/00006982-200310000-00030
225. Peachey NS, Fishman GA, Derlacki DJ, Brigell MG. Psychophysical and electroretinographic findings in X-linked juvenile retinoschisis. *Arch Ophthalmol.* (1987) 105:513–6. doi: 10.1001/archopht.1987.01060040083038

226. Riveiro-Alvarez R, Trujillo-Tiebas MJ, Gimenez-Pardo A, Garcia-Hoyos M, Lopez-Martinez MA, Aguirre-Lamban J, et al. Correlation of genetic and clinical findings in Spanish patients with X-linked juvenile retinoschisis. *Invest Ophthalmol Vis Sci.* (2009) 50:4342–50. doi: 10.1167/iovs.09-3418
227. Apushkin MA, Fishman GA, Rajagopalan AS. Fundus findings and longitudinal study of visual acuity loss in patients with X-linked retinoschisis. *Retina*. (2005) 25:612–8. doi: 10.1097/00006982-200507000-00012
228. Tanimoto N, Usui T, Takagi M, Hasegawa S, Abe H, Sekiya K, et al. Electroretinographic findings in three family members with X-linked juvenile retinoschisis associated with a novel Pro192Thr mutation of the XLRS1 gene. *Jpn J Ophthalmol.* (2002) 46:568–76. doi: 10.1016/S0021-5155(02)00539-7
229. Romano F, Arrigo A, Ch'ng SW, Battaglia Parodi M, Manitto MP, Martina E, et al. Capillary network alterations in X-linked retinoschisis imaged on optical coherence tomography angiography. *Retina.* (2019) 39:1761–7. doi: 10.1097/IAE.0000000000002222
230. Grayson C, Reid SN, Ellis JA, et al. Retinoschisin, the X-linked retinoschisis protein, is a secreted photoreceptor protein, and is expressed and released by Weri-Rb1 cells. *Hum Mol Genet.* (2000) 9:1873–9. doi: 10.1093/hmg/9.12.1873
231. Molday LL, Hicks D, Sauer CG, Weber BH, Molday RS. Expression of X-linked retinoschisis protein RS1 in photoreceptor and bipolar cells. *Invest Ophthalmol Vis Sci.* (2001) 42:816–25.
232. Reid SN, Yamashita C, Farber DB. Retinoschisin, a photoreceptor-secreted protein, and its interaction with bipolar and muller cells. *J Neurosci.* (2003) 23:6030–40. doi: 10.1523/JNEUROSCI.23-14-06030.2003
233. Wu WW, Wong JP, Kast J, Molday RS. RS1, a discoidin domain-containing retinal cell adhesion protein associated with X-linked retinoschisis, exists as a novel disulfide-linked octamer. *J Biol Chem.* (2005) 280:10721–30. doi: 10.1074/jbc.M413117200
234. Wang T, Zhou A, Waters CT, O'Connor E, Read RJ, Trump D. Molecular pathology of X linked retinoschisis: mutations interfere with retinoschisin secretion and oligomerisation. *Br J Ophthalmol.* (2006) 90:81–6. doi: 10.1136/bjo.2005.078048
235. Bush RA, Zeng Y, Colosi P, Kjellstrom S, Hiriyanna S, Vijayasarathy C, et al. Preclinical dose-escalation study of intravitreal AAV-RS1 gene therapy in a mouse model of X-linked retinoschisis: dose-dependent expression and improved retinal structure and function. *Hum Gene Ther.* (2016) 27:376–89. doi: 10.1089/hum.2015.142
236. Janssen A, Min SH, Molday LL, Tanimoto N, Seeliger MW, Hauswirth WW, et al. Effect of late-stage therapy on disease progression in AAV-mediated rescue of photoreceptor cells in the retinoschisin-deficient mouse. *Mol Ther.* (2008) 16:1010–7. doi: 10.1038/mt.2008.57
237. Min SH, Molday LL, Seeliger MW, Dinculescu A, Timmers AM, Janssen A, et al. Prolonged recovery of retinal structure/function after gene therapy in an Rs1h-deficient mouse model of x-linked juvenile retinoschisis. *Mol Ther.* (2005) 12:644–51. doi: 10.1016/j.ymthe.2005.06.002
238. Marangoni D, Bush RA, Zeng Y, Wei LL, Ziccardi L, Vijayasarathy C, et al. Ocular and systemic safety of a recombinant AAV8 vector for X-linked retinoschisis gene therapy: GLP studies in rabbits and Rs1-KO mice. *Mol Ther Methods Clin Dev.* (2016) 5:16011. doi: 10.1038/mtm.2016.11
239. Cukras C, Wiley HE, Jeffrey BG, Sen HN, Turriff A, Zeng Y, et al. Retinal AAV8-RS1 gene therapy for X-linked retinoschisis: initial findings from a phase I/IIa trial by intravitreal delivery. *Mol Ther.* (2018) 26:2282–94. doi: 10.1016/j.ymthe.2018.05.025
240. Tanna P, Strauss RW, Fujinami K, Michaelides M. Stargardt disease: clinical features, molecular genetics, animal models and therapeutic options. *Br J Ophthalmol.* (2017) 101:25–30. doi: 10.1136/bjophthalmol-2016-308823
241. Voigt M, Querques G, Atmani K, Leveziel N, Massamba N, Puche N, et al. Analysis of retinal flecks in fundus flavimaculatus using high-definition spectral-domain optical coherence tomography. *Am J Ophthalmol.* (2010) 150:330–7. doi: 10.1016/j.ajo.2010.04.001
242. Gomes NL, Greenstein VC, Carlson JN, Tsang SH, Smith RT, Carr RE, et al. A comparison of fundus autofluorescence and retinal structure in patients with Stargardt disease. *Invest Ophthalmol Vis Sci.* (2009) 50:3953–9. doi: 10.1167/iovs.08-2657
243. Klufas MA, Tsui I, Sadda SR, Hosseini H, Schwartz SD. Ultrawidefield autofluoresence in Abca4 Stargardt disease. *Retina*. (2018) 38:403–15. doi: 10.1097/IAE.0000000000001567
244. Arrigo A, Romano F, Aragona E, di Nunzio C, Sperti A, Bandello F, et al. OCTA-based identification of different vascular patterns in Stargardt disease. *Transl Vis Sci Technol.* (2019) 8:26. doi: 10.1167/tvst.8.6.26
245. Arrigo A, Grazioli A, Romano F, Aragona E, Marchese A, Bordato A, et al. Multimodal evaluation of central and peripheral alterations in Stargardt disease: a pilot study. *Br J Ophthalmol.* (2020) 104:1234–8. doi: 10.1136/bjophthalmol-2019-315148
246. Allikmets R, Singh N, Sun H, Shroyer NF, Hutchinson A, Chidambaram A, et al. A photoreceptor cell-specific ATP-binding transporter gene (ABCR) is mutated in recessive Stargardt macular dystrophy. *Nat Genet.* (1997) 15:236–46. doi: 10.1038/ng0397-236
247. Yi J, Li S, Jia X, Xiao X, Wang P, Guo X, et al. Evaluation of the ELOVL4, PRPH2 and ABCA4 genes in patients with Stargardt macular degeneration. *Mol Med Rep.* (2012) 6:1045–9. doi: 10.3892/mmr.2012.1063
248. Zhang X, Ge X, Shi W, Huang P, Min Q, Li M, et al. Molecular diagnosis of putative Stargardt disease by capture next generation sequencing. *PLoS One.* (2014) 9:e95528. doi: 10.1371/journal.pone.0095528
249. Fujinami K, Lois N, Mukherjee R, McBain VA, Tsunoda K, Tsubota K, et al. A longitudinal study of Stargardt disease: quantitative assessment of fundus autofluorescence, progression, and genotype correlations. *Invest Ophthalmol Vis Sci.* (2013) 54:8181–90. doi: 10.1167/iovs.13-12104
250. Riveiro-Alvarez R, Lopez-Martinez MA, Zernant J, Aguirre-Lamban J, Cantalapiedra D, Avila-Fernandez A, et al. Outcome of ABCA4 disease-associated alleles in autosomal recessive retinal dystrophies: retrospective analysis in 420 Spanish families. *Ophthalmology.* (2013) 120:2332–7. doi: 10.1016/j.ophtha.2013.04.002
251. Fujinami K, Sergouniotis PI, Davidson AE, Mackay DS, Tsunoda K, Tsubota K, et al. The clinical effect of homozygous ABCA4 alleles in 18 patients. *Ophthalmology.* (2013) 120:2324–31. doi: 10.1016/j.ophtha.2013.04.016
252. Cella W, Greenstein VC, Zernant-Rajang J, Smith TR, Barile G, Allikmets R, et al. G1961E mutant allele in the Stargardt disease gene ABCA4 causes bull's eye maculopathy. *Exp Eye Res.* (2009) 89:16–24. doi: 10.1016/j.exer.2009.02.001
253. Lambertus S, van Huet RA, Bax NM, Hoefsloot LH, Cremers FP, Boon CJ, et al. Early-onset stargardt disease: phenotypic and genotypic characteristics. *Ophthalmology.* (2015) 122:335–44. doi: 10.1016/j.ophtha.2014.08.032
254. Simonelli F, Testa F, Zernant J, Nesti A, Rossi S, Allikmets R, et al. Genotype-phenotype correlation in Italian families with Stargardt disease. *Ophthalmic Res.* (2005) 37:159–67. doi: 10.1159/000086073
255. Gemenetzi M, Lotery AJ. Phenotype/genotype correlation in a case series of Stargardt's patients identifies novel mutations in the ABCA4 gene. *Eye (Lond).* (2013) 27:1316–9. doi: 10.1038/eye.2013.176
256. Zernant J, Lee W, Collison FT, Fishman GA, Sergeev YV, Schuerch K, et al. Frequent hypomorphic alleles account for a significant fraction of ABCA4 disease and distinguish it from age-related macular degeneration. *J Med Genet.* (2017) 54:404–12. doi: 10.1136/jmedgenet-2017-104540
257. Braun TA, Mullins RF, Wagner AH, Andorf JL, Johnston RM, Bakall BB, et al. Non-exomic and synonymous variants in ABCA4 are an important cause of Stargardt disease. *Hum Mol Genet.* (2013) 22:5136–45. doi: 10.1093/hmg/ddt367
258. Bauwens M, De Zaeytijd J, Weisschuh N, Kohl S, Meire F, Dahan K, et al. An augmented ABCA4 screen targeting noncoding regions reveals a deep intronic founder variant in Belgian Stargardt patients. *Hum Mutat.* (2015) 36:39–42. doi: 10.1002/humu.22716
259. Kong J, Kim SR, Binley K, Pata I, Doi K, Mannik J, et al. Correction of the disease phenotype in the mouse model of Stargardt disease by lentiviral gene therapy. *Gene Ther.* (2008) 15:1311–20. doi: 10.1038/gt.2008.78
260. Dyka FM, Molday LL, Chiodo VA, Molday RS, Hauswirth WW. Dual ABCA4-AAV vector treatment reduces pathogenic retinal A2E accumulation in a mouse model of autosomal recessive Stargardt disease. *Hum Gene Ther.* (2019) 30:1361–70. doi: 10.1089/hum.2019.132
261. Sun D, Sun W, Gao SQ, Wei C, Naderi A, Schilb AL, et al. Formulation and efficacy of ECO/pRHO-ABCA4-SV40 nanoparticles for nonviral gene therapy of Stargardt disease in a mouse model. *J Control Release.* (2021) 330:329–40. doi: 10.1016/j.jconrel.2020.12.010

262. Sun D, Schur RM, Sears AE, Gao SQ, Vaidya A, Sun W, et al. Non-viral gene therapy for Stargardt disease with ECO/pRHO-ABCA4 self-assembled nanoparticles. *Mol Ther.* (2020) 28:293–303. doi: 10.1016/j.ymthe.2019.09.010
263. Glover DJ, Lipps HJ, Jans DA. Towards safe, non-viral therapeutic gene expression in humans. *Nat Rev Genet.* (2005) 6:299–310. doi: 10.1038/nrg1577
264. Michaelides M, Hunt DM, Moore AT. The cone dysfunction syndromes. *Br J Ophthalmol.* (2004) 88:291–7. doi: 10.1136/bjo.2003.027102
265. Aboshiha J, Dubis AM, Carroll J, Hardcastle AJ, Michaelides M. The cone dysfunction syndromes. *Br J Ophthalmol.* (2016) 100:115–21. doi: 10.1136/bjophthalmol-2014-306505
266. Hirji N, Aboshiha J, Georgiou M, Bainbridge J, Michaelides M. Achromatopsia: clinical features, molecular genetics, animal models and therapeutic options. *Ophthalmic Genet.* (2018) 39:149–57. doi: 10.1080/13816810.2017.1418389
267. Andreasson S, Tornqvist K. Electroretinograms in patients with achromatopsia. *Acta Ophthalmol (Copenh).* (1991) 69:711–6. doi: 10.1111/j.1755-3768.1991.tb02048.x
268. Thiadens AA, Slingerland NW, Roosing S, van Schooneveld MJ, van Lith-Verhoeven JJ, van Moll-Ramirez N, et al. Genetic etiology and clinical consequences of complete and incomplete achromatopsia. *Ophthalmology.* (2009) 116:1984.e1–9.e1. doi: 10.1016/j.ophtha.2009.03.053
269. Sundaram V, Wilde C, Aboshiha J, Cowing J, Han C, Langlo CS, et al. Retinal structure and function in achromatopsia: implications for gene therapy. *Ophthalmology.* (2014) 121:234–45. doi: 10.1016/j.ophtha.2013.08.017
270. Aboshiha J, Dubis AM, Cowing J, Fahy RT, Sundaram V, Bainbridge JW, et al. A prospective longitudinal study of retinal structure and function in achromatopsia. *Invest Ophthalmol Vis Sci.* (2014) 55:5733–43. doi: 10.1167/iovs.14-14937
271. Scoles D, Flatter JA, Cooper RF, Langlo CS, Robison S, Neitz M, et al. Assessing photoreceptor structure associated with ellipsoid zone disruptions visualized with optical coherence tomography. *Retina.* (2016) 36:91–103. doi: 10.1097/IAE.0000000000000618
272. Remmer MH, Rastogi N, Ranka MP, Ceisler EJ. Achromatopsia: a review. *Curr Opin Ophthalmol.* (2015) 26:333–40. doi: 10.1097/ICU.0000000000000189
273. Aligianis IA, Forshew T, Johnson S, Michaelides M, Johnson CA, Trembath RC, et al. Mapping of a novel locus for achromatopsia (ACHM4) to 1p and identification of a germline mutation in the alpha subunit of cone transducin (GNAT2). *J Med Genet.* (2002) 39:656–60. doi: 10.1136/jmg.39.9.656
274. Thiadens AA, den Hollander AI, Roosing S, Nabuurs SB, Zekveld-Vroon RC, Collin RW, et al. Homozygosity mapping reveals PDE6C mutations in patients with early-onset cone photoreceptor disorders. *Am J Hum Genet.* (2009) 85:240–7. doi: 10.1016/j.ajhg.2009.06.016
275. Kohl S, Coppieters F, Meire F, Schaich S, Roosing S, Brennenstuhl C, et al. A nonsense mutation in PDE6H causes autosomal-recessive incomplete achromatopsia. *Am J Hum Genet.* (2012) 91:527–32. doi: 10.1016/j.ajhg.2012.07.006
276. Kohl S, Zobor D, Chiang WC, Weisschuh N, Staller J, Gonzalez Menendez I, et al. Mutations in the unfolded protein response regulator ATF6 cause the cone dysfunction disorder achromatopsia. *Nat Genet.* (2015) 47:757–65. doi: 10.1038/ng.3319
277. Mühlfriedel R, Tanimoto N, Schön C, Sothilingam V, Garcia Garrido M, Beck SC, et al. AAV-mediated gene supplementation therapy in achromatopsia type 2: preclinical data on therapeutic time window and long-term effects. *Front Neurosci.* (2017) 11:292. doi: 10.3389/fnins.2017.00292
278. Michalakis S, Mühlfriedel R, Tanimoto N, Krishnamoorthy V, Koch S, Fischer MD, et al. Restoration of cone vision in the CNGA3$^{-/-}$ mouse model of congenital complete lack of cone photoreceptor function. *Mol Ther.* (2010) 18:2057–63. doi: 10.1038/mt.2010.149
279. Carvalho LS, Xu J, Pearson RA, Smith AJ, Bainbridge JW, Morris LM, et al. Long-term and age-dependent restoration of visual function in a mouse model of CNGB3-associated achromatopsia following gene therapy. *Hum Mol Genet.* (2011) 20:3161–75. doi: 10.1093/hmg/ddr218
280. Pang JJ, Deng WT Dai X, Lei B, Everhart D, Umino Y, et al. AAV-mediated cone rescue in a naturally occurring mouse model of CNGA3-achromatopsia. *PLoS ONE.* (2012) 7:e35250. doi: 10.1371/journal.pone.0035250
281. Alexander JJ, Umino Y, Everhart D, Chang B, Min SH Li Q, et al. Restoration of cone vision in a mouse model of achromatopsia. *Nat Med.* (2007) 13:685–7. doi: 10.1038/nm1596
282. Gootwine E, Abu-Siam M, Obolensky A, Rosov A, Honig H, Nitzan T, et al. Gene augmentation therapy for a missense substitution in the cGMP-binding domain of ovine CNGA3 gene restores vision in day-blind sheep. *Invest Ophthalmol Vis Sci.* (2017) 58:1577–84. doi: 10.1167/iovs.16-20986
283. Banin E, Gootwine E, Obolensky A, Ezra-Elia R, Ejzenberg A, Zelinger L, et al. Gene augmentation therapy restores retinal function and visual behavior in a sheep model of CNGA3 achromatopsia. *Mol Ther.* (2015) 23:1423–33. doi: 10.1038/mt.2015.114
284. Komáromy AM, Rowlan JS, Corr AT, Reinstein SL, Boye SL, Cooper AE, et al. Transient photoreceptor deconstruction by CNTF enhances rAAV-mediated cone functional rescue in late stage CNGB3-achromatopsia. *Mol Ther.* (2013) 21:1131–41. doi: 10.1038/mt.2013.50

Conflict of Interest: FB consultant for Alcon (Fort Worth, Texas, USA), Alimera Sciences (Alpharetta, Georgia, USA), Allergan Inc. (Irvine, California, USA), Farmila-Thea (Clermont-Ferrand, France), Bayer Shering-Pharma (Berlin, Germany), Bausch and Lomb (Rochester, New York, USA), Genentech (San Francisco, California, USA), Hoffmann-La-Roche (Basel, Switzerland), NovagaliPharma (Évry, France), Novartis (Basel, Switzerland), Sanofi-Aventis (Paris, France), Thrombogenics (Heverlee, Belgium), and Zeiss (Dublin, USA).

The remaining authors declare that the research was conducted in the absence of any commercial or financial relationships that could be construed as a potential conflict of interest.

Publisher's Note: All claims expressed in this article are solely those of the authors and do not necessarily represent those of their affiliated organizations, or those of the publisher, the editors and the reviewers. Any product that may be evaluated in this article, or claim that may be made by its manufacturer, is not guaranteed or endorsed by the publisher.

frontiers in Medicine

ORIGINAL RESEARCH
published: 27 October 2021
doi: 10.3389/fmed.2021.755816

Outcomes of Primary 27-Gauge Vitrectomy for 73 Consecutive Cases With Uveitis-Associated Vitreoretinal Disorders

Kyung Woo Kim, Sentaro Kusuhara, Hisanori Imai, Noriyuki Sotani, Ryuto Nishisho, Wataru Matsumiya and Makoto Nakamura*

Division of Ophthalmology, Department of Surgery, Kobe University Graduate School of Medicine, Kobe, Japan

OPEN ACCESS

Edited by:
Ryoji Yanai,
Yamaguchi University, Japan

Reviewed by:
Steve Charles,
University of Tennessee Health Science Center (UTHSC), United States
Manami Ohta,
Yamaguchi University, Japan

***Correspondence:**
Sentaro Kusuhara
kusu@med.kobe-u.ac.jp

Specialty section:
This article was submitted to Ophthalmology, a section of the journal Frontiers in Medicine

Received: *09 August 2021*
Accepted: *04 October 2021*
Published: *27 October 2021*

Citation:
Kim KW, Kusuhara S, Imai H, Sotani N, Nishisho R, Matsumiya W and Nakamura M (2021) Outcomes of Primary 27-Gauge Vitrectomy for 73 Consecutive Cases With Uveitis-Associated Vitreoretinal Disorders. Front. Med. 8:755816. doi: 10.3389/fmed.2021.755816

Background: Since the advent of 27-gauge microincision vitrectomy system a decade ago, evidence regarding the feasibility, safety, and effectiveness of 27-gauge pars plana vitrectomy (PPV) has increased.

Aim: To assess the effectiveness and safety profile of 27-gauge PPV for various vitreoretinal conditions associated with uveitis.

Methods: We retrospectively investigated 73 consecutive cases that underwent primary 27-gauge PPV for uveitis-related ocular disorders between October 2014 and April 2021. The primary outcome measures were mean change in logMAR best-corrected decimal visual acuity (BCVA) pre-operatively to 3 months post-operatively, the proportion of BCVA improvement category defined as the degree of logMAR BCVA difference ("improved" [≤ -0.3], "unchanged" [-0.3 to 0.3], and "worsened" [≥ 0.3]) pre-operatively to 3 months post-operatively, the mean change in intraocular inflammation scores pre-operatively to 3 months post-operatively; and intraoperative and post-operative complications.

Results: The mean logMAR BCVA significantly improved from 0.69 pre-operatively to 0.42 at 3 months post-operatively ($P = 0.017$). The percentages of eyes with "improved," "unchanged," and "worsened" BCVA at 3 months post-operatively were 37, 50, and 13%, respectively. The mean anterior chamber cell score was 0.6 pre-operatively and 0.2 at 3 months post-operatively ($P = 0.001$), the mean anterior chamber flare score was 0.4 pre-operatively and 0.1 at 3 months post-operatively ($P = 0.004$), and the mean vitreous haze score was 1.9 pre-operatively and 0.1 at 3 months post-operatively ($P < 0.001$). Surgery-related complications occurred in 35 (48%) eyes, 68% of which were related to intraocular pressure and transient.

Conclusions: Given its risk–benefit profile, 27-gauge PPV is a promising option for the treatment of vitreoretinal disorders in uveitis.

Keywords: uveitis, 27-gauge, vitrectomy, visual acuity, inflammation, complication

INTRODUCTION

Medical therapy is the cornerstone for the management of uveitis, a potentially sight-threatening intraocular inflammatory disorder (1, 2). However, pars plana vitrectomy (PPV) may be performed when medical therapy fails, secondary vitreoretinal complications develop, or diagnostic vitreous/retinal sampling is necessary (3–12). The benefits of PPV in eyes with uveitis chiefly stem from the removal of vitreous gel and abnormal tissues that cause media opacification, intraocular accumulation of inflammatory mediators, and/or retinal complications (12). However, the surgical stress associated with PPV increases the risk of intraoperative and post-operative complications in inflamed eyes (7, 12, 13). Therefore, balancing benefits with risks has become the primary concern when performing PPV for uveitis (12, 14, 15).

The microincision vitrectomy system (MIVS), first appeared as 25-gauge PPV, was developed nearly two decades ago (16) and has gradually become the standard surgical platform for various indications, including uveitis-related vitreoretinal disorders (8, 9). Recent technological advances have enabled PPV using 27-gauge instruments (27-gauge PPV) as Oshima and associates documented in 2010 (17). This smaller-gauge instrumentation can enhance the advantages of MIVS, such as reduced patient discomfort, minimal scarring, and rapid recovery of vision post-operatively. Thus far, many researchers have reported the feasibility, safety, and efficiency of 27-gauge PPV (17–24). Given its less invasive nature, 27-gauge PPV should be suitable for vitreoretinal disorders secondary to uveitis. However, to the best of our knowledge, the usefulness of 27-PPV for eyes with uveitis remains unknown. To address this research gap, this study aimed to assess the effectiveness and safety profile of 27-gauge PPV for various vitreoretinal conditions associated with uveitis.

MATERIALS AND METHODS

Study Design and Patients

This single-center retrospective study was approved by the institutional review board of the Kobe University Graduate School of Medicine (permission number: 170115) and adhered to the tenets of the Declaration of Helsinki for research involving human subjects. Informed consent was not obtained from patients due to the retrospective, observational nature of this study. However, patients were able to withdraw their consent anytime through the opt-out choice provided on the hospital homepage.

We reviewed the medical records of 73 consecutive eyes from 73 patients who underwent primary 27-gauge PPV for uveitis-related ocular disorders between October 2014 and April 2021 at Kobe University Hospital. Patients with a history of 27-gauge PPV for the fellow eye were excluded ($n = 13$) to evade inter-eye correlation in statistical analyses. The collected data included the following: age, sex, laterality of the operated eye, anatomical type of uveitis, cause of uveitis, lens status, best-corrected decimal visual acuity (BCVA) (converted to the logarithm of the minimum angle of resolution [logMAR] for analysis), intraocular pressure, anterior chamber cell, anterior chamber flare, vitreous haze, presence or absence of retinal and/or choroidal lesion, purpose of surgery, date of surgery, concomitant cataract surgery, tamponade agent, surgical time, complications, and final visit date. Intraocular inflammation scoring for the anterior chamber cell, anterior chamber flare, and vitreous haze was carried out according to the National Eye Institute criteria adapted by the Standardization of Uveitis Nomenclature Working Group (25).

Surgical Technique

All surgeries were performed by two experienced surgeons (SK and HI). All patients received local anesthesia consisting of 4% lidocaine eye drops and sub-Tenon injection of ∼4 mL of 2% lidocaine or 0.75% ropivacaine hydrochloride. General anesthesia was performed as necessary. Patients' skin and ocular surfaces were disinfected using 5% povidone-iodine and eight-fold diluted PA · IODO Ophthalmic and Eye washing Solution Disinfection (Nitten Pharmaceutical Co., Nagoya, Japan). The Constellation Vision System (Alcon Laboratories, Inc., Fort Worth, TX, USA) combined with a 27+ Combined Procedure Pak (Alcon Laboratories, Inc.) and a wide-angle non-contact viewing system (Resight 500 or 700, Carl Zeiss Meditec AG, Jena, Germany) were used for all surgeries. A 27G Oshima Vivid chandelier (Bausch and Lomb, St. Louis, MO) was utilized for illumination as needed. Combined cataract surgery, phacoemulsification, and intraocular lens implantation were performed using the Constellation Vision System (Alcon Laboratories) as needed. We routinely removed as much vitreous gel as possible irrespective of the purpose of the surgery.

Outcomes

The primary outcome measures were mean change in logMAR BCVA pre-operatively to 3 months post-operatively, the proportion of BCVA improvement category defined as the degree of logMAR BCVA difference ("improved" [≤ -0.3], "unchanged" [-0.3 to 0.3], "worsened" [≥ 0.3]) pre-operatively to 3 months post-operatively, the mean changes in intraocular inflammation scores pre-operatively to 3 months post-operatively, and intraoperative and post-operative complications.

Statistical Analyses

All statistical analyses were carried out as complete case analyses; cases with any missing data were excluded from analysis at each time point. The Wilcoxon test was used for time comparisons (baseline and 3 months post-operatively) for each variable. Statistical analyses were performed using MedCalc v.16.8.4 software (MedCalc Software, Belgium). P-value < 0.05 was considered statistically significant.

RESULTS

The pre-operative characteristics of the included patients are summarized in **Table 1**. The purposes of surgery (number of eyes) were biopsy (38 [52%]), removal of vitreous opacity (12 [16%]), epiretinal membrane peeling (7 [10%]), reduction of infectious pathogens (6 [8%]), repair of retinal detachment (3 [4%]), removal of vitreous hemorrhage (3 [4%]), removal of retained lens fragment (2 [3%]), closure of macular hole (1

TABLE 1 | Pre-operative characteristics of the included patients.

Characteristic	Data
Number of patients/affected eyes, n/n	73/73
Age (years), mean (SD)	66.8 (13.3)
Sex, men/women, n (%)/n (%)	33 (45)/40 (55)
Eye, right/left, n (%)/n (%)	44 (60)/29 (40)
Anatomical type of uveitis, n (%)	
Anterior uveitis	1 (1)
Intermediate uveitis	12 (16)
Posterior uveitis	13 (18)
Panuveitis	41 (56)
Unspecified	6 (8)
Cause of uveitis, n (%)	
Vitreoretinal lymphoma	22 (30)
Acute retinal necrosis	7 (10)
Cytomegalovirus retinitis	6 (8)
Post-operative infectious endophthalmitis	4 (5)
Others	7 (10)
Unclassified	27 (37)
Lens status, n (%)	
Phakia	39 (53)
Pseudophakia	33 (45)
Aphakia	1 (1)
Best-corrected visual acuity (decimal), median (range)	0.4 (LP−1.5)
Best-corrected visual acuity (logMAR), mean (SD)	0.687 (0.802)
Intraocular pressure (mmHg), mean (SD)	15.9 (8.0)
Anterior chamber cells (grade), mean (SD)	0.6 (0.8)
Anterior chamber flare (grade), mean (SD)	0.4 (0.9)
Vitreous haze (grade), mean (SD)	1.9 (1.2)

SD, standard deviation; logMAR, logarithm of the minimum angle of resolution; LP, light perception.

[1%]), and improvement of macular edema (1 [1%]). Of the total 39 phakic eyes, 38 (97%) underwent concomitant cataract surgery (phacoemulsification and intraocular lens implantation). Intraocular tamponade was performed in 13 (18%) eyes. The tamponade agents used (number of eyes) were air (5 [38%]), 20% SF_6 gas (2 [15%]), and silicone oil (6 [46%]). The mean surgical time was 47.1 ± 26.1 min and the mean follow-up time was 14.6 ± 15.1 months. Post-operatively, 25 (34%) continued corticosteroid eye drops for more than 1 month.

Overall, the mean logMAR BCVA was 0.69 ± 0.80 pre-operatively, 0.40 ± 0.72 at 1 month post-operatively, 0.42 ± 0.78 at 3 months post-operatively, 0.35 ± 0.70 at 6 months post-operatively, 0.40 ± 0.76 at 9 months post-operatively, and 0.33 ± 0.72 at 12 months post-operatively ($P = 0.017$, pre-operatively vs. 3 months post-operatively; **Figure 1**). The mean logMAR BCVA showed a significant difference at each post-operative time point as compared to pre-operatively ($P < 0.001$ at 1 month, $P = 0.017$ at 3 months, $P = 0.021$ at 6 months, $P = 0.027$ at 9 months, and $P = 0.016$ at 12 months). The percentages of eyes with "improved," "unchanged," and "worsened" BCVA at 3 months after surgery were 37, 50, and 13%, respectively. The percentages of eyes with a BCVA of 20/200 or better and 20/40 or better were 74 and 50% pre-operatively and 91% and 76% at 12 months post-operatively, respectively. According to diagnosis, the mean logMAR BCVA pre-operatively and at 12 months post-operatively were 0.59 ± 0.84 and −0.04 ± 0.13 in vitreoretinal lymphoma, 0.67 ± 0.89 and 1.35 ± 1.77 in acute retinal necrosis, 0.73 ± 0.89 and 0.61 ± 0.13 in cytomegalovirus retinitis, 1.25 ± 1.09 and 0.37 ± 0.46 in post-operative infectious endophthalmitis, 1.13 ± 0.96 and 0.07 ± 0.21 in others, and 0.58 ± 0.66 and 0.43 ± 0.82 in unclassified conditions, respectively (**Figure 2**).

The cell and flare scores in the anterior chamber as well as the vitreous haze score, significantly improved after surgery (**Figure 3**). The mean anterior chamber cell score was 0.6 ± 0.8 pre-operatively and 0.2 ± 0.4 at 3 months post-operatively ($P = 0.001$). The mean anterior chamber flare score was 0.4 ± 0.9 pre-operatively and 0.1 ± 0.3 at 3 months post-operatively ($P = 0.004$). The mean vitreous haze score was 1.9 ± 1.2 pre-operatively and 0.1 ± 0.5 at 3 months post-operatively ($P < 0.001$). Of the 73 eyes, 41% had 1+ or greater anterior chamber cells, 27% showed 1+ or greater anterior chamber flare, and 90% exhibited 1+ or greater vitreous haze before surgery. At 3 months post-operatively, the percentage of eyes demonstrating a 1+ or greater score decreased to 29% in anterior chamber cells, 6% in anterior chamber flare, and 4% in vitreous haze. The development of new retinal/choroidal lesions was observed in 13 (18%) eyes up to 3 months post-operatively.

Surgery-related complications occurred in 35 (48%) eyes; 6 (8%) occurred intraoperatively, 24 (33%) occurred within 2 weeks post-operatively, and 11 (15%) occurred after 2 weeks post-operatively (some cases were overlapping), as listed in **Table 2**. The most common intraoperative complication was retinal breaks, which were properly treated via laser photocoagulation. One eye experienced choroidal effusion due to slippage of the infusion cannula out of a sclerotomy. Ocular hypertension was the most frequent complication within 2 weeks post-operatively. Although it was transient in most cases, some eyes required glaucoma eye drops. Transient post-operative ocular hypotension also occurred during the same time frame and was often accompanied by choroidal detachment. Beyond 2 weeks post-operatively, retinal detachment was the most common complication and was successfully treated via additional vitrectomy. The incidence rate of complications between the biopsy and non-biopsy groups and among the cause of uveitis was not significant at any post-operative time point. In the comparison between eyes with and without glaucoma/ocular hypertension pre-operatively, the difference in the incidence rate of postsurgical ocular inflammation did not reach a statistical significance ($P = 0.279$).

DISCUSSION

In the present study, we retrospectively analyzed 73 consecutive cases that underwent primary 27-gauge PPV for various vitreoretinal disorders associated with uveitis. Henry et al. conducted a systematic literature review of PPV for uveitis and summarized the data of 34 recent articles (12). The review reported the following mean or median patient demographics for

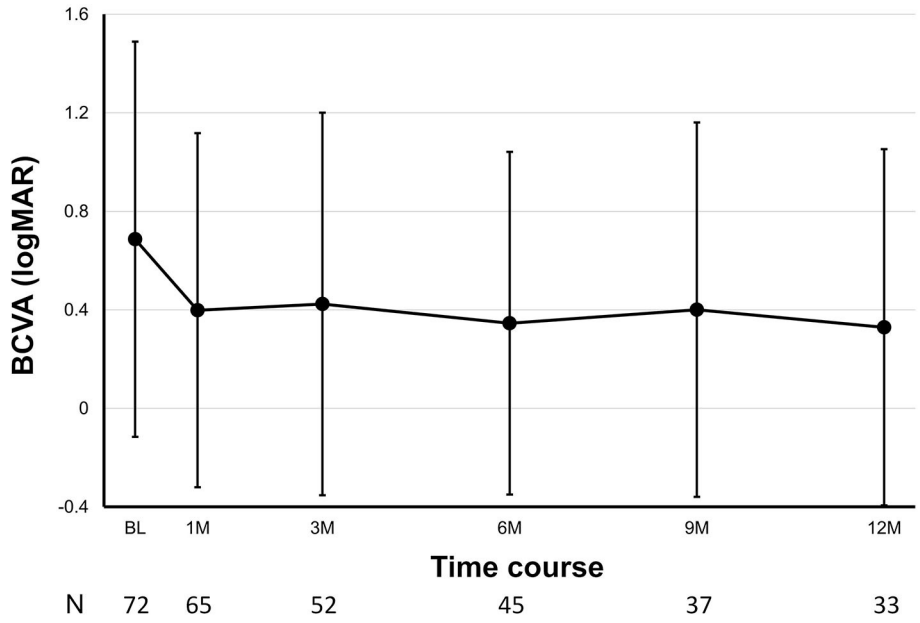

FIGURE 1 | Post-operative changes in best-corrected visual acuity (BCVA) over time. Number of eyes (N) is provided at each time point.

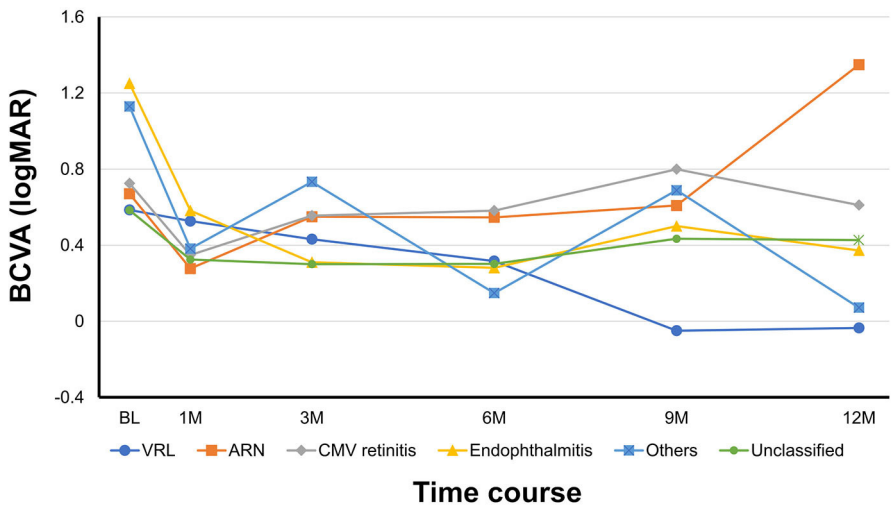

VRL	22	18	13	13	9	10
ARN	7	7	6	6	5	2
CMV retinitis	6	3	4	3	3	2
Endophthalmitis	4	4	2	3	2	2
Others	6	7	5	3	4	2
Unclassified	27	26	22	17	14	15

FIGURE 2 | Post-operative changes in best-corrected visual acuity (BCVA) over time according to diagnosis. Number of eyes (N) is provided at each time point. VRL, vitreoretinal lymphoma; ARN, acute retinal necrosis; CMV, cytomegalovirus.

each included study: number of eyes (13.5), age at the time of PPV (42.8 years), and follow-up time after PPV (19.0 months). Compared with these data, the current study had a larger number of eyes (73), older age at time of PPV (66.8 years), and similar follow-up time after PPV (14.6 months). The reason for the older age at time of PPV in our study could be attributed to the smaller number of eyes with young-onset uveitis. In Henry's review, Behçet's disease and juvenile idiopathic arthritis accounted for

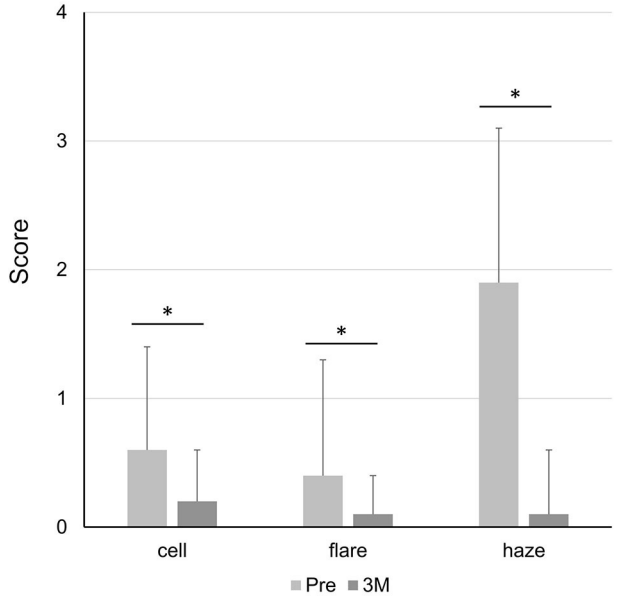

FIGURE 3 | Post-operative change in inflammation scores. cell, cells in the anterior chamber; flare, flare in the anterior chamber; haze, vitreous haze; Pre, pre-operatively; 3M, at 3 months post-operatively. *$P < 0.05$.

TABLE 2 | Surgical complications.

Complication	Intraoperative	Post-operative (within 2 weeks)	Post-operative (after 2 weeks)
Iatrogenic retinal break	2 (3)	0 (0)	0 (0)
Discovery of retinal tear	2 (3)	0 (0)	0 (0)
Bleeding from iris neovascularization	1 (1)	0 (0)	0 (0)
Choroid effusion	1 (1)	0 (0)	0 (0)
Ocular hypertension	0 (0)	13 (18)	2 (3)
Ocular hypotension	0 (0)	8 (11)	0 (0)
Choroidal detachment	0 (0)	4 (5)	0 (0)
Retinal detachment	0 (0)	2 (3)	4 (5)
Hyphema	0 (0)	2 (3)	0 (0)
Vitreous hemorrhage	0 (0)	1 (1)	1 (1)
Corneal erosion	0 (0)	1 (1)	0 (0)
Dislocation of intraocular lens	0 (0)	0 (0)	1 (1)
Epiretinal membrane	0 (0)	0 (0)	1 (1)
Macular edema	0 (0)	0 (0)	1 (1)
Suture-related infection	0 (0)	0 (0)	1 (1)

Data are provided as n (%).

8.1% and 9.3% of all eyes, respectively (12). In contrast, none of the cases in our study had Behçet's disease or juvenile idiopathic arthritis. The specified anatomical location of uveitis was similar between studies, in that ∼50% of eyes had panuveitis. In the cause of uveitis, vitreoretinal lymphoma comprised 30% of all eyes, which is the greatest feature of our cohort and may affect the surgical outcomes as described below. Note that the mean surgical time of 47.1 min in our study is longer than that reported in previous studies (20.2–38.8 min for non-uveitic eyes) (17, 18, 24). This difference may be attributed to the higher rate of concomitant cataract surgery, the need to educate unexperienced nurses and assistants during surgery, or both. As surgical time in MIVS is one of the most interesting points for vitreous surgeons, further studies are required to understand the real impact of 27-gauge PPV on surgical time in eyes with uveitis.

Overall, the visual outcomes of 27-gauge PPV for uveitis in our study were promising. The mean logMAR BCVA significantly improved, with 37% of eyes attaining logMAR BCVA improvement of ≤ -0.3 and 76% of eyes with a BCVA of 20/40 or better at 12 months post-operatively. The subgroup analyses based on diagnosis showed a similar tendency, with the exception of the acute retinal necrosis group wherein the mean logMAR BCVA worsened during follow-up as cases with good vision recovery returned to a local doctor. It should be noted that the method of reporting visual outcome results differs among studies, including the definition of BCVA improvement and time points of BCVA evaluation. The factors affecting post-operative visual recovery (e.g., cause of uveitis, pre-operative BCVA, and pre-operative inflammatory status) may also vary. In an analysis of 519 eyes with uveitis from 31 studies, BCVA improved in 69% of eyes, was unchanged in 18% of eyes, and worsened in 13% of eyes (12). In 25-gauge PPV for uveitis, Soheilian et al. reported that 59% of patients showed BCVA improvement (9), whereas Kamei et al. reported a mean logMAR BCVA of 0.58 at 12 weeks post-operatively (8). In the current study, 87% of eyes had improved/unchanged BCVA at 3 months post-operatively, 76% of eyes attained a BCVA of 20/40 or better at 12 months post-operatively, and the mean logMAR BCVA was 0.423 at 3 months post-operatively. Although it is not meaningful to directly compare visual outcomes among studies due to the aforementioned reasons, the visual outcomes following 27-gauge PPV in our study were generally satisfactory.

Post-operative inflammation is a concern to ophthalmologists operating on eyes with uveitis because the underlying uveitis may be exacerbated following surgery. According to a systematic literature review, intraocular inflammation generally subsides following PPV (12), which is consistent with the findings of our study. However, as most previous studies did not apply standardized grading, it is difficult to properly compare the degree of inflammation among studies. Kamei et al. reported changes in ocular inflammation in 20 eyes with uveitis that underwent 25-gauge PPV. In their report, the percentage of eyes with anterior chamber cells of 1+ or greater was 30% pre-operatively but only 5% at 12 weeks post-operatively (8). Examining data from a systematic review (12), we calculated that the percentage of eyes with anterior chamber cells of 1+ or greater was 92% pre-operatively and 52% post-operatively. In our study, the percentage of eyes with anterior chamber cells of 1+ or greater was 41% pre-operatively and 29% at 3 months post-operatively. Regarding other inflammatory signs, Kamei et al. reported that the percentage of eyes with anterior chamber flare of 1+ or greater was 25% pre-operatively and 5% at 12 weeks

post-operatively, and the percentage of eyes with vitreous haze of 1+ or greater was 100% pre-operatively and 5% at 12 weeks post-operatively (8). In our study, the percentage of eyes with anterior chamber flare of 1+ or greater was 27% pre-operatively and 6% at 3 months post-operatively, and the percentage of eyes with vitreous haze of 1+ or greater was 90% pre-operatively and 4% at 3 months post-operatively. In the era of MIVS—including 27-gauge PPV—post-operative inflammation is expected to be minimal even in eyes with uveitis.

Surgery-related complications are another concern in PPV for uveitis. Although 48% of eyes experienced complications in the present study, most were mild and transient. As shown in **Table 2**, complications related to intraocular pressure accounted for 68% of overall complications (18% of all eyes) within post-operative 2 weeks, which is consistent with a previous report (19). Khan et al. conducted a multicenter retrospective study of 360 patients who underwent 27-gauge PPV for posterior segment disease (not limited to uveitis) and found that 16% of eyes showed ocular hypertension or hypotony post-operatively (19). The extent of intraoperative and post-operative complications in PPV for uveitis is best summarized by Henry et al. (12). After reviewing 34 articles published from 2005 to 2014 and analyzing 708 eyes (∼25% of which were treated with 25-gauge PPV and no cases treated with 27-gauge PPV), they reported the following frequencies of surgery-related complications: cataract (24%), glaucoma (17%), epiretinal membrane (15%), band keratopathy/corneal decompression (11%), pupillary block (9.3%), etc. The rates of complications in Henry et al.'s review are obviously more severe compared with those reported in our study, suggesting that the 27-gauge system contributes to safer vitreous surgery in uveitis eyes.

This study has some limitations inherent to its retrospective nature. First, the surgical technique was generally standardized, but the use of adjunctive procedures (e.g., concomitant cataract surgery, intraoperative triamcinolone acetonide injection, suture placement at sclerotomies, etc.) was performed at the surgeon's discretion and may have affected surgical outcomes. Second, we included various types of surgical indications. Although it might help to understand the overall picture of surgical outcomes following 27-gauge PPV for uveitis, the number of eyes by diagnosis or by purpose of surgery was insufficient to perform detailed analyses. Third, because we only included subjects having eyes treated with primary 27-gauge PPV, no data were provided on 27-gauge PPV for previously vitrectomized eyes or inter-eye comparison for patients who underwent 27-gauge PPV in both eyes. Further well-designed clinical studies are warranted to address these concerns.

In conclusion, we have reported the clinical outcomes of primary 27-gauge PPV for various vitreoretinal disorders associated with uveitis. In 27-gauge PPV for uveitis, BCVA was maintained or improved in most cases, whereas intraocular inflammation typically subsided post-operatively. Although nearly half of the patients experienced surgery-related complications, they tended to be mild and transient. Given its risk–benefit profile, 27-gauge PPV is a promising option for the treatment of vitreoretinal disorders in uveitis.

DATA AVAILABILITY STATEMENT

The raw data supporting the conclusions of this article will be made available by the authors, without undue reservation.

ETHICS STATEMENT

The studies involving human participants were reviewed and approved by the Institutional Review Board of the Kobe University Graduate School of Medicine. Written informed consent for participation was not required for this study in accordance with the national legislation and the institutional requirements.

AUTHOR CONTRIBUTIONS

KK, SK, and WM conceived and designed the study. KK, NS, and RN contributed to data acquisition. HI, WM, and MN provided critical advice for the revision of the manuscript. SK had full access to all data in the study and takes responsibility for the integrity of the data and accuracy of the data analysis. All authors participated in data interpretation and approved the final version for publication.

REFERENCES

1. de Smet MD, Taylor SR, Bodaghi B, Miserocchi E, Murray PI, Pleyer U, et al. Understanding uveitis: the impact of research on visual outcomes. *Prog Retin Eye Res*. (2011) 30:452–70. doi: 10.1016/j.preteyeres.2011.06.005
2. Dick AD, Rosenbaum JT, Al-Dhibi HA, Belfort R Jr, Brezin AP, Chee SP, et al. Guidance on noncorticosteroid systemic immunomodulatory therapy in noninfectious uveitis: Fundamentals Of Care for UveitiS (FOCUS) initiative. *Ophthalmology*. (2018) 125:757–73. doi: 10.1016/j.ophtha.2017.11.017
3. Gutfleisch M, Spital G, Mingels A, Pauleikhoff D, Lommatzsch A, Heiligenhaus A. Pars plana vitrectomy with intravitreal triamcinolone: effect on uveitic cystoid macular oedema and treatment limitations. *Br J Ophthalmol*. (2007) 91:345–8. doi: 10.1136/bjo.2006.101675
4. Soheilian M, Mirdehghan SA, Peyman GA. Sutureless combined 25-gauge vitrectomy, phacoemulsification, and posterior chamber intraocular lens implantation for management of uveitic cataract associated with posterior segment disease. *Retina*. (2008) 28:941–6. doi: 10.1097/IAE.0b013e31816ed5c7
5. Woo SJ, Yu HG, Chung H. Surgical outcome of vitrectomy for macular hole secondary to uveitis. *Acta Ophthalmol*. (2010) 88:e287–8. doi: 10.1111/j.1755-3768.2009.01667.x
6. Svozilkova P, Heissigerova J, Brichova M, Kalvodova B, Dvorak J, Rihova E. The role of pars plana vitrectomy in the diagnosis and treatment of uveitis. *Eur J Ophthalmol*. (2011) 21:89–97. doi: 10.5301/EJO.2010.4040
7. Androudi S, Praidou A, Symeonidis C, Tsironi E, Iaccheri B, Fiore T, et al. Safety and efficacy of small incision, sutureless pars plana vitrectomy for patients with posterior segment complications secondary to uveitis. *Acta Ophthalmol*. (2012) 90:e409–10. doi: 10.1111/j.1755-3768.2011.02258.x
8. Kamei RR, Arantes TE, Garcia CR, Muccioli C. Twenty-five gauge vitrectomy in uveitis. *Arq Bras Oftalmol*. (2012) 75:107–10. doi: 10.1590/S0004-27492012000200007

9. Soheilian M, Ramezani A, Soheilian R. 25-gauge Vitrectomy for complicated chronic endogenous/autoimmune uveitis: predictors of outcomes. *Ocul Immunol Inflamm*. (2013) 21:93–101. doi: 10.3109/09273948.2012.734536
10. Oahalou A, Schellekens PA, de Groot-Mijnes JD, Rothova A. Diagnostic pars plana vitrectomy and aqueous analyses in patients with uveitis of unknown cause. *Retina*. (2014) 34:108–14. doi: 10.1097/IAE.0b013e31828e6985
11. Schoenberger SD, Kim SJ, Thorne JE, Mruthyunjaya P, Yeh S, Bakri SJ, et al. Diagnosis and treatment of acute retinal necrosis: a report by the american academy of ophthalmology. *Ophthalmology*. (2017) 124:382–92. doi: 10.1016/j.ophtha.2016.11.007
12. Henry CR, Becker MD, Yang Y, Davis JL. Pars Plana vitrectomy for the treatment of uveitis. *Am J Ophthalmol*. (2018) 190:142–9. doi: 10.1016/j.ajo.2018.03.031
13. Bansal R, Gupta A, Gupta V, Mulkutkar S, Dogra M, Katoch D, et al. Safety and outcome of microincision vitreous surgery in uveitis. *Ocul Immunol Inflamm*. (2017) 25:775–84. doi: 10.3109/09273948.2016.1165259
14. Becker M, Davis J. Vitrectomy in the treatment of uveitis. *Am J Ophthalmol*. (2005) 140:1096–105. doi: 10.1016/j.ajo.2005.07.017
15. Bansal R, Dogra M, Chawla R, Kumar A. Pars plana vitrectomy in uveitis in the era of microincision vitreous surgery. *Indian J Ophthalmol*. (2020) 68:1844–51. doi: 10.4103/ijo.IJO_1625_20
16. Fujii GY, De Juan E Jr, Humayun MS, Pieramici DJ, Chang TS, Awh C, et al. A new 25-gauge instrument system for transconjunctival sutureless vitrectomy surgery. *Ophthalmology*. (2002) 109:1807–12. doi: 10.1016/S0161-6420(02)01179-X
17. Oshima Y, Wakabayashi T, Sato T, Ohji M, Tano Y. A 27-gauge instrument system for transconjunctival sutureless microincision vitrectomy surgery. *Ophthalmology*. (2010) 117:93–102 e2. doi: 10.1016/j.ophtha.2009.06.043
18. Mitsui K, Kogo J, Takeda H, Shiono A, Sasaki H, Munemasa Y, et al. Comparative study of 27-gauge vs 25-gauge vitrectomy for epiretinal membrane. *Eye (Lond)*. (2016) 30:538–44. doi: 10.1038/eye.2015.275
19. Khan MA, Kuley A, Riemann CD, Berrocal MH, Lakhanpal RR, Hsu J, et al. Long-term visual outcomes and safety profile of 27-gauge pars plana vitrectomy for posterior segment disease. *Ophthalmology*. (2018) 125:423–31. doi: 10.1016/j.ophtha.2017.09.013
20. Li J, Liu SM, Dong WT, Li F, Zhou CH, Xu XD, et al. Outcomes of transconjunctival sutureless 27-gauge vitrectomy for vitreoretinal diseases. *Int J Ophthalmol*. (2018) 11:408–15. doi: 10.18240/ijo.2018.03.10
21. Li J, Zhao B, Liu S, Li F, Dong W, Zhong J. Retrospective comparison of 27-gauge and 25-gauge microincision vitrectomy surgery with silicone oil for the treatment of primary rhegmatogenous retinal detachment. *J Ophthalmol*. (2018) 2018:7535043. doi: 10.1155/2018/7535043
22. Otsuka K, Imai H, Fujii A, Miki A, Tagami M, Azumi A, et al. Comparison of 25- and 27-gauge pars plana vitrectomy in repairing primary rhegmatogenous retinal detachment. *J Ophthalmol*. (2018) 2018:7643174. doi: 10.1155/2018/7643174
23. Shinkai Y, Oshima Y, Yoneda K, Kogo J, Imai H, Watanabe A, et al. Multicenter survey of sutureless 27-gauge vitrectomy for primary rhegmatogenous retinal detachment: a consecutive series of 410 cases. *Graefes Arch Clin Exp Ophthalmol*. (2019) 257:2591–600. doi: 10.1007/s00417-019-04448-2
24. Saleh OA, Alshamarti SA, Abu-Yaghi NE. Comparison of characteristics and clinical outcomes in 27-gauge versus 23-gauge vitrectomy surgery. *Clin Ophthalmol*. (2020) 14:1553–8. doi: 10.2147/OPTH.S255162
25. Nussenblatt RB, Palestine AG, Chan CC, Roberge F. Standardization of vitreal inflammatory activity in intermediate and posterior uveitis. *Ophthalmology*. (1985) 92:467–71. doi: 10.1016/S0161-6420(85)34001-0

Conflict of Interest: The authors declare that the research was conducted in the absence of any commercial or financial relationships that could be construed as a potential conflict of interest.

frontiers in Medicine

ORIGINAL RESEARCH
published: 18 November 2021
doi: 10.3389/fmed.2021.732427

Methotrexate Effectively Controls Ocular Inflammation in Japanese Patients With Non-infectious Uveitis

Yosuke Harada†, Tomona Hiyama† and Yoshiaki Kiuchi*

Department of Ophthalmology and Visual Science, Graduate School of Biomedical Sciences, Hiroshima University, Hiroshima, Japan

OPEN ACCESS

Edited by:
Ryoji Yanai, Yamaguchi University, Japan

Reviewed by:
Selçuk Yüksel, Pamukkale University, Turkey
Georgios Panos, Nottingham University Hospitals NHS Trust, United Kingdom

***Correspondence:**
Yosuke Harada
yharada@hiroshima-u.ac.jp

†*These authors have contributed equally to this work*

Specialty section:
This article was submitted to Ophthalmology, a section of the journal Frontiers in Medicine

Received: *29 June 2021*
Accepted: *20 October 2021*
Published: *18 November 2021*

Citation:
Harada Y, Hiyama T and Kiuchi Y (2021) Methotrexate Effectively Controls Ocular Inflammation in Japanese Patients With Non-infectious Uveitis. Front. Med. 8:732427. doi: 10.3389/fmed.2021.732427

This single-center retrospective study investigated the clinical characteristics and efficacy of methotrexate (MTX) for the treatment of non-infectious uveitis for more than 6 months at Hiroshima University, from February 2016 to May 2021. Outcome variables included changes in systemic immunosuppressive treatment and intraocular inflammation. Out of 448 patients with non-infectious uveitis, 35 patients (14 male patients and 21 female patients; 65 eyes) treated with MTX for more than 6 months were analyzed. There were 15 patients with anterior uveitis and 20 with posterior and panuveitis. The mean dose of systemic corticosteroids decreased from 12.1 mg/day at baseline to 1.3 mg/day at 6 months and 0.6 mg at 12 months after starting MTX, and approximately 90% of patients were corticosteroid-free at 12 months. The percentage of eyes with inactive uveitis at 6, 12, and 24 months was 49.2%, 59.6%, and 90.0%, respectively. Mean relapse rate score also significantly decreased from 2.88 at baseline to 0.85 at 12 months ($p < 0.001$). Inflammatory control was achieved with MTX doses of 8–16 mg/week, with a median dose of 12 mg/week. Adverse effects of MTX were observed in 34.3% of patients, and 11.4% required discontinuation; most commonly hepatotoxicity (58.3%), followed by fatigue (25.0%), and hair loss (16.7%). No significant differences were found between the survival curves of patients with anterior uveitis and posterior/panuveitis (Wilcoxon rank-sum test). The percentage of eyes without IOP-lowering eye drops was significantly higher in patients with posterior/panuveitis at 24 months ($p = 0.001$). Our study suggests that MTX is effective in controlling ocular inflammation for Japanese patients with non-infectious uveitis. Relatively high incidence of MTX-related adverse effects in the Japanese population indicates that careful monitoring and dose adjustments are crucial for the long-term use of this therapy.

Keywords: uveitis, non-infectious uveitis, methotrexate, immunosuppressive therapy, intraocular inflammation, Japanese

INTRODUCTION

Uveitis is one of the major causes of vision loss and is estimated to cause approximately 10% of blindness in developed countries (1, 2). Immunosuppressive therapy is the main treatment for non-infectious uveitis; local or systemic corticosteroids are the first-line treatment. However, prolonged corticosteroid use leads to severe ocular (such as cataracts or intraocular elevation) and systemic (such as diabetes mellitus, gastrointestinal complications, or osteoporosis) side effects (3). Thus, corticosteroid-sparing agents should be considered when patients require ongoing treatment and are unable to taper to $\leq$ 10 mg/day of systemic corticosteroids (4).

Currently, infliximab is approved for Behcet's disease only, and cyclosporine and adalimumab are approved and reported to be efficient for the treatment of non-infectious uveitis in Japan (5–8). Methotrexate (MTX) is a commonly used antimetabolite for ocular inflammation (4, 9–12). Although MTX is administered as a first-line corticosteroid-sparing agent in countries, such as the United States or European countries, there are limited reports from Asian countries, including Japan (13–15). This is because the use of MTX to treat non-infectious uveitis has not yet been established or approved in Japan. Recently, we showed that the administration of MTX at a dose of 8–16 mg/week effectively controlled inflammation in patients with refractory non-infectious scleritis and those who could not tolerate systemic corticosteroids (16). Here, we investigated the efficacy and safety of MTX in the treatment of Japanese patients with non-infectious uveitis.

PATIENTS AND METHOD

Study Population

This retrospective study included patients with chronic non-infectious uveitis who were treated with MTX for $\geq$ 6 months from February 2015 to May 2021 at the uveitis center of Hiroshima University Hospital (Hiroshima, Japan). All patients had active ocular inflammation at the time of MTX initiation despite the use of conventional topical or systemic steroid therapy. The study protocol was approved by the University of Hiroshima Institutional Review Board (protocol number/2122), and the requirement for informed consent was waived.

Objectives

The primary objectives were to control ocular inflammation and evaluate treatment safety. The secondary objectives included evaluating changes in systemic treatments (e.g., oral corticosteroids) and topical steroids, intraocular pressure (IOP)-lowering therapy, visual acuity improvement, and laser flare photometry results if available.

Data Collection

For patients treated with MTX, the following data were collected: sex, age at uveitis onset, duration of uveitis, type of uveitis (anterior, intermediate, posterior, or panuveitis), involvement (unilateral or bilateral), diagnosis of uveitis, previous treatment history, surgical history, ophthalmological findings [best-corrected visual acuity, anterior chamber cell grade, vitreous haze grade, retinal/choroidal lesions, and cystoid macular edema (CME)], peripheral anterior synechia, and changes in local and systemic corticosteroid therapy. Adverse events caused by MTX (e.g., hepatotoxicity, fatigue, or hair loss) and the number of patients who required other immunosuppressive treatments were also recorded. Patients who underwent intraocular surgeries within 6 months after the initiation of MTX treatment were excluded from the data analysis. The classification and grading of uveitis were based on the 2005 Standardization of Uveitis Nomenclature criteria (17). For topical steroid therapy, a betamethasone sodium phosphate ophthalmic solution and 0.1% fluorometholone ophthalmic suspension were used for severe and mild anterior uveitis, respectively. Additionally, laser flare photometry values (objective and quantitative measurements of aqueous humor protein levels in the anterior chamber) were analyzed for patients whose flare values were recorded before and after MTX treatment.

Inactive uveitis was defined as an anterior chamber grade $\leq$ 0.5+, vitreous haze grade $\leq$ 0.5+, no active retinal/choroidal lesion, and no CME for 3 months. Treatment failure was defined as a two-step increase in the level of inflammation, an increase from grade 3+ to 4+ in the anterior chamber or vitreous haze score, new CME or retinal/choroidal lesion activity, and/or a requirement for corticosteroid rescue therapy. The treatment of patients with bilateral involvement was considered successful only if inactive uveitis was achieved in both eyes. The number of relapses per year was recorded before and after MTX treatment using the following relapse rate scoring system: 0, zero relapses; 1, one relapse; 2, two relapses; 3, three relapses; and 4, $\geq$ 4 relapses. Steroid-induced ocular hypertension was defined as IOP elevation $>$ 10 mmHg from baseline during topical and systemic corticosteroids therapy.

Diagnosis

Sarcoidosis and Vogt–Koyanagi–Harada disease were diagnosed in accordance with international diagnostic criteria (18, 19). Sympathetic ophthalmia was diagnosed clinically (20). The diagnosis of multifocal choroiditis was based on the characteristic clinical manifestation of panuveitis and the presence of multiple pigmented chorioretinal lesions in the posterior and mid peripheral retina without any associated systemic or infectious etiologies (21). A patient was diagnosed with retinal vasculitis when a vascular alteration was observed by fluorescein angiography without any associated systemic, infectious, or ocular disorders and associated neoplasms (22).

MTX Administration

Permission was granted from the Evaluation Committee on Unapproved or Off-labeled Drugs with High Medical Needs at Hiroshima University for unapproved usage of MTX. MTX was initiated when $>$ 10 mg/day systemic corticosteroids were required to control ocular inflammation or patients could not tolerate corticosteroids (e.g., those with steroid-induced ocular hypertension or diabetes mellitus). Patients who were given MTX for systemic diseases, such as rheumatoid arthritis, were excluded

TABLE 1 | Baseline demographic and clinical characteristics of patients with non-infectious uveitis treated with methotrexate.

	Total	%
Patients	35	
Eyes	65	
Sex		
Male	14	40
Female	21	60
Age at Uveitis Onset, Median in years	40	
Duration of uveitis, Median in months	62	
Type of Uveitis		
Anterior	15	42.9
Intermediate	0	0
Posterior/Pan	20	57.1
Laterality		
Unilateral	5	14.3
Bilateral	30	85.7
Diagnosis		
Idiopathic anterior uveitis	15	42.9
Retinal vasculitis	13	37.1
Sarcoidosis	4	11.4
Multifocal choroiditis	3	8.6

from this study. Prior to the administration of MTX, an extensive workup was performed, including chest radiography, exclusion of tuberculosis and syphilis, hepatitis B and C serology, complete blood count, and hepatic and renal function tests. The initial dose was 4–8 mg/week, and it was gradually increased up to 16 mg/week according to the clinical response. The maximum dose of MTX in the present study (16 mg/week) was based on the guidelines for Japanese patients with rheumatoid arthritis (23). Folic acid supplementation was given on the day after MTX administration for patients older than 20 years. To assess MTX-related adverse effects, complete blood count, C-reaction protein, and hepatic and renal function were evaluated at least every 2 months. Regular KL-6 monitoring (every 4 months) and annual chest X-rays were also performed. Tapering of MTX therapy was performed according to the preference of patients who exhibited remission for at least 12 months. MTX was tapered by 2 mg/week every 3–6 months if patients did not experience uveitis recurrence.

Statistical Analyses

Statistical analyses were performed using Microsoft Excel (Microsoft Corp., Redmond, WA, USA) and JMP version 11 (SAS Institute, Cary, NC, USA). Quantitative variables were described using means, medians, ranges (minimal and maximal values), and counts (percentages). Continuous variables were assessed using the Steel test and Dunnett test. Qualitative variables were analyzed using Fisher's exact test. Comparison of non-parametric data was performed by Mann-Whitney U test. Differences with $p < 0.05$ were considered statistically significant.

RESULTS

Demographic and Clinical Characteristics

Among 448 patients with non-infectious uveitis, 50 patients (24 male and 26 female patients) were treated with MTX. Fifteen patients were excluded from the evaluation of efficacy of MTX because it was discontinued within the first 6 months after treatment initiation for the following reasons: adverse effect (nine patients), intraocular surgery (four patients), insufficient inflammation control (one patient), or poor adherence (one patient). In total, 65 eyes in 35 patients (14 male and 21 female) were analyzed for therapeutic outcomes. Their clinical and demographic data are summarized in **Table 1**. The median age at uveitis onset was 40 years (range, 5–83 years); the median follow-up period was 45 months (range, 10–156 months). The majority of patients had posterior/panuveitis ($n = 20$, 57.1%) and bilateral involvement ($n = 30$, 85.7%). Idiopathic anterior uveitis was the most common diagnosis ($n = 15$, 42.9%). The remaining patients were diagnosed with retinal vasculitis ($n = 13$, 37.1%), biopsy-proven sarcoidosis ($n = 4$, 11.4%), and multifocal choroiditis ($n = 3$, 8.6%). Gonioscopic examination was conducted in 56 out of 65 eyes at presentation; 67% showed peripheral anterior synechia. Most patients (28/35, 80.0%) were treated with corticosteroids before the administration of MTX. Eighteen eyes (22.9%) had a history of intraocular surgeries (cataract surgery, 14 eyes; glaucoma surgery, 5 eyes; vitreous surgery, 2 eyes) before MTX therapy. The median duration of uveitis before MTX treatment was 17 months (range, 3–269 months). The median duration of MTX therapy was 18.5 months (range, 7–48 months).

Control of Ocular Inflammation and Changes in Systemic Treatment

The therapeutic outcomes of MTX therapy for the 35 patients (65 eyes) are summarized in **Table 2**. No adjustment to systemic treatment was required for non-ocular activity in any patient. The median dose of MTX was 12.0 mg/week (8–16 mg/week). Among the patients who were analyzed, more than 65% needed $\geq$ 5 mg/day systemic corticosteroids for controlling ocular inflammation (mean dose was 12.1 $\pm$ 10.5 mg/day) at baseline, and the remaining proportion could not tolerate corticosteroids due to their adverse effects. After starting MTX, the mean dose of systemic corticosteroids significantly decreased at all evaluation points (3, 6, 12, 18, and 24 months) from baseline ($p < 0.001$). The percentage of patients who no longer required corticosteroids at 6 and 12 months was 68.6 and 88.9%, respectively. A topical steroid was administered in 98.5% of patients at baseline; betamethasone $\geq$ 2 times daily was used in 80% at baseline and decreased to approximately 40% after 12 months. The proportion of patients who received the less potent topical corticosteroid fluorometholone $\leq$ 2 times daily was 8.0% at baseline and increased to 34.0% after 12 months (75% changed from betamethasone). Additionally, the proportion of topical steroid treatment-free patients was 1.5% at baseline and increased to 14.9% after 12 months. In contrast, the proportion of patients using IOP-lowering eye drops remained between 34.8 and 46.2% throughout the MTX treatment. Among the eyes treated with IOP-lowering eye drops, glaucoma surgery was

TABLE 2 | Treatment outcomes of patients with non-infectious uveitis treated with methotrexate.

	Base line	3 months	6 months	12 months	18 months	24 months
Number of patients (eyes)	35 (65)	35 (65)	35 (65)	26 (47)	17 (30)	14 (23)
Mean dose of methotrexate (mg/week)	0	9.2	10.5	10.6	9.2	9
Systemic corticosteroids						
Mean dose of systemic corticoteroids (mg/day)	12.1	3.1*	1.3*	0.6*	0*	0*
Percentage of patients with corticosteroids ≤ 5 mg	34.3	72.3	94.3	96.3	100	100
Percentage of corticosteroid-free patients	22.9	45.7	68.6	88.9	100	100
Steroid eye drops						
Percentage of patients with bethamethasone ≥ 2 times daily	80	58.4	58.4	40.3	30	43.4
Percentage of patients with fluorometholone ≤ 2 times daily	8	21.5	24.6	34	40	39.1
None	1.5	9.2	13.3	14.9	26.7	26.1
Percentage of patients with intraocular pressure-lowering eye drops	36.9	46.2	46.2	38.3	36.7	34.8
Mean best corrected visual acuity (logarithm of the minimal angle of resolution)	0.12	0.09	0.07	0.05	−0.04	−0.06
Percentage of eyes with of ≤ 0.5 + anterior chamber cells	32.3	61.5	73.8	74.5	83.3	76.2
Percentage of eyes with ≤ 0.5 + vitreous haze	72.3	86.2	87.7	89.4	100	100
Percentage of eyes with cystic macular edema	90.8	95.4	96.2	95.7	100	100
Percentage of eyes without active retinal/choroidal lesion	44.6	60	70.8	83	96.7	100
Percentage of eyes with inactive uveitis	0	29.2	49.2	59.6	80	90

Significant difference observed between baseline and evaluation point (Steel test, $p < 0.05$).

performed in 7 patients during MTX therapy. The proportion of eyes with an anterior chamber cell grade and vitreous haze grade ≤ 0.5+ had increased at all evaluation points from base line after starting MTX therapy. The mean best-corrected visual acuity improved from 0.12 logarithm of the minimum angle of resolution at baseline to 0.07, 0.05, and −0.06 at 6, 12, and 24 months, respectively. The proportion of eyes with CME and active retinal/choroidal lesions also decreased after starting MTX. The percentage of eyes (patients) with inactive uveitis at 6, 12, and 24 months was 49.2 (40.0), 59.6 (65.4), and 90.0 (78.5)%, respectively. Additionally, the mean relapse rate score significantly decreased from 2.88 at baseline to 0.85 at 12 months ($p < 0.001$). Treatment failure occurred in 13 patients (37.1%) with a mean survival time of 15.7 months. In six patients (17.1%; five posterior uveitis, one anterior uveitis), after exhibiting remission for at least 12 months, MTX was slowly tapered and discontinued after a median of 23.5 months (range, 21–48 months).

Treatment outcomes were compared between patients with anterior uveitis (15 patients, 25 eyes) and those with posterior/panuveitis (20 patients, 40 eyes) (**Table 3**). Although the median follow-up period was 44 months in both groups, the duration of uveitis before starting MTX was significantly longer in patients with anterior uveitis than in those with posterior/panuveitis (median 63.6 months in anterior vs. 13.6 months in posterior/panuveitis, $p = 0.012$). The proportions of patients with peripheral anterior synechia and steroid-induced ocular hypertension were not significantly different between the two groups ($p = 0.78$ and 0.80, respectively). The mean dose of corticosteroids at baseline was 12.6 mg/day and 11.6 mg/day in patients with anterior and posterior/panuveitis, respectively, which decreased to 1.1 mg/day and 0.1 mg/day at 12 months after starting MTX. The percentage of eyes who showed inflammatory control at 12 months after MTX therapy was 59.1% in eyes with anterior uveitis and 60.0% in eyes with posterior/panuveitis, respectively. No significant differences were found between the survival curves of patients with anterior uveitis and posterior/panuveitis according to the Wilcoxon rank-sum test ($p = 0.70$). Five out of 20 (25.0%) patients with posterior/panuveitis discontinued MTX following tapering without recurrence, whereas only one patient with anterior uveitis (6.7%) achieved the discontinuation of therapy. The percentage of eyes without

TABLE 3 | Treatment outcomes of patients with anterior uveitis and posterior/panuveitis treated with methotrexate.

	Anterior uveitis	Posterior/Panuveitis
Number of patients, eyes	15 patients, 25 eyes	20 patients, 40 eyes
Median age of onset	39	43
Median follow-up period (months)	44	44
Duration of uveitis before starting methorexate (months)	63.6	12.6*
Percentage of eyes with peripheral anterior synechia (%)	68	52.5
Percentage of eyes with steroid induced intraocular pressure elevation (%)	40	45
Mean dose of corticosteroids (mg/day)	12.6	11.6
Baseline		
12 months	1.1	0.1
Percentage of eyes with inactive uveitis at 12 months (%)	59.1	60.1

Significant difference observed (Mann-Whitney U test, $p < 0.05$).

IOP-lowering eye drops was significantly higher in patients with posterior/panuveitis at 24 months ($p = 0.001$) (**Figure 1**). The number of IOP-lowering eye drops was significantly lower in those with posterior/panuveitis at 18 and 24 months (1.23 in anterior uveitis vs. 0.35 in posterior/panuveitis at 18 months, $p = 0.046$ and 1.89 in anterior uveitis vs. 0.14 in posterior/panuveitis at 24 months, $p = 0.0007$). Among the five patients (eight eyes) with anterior uveitis who started MTX < 1 year after uveitis onset, only one eye was treated with IOP-lowering eye drops before MTX therapy and required no extra IOP-lowering eye drops after the initiation of MTX.

Laser Flare Photometry

Laser flare photometry values were recorded for 17 patients (anterior uveitis: $n = 9$, posterior uveitis: $n = 7$, panuveitis: $n = 1$) before and after MTX therapy. The mean laser flare photometry value was 51.9 ph/ms at baseline and 34.3 ph/ms at 12 months ($p = 0.93$). The patients were then divided into groups according to the duration of uveitis before MTX treatment (**Table 4**). The mean laser flare photometry value of patients with uveitis for < 15 months (8 patients, 15 eyes) significantly decreased from 27.5 ph/ms at baseline to 10.1 ph/ms at 12 months ($p = 0.04$). On the contrary, the mean laser flare photometry value of patients with uveitis for ≥ 15 months (9 eyes, 14 patients) was 76.5 ph/ms at baseline and remained as high as 60.2 ph/ms at 12 months ($p = 0.99$). Five patients with uveitis for ≥ 15 months (62.5%) underwent intraocular surgery (three glaucoma surgery, one cataract surgery, one vitrectomy), whereas only one patient with uveitis for < 15 months (12.5%) required intraocular surgery (glaucoma surgery). In contrast to the laser flare results, anterior chamber cell grade improved regardless of laser flare values or uveitis duration before MTX administration.

Adverse Effects

Among 35 patients treated with MTX, 12 patients (34.3%) experienced an adverse effect at some point during the follow-up period. These included hepatotoxicity ($n = 7$), fatigue ($n = 3$), hair loss ($n = 2$) Four out of 12 patients discontinued MTX therapy due to adverse effects (11.4%). The median dose of MTX that caused an adverse effect was 10 mg/week (range, 6–16 mg/week).

DISCUSSION

Our findings indicated that MTX is effective for controlling inflammation and reducing the relapse rate in Japanese patients with non-infectious uveitis. Ocular inflammation was controlled in approximately 65 and 80% of patients at 12 and 24 months, respectively. The mean systemic corticosteroid dose decreased significantly after MTX therapy. More than 85% of patients no longer required steroid treatment at 12 months after MTX initiation. A median dose of 12 mg/week was required to control ocular inflammation. No improvement was observed in the number of IOP-lowering eye drops before and after MTX therapy, especially in patients with anterior uveitis. This study also suggested a benefit of early MTX administration in reducing the risk of ocular complications due to elevation of laser flare values, owing to irreversible disruption of blood-aqueous barrier.

MTX is one of the most commonly used immunosuppressive agents for non-infectious uveitis and several reports have demonstrated the efficacy of MTX for non-infectious uveitis; most of these studies were reported in patients from the United States, Europe, South America, Australia, or India (9–12, 24). The median dosage of MTX that most uveitis specialists in the American Uveitis Society administer is 20 mg/week (25). However, considerably higher incidence of some serious adverse events of MTX (such as pneumocystis pneumonia, lymphoproliferative disorders, and hepatotoxicity) have been reported among Japanese patients than in those from other countries (23). For Japanese patients with rheumatoid arthritis, the maximum dose of MTX is limited to 16 mg/week and Japan College of Rheumatology guidelines recommends the dose escalation up to 10-12 mg/week, because it has been reported that these doses can maintain the adequate concentration of MTX to suppress inflammation with limited adverse effects on liver function (23, 26). Only few studies from East Asian countries have demonstrated the use of MTX to treat non-infectious uveitis; lower doses of MTX ≤ 8 mg/week was administered in some of the reports (13–16, 27). In our study, inflammatory control was achieved with MTX doses of 8–16 mg/week, with a median dose of 12 mg/week, which is similar to the dose used for Japanese patients with RA. These results indicate that although it is still lower than the MTX which is usually prescribed in Western countries, higher doses of MTX than previously reported in East Asian populations may be required to control ocular inflammation. Despite the small number of patients, we believe it is worthwhile reporting our clinical experience using MTX for the treatment of non-infectious uveitis. Additional prospective studies from East Asia are needed to determine the adequate dose of MTX for ocular inflammation.

According to previous studies from Western countries, the incidence of MTX-related adverse events varied greatly; the percentage of discontinuation caused by adverse events ranged from 2.8 to 26% (10, 11, 24, 28). In our study, 34.3% of patients experienced adverse effects, and 11.4% had to discontinue MTX. Although there were no serious adverse events, such as lymphoproliferative disease, close monitoring during MTX therapy for non-infectious uveitis is essential.

The difference in MTX treatment efficacy among various types of uveitis remains controversial. Gangaputra et al. (10) reported that posterior or panuveitis responded less to MTX therapy than other types of uveitis, whereas Rathinam et al. (12) showed a better response of posterior or panuveitis than anterior and intermediate uveitis. Our results were consistent with the latter report; patients with posterior and panuveitis required a lower dose of MTX and achieved better efficacy than those with anterior uveitis. Additionally, the rate of MTX discontinuation due to remission was higher in patients with posterior/panuveitis. There are several reasons to explain these results. First, the duration between uveitis onset and MTX therapy was longer in patients with anterior uveitis than in those

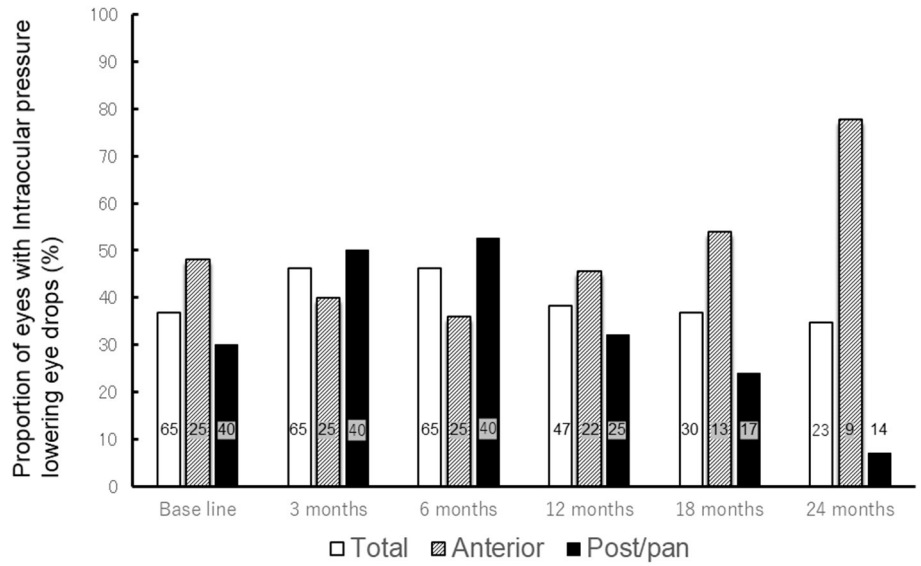

FIGURE 1 | Change in proportion of eyes with intraocular pressure-lowering eye drops after methotrexate therapy. The bar graph shows the change in proportion of eyes with intraocular pressure lowering eye drops after methotrexate treatment (All patients, patients with anterior uveitis, and patients with posterior/panuveitis). The proportion of all eyes with intraocular pressure-lowering eye drops remained between 34.8 and 46.2% throughout methotrexate therapy. While proportion of eyes with intraocular pressure-lowering eye drops decreased from 30.0% at base line to 7.7% at 24 months in patients with posterior/panuveitis, it increased from 48.0% at baseline to 77.8% at 24 months in those with anterior uveitis. The numbers in each bar graph represents the number of eyes using intraocular pressure-lowering eye drops. Total = all patients, Ant = patients with anterior uveitis, Post/pan = patients with posterior/panuveitis.

TABLE 4 | Change in laser flare photometry values and inflammatory variables according to uveitis duration before methotrexate therapy.

	Base line	12 months
Total (17 patients, 29 eyes) Mean laser flare photometry value (ph/ms)	51.9	34.3
Percentage of eyes with anterior chamber cell grade ≤ 0.5+	17.2	72.4*
Patients with uveitis duration < 15 months (8 patients, 15 eyes) Mean laser flare photometry value (ph/ms)	27.5	10.1**
Percentage of eyes with anterior chamber cell grade ≤ 0.5+	13.3	66.7*
Patients with uveitis duration ≥ 15 months (9 patients, 14 eyes) Mean laser flare photometry value (ph/ms)	76.5	60.2
Percentage of eyes with anterior chamber cell grade ≤ 0.5+	21.4	78.6*

*ph/ms, photons/millisecond. *Significant difference observed (Fisher's test, $p < 0.05$). **Significant difference observed (Dunnett test, $p < 0.05$).*

with posterior/panuveitis. Most patients were treated solely with local corticosteroids for a longer period before being referred to our uveitis center. In fact, a longer duration of chronic anterior uveitis is reported to be one of the factors associated with failure to achieve remission (29). Second, patients with anterior uveitis included in this study may have had more severe forms of inflammation at baseline than patients with posterior/panuveitis. Further studies with a larger number of patients are needed to address this question.

Ocular hypertension and glaucoma are common and one of the serious complications of uveitis (30–33). Reduced local and systemic corticosteroid use and rates of ocular hypertension may be obtained from the introduction of immunosuppressive therapy (31). In this study, despite the reduction in local and systemic steroid therapies, there was no decrease in the number of IOP-lowering eye drops, especially for patients with anterior uveitis. The longer duration of active inflammation before MTX initiation, which causes irreversible structural changes to the trabecular meshwork, may have contributed to this result. In fact, only one out of eight eyes was treated with IOP-lowering eye drops before MTX therapy, and no eye drops were added after treatment in patients with anterior uveitis for < 12 months before MTX initiation.

Previously, it has been reported that high laser flare values are associated with ocular complications, regardless of the presence of anterior chamber cell grade (6, 34–36). In our study, patients who received early MTX treatment achieved reduced laser flare photometry values and surgical requirements for ocular complications. The findings support the need for MTX administration before the

irreversible disruption of the blood-aqueous barrier due to chronic inflammation.

The current study had several limitations. First, it was a retrospective study. Second, although the number of patients is larger than previous reports from East Asia, it is still limited. Our study would have been strengthened by including multiple Japanese institutions to determine the efficacy, safety, and adequate dose of MTX in the Japanese population. Third, a longer follow-up period is necessary for further assessment of MTX efficacy and adverse effects. Finally, we collected data from all eyes affected with uveitis (both eyes for some patients) to prevent a potential loss of information, which can affect the independence of the sample and the statistical analysis about clinical findings of each eye.

In conclusion, this study demonstrated that MTX treatment is effective in controlling ocular inflammation for Japanese patients with non-infectious uveitis. MTX dose similar to that used for Japanese patients with rheumatoid arthritis was sufficient to control ocular inflammation. Although MTX had a corticosteroid-sparing effect both topically and systemically, it did not decrease the use of IOP-lowering eye drops for patients with ocular hypertension. Relatively high incidence of MTX-related adverse effects in the Japanese population indicates that careful monitoring and dose adjustments are crucial for the long-term use of this therapy.

DATA AVAILABILITY STATEMENT

The data that support the findings of this study are available on request from the corresponding author, YH. The data are not publicly available due to their containing information that could compromise the privacy of research participants.

ETHICS STATEMENT

The studies involving human participants were reviewed and approved by University of Hiroshima Institutional Review Board. Written informed consent to participate in this study was provided by the participant's legal guardian/next of kin.

AUTHOR CONTRIBUTIONS

YH and TH contributed to conception and design of the study, organized the database, performed the statistical analysis, and wrote the first draft of the manuscript. All authors contributed to manuscript revision, read, and approved the submitted version.

ACKNOWLEDGMENTS

We thank Melissa Crawford, PhD, from Edanz (https://jp.edanz.com/ac) for editing a draft of this manuscript.

REFERENCES

1. Suttorp-Schulten MS, Rothova A. The possible impact of uveitis in blindness: a literature survey. *Br J Ophthalmol.* (1996) 80:844–8. doi: 10.1136/bjo.80.9.844
2. Rothova A, Buitenhuis HJ, Meenken C, Brinkman CJJ, Linssen A, Alberts C, et al. Uveitis and systemic disease. *Br J Ophthalmol.* (1992) 76:137–41. doi: 10.1136/bjo.76.3.137
3. Renfro L, Snow JS. Ocular effects of topical and systemic steroids. *Dermatol Clin.* (1992) 10:505–12. doi: 10.1016/S0733-8635(18)30318-8
4. Castiblanco C, Foster CS. Review of systemic immunosuppression for autoimmune uveitis. *Ophthalmol Ther.* (2014) 3:17–36. doi: 10.1007/s40123-014-0023-x
5. Nakayama M, Keino H, Watanabe T, Okada AA. Clinical features and visual outcomes of 111 patients with new-onset acute Vogt-Koyanagi-Harada disease treated with pulse intravenous corticosteroids. *Br J Ophthalmol.* (2019) 103:274–8. doi: 10.1136/bjophthalmol-2017-311691
6. Hiyama T, Harada Y, Kiuchi Y. Efficacy and safety of adalimumab therapy for the treatment of non-infectious uveitis: efficacy comparison among uveitis aetiologies. *Ocul Immunol Inflamm.* (2021). doi: 10.1080/09273948.2020.1857791. [Epub ahead of print].
7. Kunimi K, Usui Y, Asakage M, Maehara C, Tsubota K, Mitsuhashi R, et al. Anti-TNF-α therapy for refractory uveitis associated with behçet's syndrome and sarcoidosis: a single center study of 131 patients. *Ocul Immunol Inflamm.* (2020). doi: 10.1080/09273948.2020.1791346. [Epub ahead of print].
8. Ohno S, Umebayashi I, Matsukawa M, Goto T, Yano T. Safety and efficacy of infliximab in the treatment of refractory uveoretinitis in Behçet's disease: a large-scale, long-term postmarketing surveillance in Japan. *Arthritis Res Ther.* (2019) 21:2. doi: 10.1186/s13075-018-1793-7
9. Gangaputra S, Newcomb CW, Liesegang TL, Kaçmaz RO, Jabs DA, Levy-Clarke GA, et al. Methotrexate for ocular inflammatory diseases. *Ophthalmology.* (2009) 116: 2188–98. doi: 10.1016/j.ophtha.2009.04.020
10. Gangaputra SS, Newcomb CW, Joffe MM, Dreger K, Begum H, Artornsombudh P, et al. Comparison between methotrexate and mycophenolate mofetil monotherapy for the control of noninfectious ocular inflammatory diseases. *Am J Ophthalmol.* (2019) 208:68–75. doi: 10.1016/j.ajo.2019.07.008
11. Kaplan-Messas A, Barkana Y, Avni I, Neumann R. Methotrexate as a first-line corticosteroid-sparing therapy in a cohort of uveitis and scleritis. *Ocul Immunol Inflamm.* (2003) 11:131–9. doi: 10.1076/ocii.11.2.131.15919
12. Rathinam SR, Gonzales JA, Thundikandy R, Kanakath A, Murugan SB, Vedhanayaki R, et al. Effect of corticosteroid-sparing treatment with mycophenolate mofetil vs methotrexate on inflammation in patients with uveitis: a randomized clinical trial. *JAMA.* (2019) 322:936–45. doi: 10.1001/jama.2019.12618
13. Kondo Y, Fukuda K, Suzuki K, Nishida T. Chronic noninfectious uveitis associated with Vogt-Koyanagi-Harada disease treated with low-dose weekly systemic methotrexate. *Jpn J Ophthalmol.* (2012) 56:104–6. doi: 10.1007/s10384-011-0092-5
14. You C, Ma L, Anesi SD. Bilateral papillitis and vitritis as the initial ophthalmologic finding in a patient with complex medical history, leading to diagnosis of multisystem sarcoidosis. *Am J Ophthalmol Case Rep.* (2019) 13:122–6. doi: 10.1016/j.ajoc.2018.12.020
15. Yang P, Ye Z, Du L, Zhou Q, Qi J, Liang L, et al. Novel treatment regimen of Vogt–Koyanagi–Harada disease with a reduced dose of corticosteroids combined with immunosuppressive agents. *Curr Eye Res.* (2018) 43:254–61. doi: 10.1080/02713683.2017.1383444
16. Hiyama T, Harada Y, Kiuchi Y. Clinical characteristics and efficacy of methotrexate in Japanese patients with noninfectious scleritis. *Jpn J Ophthalmol.* (2021) 65:97–106. doi: 10.1007/s10384-020-00778-5
17. Jabs DA, Nussenblatt RB, Rosenbaum JT, Atmaca LS, Becker MD, Brezin AP, et al. Standardization of uveitis nomenclature for reporting clinical data. results of the first international workshop. *Am J Ophthalmol.* (2005) 140:509–16. doi: 10.1016/j.ajo.2005.03.057
18. Mochizuki M, Smith JR, Takase H, Kaburaki T, Acharya NR, Rao NA. Revised criteria of International Workshop on Ocular Sarcoidosis (IWOS)

for the diagnosis of ocular sarcoidosis. *Br J Ophthalmol*. (2019) 103:1418–22. doi: 10.1136/bjophthalmol-2018-313356
19. Read RW, Holland GN, Rao NA, Tabbara KF, Ohno S, Arellanes-Garcia L, et al. Revised diagnostic criteria for Vogt-Koyanagi-Harada disease: report of an international committee on nomenclature. *Am J Ophthalmol.* (2001) 131:647–52. doi: 10.1016/S0002-9394(01)00925-4
20. Chu XK, Chan C-CC. Sympathetic ophthalmia: to the twenty-first century and beyond. *J Ophthalmic Inflamm Infect*. (2013) 3:49. doi: 10.1186/1869-5760-3-49
21. Dreyer RF, Gass JDM. Multifocal choroiditis and panuveitis: a syndrome that mimics ocular histoplasmosis. *Arch Ophthalmol.* (1984) 102:1776–84. doi: 10.1001/archopht.1984.01040031440019
22. Abu El-Asrar AM, Herbort CP, Tabbara KF. Retinal vasculitis. *Ocul Immunol Inflamm*. (2005) 13:415–33. doi: 10.1080/09273940591003828
23. Kameda H, Fujii T, Nakajima A, Koike R, Sagawa A, Kanbe K, et al. Japan college of rheumatology guideline for the use of methotrexate in patients with rheumatoid arthritis. *Mod Rheumatol*. (2019) 29:31–40. doi: 10.1080/14397595.2018.1472358
24. Samson CM, Waheed N, Baltatzis S, Foster CS. Methotrexate therapy for chronic noninfectious uveitis: analysis of a case series of 160 patients. *Ophthalmology*. (2001) 108:1134–9. doi: 10.1016/S0161-6420(01)00576-0
25. Ali A, Rosenbaum JT. Use of methotrexate in patients with uveitis. *Clin Exp Rheumatol*. (2010) 28:S145–50.
26. Takahashi C, Kaneko Y, Okano Y, Taguchi H, Oshima H, Izumi K, et al. Association of erythrocyte methotrexate-polyglutamate levels with the efficacy and hepatotoxicity of methotrexate in patients with rheumatoid arthritis: a 76-week prospective study. *RMD Open*. (2017) 3:e000363. doi: 10.1136/rmdopen-2016-000363
27. Woo SJ, Kim MJ, Park KH, Lee YJ, Hwang JM. Resolution of recalcitrant uveitic optic disc edema following administration of methotrexate: two case reports. *Korean J Ophthalmol.* (2012) 26:61–4. doi: 10.3341/kjo.2012.26.1.61
28. Rathinam SR, Babu M, Thundikandy R, Kanakath A, Nardone N, Esterberg E, et al. A randomized clinical trial comparing methotrexate and mycophenolate mofetil for noninfectious uveitis. *Ophthalmology.* (2014) 121:1863–70. doi: 10.1016/j.ophtha.2014.04.023
29. Sobrin L, Pistilli M, Dreger K, Kothari S, Khachatryan N, Artornsombudh P, et al. Factors predictive of remission of chronic anterior uveitis. *Ophthalmology*. (2020) 127:826–34. doi: 10.1016/j.ophtha.2019.11.020
30. Baneke AJ, Lim KS, Stanford M. The pathogenesis of raised intraocular pressure in uveitis. *Current Eye Res.* (2016) 41:137–49. doi: 10.3109/02713683.2015.1017650
31. Muñoz-Negrete FJ, Moreno-Montañés J, Hernández-Martínez P, Rebolleda G. Current approach in the diagnosis and management of uveitic glaucoma. *BioMed Res Int*. (2015) 2015:742792. doi: 10.1155/2015/742792
32. Sng CCA, Ang M, Barton K. Uveitis and glaucoma: new insights in the pathogenesis and treatment. *Prog Brain Res.* (2015) 221:243–69. doi: 10.1016/bs.pbr.2015.06.008
33. Siddique SS, Suelves AM, Baheti U, Foster CS. Glaucoma and uveitis. *Surv Ophthalmol*. (2013) 58:1–10. doi: 10.1016/j.survophthal.2012.04.006
34. Hiyama T, Harada Y, Doi T, Kiuchi Y. Early administration of adalimumab for paediatric uveitis due to Behçet's disease. *Pediatr Rheumatol*. (2019) 17:29. doi: 10.1186/s12969-019-0333-6
35. Gonzales CA, Ladas JG, Davis JL, Feuer WJ, Holland GN. Relationships between laser flare photometry values and complications of uveitis. *JAMA Ophthalmol.* (2001) 119:1763–9. doi: 10.1001/archopht.119.12.1763
36. Davis JL, Dacanay LM, Holland GN, Berrocal AM, Giese MJ, Feuer WJ. Laser flare photometry and complications of chronic uveitis in children. *Am J Ophthalmol.* (2003) 135:763–71. doi: 10.1016/S0002-9394(03)00315-5

Conflict of Interest: The authors declare that the research was conducted in the absence of any commercial or financial relationships that could be construed as a potential conflict of interest.

Publisher's Note: All claims expressed in this article are solely those of the authors and do not necessarily represent those of their affiliated organizations, or those of the publisher, the editors and the reviewers. Any product that may be evaluated in this article, or claim that may be made by its manufacturer, is not guaranteed or endorsed by the publisher.

frontiers in Medicine

ORIGINAL RESEARCH
published: 24 December 2021
doi: 10.3389/fmed.2021.733523

Evaluation of Cyclooxygenase-2 and p53 Expression in Pterygium Tissue Following Preoperative Intralesional Ranibizumab Injection

Ahmad Razif Omar[1], *Mohtar Ibrahim*[1,2]*, *Hasnan Jaafar*[2,3], *Ab Hamid Siti-Azrin*[4] and *Embong Zunaina*[1,2]

[1] Department of Ophthalmology and Visual Science, School of Medical Sciences, Universiti Sains Malaysia, Kubang Kerian, Malaysia, [2] Hospital Universiti Sains Malaysia, Kubang Kerian, Malaysia, [3] Department of Pathology, School of Medical Sciences, Universiti Sains Malaysia, Kubang Kerian, Malaysia, [4] Biostatistics and Research Methodology Unit, School of Medical Sciences, Universiti Sains Malaysia, Kubang Kerian, Malaysia

OPEN ACCESS

Edited by:
Michele Lanza,
University of Campania Luigi Vanvitelli, Italy

Reviewed by:
Monika Riederer,
FH Joanneum, Austria
Daniel Marks,
AstraZeneca, United Kingdom
Anna A. Brozyna,
Nicolaus Copernicus University, Poland

***Correspondence:**
Mohtar Ibrahim
mohtar@usm.my

Specialty section:
This article was submitted to Ophthalmology, a section of the journal Frontiers in Medicine

Received: 30 June 2021
Accepted: 29 November 2021
Published: 24 December 2021

Citation:
Omar AR, Ibrahim M, Jaafar H, Siti-Azrin AH and Zunaina E (2021) Evaluation of Cyclooxygenase-2 and p53 Expression in Pterygium Tissue Following Preoperative Intralesional Ranibizumab Injection. Front. Med. 8:733523. doi: 10.3389/fmed.2021.733523

Introduction: Overexpression of vascular endothelial growth factor (VEGF), cyclooxygenase-2 (COX-2), and p53 are the postulated aetiopathogenesis in pterygium. VEGF is responsible for the induction of COX-2 expression, whereas p53 plays an important role in the regulation of VEGF. This study aimed to evaluate the immunohistochemistry of COX-2 and p53 expressions from excised pterygium tissue from patients who received intralesional ranibizumab (anti-VEGF) injection 2 weeks prior to pterygium surgery.

Materials and Methods: An interventional comparative study involving patients presenting with primary pterygium was conducted between September 2015 and November 2017. The patients were randomized into either the intervention or control group. Patients in the intervention group were injected with intralesional ranibizumab (0.5 mg/0.05 ml) 2 weeks prior to surgery. Both groups underwent pterygium excision followed by conjunctival autograft. Immunohistochemistry staining was performed to evaluate COX-2 and p53 expressions in the excised pterygium tissue.

Results: A total of 50 patients (25 in both the intervention and control groups) were recruited. There were 34 (68%) patients with grade III pterygium and 16 (32%) patients with grade IV pterygium. There was statistically significant difference in reduction of COX-2 expression in the epithelial layer [84.0% (95% CI: 63.9, 95.5)] ($p = 0.007$) and stromal layer [84.0% (95% CI: 63.9, 95.5)] ($p < 0.001$) between intervention and control groups. There was no significant difference in the reduction of p53 expression between the two groups.

Conclusion: This study demonstrated the possible use of intralesional anti-VEGF treatment prior to pterygium excision as a potential future modality of adjunctive therapy for pterygium surgery.

Keywords: anti-vascular endothelial growth factor, cyclooxygenase-2, primary pterygium, immunohistochemistry 2, p53 expression

INTRODUCTION

Pterygium appears as a triangular, wing-like fibrovascular growth from the bulbar conjunctiva over the limbus onto the cornea. Human pterygium exhibits both degenerative and hyperplastic conditions and is characterized by chronic proliferative fibrovascular tissue growth (1–3). Pterygium is a common ocular surface disease in countries in equatorial locations, namely, Malaysia. Its prevalence is as high as 22% in equatorial areas (compared to 2% in latitudes above 40°) (4). However, total prevalence worldwide ranges from 0.7 to 33% (5).

Pterygium has been associated with environmental factors, such as UV radiation, heat, dust, dryness, windy atmospheres, and increasing age (6, 7). Current studies suggested that UV radiation is the most important factor for pterygium formation (3, 8). It is postulated that UV-B radiation causes activation of the nuclear factor-kappa B (NF-kB) signaling pathway and leads to overexpression of cyclooxygenase-2 (COX-2) and vascular endothelial growth factor (VEGF). Overexpression of COX-2 and VEGF plays an important role in the angiogenesis and proliferating of fibrovascular tissue in the formation of pterygium (9, 10). Recent studies have also reported that overexpression of VEGF is produced by corneal fibroblasts in response to local conjunctival inflammation caused by environmental UV radiation, dryness, or dust (11–14). Park et al. (15) found that there was strongly expressed COX-2 and VEGF in macrophages of pterygium tissue. In addition, COX-2 overexpression is correlated with vessel density and VEGF expression (16).

Cyclooxygenase-2 is an enzyme that is responsible for inflammatory cytokine-induced angiogenesis. It is rapidly induced by growth factors, cytokines, and tissue damage. Some studies have reported that COX-2 overexpression was found in more than 80% of pterygium tissues (15, 17). Chiang et al. (17) suggested that COX-2 may play a role in pterygium formation. They reported that 75 out of 90 (83.3%) pterygium specimens were stained positive for COX-2, while all specimens from normal conjunctiva and limbi were stained negative for COX-2. In another study, COX-2 expression was detected in all pterygium tissues, while no COX-2 expression was observed in normal conjunctiva (15). Strong COX-2 expression has also been suggested as one of the risk factors for the recurrence of pterygium (18, 19). In addition to environmental factors, various theories have been postulated for the etiopathogenesis of pterygium, such as expression of p53 oncogenes, genetic and hereditary factors, and infective and immunological factors (3, 20–23).

The gene p53 (wild type) is a tumor suppressor gene that controls the cell cycle (24). Tumor suppressor genes protect cells from converting to cancer cells (25). The p53 gene product, the p53 protein, is a nuclear phosphoprotein, which binds to the DNA (26). In normal cells, wild-type p53 proteins have a short half-life, and the concentration is very low. They are almost undetectable by immunohistochemistry, so the cells stain negative (24, 26, 27). Mutations in the p53 gene can lead to the synthesis of abnormal p53 proteins, which has increased in protein stability resulting in prolonged half-life (26, 27). In many types of neoplastic cells, its concentration is higher hence immunohistochemical staining for the p53 protein becomes positive (24, 26). p53 expression is an indicator of p53 mutation (27, 28).

Ultraviolet radiation can inactivate p53 through mutation and subsequently lead to cell proliferation and genomic instability (29). Overexpression of p53 was found in the epithelium of pterygium tissue, thus suggesting that pterygium could be a result of uncontrolled cell proliferation (26). Expression of p53 in primary pterygium varies between 54% and 100% (26, 30–32). Kieser et al. (33) reported that p53 mutation is associated with VEGF expression.

Ranibizumab (Lucentis®; Genentech, Inc., South San Francisco, CA, United States) is a recombinant humanized anti-VEGF antibody that binds to VEGF-A. Through binding to VEGF-A, ranibizumab interrupts the VEGF-receptors interaction and thus prevents new vessels proliferation. Several studies (9, 34, 35) have demonstrated the beneficial effects of subconjunctival anti-VEGF, not only in regression of pterygium size and proliferation of vessels but also in the reduction of recurrence rate. However, there has been no study done to evaluate the immunohistochemistry of COX-2 and p53 expressions following anti-VEGF administration.

Therefore, the aim of this study was to compare the immunohistochemistry of COX-2 and p53 expressions from excised pterygium tissues following intralesional ranibizumab injection 2 weeks prior to pterygium surgery vs. the control group. Intralesional anti-VEGF treatment may provide future modalities of adjunctive therapy for pterygium surgery.

MATERIALS AND METHODS

An interventional comparative study involving patients with primary pterygium was conducted between September 2015 and November 2017. The study followed the tenets of the Declaration of Helsinki and was approved by the local ethical boards USM/JEPeM/[269.3 (1)].

The sample size was calculated using PS Power and Sample Size Calculation 3.1.2 based on an independent, prospective, two-proportion, and uncorrected chi-square test design. Power was set at 0.8, and the input was as follows: $\alpha = 0.05$, $p0 = 0.7$, $p1 = 0.3$, $m = 1$. The estimated sample size was based on several studies showing that COX-2 expression in primary pterygium is 80–100% (15, 17, 19). The calculated sample size was 25 with a 10% dropout. A total of 50 patients with primary pterygium were recruited for this study (25 patients for the intervention group and 25 patients for the control group).

This study was conducted among patients with grades III–IV primary nasal pterygium. Those patients with temporal or double-headed (nasal and temporal) pterygium, previous ocular surgery or trauma, ocular surface disorder, corneal pathology, primary or secondary glaucoma, history of taking regular eye drops, or history of a systemic thromboembolic event were excluded from this study. Pregnant women and lactating mothers were also excluded.

Patients who fulfilled the selection criteria and agreed to undergo surgical excision of pterygium were explained the nature

of the study, and written consent was obtained. Data regarding demographics (age and gender), medical history, previous ocular surgery or treatment, and previous systemic diseases were obtained through direct questioning from patients and from medical records.

Clinical Classification of Pterygium

A thorough slit lamp examination was performed by an independent ophthalmologist to clinically grade the pterygium. The clinical classification of pterygium was based on a modified classification system (36). The pterygium was rated as stage I (tissue involvement of the limbus), stage II (the tissue just on the limbus), stage III (the tissue between the limbus and pupillary margin), and stage IV (tissue central to the pupillary margin).

Randomization

Patients with grades III–IV primary nasal pterygium only were selected. Those who agreed to participate in the study were randomized into either the intervention or control group. The eligible patients were randomized into two groups by using the opaque sealed envelope technique. A piece of paper written with "Intervention" was placed in 25 envelopes, and the remaining 25 envelopes were written with "Control". These envelopes were shuffled and stored at the randomization room after random numbering the allocation sequence that was generated using a digital table by the primary investigator. The envelope was drawn for each patient by a co-investigator, who was not involved in the preparation of these opaque sealed envelopes. Patients in the intervention group were given an intralesional injection of ranibizumab. Patients in the control group were not given any injection or placebo.

Intralesional Injection of Ranibizumab

Patients in the intervention group were given an intralesional injection of ranibizumab (Lucentis®; Genentech, Inc., United States) 2 weeks before their pterygium surgery. The injection was given in an operating theater using an aseptic technique. The patient was lying supine, and the eye was anesthetized with topical proparacaine (0.5%). Then, the eye was cleaned and draped, and a lid speculum was applied. Topical povidone (5%) was applied to the conjunctiva and then washed thoroughly. Ranibizumab 0.5 mg/0.05 ml was then injected into the body of the pterygium along the limbus. After the procedure, each patient was treated with 0.5% topical chloramphenicol every 6 h for 1 week. Each patient was scheduled for pterygium excision surgery 2 weeks post-procedure. This 2-week post-intralesional ranibizumab period was chosen for pterygium excision because a study done by Mandalos et al. (37) showed that pterygium attained the lowest vessel density after 2 weeks of anti-VEGF injection.

Pterygium Surgery

Patients in both the intervention and control groups were admitted for the pterygium surgery procedure. General and ocular assessments had been performed preoperatively. Any side effects or complications related to intralesional injection of ranibizumab were recorded for those in the intervention group.

The pterygium excision surgery was carried out in an operating theater under topical anesthesia using 5% proparacaine. Topical phenylephrine (2.5%) was given to reduce bleeding during the excision. The surgical area was then cleaned and draped, and a lid speculum was applied. Topical povidone (5%) was applied to the cul-de-sac for 3 min and then washed thoroughly. Intralesional lignocaine (1%) was injected into the pterygium body. The pterygium was excised from the apex to the base using a Tooke corneal knife and Westcott scissors. Part of the pterygium head was excised, and fibrovascular tissue was scraped using a Tooke corneal knife. Hemostasis was achieved by applying pressure to the bleeding site using cotton bud tips. Conjunctiva autograft was harvested from the superior or inferior bulbar conjunctiva and then applied with the correct orientation of limbal edge to the bare sclera. The conjunctival autograft was either secured using fibrin adhesive glue (Tisseel VH; Baxter Healthcare Corp., Deerfield, IL, USA) or sutured using absorbable suture vicryl 8/0 depending on the availability of fibrin adhesive glue during the surgery.

This part of this study was open-label in which both the patient and the operating surgeon were aware of the treatment allocation.

Paraffin-Embedded Tissue Block Preparation

Excised pterygium tissue was transported to the pathology laboratory in 10% normal buffered formalin for tissue fixation for histological diagnosis. After 48 h, the formalin was exchanged with 80–95% ethanol and absolute alcohol for the tissue dehydration procedure, and the excised pterygium tissues were processed and embedded in paraffin wax. The tissue processing and paraffin-embedded tissue blocks had been prepared by the principal investigator, co-investigator, and laboratory technician.

Immunohistochemical Analysis of COX-2

Sections of approximately 3–4 μm in thickness were obtained from paraffin-embedded tissue blocks. All sections were deparaffinized in xylene, rehydrated through a graded series of alcohols, and washed with phosphate-buffered saline. This buffer was used for all subsequent washes. Sections for COX-2 detection were heated in a pressure cooker for 3 min at full pressure in citrate buffer (pH 6.0). Dako REAL Peroxidase blocking solution (Dako, Denmark) was used to block endogenous peroxidase and was incubated for 5 min. Monoclonal mouse anti-COX-2 antibody at a dilution of 1:200 (Clone CX-294; Dako, North America) was used as the primary antibody. The primary antibody was incubated with the tissue sample to allow binding to the target antigen. The incubation time was 1 h at room temperature. Dako REAL EnVision Horse Reddish Peroxidase (HRP) rabbit/mouse (ready-to-use) (Dako, Denmark) was the secondary antibody, with specificity for the primary antibody, was incubated with the tissue sample to allow binding to the primary antibody. This incubation step was 30 min at room temperature. Signals were developed with 3,3'-diaminobenzidine (DAB) for 5 min and counterstained with hematoxylin. Negative controls were obtained by leaving out the primary antibody.

COX-2 expression in colon adenocarcinoma tissue was used as a positive control.

Clone CX-294 (Clone CX294; Dako North America) is specific to the peptide used for immunization. In Western blotting and immunoprecipitation experiments, CX-294 was shown to identify the inducible human COX-2 using interleukin-1 alpha-stimulated human umbilical vein endothelial cells (HUVEC); peptide blocking of the antibody with the COX-2 immunogen eliminated all reactivity.

Evaluation and scoring of immunohistochemical staining of COX-2 expression were performed by two independent researchers for test-retest reliability. Both researchers were single blinded to the treatment allocation. COX-2 expression in the epithelial layer was scored according to the percentage of positive cell staining: score 0, negative staining; score 1+, 1–10% positive cell staining; score 2+, 11–50% positive cell staining; and score 3+, >50% positive cell staining. COX-2 expression in the stromal layer was scored according to the average number of COX-2-expressing cells calculated over ten random high-power fields (magnification 400×): score 0, negative staining; score 1+, 1–5 positive cells staining; score 2+, 6–10 positive cells staining; and score 3+, >10 positive cells staining. The scoring method that was used in this study was based on the scoring described by Park et al. (15).

Immunohistochemical Analysis of p53

Sections of approximately 3–4 μm in thickness were obtained from paraffin-embedded tissue blocks. All sections were deparaffinized in xylene, rehydrated through a graded series of alcohols, and washed with phosphate-buffered saline. This buffer was used for all subsequent washes. Sections for p53 detection were heated in a pressure cooker for 3 min at full pressure in crisEDTA buffer (pH 9.0). Dako REAL Peroxidase blocking solution (Dako, Denmark) was used to block endogenous peroxidase and was incubated for 5 min. Monoclonal mouse anti-p53 antibody, DO-7, at dilution 1:100 (Code number M 7001; Dako, Denmark) was used as the primary antibody. The primary antibody was incubated with the tissue sample to allow binding to the target antigen. The incubation time was 1 h at room temperature. Dako REAL EnVision (HRP rabbit/mouse (ready-to-use) (Dako, Denmark) was the secondary antibody, with specificity for the primary antibody, was incubated with the tissue sample to allow binding to the primary antibody. This incubation step was 30 min at room temperature. Signals were developed with DAB for 5 min and counterstained with hematoxylin. Negative controls were obtained by leaving out the primary antibody. p53 expression in colon adenocarcinoma tissue was used as a positive control.

Evaluation and scoring of immunohistochemical staining of p53 expression were performed by two independent researchers for test-retest reliability. Both researchers were single blinded to treatment allocation. p53 expression was observed in the nuclei of the epithelial layer of excised pterygium tissue. The immunohistochemical p53 results were scored according to the percentage of cells with positive nuclei staining: score 0, negative staining in the nuclei; score 1+, 1–10% positive staining in the nuclei; score 2+, 11–50% positive staining in the nuclei; score 3+, >50% positive staining in the nuclei. The scoring method that was used in this study was based on the scoring described by Tsai et al. (38).

TABLE 1 | Distribution of age, gender, and method of conjunctival autograft for both groups.

Parameters	Intervention $n = 25$	Control $n = 25$
Age (years)		
Mean	52.64 ± 8.8	51.96 ± 9.5
Range	36–67	37–68
Gender (n, %)		
Male	13 (52)	13 (52)
Female	12 (48)	12 (48)
Methods of conjunctival autograft (n, %)		
Fibrin glue	18 (72)	22 (88)
Suturing	7 (28)	3 (12)

Statistical Analysis

Statistical analysis was carried out using the Statistical Package for Social Sciences (SPSS) version 22. Fisher's exact test was used for the association of COX-2 and p53 expressions between the intralesional ranibizumab and control groups. Fisher's exact tests were conducted using STATA version 14, and a value of $p < 0.05$ indicated statistical significance.

RESULTS

Demographic Data

A total of 50 patients (25 patients in the intervention group and 25 patients in the control group) were recruited. Among these two groups, there were 34 (68%) patients with grade III pterygium and 16 (32%) patients with grade IV pterygium. There were 13 (52%) men and 12 (48%) women in each group. Ages in the intervention group ranged from 36 to 67 years, with a mean age of 52.64 ± 8.8 years. In the control group, ages ranged from 37 to 68, with a mean age of 51.96 ± 9.5 years (**Table 1**).

Post-pterygium excision, the conjunctival autograft was performed using fibrin adhesive glue in 18 (72%) patients in the intervention group and 22 (88%) patients in the control group. Suturing of conjunctival autograph was done in the other 10 patients (seven patients in intervention and three patients in control groups) (**Table 1**). There were no side effects or complications post-intralesional ranibizumab injection observed among the patients in the intervention group.

COX-2 Expression in Excised Pterygium Tissue

Cyclooxygenase-2 expression was observed in both the epithelial layer and stromal layer of excised pterygium tissue. There were a greater number of positive cells staining in the epithelial

TABLE 2 | Association of cyclooxygenase-2 (COX-2) and p53 expression in excised pterygium tissue between intervention and control groups post-intralesional injection of ranibizumab.

Immunohistochemical analysis	Intervention group *n* (%)	Control group *n* (%)	Point estimate	95% CI	*p* value
COX-2 epithelial cells staining					
Score 0	4 (16)	0 (0)			
Score 1+	10 (40)	6 (24)	84.0%	63.9, 95.5	0.007
Score 2+	10 (40)	10 (40)			
Score 3+	1 (4)	9 (36)			
COX-2 stromal cells staining					
Score 0	4 (16)	0 (0)			
Score 1+	15 (60)	6 (24)	84.0%	63.9, 95.5	<0.001
Score 2+	6 (24)	14 (56)			
Score 3+	0 (0)	5 (20)			
p53 epithelial cells staining					
Score 0	1 (4)	0 (0)			
Score 1+	9 (36)	3 (12)	96.0%	79.6, 99.9	0.085
Score 2+	9 (36)	10 (40)			
Score 3+	6 (24)	12 (48)			

Fisher's exact test, $p < 0.05$ significant.
CI, confidence interval; COX-2, cyclooxygenase-2.

layer as compared to the stromal layer. The epithelial layer showed few focal areas of hyperplasia indicate a disturbance of cell proliferation. Immunohistochemical scoring of COX-2 expression of pterygium tissues showed different staining intensities from weak to moderate and strong staining intensity.

In the epithelial layer, COX-2 expression was observed mainly in the basal epithelia. The distribution of COX-2 expression in epithelial cells between the two groups is shown in **Table 2**. Higher scoring (score 3+) was seen more in the control group as compared to the intervention group. There were 4 (16%) pterygium tissues in the intervention group that showed negative epithelial cell staining of COX-2. None of the tissues from the control group showed negative staining of COX-2 in epithelial cells. There was a statistically significant difference in the reduction of COX-2 expression in the surface epithelium between intervention and control groups [84.0% (95% CI: 63.9, 95.5)] ($p = 0.007$) post-intralesional injection of ranibizumab.

In the stromal layer, COX-2 staining was observed in stromal inflammatory cells, capillary vessels, and fibroblasts. The distribution of COX-2 expression in stromal cells between the two groups is shown in **Table 2**. Score 2+ was observed higher in the control group as compared to the intervention group. On the contrary, a score 1+ was higher in the intervention group as compared to the control group. There were 4 (16%) pterygium tissues in the intervention group that showed negative stromal cell staining of COX-2. None of the tissues from the control group showed negative staining of COX-2 in stromal cells. There was a statistically significant difference in the reduction of COX-2 expression in stromal cells between intervention and control groups [84.0% (95% CI: 63.9, 95.5)] ($p < 0.001$) post-intralesional injection of ranibizumab.

p53 Expression in Excised Pterygium Tissue

p53 immunostaining was observed in the nuclei of the surface epithelia. The distribution of p53 expression in epithelial cells between the two groups is shown in **Table 2**. Intervention group showed 4% negative staining, 36% in score 1+, and 24% in score 3+ as compared to control group with 0, 12, and 48%, respectively. There was only one (4%) pterygium tissue in the intralesional ranibizumab group that showed negative epithelial cell staining of p53, and none from the control group. However, there was no significant difference in the reduction of p53 expression between intervention and control groups [96.0% (95% CI: 79.6, 99.9)] ($p = 0.085$) post-intralesional injection of ranibizumab.

Immunohistochemical scoring of COX-2 expression in the epithelial layer, COX-2 expression in the stromal layer, and p53 expression in the epithelia layer of pterygium tissues are shown in **Supplementary Figures 1–3**, respectively, as supplementary files. In view of the inability to use of scale slide, the images were captured without a scale bar.

DISCUSSION

There are various proposed etio-histopathologies of pterygia. Overexpression of VEGF in response to numerous stimuli plays a role in pterygium formation (11–14). Apart from that, several studies have shown that COX-2 and p53 overexpressions play important roles in the pathogenesis of pterygium. COX-2 is the significant enzyme for inflammatory cytokine-induced angiogenesis, and it was found in 80–100% of primary pterygia (15, 17, 19). Expression of p53 in primary pterygia varies between 54 and 100% (26, 30–32). It has been suggested that pterygium could result from uncontrolled cell proliferation (26).

Several studies have demonstrated the effectiveness of subconjunctival anti-VEGF in regression of pterygium size (9), vascularity (9, 39, 40), and the recurrence rate (39, 41). VEGF is a regulator of angiogenesis and inhibition of VEGF can prevent new vessel proliferation (9). Mohamed et al. (40) demonstrated that pterygium with anti-VEGF injection showed a reduction in mean vessel count and VEGF expression.

Vascular endothelial growth factor is induced by hypoxic stimuli and is responsible for the induction of COX-2 expression in endothelial cells (42). In our study, there were significant reductions in COX-2 expression in the surface epithelium ($p = 0.007$) and stromal cells ($p < 0.001$) in pterygium tissue post-intralesional injection of ranibizumab as compared to the control group. Liu et al. (10) reported that there was a significant correlation between COX-2 upregulation and VEGF expression in pterygium tissue. They found that the expression of COX-2 showed a significant correlation with the density of the microvessels. The finding was supported by Mohamed et al. (40) showed that intralesional injection of anti-VEGF in pterygium decreased vascularity and VEGF expression. We postulated that inhibition of VEGF is associated with a reduction of COX-2 expression and vascularity.

However, only 16% of pterygium tissue in the intervention group in our study showed negative staining for COX-2 expression. Multiple factors might be responsible for COX-2 expression. Application of COX inhibitor demonstrated inhibition of COX-2 expression (43), indicating COX-2-prostaglandin-E2 pathway is the possible mechanism (44).

Abnormal expression of p53 has also been demonstrated in pterygium suggesting that p53 plays a possible role in the pathogenesis of pterygium (28). The expression of p53 could be associated with an increase in VEGF production (45). In our study, p53 immunostaining was observed in the nuclei of the surface epithelium. Although there was no significant difference in the reduction of p53 expression in pterygium tissue post-intralesional injection of ranibizumab between the two groups ($p = 0.085$), the trend of scoring is more favorable in the intervention group. Lower scoring (score 1+) was seen more in the intervention group as compared to the control group. Our finding showed that VEGF inhibition plays a minor role in the reduction of p53 expression. We postulated that the possibility of UV radiation-induced p53 mutation is the major mechanism for p53 expression.

Several studies have reported that there is a relationship between UV radiation and the prevalence of pterygium (46–48). Those who are living at high altitudes (above 3,000 m) were exposed to high UV-B sunlight and had high prevalence rates of pterygium (46, 47) and those who are living at low altitudes (below 3,000 m) had a low prevalence of pterygium (48). Recent reports have suggested that p53 expression in the epithelium of pterygium is probably a result of UV radiation exposure (24, 26, 30, 32). p53 expression was observed to be increasing with increasing duration and severity of pterygium (49).

The different scoring system of COX-2 expression was used for the epithelial layer and stromal layer. Scoring according to the percentage of positive cell staining was used in the epithelial layer, whereas in the stromal layer was scored according to the average number of COX-2-expressing cells. Histologically, pterygia are characterized by a hyperplastic, epithelial mesenchymal transition, clusters of basal cells aggregation beside an activated fibroblastic stroma with inflammation and matrix remodeling (1). Small clusters of aggregation basal cells illustrated smaller cell size and had increased nuclear-to-cytoplasm ratio (1). Dense epithelial cells in a few clusters of epithelial layers with different staining intensity, COX-2 expression in the epithelial layer was scored according to the percentage of positive cell staining. On the other hand, absolute cell number was used for scoring of cell staining in the stromal layer in view of less abundant stromal cells.

With the emergence and availability of anti-VEGF, intralesional of anti-VEGF on pterygium tissue was suggested as a possible adjunctive therapy for pterygium excision by decreasing the blood vessel formation (9, 40, 50). Strong COX-2 expression has been suggested as a risk factor for the recurrence of pterygium (18, 19). However, p53 expression in the epithelium overlying the pterygium is not associated with the recurrence of pterygium (51).

The use of subconjunctival anti-VEGF injection as an adjunct therapy to the surgery is relatively safe (40, 52). There were no side effects or complications post-intralesional ranibizumab injection observed in our study.

Limitation and Recommendation

This study does have some limitations. Firstly, the specific mechanism of COX-2 and p53 overexpressions was not fully understood. Therefore, detailed information about each patient's lifestyle, sun exposure, irradiation, family history, and medication intake should be obtained and considered during analysis, as all these factors can affect COX-2 and p53 overexpressions in pterygium tissue.

In this study, the sealed envelope technique was used as the technique for the randomization method. However, this sealed envelopes technique is not a robust method for allocation concealment. Other methods of randomization such as block or stratified randomization are the better randomization technique in order to produce a comparable group and eliminate the source of bias in the intervention group.

The COX-2 expression in the stromal layer was analyzed as a total of all cells. Analysis of the COX-2 expression according to the different stroma cell types was not performed. The information regarding COX-2 expression according to the different stroma cell types might strengthen the findings. We recommend analyzing the COX-2 expression based on the different types of cells in the stromal layer in future studies.

Images of immunohistochemical scoring of COX-2 expression and p53 expression in pterygium tissues (**Supplementary Files**) were captured without a scale bar because we were not being able to use a scale slide during capturing the image. Since scale bar information allows a quicker and reliable way to assess the size of features shown in images, we advise any microscopic images should have a scar bar either using a scale slide or specific software.

Intralesional ranibizumab would have an effect on VEGF expression and reflect the effect of ranibizumab on the treatment

efficacy. However, due to limited funds, VEGF expression was not analyzed in this study. We strongly recommend analyzing the VEGF expression in future studies that used anti-VEGF as a treatment option.

Due to the various postulated etiopathogenesis of pterygium that exists currently, evaluating the effect of intralesional ranibizumab injection on oxidative stress markers in pterygium such as 8-hydroxy-20-deoxyguanosine and on CD34 expression in endothelial cells might be useful.

Lignocaine, is an amide local anesthetic, was administered during the procedure of pterygium surgery. The mechanism of action of lignocaine for local anesthesia is by reversible blockade of nerve fiber impulse propagation (53). It was reported that lignocaine significantly inhibits the VEGF by suppressing VEGF receptor-2 signaling (54, 55). Suppression of VEGF in the intervention group might also be caused by lignocaine administration besides intralesional injection of anti-VEGF. Further study needs to be evaluated to determine the impact of administration of local anesthesia on the effect of COX-2 and p53 overexpression. In our study, both groups were given lignocaine anesthesia during pterygium surgery. Therefore, the effect of VEGF inhibition by lignocaine was standardized in both groups.

In our study, the recurrence rate was not evaluated in both groups. The surgical technique for conjunctiva autograft application post-pterygium excision for our patients was not standardized due to the limited availability of fibrin adhesive glue during the surgeries. In our study, pterygium excision was performed with a conjunctiva autograft application, using either fibrin adhesive glue or absorbable sutures. In view of different surgical techniques, so this will affect the long-term recurrence rates between these two groups. Future studies should standardize the surgical method and evaluate the recurrence rate of pterygium between intervention and control groups.

CONCLUSION

Intralesional ranibizumab has the effect of reducing both COX-2 and p53 expressions in primary pterygium tissue compared to the control group. However, only the COX-2 expression showed a significant result. This study demonstrated the possible use of intralesional anti-VEGF treatment prior to pterygium excision as a potential future modality of adjunctive therapy for pterygium surgery.

DATA AVAILABILITY STATEMENT

The raw data supporting the conclusions of this article will be made available by the authors, without undue reservation.

ETHICS STATEMENT

The studies involving human participants were reviewed and approved by Local Ethical Boards USM/JEPeM/[269.3 (1)] from Universiti Sains Malaysia. The patients/participants provided their written informed consent to participate in this study.

AUTHOR CONTRIBUTIONS

AO, MI, and HJ contributed to the design of the study. AO, MI, and HJ were involved in data collection. HJ and AO contributed to laboratory analysis. AS-A and AO contributed to statistical analysis. AO and MI drafted the manuscript. MI and EZ crucially revised the manuscript. All authors have read and approved the final manuscript.

FUNDING

This work was supported by a short term grant (Account Number: 304/PPSP/61313145) from Universiti Sains Malaysia.

ACKNOWLEDGMENTS

We would like to thank all staff from the Department of Ophthalmology and Visual Science and the Department of Pathology for their direct and indirect support and help.

SUPPLEMENTARY MATERIAL

The Supplementary Material for this article can be found online at: https://www.frontiersin.org/articles/10.3389/fmed.2021.733523/full#supplementary-material

Supplementary Figure 1 | Immunohistochemical analysis of cyclooxygenase-2 (COX-2) protein expression in the epithelial layer of excised pterygium tissue. **(A)** This panel shows negative expression (no positive cell staining). **(B)** Positive immunostaining of scores 1+, 1–10% positive cells staining. **(C)** Positive immunostaining of scores 2+, 11–50% positive cells staining. **(D)** Positive immunostaining of scores 3+, more than 50% positive cells staining (IHC stain: magnification 200×). IHC, Immunohistochemistry.

Supplementary Figure 2 | Immunohistochemical analysis of cyclooxygenase-2 (COX-2) protein expression in the stromal layer of excised pterygium tissue. **(E)** This panel shows negative expression (no positive cell staining). **(F)** Positive immunostaining of scores 1+, 1–5 positive cells staining. **(G)** Positive immunostaining of scores 2+, 6–10 positive cells staining. **(H)** Positive immunostaining of scores 3+, more than 10 positive cells staining (IHC stain: magnification 200×). IHC, Immunohistochemistry.

Supplementary Figure 3 | Immunohistochemical analysis of p53 protein expression in the epithelial layer of excised pterygium tissue. **(J)** This panel shows negative expression (no positive staining in the nuclei of all cells). **(K)** Positive immunostaining of scores 1+, 1–10% positive staining in the nuclei. **(L)** Positive immunostaining of scores 2+, 10–50% positive staining in the nuclei. **(M)** Positive immunostaining of scores 3+, more than 50% positive staining in the nuclei (IHC stain: magnification 200×). IHC, Immunohistochemistry.

REFERENCES

1. Chui J, Coroneo MT, Tat LT, Crouch R, Wakefield D, Di Girolamo N. Ophthalmic pterygium: a stem cell disorder with premalignant features. *Am J Pathol.* (2011) 178:817–27. doi: 10.1016/j.ajpath.2010.10.037
2. Bradley JC, Yang W, Bradley RH, Reid TW, Schwab IR. The science of pterygia. *Br J Ophthalmol.* (2010) 94:815–20. doi: 10.1136/bjo.2008.151852
3. Di Girolamo N, Chui J, Coroneo MT, Wakefield D. Pathogenesis of pterygia: role of cytokines, growth factors, and matrix metalloproteinases. *Prog Retin Eye Res.* (2004) 23:195–228. doi: 10.1016/j.preteyeres.2004.02.002

4. Dake Y, Mukae R, Soda Y, Kaneko M, Amemiya T. Immunohistochemical localization of collagen types I, II, III, and IV in pterygium tissues. *Acta Histochem.* (1989) 87:71–4. doi: 10.1016/S0065-1281(89)80035-2
5. Droutsas K, Sekundo W. Epidemiologie des pterygiums. *Ophthalmologe.* (2010) 107:511–6. doi: 10.1007/s00347-009-2101-3
6. Saw S-M, Tan D. Pterygium: prevalence, demography and risk factors. *Ophthalmic Epidemiol.* (1999) 6:219–28. doi: 10.1076/opep.6.3.219.1504
7. Zhong H, Cha X, Wei T, Lin X, Li X, Li J, et al. Prevalence of and risk factors for pterygium in rural adult Chinese populations of the Bai Nationality in Dali: the Yunnan Minority Eye Study. *Invest Ophthalmol Vis Sci.* (2012) 53:6617–21. doi: 10.1167/iovs.11-8947
8. Chui J, Di Girolamo N, Wakefield D, Coroneo MT. The pathogenesis of pterygium: current concepts and their therapeutic implications. *Ocul Surf.* (2008) 6:24–43. doi: 10.1016/S1542-0124(12)70103-9
9. Singh P, Sarkar L, Sethi HS, Gupta VS, A. randomized controlled prospective study to assess the role of subconjunctival bevacizumab in primary pterygium surgery in Indian patients. *Indian J Ophthalmol.* (2015) 63:779–84. doi: 10.4103/0301-4738.171508
10. Liu D, Peng C, Jiang Z, Tao L. Relationship between expression of cyclooxygenase 2 and neovascularization in human pterygia. *Oncotarget.* (2017) 8:105630–6. doi: 10.18632/oncotarget.22351
11. Blaudschun R, Sunderkötter C, Brenneisen P, Hinrichs R, Peters T, Schneider L, et al. Vascular endothelial growth factor causally contributes to the angiogenic response upon ultraviolet B irradiation in vivo. *Br J Dermatol.* (2002) 146:581–7. doi: 10.1046/j.1365-2133.2002.04669.x
12. Detorakis ET, Spandidos DA. Pathogenetic mechanisms and treatment options for ophthalmic pterygium: trends and perspectives. *Int J Mol Med.* (2009) 23:439–47. doi: 10.3892/ijmm_00000149
13. Lee DH, Cho HJ, Kim JT, Choi JS, Joo CK. Expression of vascular endothelial growth factor and inducible nitric oxide synthase in pterygia. *Cornea.* (2001) 20:738–42. doi: 10.1097/00003226-200110000-00013
14. Yan M, Li Z, Liu G, Peng C, Zhou Y, Wang F. Blood vessel multiply and significance of expression of Cox-2, VEGF in pterygium. *Yan Ke Xue Bao.* (2007) 23:20–4.
15. Park CY, Choi JS, Lee SJ, Hwang SW, Kim E-J, Chuck RS. Cyclooxygenase-2-expressing macrophages in human pterygium co-express vascular endothelial growth factor. *Mol Vis.* (2011) 17:3468–80.
16. Luo H, Chen Z, Jin H, Zhuang M, Wang T, Su C, et al. Cyclooxygenase-2 up-regulates vascular endothelial growth factor via a protein kinase C pathway in non-small cell lung cancer. *J Exp Clin Cancer Res.* (2011) 30:6. doi: 10.1186/1756-9966-30-6
17. Chiang CC, Cheng YW, Lin CL, Lee H, Tsai FJ, Tseng SH, et al. Cyclooxygenase 2 expression in pterygium. *Mol Vis.* (2007) 13:635–8.
18. Adiguzel U, Karabacak T, Sari A, Oz O, Cinel L. Cyclooxygenase-2 expression in primary and recurrent pterygium. *Eur J Ophthalmol.* (2007) 17:879–84. doi: 10.1177/112067210701700602
19. Karahan N, Baspinar S, Ciris M, Baydar CL, Kapucuoglu N. Cyclooxygenase-2 expression in primary and recurrent pterygium. *Indian J Ophthalmol.* (2008) 56:279–83. doi: 10.4103/0301-4738.39663
20. Hill JC, Maske R. Pathogenesis of pterygium. *Eye.* (1989) 3:218–26. doi: 10.1038/eye.1989.31
21. Tan D, Lim A, Goh H-S, Smith DR. Abnormal expression of the p53 tumor suppressor gene in the conjunctiva of patients with pterygium. *Am J Ophthalmol.* (1997) 123:404–5. doi: 10.1016/S0002-9394(14)70141-2
22. Tsironi S, Ioachim E, Machera M, Aspiotis M, Agnantis N, Psillas K. Immunohistochemical HLA-DR antigen expression with lymphocyte subsets and proliferative activity in pterygium. *In Vivo.* (2002) 16:299–306.
23. Pinkerton OD, Hokama Y, Shigemura LA. Immunologic basis for the pathogenesis of pterygium. *Am J Ophthalmol.* (1984) 98:225–8. doi: 10.1016/0002-9394(87)90358-8
24. Anthwal D, Gupta M, Dasgupta S, Tyagi R. p53 Expression in pterygium amongst natives of high versus low altitude. *Int J Ophthalmol Eye Res.* (2017) 5:334–40. doi: 10.19070/2332-290X-1700068
25. Feng QY, Hu ZX, Song XL, Pan HW. Aberrant expression of genes and proteins in pterygium and their implications in the pathogenesis. *Int J Ophthalmol.* (2017) 10:973–81.
26. Weinstein O, Rosenthal G, Zirkin H, Monos T, Lifshitz T, Argov S. Overexpression of p53 tumor suppressor gene in pterygia. *Eye.* (2002) 16:619–21. doi: 10.1038/sj.eye.6700150
27. Pelit A, Bal N, Akova YA, Demirhan B. p53 expression in pterygium in two climatic regions in Turkey. *Indian J Ophthalmol.* (2009) 57:203–6. doi: 10.4103/0301-4738.49394
28. Shimmura S, Ishioka M, Hanada K, Shimazaki J, Tsubota K. Telomerase activity and p53 expression in pterygia. *Invest Ophthalmol Vis Sci.* (2000) 41:1364–9.
29. Perra MT, Maxia C, Corbu A, Minerba L, Demurtas P, Colombari R, et al. Oxidative stress in pterygium: relationship between p53 and 8-hydroxydeoxyguanosine. *Mol Vis.* (2006) 12:1136–42.
30. Dushku N, Reid TW. P53 expression in altered limbal basal cells of pingueculae, pterygia, and limbal tumors. *Curr Eye Res.* (1997) 16:1179–92. doi: 10.1076/ceyr.16.12.1179.5036
31. Tan DT, Tang WY, Liu YP, Goh H-S, Smith DR. Apoptosis and apoptosis related gene expression in normal conjunctiva and pterygium. *Br J Ophthalmol.* (2000) 84:212–6. doi: 10.1136/bjo.84.2.212
32. Onur C, Orhan D, Orhan M, Sak SD, Tulunay Ö, Irkeç M. Expression of p53 protein in pterygium. *Eur J Ophthalmol.* (1998) 8:157–61. doi: 10.1177/112067219800800307
33. Kieser A, Weich HA, Brandner G, Marme D, Kolch W. Mutant p53 potentiates protein kinase C induction of vascular endothelial growth factor expression. *Oncogene.* (1994) 9:963–70.
34. Alhammami H, Farhood Q, Shuber H. Subconjuctival bevacizumab injection in treatment of recurrent pterigym. *J Clin Exp Ophthalmol.* (2013) 4:267. doi: 10.4172/2155-9570.1000267
35. Stival LR, Lago AM, Figueiredo MN, Bittar RH, Machado ML, Nassaralla Junior JJ. Efficacy and safety of subconjunctival bevacizumab for recurrent pterygium. *Arq Bras Oftalmol.* (2014) 77:4–7. doi: 10.5935/0004-2749.20140003
36. Johnston SC, Williams PB, Sheppard JD, A. comprehensive system for pterygium classification. *Invest Ophthalmol & Vis Sci.* (2004) 45:2940.
37. Mandalos A, Tsakpinis D, Karayannopoulou G, Tsinopoulos I, Karkavelas G, Chalvatzis N, et al. The effect of subconjunctival ranibizumab on primary pterygium: a pilot study. *Cornea.* (2010) 29:1373–9. doi: 10.1097/ICO.0b013e3181d927b9
38. Tsai YY, Cheng YW, Lee H, Tsai FJ, Tseng SH, Chang KC. P53 gene mutation spectrum and the relationship between gene mutation and protein levels in pterygium. *Mol Vis.* (2005) 11:50–5.
39. El Shafie AM, Mohamed AS, Sayed MF. The outcome of preoperative subconjunctival bevacizumab injection in pterigium surgery. *J Egypt Ophthalmol Soc.* (2014) 107:113–6. doi: 10.4103/2090-0686.140643
40. Mohamed TA, Soliman W, Fathalla AM, El Refaie A. Effect of single subconjunctival injection of bevacizumab on primary pterygium: clinical, histopathological and immunohistochemical study. *Int J Ophthalmol.* (2018) 11:797–801. doi: 10.18240/ijo.2018.05.13
41. Bahar I, Kaiserman I, McAllum P, Rootman D, Slomovic A. Subconjunctival bevacizumab injection for corneal neovascularization in recurrent pterygium. *Curr Eye Res.* (2008) 33:23–8. doi: 10.1080/02713680701799101
42. Wu G, Luo J, Rana JS, Laham R, Frank W. Sellke FW, Li J. Involvement of COX-2 in VEGF-induced angiogenesis via P38 and JNK pathways in vascular endothelial cells. *Cardiovasc Res.* (2006) 69:512–9. doi: 10.1016/j.cardiores.2005.09.019
43. Yao B, Wang F, Zhao X, Wang B, Yue X, Ding Y, et al. Effect of a topical nonsteroidal anti-inflammatory drug (01% pranoprofen) on VEGF and COX-2 expression in primary pterygium. *Front Pharmacol.* (2021) 12:709251. doi: 10.3389/fphar.2021.709251
44. Xu L, Croix BS. Improving VEGF-targeted therapies through inhibition of COX-2/PGE[[sb]]2 [[/s]]signaling. *Mol Cell Oncol.* (2014) 1:e969154. doi: 10.4161/23723548.2014.969154
45. Cavazzola LT, Rosa ARP, Schirmer CC, Gurski RR, Telles JPB, Médico FM, et al. Immunohistochemical evaluation for P53 and VEGF (Vascular Endothelial Growth Factor) is not prognostic for long term survival in end stage esophageal adenocarcinoma. *Rev Col Bras Cir.* (2009) 36:024–34. doi: 10.1590/S0100-69912009000100007

46. Lu P, Chen X, Kang Y, Ke L, Wei X, Zhang W. Pterygium in Tibetans: A population-based study in China. *Clin Experiment Ophthalmol*. (2007) 35:828–33. doi: 10.1111/j.1442-9071.2007.01630.x
47. Lu J, Wang Z, Lu P, Chen X, Zhang W, Shi K, et al. Pterygium in an aged Mongolian population: a population-based study in China. *Eye*. (2009) 23:421–7. doi: 10.1038/sj.eye.6703005
48. Alqahtani JM. The prevalence of pterygium in Alkhobar: A hospital-based study. *J Family Community Med*. (2013) 20:159–61. doi: 10.4103/2230-8229.121980
49. Mahesh M, Mittal SK, Kishore S, Singh A, Gupta N, Rana R. Expression of p53 and Ki-67 proteins in patients with increasing severity and duration of pterygium. *Indian J Ophthalmol*. (2021) 69:847–50. doi: 10.4103/ijo.IJO_1034_20
50. Fouda SM. Evaluation of the additive effect of bevacizumab eye drops to mitomycin C in primary pterygium. *Adv Ophthalmol Vis Syst*. (2017) 6:53–6. doi: 10.15406/aovs.2017.06.00171
51. Chowers I. Pe'er J, Zamir E, Livni N, Ilsar M, Frucht-Pery J. Proliferative activity and p53 expression in primary and recurrent pterygia. *Ophthalmology*. (2001) 108:985–8. doi: 10.1016/S0161-6420(00)00651-5
52. Nuzzi R, Tridico F. Efficacy of subconjunctival bevacizumab injections before and after surgical excision in preventing pterygium recurrence. *J Ophthalmol*. (2017) 1–7. doi: 10.1155/2017/6824670
53. Weinberg L, Peake B, Tan C, Nikfarjam M. Pharmacokinetics and pharmacodynamics of lignocaine: A review. *World J Anesthesiol*. (2015) 4:17–29. doi: 10.5313/wja.v4.i2.17
54. Goa J, Hu H, Wang X. Clinically relevant concentrations of lidocaine inhibit tumor angiogenesis through suppressing VEGF/VEGFR2 signaling. *Cancer Chemother Pharmacol*. (2019) 83:1007–15. doi: 10.1007/s00280-019-03815-4
55. Suzuku S, Mori A, Fukui A, Ema Y, Nishiwaki K. Lidocaine inhibits vascular endothelial growth factor-A-induced angiogenesis. *J Anesth*. (2020) 34:857–64. doi: 10.1007/s00540-020-02830-7

Conflict of Interest: The authors declare that the research was conducted in the absence of any commercial or financial relationships that could be construed as a potential conflict of interest.

Publisher's Note: All claims expressed in this article are solely those of the authors and do not necessarily represent those of their affiliated organizations, or those of the publisher, the editors and the reviewers. Any product that may be evaluated in this article, or claim that may be made by its manufacturer, is not guaranteed or endorsed by the publisher.

frontiers in Medicine

ORIGINAL RESEARCH
published: 06 January 2022
doi: 10.3389/fmed.2021.730215

Clinical Characteristics and Efficacy of Adalimumab and Low-Dose Methotrexate Combination Therapy in Patients With Vogt–Koyanagi–Harada Disease

Tomona Hiyama, Yosuke Harada and Yoshiaki Kiuchi*

Department of Ophthalmology and Visual Science, Graduate School of Biomedical Sciences, Hiroshima University, Hiroshima, Japan

OPEN ACCESS

Edited by:
Ryoji Yanai,
Yamaguchi University, Japan

Reviewed by:
Ali Osman Saatci,
Dokuz Eylül University, Turkey
Lilian Julian,
Cleveland Clinic Abu Dhabi,
United Arab Emirates

****Correspondence:***
Yosuke Harada
yharada@hiroshima-u.ac.jp

Specialty section:
This article was submitted to Ophthalmology, a section of the journal Frontiers in Medicine

Received: *24 June 2021*
Accepted: *07 December 2021*
Published: *06 January 2022*

Citation:
Hiyama T, Harada Y and Kiuchi Y (2022) Clinical Characteristics and Efficacy of Adalimumab and Low-Dose Methotrexate Combination Therapy in Patients With Vogt–Koyanagi–Harada Disease. Front. Med. 8:730215. doi: 10.3389/fmed.2021.730215

This retrospective study investigated the clinical characteristics and efficacy of adalimumab and low-dose methotrexate combination therapy in patients with Vogt–Koyanagi–Harada disease who were treated at Hiroshima University from February 2012 to May 2021. The patients' demographics, clinical features at administration of immunosuppressive therapy, steroid-sparing immunosuppressive therapy, side effects, and relapses were recorded. The efficacies of steroid-sparing immunosuppressive therapy (methotrexate, cyclosporine A, adalimumab, and adalimumab and methotrexate combination therapy) were analyzed. Among 62 patients, the median age at diagnosis was 47 years and the median duration of uveitis was 51 months. Systemic corticosteroid therapy was administered to 93.5% of patients ($n = 58$). Thirty-four patients (54.8%) were treated with steroid-sparing immunosuppressive therapy. Methotrexate and cyclosporine A were administered to 12 and 22 patients, respectively; relapse occurred in 50.0% and 22.7% of the patients, respectively. Discontinuation of cyclosporine A was required in 63.6% of patients because of side effects. Adalimumab was administered to 14 patients. Recurrence occurred in 11 patients, requiring methotrexate concomitantly. The mean dose of methotrexate at inflammatory quiescence after side effect-related dose decrease was 8.0 mg/week (0.13 mg/kg). The median duration of combination therapy without recurrence was 20 months. There were no serious adverse events during adalimumab therapy. A high relapse rate was observed in patients receiving methotrexate; a high rate of side effects requiring discontinuation was observed in patients receiving Cyclosporine A. Patients with late-stage Vogt–Koyanagi–Harada disease may achieve better control with adalimumab and methotrexate combination therapy.

Keywords: Vogt-Koyanagi-Harada disease, uveitis, adalimumab, methotrexate, cyclosporine A, tumor necrosis factor-alpha

INTRODUCTION

Vogt–Koyanagi–Harada disease (VKH) is an autoimmune bilateral panuveitis often associated with neurological and cutaneous involvement (1). In the early-stage of disease, granulomatous choroiditis occurs with exudative retinal detachment and optic disc swelling, causing a bilateral reduction of visual acuity (2, 3). Late-stage disease occurs in patients with insufficient treatment; this phase is characterized by depigmentation signs such as "sunset glow fundus" and recurrent uveitis, with an increased risk of ocular complications (1–4). Early and aggressive systemic corticosteroid therapy is the basic treatment; however, systemic corticosteroid therapy alone cannot prevent the onset of late-stage disease (1, 5). The early administration of additional steroid-sparing immunosuppressive therapy within 2–3 weeks of onset was reported to prevent the onset of late-stage VKH (6). Recently, mycophenolate mofetil and mycophenolic acid were found to prevent the onset of chronic VKH (7). Unfortunately, the choice of immunosuppressive therapy depends on drug availability and local regulations—in Japan, only cyclosporine A (CsA) and adalimumab (ADA) are approved for the treatment of non-infectious uveitis. VKH is the second most diagnosed intraocular inflammatory disease after sarcoidosis in Japan; many affected patients are treated solely with systemic corticosteroids at general ophthalmology hospitals. Although vigorous early immunosuppressive therapy is recommended to prevent the onset of late-stage VKH, it is not always possible in clinical practice because of treatment availability and cost. Furthermore, it is challenging to control ocular inflammation in patients with late-stage VKH (8). In this study, we analyzed the clinical characteristics and treatment efficacies of immunosuppressive therapies in patients with VKH and focused on the treatment of patients with late-stage VKH.

MATERIALS AND METHODS

This retrospective study reviewed data from patients with VKH who were treated at Hiroshima University Hospital (Hiroshima, Japan) from February 2012 to May 2021. The study was performed with approval from the University of Hiroshima Institutional Review Board. Written informed consent was obtained from all patients. Permission was granted by the Evaluation Committee on Unapproved or Off-labeled Drugs with High Medical Needs at Hiroshima University for methotrexate (MTX) for patients with non-infectious uveitis.

VKH was diagnosed in accordance with international diagnostic criteria (9). Patients were initially treated with oral corticosteroids or intravenous pulse corticosteroid therapy (1,000 mg methylprednisolone per day for 3 consecutive days) followed by the tapering of oral corticosteroids. Topical treatments were used if necessary. The study included all patients who were followed up for more than 6 months. Patients were excluded if they had an unknown date of onset or were lost to follow-up during treatment. Early-stage and late-stage VKH were diagnosed according to the classification criteria for VKH by the standardization of uveitis nomenclature working group (3).

The data collected in this study included patient age at diagnosis, sex, duration of uveitis, initial treatment, use of steroid-sparing immunosuppressive therapy, time until the first immunosuppressive therapy, dose of oral corticosteroids at baseline, ocular findings at baseline (anterior chamber cells $\geq$1+, posterior synechiae, exudative retinal detachment, choroidal thickening/folding, sunset glow fundus, chorioretinal atrophy, choroidal neovascularization), neurological (headache/tinnitus/dysacusis/meningismus/cerebrospinal fluid pleocytosis)/cutaneous (vitiligo, poliosis, alopecia) features at baseline, best-corrected visual acuity at baseline, relapse during the immunosuppressive therapy, and side effects of immunosuppressive therapy. Inflammatory relapse was defined as the presence of the following: anterior chamber cells $\geq$1+ (according to Standardization of Uveitis Nomenclature Working Group criteria), increase in subfoveal choroidal thickness or choroidal folding based on enhanced depth imaging optical coherence tomography, and indocyanine green angiography signs (e.g., choroidal vasculitis and hypofluorescent dark dots representing choroidal granulomas) (10). For patients treated with ADA and MTX combination therapy, data were obtained including previous immunosuppressive therapy, duration from onset of VKH to ADA administration, duration from ADA administration to MTX administration, dose of concomitant MTX, relapse after the combination therapy, and relapse-free period under the combination therapy.

Prior to the administration of immunosuppressive therapies (e.g., MTX, CsA, and ADA), an extensive work-up was performed including complete blood count, hepatic and renal function tests, exclusion of tuberculosis and syphilis, hepatitis B and C serology, serum angiotensin converting enzyme, and chest radiography. Laboratory tests and chest radiography were performed regularly during immunosuppressive therapy. CsA blood concentration was monitored regularly. Electrocardiograms were routinely performed before starting ADA for screening heart disease (11, 12). An initial dose of 80 mg ADA was administered subcutaneously, followed by 40 mg ADA subcutaneously at 2-week intervals, beginning 1 week after the initial dose. All patients were examined by several ophthalmologists at each visit at intervals of $\leq$2 months. ADA was initiated when conventional therapy (i.e., oral corticosteroids $>$5 mg, with or without oral immunosuppressants) failed to control ocular inflammation or when patients could not tolerate corticosteroids (e.g., in patients with diabetes mellitus or steroid-induced glaucoma) or other oral immunosuppressants (MTX or CsA). MTX or CsA were discontinued at administration of ADA. On the basis of factors such as age, severity of ocular inflammation, and range of ocular complications, some patients received ADA as a first-line steroid-sparing immunosuppressive therapy. Concomitant MTX was administered when inflammatory relapse occurred in patients who were treated with ADA.

Statistical analysis was performed using Microsoft Excel (Microsoft Corporation, Redmond, WA, USA) and JMP Pro, version 15 (SAS, Cary, NC, USA). Quantitative variables were summarized using counts (percentages), as well as means and medians (ranges). Qualitative variables were analyzed using

TABLE 1 | Demographics of patients with Vogt–Koyanagi–Harada disease.

Characteristics	*n*	%
Patients	62	
Male	25	36.8
Female	37	54.4
Age at diagnosis, median in years (range)	47 (18–77)	
Duration of uveitis, median in months (range)	51 (15–148)	
Initial treatment of Vogt–Koyanagi–Harada disease onset		
Pulse corticosteroid therapy	58	93.5
Oral corticosteroid thearpy	4	6.5

Fisher's exact test. Differences with P-values < 0.05 were considered statistically significant.

RESULTS

Overall, 62 patients (25 men, 37 women) with VKH were included in the study. The patient demographics are summarized in **Table 1**. The median age at diagnosis was 47 years (range, 18–77 years). The duration of uveitis was 51 months (range, 15–148 months). Systemic corticosteroid therapy was administered in 93.5% of the patients ($n = 58$). Thirty-four patients (54.8 %) were treated with steroid-sparing immunosuppressive therapy, 10 were administered treatment at the early-stage of the disease, and 24 were administered treatment at the late-stage of disease.

The baseline clinical characteristics of patients with early-stage ($n = 10$) and late-stage ($n = 24$) VKH at immunosuppressive therapy administration are summarized in **Table 2**. The median dose of oral corticosteroids at baseline was 37.5 mg and 11.3 mg in early- and late-stage VKH, respectively. The most common first choice immunosuppressive therapy was CsA in both groups. Anterior chamber cells >1+ were present in more than 50% of patients in both groups. Exudative retinal detachment was present in 80.0% of the patients with early-stage VKH. At baseline, choroidal thickening/folding were observed in ∼80% of the patients in the early- and late-stage VKH groups. All patients with late-stage VKH presented with sunset glow fundus. Best-corrected visual acuity was better than 20/50 in more than 80% of the eyes in both groups.

Table 3 shows the details of immunosuppressive therapy administered to patients with VKH disease. MTX was administered to 12 patients; 11 of whom were administered MTX as a second choice. Relapse during MTX treatment occurred in 50% ($n = 6$) of the patients. MTX was discontinued in 25.0% ($n = 3$) of the patients because of side effects (alopecia, myelosuppression, nephrotoxicity). Of 22 patients who received CsA, 21 were administered it as a first choice. Relapse occurred in 22.7% ($n = 5$) of the patients. The discontinuation of CsA because of side effects occurred in 63.6% ($n = 14$) of the patients (nephrotoxicity, myelosuppression, hepatotoxicity, hematuria, edema, numbness, fever); this rate of side effects was higher than that among patients who received MTX (Fisher's exact test, $P = 0.0354$). The median dose of CsA at which side effects occurred was 137.5 mg/day (2.3 mg/kg). ADA was administered to 14 patients; as the first choice in 8 patients, as the second choice in 4 patients, and as the third choice in 2 patients. Of 14 patients, 13 were administered ADA at late-stage disease. Relapse during ADA occurred in 11 patients, who then required concomitant MTX. No side effects were observed during ADA therapy.

TABLE 2 | Baseline clinical characteristics of patients with Early-Stage and Late-Stage Vogt-Koyanagi-Harada disease at time of administration of immunosuppressive therapy.

Clinical characteristics	Early-stage $n = 10$	Late-stage $n = 24$
Duration from onset to first immunosuppressive therapy, Median in months (range)	0.5 (0–2)	8 (0–105)
Dose of oral corticosteroids at baseline, Median in milligram (range)	37.5 (20–50)	11.3 (0–60)
First choice immunosuppressive therapy		
Methotrexate	1	4
Cyclosporine A	8	13
Adalimumab	1	7
Ocular findings at baseline		
Anterior chamber cell (%)	7 (70.0)	14 (58.3)
Posterior synechiae (%)	1 (10.0)	2 (8.3)
Exudative retinal detachment (%)	8 (80.0)	4 (16.7)
Choroidal thickening/folding (%)	8 (80.0)	19 (79.2)
Sunset glow fundus (%)	0 (0)	24 (100)
Chorioretinal atrophy (%)	0 (0)	6 (25.0)
Choroidal neovascularization (%)	0 (0)	2 (8.3)
Neurological[a]/Cutaneous[b] features at baseline (%)	2 (20.0)	7 (29.2)
Best corrected visual acuity at baseline	20 eyes	48 eyes
Better than 20/50 (%)	16 (80.0)	44 (91.7)
20/50 to 20/200 (%)	3 (15.0)	3 (6.3)
Worse than 20/200 (%)	1 (5.0)	1 (2.1)

[a] *Headache/tinnitus/dysacusis/meningismus/cerebrospinal fluid pleocytosis.*
[b] *Vitiligo/poliosis/alopecia.*

The 11 patients treated with ADA and MTX combination therapy following relapse during ADA monotherapy are summarized in **Table 4**. All 11 patients were administered ADA at late-stage disease. The median duration from onset to ADA administration was 5 months (range, 0–105 months). Nine out of 11 patients relapsed within the first 6 months after starting ADA, and received concomitant MTX. All 11 patients had received MTX by 12 months (median, 2 months; range, 0–12 months). The mean maximum dose of concomitant MTX was 11.5 mg/week (0.18 mg/kg). A dose adjustment of MTX was required in five patients (45.5%) because of side effects (hepatotoxicity and fatigue). The mean dose of MTX at inflammatory quiescence after dose adjustment was 8.0 mg/week (0.13 mg/kg). Inflammatory relapse occurred in three patients (27.3%) after 4, 6, and 12 months of combination therapy (patients 6, 10, and 11): subsequently, the MTX dose was increased in these three patients. The median duration of ADA and MTX combination therapy without relapse was 20 months (range, 4–31).

TABLE 3 | Immunosuppressive therapy in patients with Vogt–Koyanagi–Harada disease.

	n	%
Methotrexate (*n* = 12)		
First choice	1	8.3
Second choice	11	91.7
Early-stage	5	41.7
Late-stage	7	58.3
Relapse during methotrexate therapy	6	50.0
Discontinuation due to side effects	3	25.0
Cyclosporine A (*n* = 22)		
First choice	21	95.5
Second choice	1	4.5
Early-stage	8	36.4
Late-stage	14	63.6
Relapse during cyclosporine A therapy	5	22.7
Discontinuation due to side effects	14	63.6
Adalimumab (*n* = 14)		
First choice	8	57.1
Second choice	4	28.6
Third choice	2	14.3
Early-stage	1	7.1
Late-stage	13	92.9
Relapse during Adalimumab therapy	11	78.6
Discontinuation due to side effects	0	0.0
Monotherapy	3	21.4
Adalimumab and Methotrexate combination therapy	11	78.6

There were no serious adverse events associated with ADA treatment in this study. Side effects occurred in 11 out of 21 patients (52.4%) who received MTX (including MTX monotherapy and combination therapy). Side effects were managed by dose adjustment in 8 out of 21 patients (38.1%), and, 14.3% ($n = 3$) discontinued MTX. In contrast, side effects of CsA that required discontinuation were observed in 63.6% of the patients; nephrotoxicity was the most common side effect.

DISCUSSION

Recently, combinations of steroidal and steroid-sparing immunosuppressive therapies for VKH were proposed to prevent chronic recurrent disease (6). In the present study, we focused on the clinical characteristics and treatment efficacies of MTX and CsA in patients with VKH, as well as the use of ADA and low-dose MTX combination therapy for the treatment of late-stage VKH in Japanese patients.

In this study, 54.8% of all patients with VKH were treated with steroid-sparing immunosuppressive therapies, including MTX, CsA, and ADA. In many instances, CsA was chosen first, as this is approved for the treatment of non-infectious uveitis. Patients with early-stage VKH received immunosuppressive therapy approximately within 1 month of diagnosis, during the tapering of oral corticosteroids. Anterior chamber cells and exudative retinal detachment were more prominent in patients with early-stage VKH, whereas choroidal thickening/folding was present in patients with early- and late-stage VKH at baseline when they received immunosuppressive therapy. Sunset glow fundus, a characteristic depigmentation sign of VKH, was present in all patients with late-stage VKH. Neurological and cutaneous features were slightly less prominent in patients who received immunosuppressive therapy at the early-stage of disease, which may have been improved because of the aggressive corticosteroid therapy. Inflammatory relapse occurred in 50.0% and 22.7% of patients treated with MTX or CsA, respectively. Notably, the rate of side effects requiring discontinuation of medication was higher in patients treated with CsA than in patients treated with MTX. In Japan, the approved maximum dose of MTX is 16 mg/week because of the increased prevalence of adverse events in Japanese patients (13). The higher recurrence rate in the MTX group may be associated with the insufficient MTX dose, which had been adjusted because of side effects. Furthermore, regardless of the concurrent initiation of MTX with systemic corticosteroid treatment, its effects were not apparent until a few months after administration, unlike immediate-acting agents such as CsA and ADA (14). Thus, the use of delayed-acting agents such as MTX alone may be inappropriate to prevent ongoing subclinical choroidal inflammation in patients with early-stage VKH.

As we previously suggested, VKH may require stronger anti-inflammatory treatment, compared with other uveitis etiologies (15). Adalimumab is more effective when used in combination with disease-modifying antirheumatic drugs (e.g., MTX) than when used alone (16–18). In the current study, 13 out of 14 patients who were treated with ADA received the treatment at late-stage. Of these 13 patients, relapse occurred in 11, which required ADA and MTX combination therapy. After the onset of late-stage VKH, the immunosuppressive effect of ADA alone might unfortunately be insufficient to control ocular flares and to prevent further functional and morphological dysfunctions. In this study, ADA and MTX combination therapy was successful in 72.7% of patients with late-stage VKH; the median recurrence-free period was 20 months. Previously, an adequate concentration of MTX to suppress inflammation with limited hepatotoxicity in Japanese patients with RA was achieved using a dose of 10–12 mg/week (19). Previously we reported that the median maximum dose of MTX that achieved inflammatory quiescence in patients with sclerouveitis was 16 mg/week, and the inflammatory control of non-infectious uveitis was achieved with the median dose of 12 mg/week (20, 21). In this study, the median concomitant MTX dose required at inflammatory quiescence without any side effects was 8.0 mg/week (0.13 mg/kg), which is considered low-dose therapy. This suggests that combination therapy involving ADA and MTX (at a dose lower than generally considered adequate for monotherapy) may be sufficient to achieve inflammatory control in patients in late-stage VKH. In our study, 81.8% of patients who were treated with the combination therapy required MTX within 6 months after ADA administration. Because of the slow onset of action of MTX, we presume that it is preferable to initiate MTX concomitantly with ADA in patients with late-stage VKH. To the best of our knowledge, this study includes the largest series of patients with VKH who were treated with ADA and MTX combination therapy.

TABLE 4 | Patients treated with adalimumab and methotrexate combination therapy.

Patient	Sex	Age at diagnosis (years)	Duration of uveitis (months)	Previous immuno suppressive therapy	Duration from onset to ADA administration (months)	Duration from ADA to MTX administration (months)	MTX dose at inflammatory quiescence (mg)	Side effects of MTX that required dose adjustment	Relapse after combination therapy	Combination therapy without relapse (months)
1	F	59	19	+	5	2	10		−	12
2	F	56	56	−	14	12	4	Hepatotoxicity	−	30
3	F	45	110	+	85	0	8	Fatigue	−	25
4	M	38	24	−	0	3	8		−	20
5	F	29	141	+	105	7	8		−	28
6	M	50	57	+	23	2	14		+	12
7	M	37	36	−	2	2	4	Hepatotoxicity	−	31
8	M	42	37	−	3	2	4	Hepatotoxicity	−	31
9	M	27	20	+	8	0	4	Hepatotoxicity	−	16
10	M	22	12	−	2	0	16		+	6
11	M	59	11	−	0	0	16		+	4

M, male; F, female; ADA, adalimumab; MTX, methotrexate.

According to a previous study conducted in Japan, ∼61% of patients receiving systemic corticosteroid monotherapy eventually developed sunset glow fundus (5, 14, 22–25). Thus, if the goal of successful treatment is preventing the onset of late-stage disease, there is a risk of over-treatment in one-third of patients if steroid-sparing immunosuppressive therapy is administered at the initiation of systemic corticosteroid therapy. However, when the consequences of late-stage disease (e.g., cataract, glaucoma, contrast sensitivity, color vision deficits, and extraocular complications) are weighed against the potential side effects of steroid-sparing immunosuppressive therapy, early ADA or ADA and MTX combination may be appropriate, especially in younger patients (14).

There were several limitations in this study. First, the number of patients was limited; thus, a multicenter study in Japan is needed to determine the efficacy and the rate of side effects associated with MTX and CsA, as well as ADA and MTX combination therapy, among patients with late-stage VKH in a broader population. A direct comparison of ADA monotherapy, and ADA and MTX combination therapy should also be conducted. Second, a longer follow-up period is needed because of the chronic nature of VKH. Further assessment of ADA and MTX combination therapy in patients with early- and late-stage VKH, as well as the possibility of the suspension of therapy should be conducted. Third, the duration from VKH onset to first steroid-sparing immunosuppressive therapy varied among patients in this study. A better analysis of the treatment results of MTX and CsA might have been possible if all patients had received treatment with consistent timing. Fourth, the measurement of ADA trough levels and anti-ADA antibody levels would be useful to assess their relationship with treatment suspension. The presence of antinuclear antibodies may be a predictable consequence of sufficient anti-tumor necrosis factor-alpha blockade, which may aid the treatment suspension (26, 27). Last, this was a retrospective study and thus included various patients with different treatment backgrounds. A prospective study is needed to investigate the use of ADA and MTX therapy in patients with VKH.

In conclusion, this study demonstrated the clinical characteristics of VKH in Japanese patients; a high relapse rate was observed in patients treated with MTX and a high rate of side effects requiring discontinuation was observed in patients treated with CsA. This study showed that patients with late-stage VKH may achieve better disease control with ADA and low-dose MTX combination therapy.

DATA AVAILABILITY STATEMENT

The data that support the findings of this study are available on request from the corresponding author, Yoshiaki Kiuchi. The data are not publicly available due to their containing information that could compromise the privacy of research participants.

ETHICS STATEMENT

The studies involving human participants were reviewed and approved by University of Hiroshima Institutional Review Board. The patients/participants provided their written informed consent to participate in this study. Written informed consent was obtained from the individual(s) for the publication of any potentially identifiable data included in this article.

AUTHOR CONTRIBUTIONS

TH and YH contributed to the conception, design of the study, and organized the database. TH performed the statistical analyses and wrote the first draft of the manuscript. TH, YH, and YK contributed to the manuscript revision and reading, and approved the submitted version. All authors contributed to the article and approved the submitted version.

ACKNOWLEDGMENTS

We thank Ryan Chastain-Gross, Ph.D., and J. Ludovic Croxford, Ph.D., from Edanz (https://jp.edanz.com/ac) for editing a draft of this manuscript.

REFERENCES

1. Moorthy RS, Inomata H, Rao NA. Vogt-Koyanagi-Harada syndrome. *Surv Ophthalmol.* (1995) 39:265–92. doi: 10.1016/S0039-6257(05)80105-5
2. Du L, Kijlstra A, Yang P. Vogt-Koyanagi-Harada disease: novel insights into pathophysiology, diagnosis and treatment. *Prog Retinal Eye Res.* (2016) 52:84–111. doi: 10.1016/j.preteyeres.2016.02.002
3. Jabs DA, Denniston AK, Dick A-DD, Dunn JP, Kramer M, Mccluskey P, et al. Classification criteria for vogt-koyanagi-harada disease. *Am J Ophthalmol.* (2021) 228:205–11. doi: 10.1016/j.ajo.2021.03.036
4. Yang P, Ren Y, Li B, Fang W, Meng Q, Kijlstra A. Clinical characteristics of vogt-koyanagi-harada syndrome in chinese patients. *Ophthalmology.* (2007) 114:606–14.e3. doi: 10.1016/j.ophtha.2006.07.040
5. Nakayama M, Keino H, Watanabe T, Okada AA. Clinical science clinical features and visual outcomes of 111 patients with new-onset acute Vogt-Koyanagi-Harada disease treated with pulse intravenous corticosteroids. *Br J Ophthalmol.* (2019) 103:274–8. doi: 10.1136/bjophthalmol-2017-311691
6. Herbort CPJ, Abu El Asrar AM, Takeuchi M, Pavésio CE, Couto C, Hedayatfar A, et al. Catching the therapeutic window of opportunity in early initial-onset Vogt-Koyanagi-Harada uveitis can cure the disease. *Int Ophthalmol.* (2019) 39:1419–25. doi: 10.1007/s10792-018-0949-4
7. Abu El-Asrar AM, Dosari M, Hemachandran S, Gikandi PW, Al-Muammar A. Mycophenolate mofetil combined with systemic corticosteroids prevents progression to chronic recurrent inflammation and development of "sunset glow fundus" in initial-onset acute uveitis associated with Vogt-Koyanagi-Harada disease. *Acta Ophthalmol.* (2017) 95:85–90. doi: 10.1111/aos.13189
8. Sonoda K-H, Hasegawa E, Namba K, Okada AA, Ohguro N, Goto H. Epidemiology of uveitis in Japan: a 2016 retrospective nationwide survey. *Jpn J Ophthalmol.* (2021) 65:184–90. doi: 10.1007/s10384-020-00809-1
9. Read RW, Holland GN, Rao NA, Tabbara KF, Ohno S, Arellanes-Garcia L, et al. Revised diagnostic criteria for Vogt-Koyanagi-Harada disease: report of an international committee on nomenclature. *Am J Ophthalmol.* (2001) 131:647–52. doi: 10.1016/S0002-9394(01)00925-4
10. Jabs DA, Nussenblatt RB, Rosenbaum JT, Standardization of Uveitis Nomenclature (SUN) Working Group. Standardization of uveitis nomenclature for reporting clinical data. Results of the first international workshop. *Am J Ophthalmol.* (2005) 140:509–16. doi: 10.1016/j.ajo.2005.03.057
11. Suhler EB, Jaffe GJ, Fortin E, Lim LL, Merrill PT, Dick AD, et al. Long-term safety and efficacy of adalimumab in patients with noninfectious intermediate uveitis, posterior uveitis, or panuveitis. *Ophthalmology.* (2021) 128:899–909. doi: 10.1016/j.ophtha.2020.10.036
12. Burmester GR, Panaccione R, Gordon KB, McIlraith MJ, Lacerda APM. Adalimumab: long-term safety in 23 458 patients from global clinical trials in rheumatoid arthritis, juvenile idiopathic arthritis, ankylosing spondylitis, psoriatic arthritis, psoriasis and Crohn's disease. *Ann Rheum Dis.* (2013) 72:517–24. doi: 10.1136/annrheumdis-2011-201244
13. Kameda H, Fujii T, Nakajima A, Koike R, Sagawa A, Kanbe K, et al. Japan college of rheumatology guideline for the use of methotrexate in patients with rheumatoid arthritis. *Mod Rheumatol.* (2019) 29:31–40. doi: 10.1080/14397595.2018.1472358
14. Herbort CP, Tugal-Tutkun I, Khairallah M, Abu el Asrar AM, Pavésio CE, Soheilian M. Vogt-Koyanagi-Harada disease: recurrence rates after initial-onset disease differ according to treatment modality and geographic area. *Int Ophthalmol.* (2021) 40:2423–23. doi: 10.1007/s10792-020-01417-1
15. Hiyama T, Harada Y, Kiuchi Y. Efficacy and safety of adalimumab therapy for the treatment of non-infectious uveitis: efficacy comparison among uveitis aetiologies. *Ocul Immunol Inflamm.* (2021) doi: 10.1080/09273948.2020.1857791. [Epub ahead of print].
16. Burmester GR, Kivitz AJ, Kupper H, Arulmani U, Florentinus S, Goss SL, et al. Efficacy and safety of ascending methotrexate dose in combination with adalimumab: the randomised CONCERTO trial. *Ann Rheum Dis.* (2015) 74:1037–44. doi: 10.1136/annrheumdis-2013-204769
17. Krieckaert CL, Nurmohamed MT, Wolbink GJ. Methotrexate reduces immunogenicity in adalimumab treated rheumatoid arthritis patients in a dose dependent manner. *Ann Rheum Dis.* (2012) 71:1914 LP—15. doi: 10.1136/annrheumdis-2012-201544
18. Cordero-Coma M, Calleja-Antolín S, Garzo-García I, Nuñez-Garnés AM, Álvarez-Castro C, Franco-Benito M, et al. Adalimumab for treatment of noninfectious uveitis: immunogenicity and clinical relevance of measuring serum drug levels and antidrug antibodies. *Ophthalmology.* (2016) 123:2618–25. doi: 10.1016/j.ophtha.2016.08.025
19. Takahashi C, Kaneko Y, Okano Y, Taguchi H, Oshima H, Izumi K, et al. Association of erythrocyte methotrexate-polyglutamate levels with the efficacy and hepatotoxicity of methotrexate in patients with rheumatoid arthritis: a 76-week prospective study. *RMD Open.* (2017) 3:e000363. doi: 10.1136/rmdopen-2016-000363
20. Hiyama T, Harada Y, Kiuchi Y. Clinical characteristics and efficacy of methotrexate in Japanese patients with noninfectious scleritis. *Jpn J Ophthalmol.* (2021) 65:97–106. doi: 10.1007/s10384-020-00778-5
21. Harada Y, Hiyama T, Kiuchi Y. Methotrexate effectively controls ocular inflammation in japanese patients with non-infectious uveitis. *Front Med.* (2021) 8:2194. doi: 10.3389/fmed.2021.732427
22. Nishioka Y, Sakamoto M, Kinukawa N, Sanui H, Inomata H, Nose Y. Recurrence risk factors in patients with the Vogt-Koyanagi-Harada syndrome in Japan. *Ocul Immunol Inflamm.* (1995) 3:73–80. doi: 10.3109/09273949509085034
23. Keino H, Goto H, Usui M. Short communication sunset glow fundus in Vogt-Koyanagi-Harada disease with or without chronic ocular inflammation. *Arch Clin Exp Ophthalmol.* (2002) 240:878–82. doi: 10.1007/s00417-002-0538-z
24. Iwahashi C, Kensuke O, Noriyasu H, Kei N, Ohguro N, Nishida K. Incidence and clinical features of recurrent Vogt-Koyanagi-Harada disease in Japanese individuals. *Jpn J Ophthalmol.* (2015) 59:157–63. doi: 10.1007/s10384-015-0377-1
25. Keino H, Goto H, Mori H, Iwasaki T, Usui M. Association between severity of inflammation in CNS and development of sunset glow fundus in Vogt-Koyanagi-Harada disease. *Am J Ophthalmol.* (2006) 141:1140–2. doi: 10.1016/j.ajo.2006.01.017
26. Atzeni F, Turiel M, Capsoni F, Doria A, Meroni P, Sarzi-Puttinia P. Autoimmunity and Anti-TNF-a agents. *Ann N Y Acad Sci.* (2005) 1051:559–69. doi: 10.1196/annals.1361.100
27. Lügering A, Schmidt M, Lügering N, Pauels HG, Domschke W, Kucharzik T. Infliximab induces apoptosis in monocytes from patients with chronic active Crohn's disease by using a caspase-dependent pathway. *Gastroenterology.* (2001) 121:1145–57. doi: 10.1053/gast.2001.28702

Conflict of Interest: The authors declare that the research was conducted in the absence of any commercial or financial relationships that could be construed as a potential conflict of interest.

frontiers in Medicine

CASE REPORT
published: 14 January 2022
doi: 10.3389/fmed.2021.764067

Effectiveness of Baricitinib in Refractory Seronegative Rheumatoid Arthritis and Uveitis: A Case Report

Yutaka Kaneko[1], *Takanori Murakami*[2], *Koichi Nishitsuka*[1], *Yuya Takakubo*[3], *Michiaki Takagi*[3] *and Hidetoshi Yamashita*[1,4]*

[1] Department of Ophthalmology and Visual Sciences, Yamagata University Faculty of Medicine, Yamagata, Japan, [2] Department of Ophthalmology, Yamagata Prefectural Central Hospital, Yamagata, Japan, [3] Department of Orthopaedic Surgery, Yamagata University Faculty of Medicine, Yamagata, Japan, [4] Yamagata City Healthcare Center, Yamagata, Japan

Baricitinib is a Janus kinase (JAK) inhibitor used to treat refractory rheumatoid arthritis and blocks the subtypes JAK1 and JAK2. A 35-year-old man with seronegative rheumatoid arthritis complicated by bilateral severe non-granulomatous panuveitis was resistant to steroid treatment, multiple conventional disease-modifying antirheumatic drugs (methotrexate and salazosulfapyridine), and TNF-α inhibitors (adalimumab and infliximab). Therefore, the TNF-α inhibitors were switched to baricitinib to decrease the activity of systemic arthritis. Along with the amelioration of inflammatory activity in seronegative rheumatoid arthritis, the inflammatory activity of uveitis was decreased. Vitreous opacity, serous retinal detachment, and anterior chamber cells showed improvement. Baricitinib was effective not only in refractory systemic arthritis but also in uveitis, which may provide a new treatment option for patients with refractory uveitis.

Keywords: JAK inhibitor, baricitinib, uveitis, rheumatoid arthritis, new therapeutic target

OPEN ACCESS

Edited by:
Ryoji Yanai,
Yamaguchi University, Japan

Reviewed by:
Elena Generali,
Humanitas University, Italy
SR Rathinam,
Aravind Eye Hospitals & Postgraduate Institute of Ophthalmology, India
Maryam Hosseini,
Mashhad University of Medical Sciences, Iran

***Correspondence:**
Hidetoshi Yamashita
hidetosi.yamashita@gmail.com

Specialty section:
This article was submitted to Ophthalmology, a section of the journal Frontiers in Medicine

Received: *24 August 2021*
Accepted: *21 December 2021*
Published: *14 January 2022*

Citation:
Kaneko Y, Murakami T, Nishitsuka K, Takakubo Y, Takagi M and Yamashita H (2022) Effectiveness of Baricitinib in Refractory Seronegative Rheumatoid Arthritis and Uveitis: A Case Report. Front. Med. 8:764067. doi: 10.3389/fmed.2021.764067

INTRODUCTION

Rheumatoid arthritis (RA) is a systemic inflammatory disease associated with several extra-articular organ manifestations involving the skin, heart, lungs, and eyes. The pharmacological treatment of RA involves anti-inflammatory analgesics, steroids, conventional synthetic disease-modifying anti-rheumatic drugs (csDMARDs) such as methotrexate, and biological agents, including TNF-α inhibitors (biological DMARDs bDMARDs). Early interventions using these agents have been reported to enable clinical, structural, and functional remission. However, treatment resistance has also been noted with the use of these medications, along with long-term systemic complications caused by administering high doses of steroids and immunosuppressive agents (1). In addition, ocular manifestations of RA, such as dry eye, corneal ulcer, episcleritis, scleritis, and retinal vasculitis, often require the use of topical and systemic steroids as well as immunosuppressive agents (2–4). In recent years, a new class of targeted synthetic DMARDs (tsDMARDs), Janus kinase (JAK) inhibitors, has shown good therapeutic results in such cases (1). Therefore, the aim of this study was to present our experience with treating a patient affected by RA and uveitis using a JAK inhibitor.

CASE DESCRIPTION

A 35-year-old man with a medical history of postoperative maxillary osteomyelitis, postoperative vocal cord tumor, right scaphoid fracture, and mediastinal tumor was referred to our hospital. He presented with lower back pain and joint pain in both hands approximately a year ago, as well as the blurred vision of his right eye that he noticed 2 months prior. The postoperative maxillary osteomyelitis was observed 10 years ago and was no longer observed at the initial visit. Vocal cord tumors and mediastinal tumors were biopsied by otolaryngology and thoracic surgery in our hospital, and the pathological result was an inflammatory pseudotumor. At the first visit, his best-corrected visual acuity (BCVA) was 20/16 in both eyes, and the intraocular pressure was 14 mmHg and 10 mmHg in the right and left eyes, respectively. A slit-lamp examination demonstrated conjunctival hyperemia and anterior chamber cells in both eyes (**Figures 1A,B**). Fundus examination revealed mild vitreous opacity in the right eye (**Figure 1C**), but no vitreous opacity in the left eye. Optical coherence tomography (OCT) showed no macular edema in either eye. Furthermore, fluorescein angiography revealed retinal vasculitis in the right eye (**Figure 1D**).

He was referred to orthopedic surgery in our hospital due to lower back pain and joint pain in both hands. Radiography showed bone erosions in both wrist joints (**Figure 2**). Blood tests showed an increase in the white blood cell count (13,530/μL) and C-reactive protein (CRP) levels of 2.37 mg/dL. The rheumatoid factor (RF) and anti-citrullinated protein antibody (ACPA) levels were within normal limits, and human leukocyte antigen B27 (HLA-B27) test was negative. According to the 2010 ACR/EULAR Rheumatoid Arthritis Classification Criteria (5), a score of 7 out of 10 was obtained; the joint distribution was 5 points because he affected over 10 joints, including the bilateral wrist and shoulder joints, metacarpophalangeal (MCP) of the thumb, proximal interphalangeal (PIP) joints of his bilateral index, long, ring, and little finger. Serology was 0 points, symptom duration was 1 point (>6 weeks) and acute phase reactions were 1 point (abnormal CRP). Computed tomography showed no obvious inflammatory findings in the spine and sacroiliac joints, so sacroiliitis was excluded. His final diagnosis was bilateral panuveitis associated with seronegative RA.

Treatment with betamethasone ophthalmic solution was started at the first visit, but 2 months later, the vitreous opacity of the right eye worsened and the visual acuity of the same eye decreased to the counting finger; therefore, prednisolone (60 mg/day) was started by the ophthalmologist. After 4 months, systemic arthritis worsened. Consequently, methotrexate (12 mg/week) and salazosulfapyridine (1,000 mg/day) were added to the patient regimen by a rheumatologist. Following this, subcutaneous injection of adalimumab (40 mg/2 weeks) was administered 19 months later due to further exacerbation of arthritis; however, no improvement was observed. Subsequently, the subcutaneous injection of adalimumab was changed to an intravenous infusion of infliximab (3–6 mg/kg) 38 months later. Nevertheless, since neither his systemic arthritis nor uveitis improved after 42 months, the orthopedic surgeon changed the patient's regimen from intravenous infliximab to oral baricitinib (8 mg/day). At the start of the oral baricitinib therapy, CRP levels were as high as 11.03 mg/dL, BCVA was 20/20 and 20/16, and intraocular pressure was 12 mmHg and 11 mmHg in the right and left eyes, respectively. A slit-lamp examination

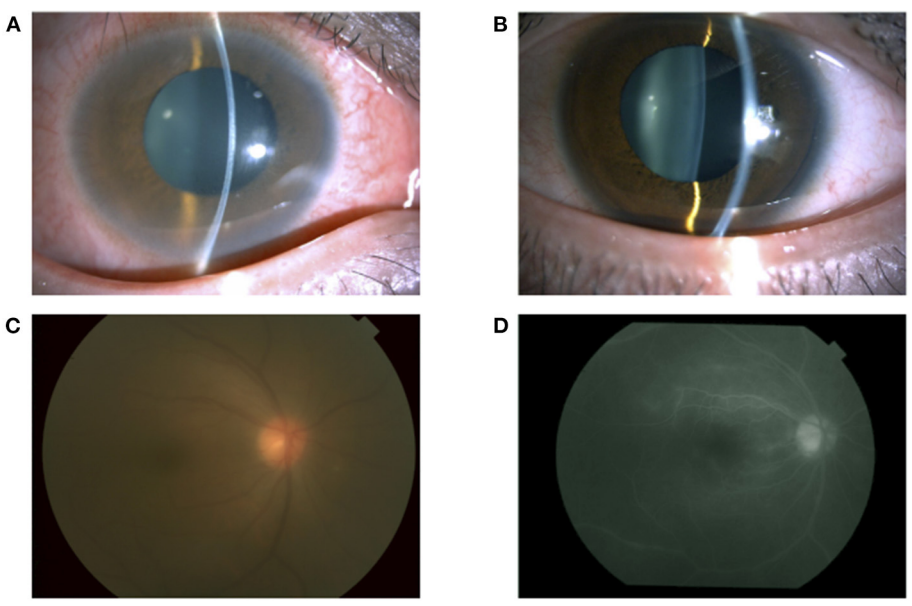

FIGURE 1 | A slit-lamp examination showing conjunctival hyperemia and anterior chamber cells in the right eye **(A)** and left eye **(B)**. A fundus photograph of the right eye showing vitreous opacity **(C)**. Fluorescein angiography of the right eye showing vascular leakage **(D)**.

FIGURE 2 | Radiography showing bone erosions of the wrist joint (red arrow) (image of right hand).

revealed corneal infiltration lesions in both eyes. Furthermore, anterior chamber cells, posterior iris synechia, and anterior subcapsular cataract were observed in the right eye, while no anterior chamber cells were seen in the left eye (**Figures 3A,B**). Fundus examination revealed vitreous opacity in both eyes (**Figures 3C,D**), and OCT revealed serous retinal detachment in the right eye (**Figure 3E**). Three months after the initiation of oral baricitinib, his CRP levels decreased to 0.26 mg/dL, and the corneal infiltrative lesions, as well as the anterior chamber cells, improved (**Figures 4A,B**). Moreover, systemic arthritis and vitreous opacity in both eyes improved (**Figures 4C,D**). OCT revealed that serous retinal detachment in the right eye had disappeared (**Figure 4E**). Two years and seven months after the initiation of baricitinib, his BCVA was 20/20 in both eyes, and no relapse of uveitis was observed. In addition, no serious side effects of oral baricitinib were observed or reported.

DISCUSSION

RA is classified as seropositive or seronegative based on the presence of RF and ACPA. The incidence of seronegative RA is estimated to be between 16 and 26% of RA patients (6, 7). Seronegative RA has been reported to have lower disease activity and better prognosis than seropositive RA (8). However, Barra et al. reported that seronegative RA showed higher inflammatory activity than seropositive RA, and bone erosion is equivalent over a 2-year course in DMARD-naive patients (6). Therefore, seronegative RA does not appear to be a benign subtype of RA and requires the same intensive treatment as seropositive RA (7). Ocular manifestations of RA include keratoconjunctivitis sicca, episcleritis, scleritis, corneal ulcer, and retinal vasculitis. In particular, corneal ulcer and scleritis are known to become intractable and cause serious visual dysfunction, such as corneal and scleral perforation, macular edema, and secondary glaucoma (2).

This case showed hypopyon, panuveitis, serous retinal detachment, and infiltrative lesions in the center of the cornea, which were not typical ocular complications, as previously reported in rheumatoid arthritis. Therefore, Behcet's disease was suspected, and he was referred to the dermatology in our hospital. However, there were no recurrent oral ulcers, recurrent genital ulcers, or skin lesions. Fluorescein angiography did not show "Fern-like" fluorescein leakage, and Behcet's disease was ruled out. Infiltrative lesions in the center of the cornea were observed simultaneously in both eyes, did not show dendritic epithelial ulcer, and improved after the start of oral baricitinib without the use of antiviral drugs. Viral etiology, such as HSV/VZV, was also ruled out. The incidence of ocular manifestations has been shown to not present any statistically significant difference between patients with seronegative and seropositive RA. The longer the duration of the disease, the larger the number of extra-articular manifestations (9); thus, these ocular manifestations require the same intensive treatment as RA.

JAK is a kinase that is constitutively bound to a cytokine receptor. When a cytokine binds to the receptor, phosphorylation of the transcription factor signal transducer and activator of transcription (STAT) is induced along with phosphorylation of JAK. Phosphorylated STATs form dimers and translocate into the nucleus without the intervention of other signaling molecules to regulate transcription, enabling the regulation of nuclear gene expression by extracellular cytokines. JAK is composed of four molecules, namely JAK1, JAK2, JAK3, and Tyk2, which are activated in different combinations by various cytokines (9).

JAK inhibitors are molecular-targeted synthetic drugs that specifically inhibit JAK. Biological agents, which are high molecular weight proteins, are limited to administration via intravenous or subcutaneous injections. On the other hand, JAK inhibitors are low molecular weight compounds that can be orally administered and are as effective as biological agents. These inhibitors competitively bind to the ATP-binding site of JAK in the cell and specifically inhibit the activity of JAK induced by cytokine stimulation (10, 11). Baricitinib inhibits JAK1 and JAK2, while tofacitinib inhibits JAK1, JAK2, and JAK3. JAK inhibitors such as these are often reported to be effective in RA that is resistant to treatment with biological agents (12–16). However, adverse events such as herpes zoster, serious heart-related events, and cancer are known to occur more frequently following the use of JAK inhibitors when compared to that of biological agents (12, 13).

At present, very little evidence is available on the use of JAK inhibitors for the treatment of ocular inflammation (17–21). Miserocchi et al. reported that baricitinib and tofacitinib showed a significant reduction in inflammatory activity in uveitis than in systemic arthritis when four cases of juvenile idiopathic arthritis-associated uveitis (JIAU) refractory to csDMARD and bDMARD were investigated (17). During their study, no serious systemic side effects required discontinuation of treatment (17).

Bauermann et al. (18) described tofacitinib as a successful strategy for severe refractory uveitis and macular edema;

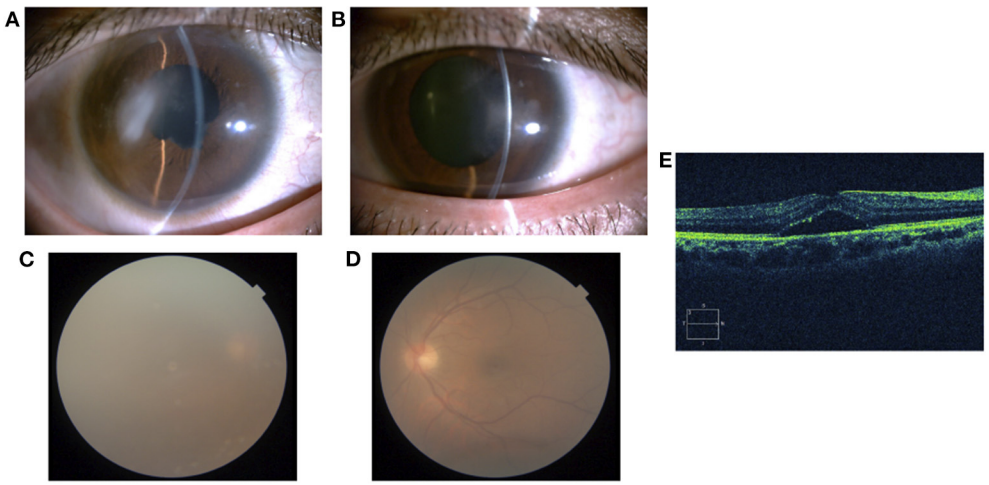

FIGURE 3 | A slit-lamp examination showing corneal infiltration lesion, anterior chamber cells, posterior iris synechia, and anterior subcapsular cataract in the right eye **(A)** and corneal infiltration lesion in the left eye **(B)**. A fundus photograph showing vitreous opacity in the right eye **(C)** and left eye **(D)**. OCT of the right eye showing serous retinal detachment **(E)**.

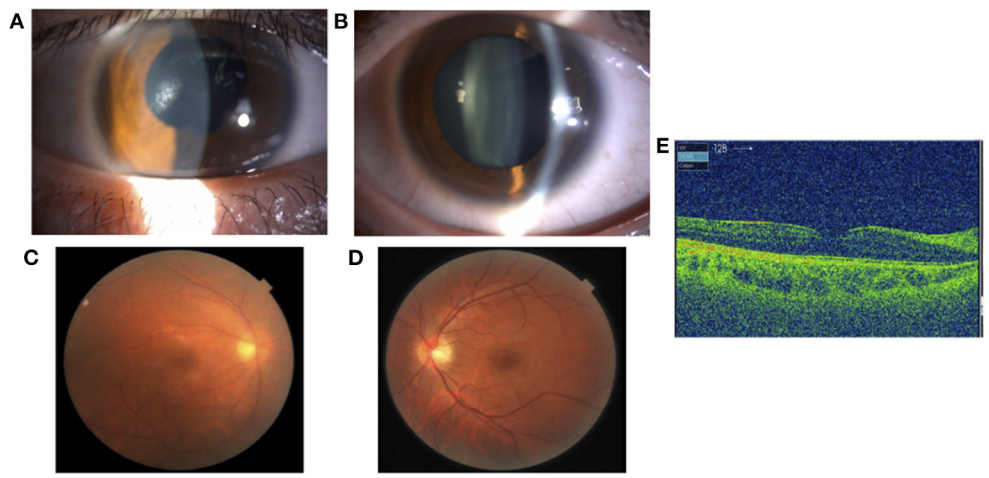

FIGURE 4 | A slit-lamp examination showing improvement of the corneal infiltrative lesions and the anterior chamber cells in the right eye **(A)** and left eye **(B)**. A fundus photograph showing improvement of vitreous opacity in both eyes **(C)** and **(D)**. OCT showing disappearance of serous retinal detachment in the right eye **(E)**.

therefore, JAK inhibitors were postulated as a treatment option in select cases that do not respond well to csDMARD and bDMARD or intraocular steroid implants.

Based on the above-mentioned findings, Chen et al. (19) reviewed the current treatment algorithms for JIAU, which are unable to taper local and oral steroids, and recommended treatment with methotrexate followed by TNF-α inhibitors such as adalimumab. IL-6 inhibitors, T cell co-stimulation modulators, JAK inhibitors, and CD20 inhibitors—which have been proven to be effective against arthritis following their recent review for the treatment of JIAU—have been proposed as remedial options when refractory to the above-mentioned treatments (19). In addition, an international, multicenter, open-label controlled study sponsored by Eli Lilly and Company [NCT04088409; 2019–present; (22)] is currently underway to compare baricitinib and adalimumab in JIAU and chronic anterior anti-nuclear antibody positive uveitis. If the effectiveness of baricitinib for these uveitis cases can be proven, it may be effective for other types of uveitis in the future.

In the current case, treatment with csDMARDs or bDMARDs did not suppress the inflammatory activity of systemic arthritis and uveitis. However, after the initiation of oral baricitinib, which is a tsDMARD, inflammatory activity improved not only in systemic arthritis but also in the uveitis of both eyes for a long time. Additionally, good visual acuity was maintained without serious side effects.

Currently, the only approved treatments for uveitis in Japan are steroids, cyclosporine, infliximab, and adalimumab, which have to be administered for a long period in refractory cases. Therefore, considering the systemic and local complications associated with the long-term use of these conventionally prescribed agents, new therapeutic agents with different mechanisms of action are desired. In this report, we highlight the efficacy and safety of baricitinib for the treatment of uveitis with RA resistant to conventional treatment. In the future, the use of a JAK inhibitor along with the involvement of a multidisciplinary team including the rheumatologist may be a viable option if the treatment by an ophthalmologist is not sufficient in similar cases.

DATA AVAILABILITY STATEMENT

The original contributions presented in the study are included in the article/supplementary material, further inquiries can be directed to the corresponding author/s.

ETHICS STATEMENT

The studies involving human participants were reviewed and approved by the Ethical Review Committee of Yamagata University Faculty of Medicine. The patients/participants provided their written informed consent to participate in this study. Written informed consent was obtained from the individual(s) for the publication of any potentially identifiable images or data included in this article.

AUTHOR CONTRIBUTIONS

YK: concept and design of study or analysis and interpretation of data. YK and YT: acquisition of data. TM, KN, YT, MT, and HY: drafting the article or revising it critically for important intellectual content and final approval of the version to be published. All authors contributed to the article and approved the submitted version.

REFERENCES

1. Smolen JS, Landewé RBM, Bijlsma JWJ, Burmester GR, Dougados M, Kerschbaumer A, et al. EULAR recommendations for the management of rheumatoid arthritis with synthetic and biological disease-modifying antirheumatic drugs: 2019 Update. *Ann Rheum Dis.* (2020) 79:685–99. doi: 10.1136/annrheumdis-2019-216655
2. Zlatanović G, Veselinović D, Cekić S, Zivković M, Dordević-Jocić J, Zlatanović M. Ocular manifestation of rheumatoid arthritis-different forms and frequency. *Bosn J Basic Med Sci.* (2010) 10:323–7. doi: 10.17305/bjbms.2010.2680
3. Martin MF, Scott DG, Gilbert C, Dieppe PA, Easty DL. Retinal vasculitis in rheumatoid arthritis. *Br Med J.* (1981) 282:1745–6. doi: 10.1136/bmj.282.6278.1745
4. Bhamra MS, Gondal I, Amarnani A, Betesh S, Zhyvotovska A, Scott W, et al. Ocular manifestations of rheumatoid arthritis: implications of recent clinical trials. *IM.Int J Clin Res Trials.* (2019) 4:139. doi: 10.15344/2456-8007/2019/139
5. Kay J, Upchurch KS. ACR/EULAR 2010 rheumatoid arthritis classification criteria. *Rheumatol Oxf Engl.* (2012) 6:51. doi: 10.1093/rheumatology/kes279
6. Barra L, Pope JE, Orav JE, Boire G, Haraoui B, Hitchon C, et al. Prognosis of seronegative patients in a large prospective cohort of patients with early inflammatory arthritis. *J Rheumatol.* (2014) 41:2361–2369. doi: 10.3899/jrheum.140082
7. Choi S, Lee KH. Clinical management of seronegative and seropositive rheumatoid arthritis: A comparative study. *PLOS ONE.* (2018) 13:e0195550. doi: 10.1371/journal.pone.0195550
8. Katchamart W, Koolvisoot A, Aromdee E, Chiowchanwesawakit P, Muengchan C. Associations of rheumatoid factor and anti-citrullinated peptide antibody with disease progression and treatment outcomes in patients with rheumatoid arthritis. *Rheumatol Int.* (2015) 35:1693–99. doi: 10.1007/s00296-015-3271-8
9. Sahatciu-Meka V, Rexhepi S, Manxhuka-Kerliu S, Rexhepi M. Extra-articular manifestations of seronegative and seropositive rheumatoid arthritis. *Bosn J Basic Med Sci.* (2010) 10:26–31. doi: 10.17305/bjbms.2010.2729
10. Yamaoka K, Saharinen P, Pesu M, Holt VE 3rd, Silvennoinen O, O'Shea JJ. The Janus kinases (Jaks). *Genome Biol.* (2004) 5:253. doi: 10.1186/gb-2004-5-12-253
11. Choy EH. Clinical significance of Janus kinase inhibitor selectivity. *Rheumatol Oxf Engl.* (2019) 58:953–62. doi: 10.1093/rheumatology/key339
12. Yamaoka K. Benefit and risk of tofacitinib in the treatment of rheumatoid arthritis: a focus on herpes zoster. *Drug Saf.* (2016) 39:823–40. doi: 10.1007/s40264-016-0430-0
13. US Food and Drug Administration. *Drug Safety Communications: Safety trial finds risk of blood clots in the lungs and death with higher dose of tofacitinib (Xeljanz, Xeljanz XR) in rheumatoid arthritis patients; FDA to investigate*. (2021). Available online at: https://www.fda.gov/drugs/drug-safety-and-availability/safety-trial-finds-risk-blood-clots-lungs-and-death-higher-dose-tofacitinib-xeljanz-xeljanz-xr (accessed July 12, 2021)
14. Mogul A, Corsi K, McAuliffe L. Baricitinib: The second FDA-approved JAK inhibitor for the treatment of rheumatoid arthritis. *Ann Pharmacother.* (2019) 53:947–53. doi: 10.1177/1060028019839650
15. Taylor PC, Keystone EC, van der Heijde D, Weinblatt ME, Del Carmen Morales L, Reyes Gonzaga J, et al. Baricitinib versus placebo or adalimumab in rheumatoid arthritis. *N Engl J Med.* (2017) 376:652–62. doi: 10.1056/NEJMoa1608345
16. Al-Salama ZT, Scott LJ. Baricitinib: A review in rheumatoid arthritis. *Drugs.* (2018) 78:761–72. doi: 10.1007/s40265-018-0908-4
17. Miserocchi E, Giuffrè C, Cornalba M, Pontikaki I, Cimaz R. JAK inhibitors in refractory juvenile idiopathic arthritis-associated uveitis. *Clin Rheumatol.* (2020) 39:847–51. doi: 10.1007/s10067-019-04875-w
18. Bauermann P, Heiligenhaus A, Heinz C. Effect of Janus kinase inhibitor treatment on anterior uveitis and associated macular edema in an adult patient with juvenile idiopathic arthritis. *Ocul Immunol Inflamm.* (2019) 27:1232–4. doi: 10.1080/09273948.2019.1605453
19. Chen JL, Abiri P, Tsui E. Recent advances in the treatment of juvenile idiopathic arthritis-associated uveitis. *Ther Adv Ophthalmol.* (2021) 13:2515841420984572. doi: 10.1177/2515841420984572
20. Paley MA, Karacal H, Rao PK, Margolis TP, Miner JJ. Tofacitinib for refractory uveitis and scleritis. *Am J Ophthalmol Case Rep.* (2019) 13:53–55. doi: 10.1016/j.ajoc.2018.12.001
21. Dutta Majumder P, Shah A, Kaushik V. Tofacitinib in Vogt–Koyanagi–Harada disease. *Indian J Ophthalmol.* (2020) 68:1938–1939. doi: 10.4103/ijo.IJO_998_20
22. Baricitinib. *A study of baricitinib (LY3009104) in participants from 2 years to less than 18 years old with active JIA-associated uveitis or chronic anterior antinuclear antibody-positive uveitis*. (2021). Available

online at: https://ClinicalTrials.gov/show/NCT04088409 (accessed July 12, 2021).

Conflict of Interest: The authors declare that the research was conducted in the absence of any commercial or financial relationships that could be construed as a potential conflict of interest.

Publisher's Note: All claims expressed in this article are solely those of the authors and do not necessarily represent those of their affiliated organizations, or those of the publisher, the editors and the reviewers. Any product that may be evaluated in this article, or claim that may be made by its manufacturer, is not guaranteed or endorsed by the publisher.

frontiers in Medicine

ORIGINAL RESEARCH
published: 24 January 2022
doi: 10.3389/fmed.2021.810070

Customized Color Settings of Digitally Assisted Vitreoretinal Surgery to Enable Use of Lower Dye Concentrations During Macular Surgery

Su Jin Park[1], *Jae Rock Do*[1], *Jae Pil Shin*[1] *and Dong Ho Park*[1,2,3]*

[1] Department of Ophthalmology, School of Medicine, Kyungpook National University, Kyungpook National University Hospital, Daegu, South Korea, [2] Kyungpook National University Bio-Medical Research Institute, Daegu, South Korea, [3] Kyungpook National University Cell and Matrix Research Institute, Daegu, South Korea

OPEN ACCESS

Edited by:
Michele Lanza,
University of Campania Luigi Vanvitelli, Italy

Reviewed by:
Yousef Ahmed Fouad,
Ain Shams University, Egypt
Takashi Ueta,
The University of Tokyo, Japan
Leandro Cabral Zacharias,
University of São Paulo, Brazil
Yutaka Imamura,
Teikyo University Mizonokuchi Hospital, Japan
Cesare Mariotti,
Marche Polytechnic University, Italy

***Correspondence:**
Dong Ho Park
DongHo_Park@knu.ac.kr

Specialty section:
This article was submitted to Ophthalmology, a section of the journal Frontiers in Medicine

Received: 05 November 2021
Accepted: 24 December 2021
Published: 24 January 2022

Citation:
Park SJ, Do JR, Shin JP and Park DH (2022) Customized Color Settings of Digitally Assisted Vitreoretinal Surgery to Enable Use of Lower Dye Concentrations During Macular Surgery. Front. Med. 8:810070. doi: 10.3389/fmed.2021.810070

Purpose: This study evaluated the color contrast ratio (CCR) of the internal limiting membrane (ILM) using different color settings of digitally assisted vitreoretinal surgery (DAVS) with different indocyanine green (ICG) concentrations.

Methods: This is a prospective comparative observational study. Consecutive patients that underwent 25G vitrectomy and ILM peeling using a standard operating microscope (SOM) (25 eyes), DAVS Ver. 1.1 (12 eyes), or DAVS Ver. 1.3 (13 eyes) were enrolled. The SOM and DAVS Ver. 1.1 groups used 0.075% ICG, and the DAVS Ver. 1.3 group used 0.025% ICG. In DAVS Ver. 1.1, macular CCR was compared between four different presets in the red, green, and blue channels: Default (Red (R) 100%, Green (G) 100%, and Blue (B) 100%); Preset 1 (R 20%, G 100%, B 100%); Preset 2 (R 80%, G 80%, B 100%), and Preset 3 (R 85%, G 100%, B 90%). In DAVS Ver. 1.3, macular CCR was evaluated using two different customized settings that modified the hue and saturation: Customized Setting 1 (R 86, G 100, B 100%, Hue +2°, Saturation 90%, Gamma 1.2) and Customized Setting 2 (R 90, G 100, B 100%, Hue +20°, Saturation 100%, Gamma 0.9). All patients underwent ophthalmologic examinations including BCVA at baseline and at 12 months.

Results: In DAVS Ver. 1.1, macular CCR was highest in Preset 3 ($P < 0.01$). The CCR of Customized Setting 2 of DAVS Ver. 1.3 using 0.025% ICG did not differ from that of Preset 3 in DAVS Ver. 1.1 using 0.075% ICG. Furthermore, there was no significant difference in BCVA between the Customized Setting 2 of DAVS Ver. 1.3 with 0.025% ICG and the Preset 3 of DAVS Ver. 1.1 with 0.075% ICG groups at baseline and at 12 months ($P > 0.05$, respectively).

Conclusion: Customized DAVS settings enabled surgeons to use a 3-fold lower ICG concentration in ILM peeling.

Keywords: vitrectomy, macular surgery, epiretinal membrane (ERM), ILM peeling, 25 gauge pars plana vitrectomy

INTRODUCTION

Since Ekardt et al. (1) first reported internal limiting membrane (ILM) peeling in full-thickness macular hole (MH) surgery in 1997, this approach has been used routinely to improve MH closure rates (2, 3). In the epiretinal membrane (ERM) and MH, a meta-analysis reported that ILM peeling improves visual acuity in long-term follow-ups and decreases ERM recurrence rates (4). According to the preference and trends (PAT) survey of the American Society of Retina Specialists (ASRS), more than 60% of vitreoretinal surgeons in the United States and Europe are performing ILM peeling during ERM surgery (5). However, the translucency of the ILM causes significant difficulty in ILM peeling. Therefore, ILM staining methods have been developed, including indocyanine green (ICG), trypan blue (TB), and brilliant blue G (BBG) (6–8). Recently, ASRS conducted a PAT survey to determine whether adjuvant dyes and which ones are used to aid in macular surgery. The survey reported that 69.0% of surgeons in the United States are still using ICG; 47.5% of surgeons in Asia/Pacific are still using ICG, and 39.9% of surgeons in Europe are using ICG or TB (5). In addition, ICG selectively stains ILM, and it is superior to TB in terms of the staining intensity which could be advantageous in cases with strong vitreoretinal adhesion (9). However, several studies have reported potential toxic effects of the ICG (10–12) and BBG dyes (13–15) used during macular surgery. Thus, protocols that minimize the use and amounts of these dyes would be clinically desirable.

Until recently, imaging devices have been designed to improve ILM contrast using multi-color endoillumination probes with light-emitting diode light sources (16). However, recently developed digitally assisted vitreoretinal surgery (DAVS), NGENUITY® 3D Visualization system (Alcon, Fort Worth, TX, USA) enables surgeons to customize the image color profiles of 3D high dynamic range (HDR) surgical images in real time (17). Although previous studies have addressed that different color channels are available in DAVS (17–19), no prior studies have quantitatively measured and compared color contrast in different color settings. Furthermore, the effect of different color settings under different ICG concentrations has not been evaluated.

The present study evaluated the color contrast ratio (CCR) of images captured during vitrectomy using different DAVS color settings. Furthermore, we determined if customizing color settings enabled surgeons to lower the ICG dye concentration as much as 3-fold in the ILM peeling process.

METHODS

Study Design and Participants

This prospective comparative observational study with consecutive patients was performed in the Department of Ophthalmology at Kyungpook National University. The protocol was approved by the Institutional Review Board of the Kyungpook National University Hospital (KNUH 01-015) and was conducted in accordance with the tenets of the Declaration of Helsinki.

The study group consisted of all consecutive Korean patients that underwent combined phacoemulsification (Centurion Vision System, Alcon) and 25G vitrectomy (Constellation Vision System, Alcon) with ILM peeling for MH or ERM. Patients enrolled from November to December 2018 were assigned to the standard operating microscope (SOM) (OMPI Lumera 700; Carl Zeiss Meditec, Inc., Germany) group. Patients enrolled in January 2019 were assigned to the DAVS version 1.1 (Ver. 1.1) (NGENUITY®, Alcon Inc., Fort Worth, TX, USA) group, and those enrolled in August 2020 were assigned to the DAVS Ver. 1.3 group. The visualization system used for surgery was not selected based on the patients' status. All surgeries were conducted by a single operator (DP). Exclusion criteria were as follows: presence of spherical equivalent $\geq$6.0 diopters or axial length $\geq$26 mm, history of previous ocular surgery, ocular trauma, and corneal diseases, including corneal opacity or corneal dystrophy.

Digitally Assisted Vitreoretinal Surgery Settings and ICG dye Concentration

The NGENUITY® system included a 3D HDR surgical camera with a complementary metal oxide semiconductor image sensor, a 3D compact image processing unit, and an OLED 3D 4K ultra high-definition 55-inch flat panel display (resolution 3,840 $\times$ 2,160 pixels; mode number: OLED55E6P; LG ltd., Seoul, Republic of Korea). The 4K OLED display was placed about 1.2 m from the operator, and operators wore passive circular polarizing eyeglasses.

Table 1 shows ICG dye concentrations and parameters for DAVS Ver. 1.1, and DAVS Ver. 1.3 groups. The 0.075% ICG dye concentration was sufficient for ILM visualization under the SOM, while 0.025% ICG was not sufficient (**Supplementary Figure 1**). Thus, all patients in the SOM group received a 0.075% solution (0.75 mg/mL) of ICG (Diagnogreen®; Daiichi Sankyo Co., Tokyo, Japan) diluted with balanced salt solution (BSS, Alcon). In the DAVS Ver. 1.1 group, the same ICG dye concentration of 0.075% was used to determine the optimal DAVS system preset. However, in the DAVS Ver. 1.3 group, to determine if the customized settings of DAVS Ver. 1.3 enabled use of a lower ICG dye concentration, the ICG dye concentration was decreased to 0.025% (0.25 mg/mL). In all the cases, after the removal of the ERM, a volume of 0.05 mL of the diluted ICG was injected only once into the vitreous cavity to stain the ILM for 30 s and then quickly washed out. The stained ILM was removed using 25G ILM forceps (GRIESHABER REVOLUTION® DSP ILM Forceps, Alcon).

In the DAVS Ver. 1.1 group, macular and vitreous images were captured four times continuously following four different color channels for each patient: Default [Red (R) 100, Green (G) 100, Blue (B) 100%]; Preset 1 (R 20, G 100, B 100%); Preset 2 (R 80, G 80, B 100%); and Preset 3 (R 85, G 100, B 90%). Hue, saturation, and gamma values were the same in all presets (+2°, 90%, and 1.2, respectively).

In the DAVS Ver. 1.3 group, macular images were captured twice continuously following two different customized settings for each patient: Customized Setting 1 (R 86, G 100, B 100%, Hue

TABLE 1 | Concentrations of indocyanine green dye and parameters for digitally assisted vitreoretinal surgery groups.

	DAVS Ver. 1.1				DAVS Ver. 1.3	
Variables	**Default**	**Preset 1**	**Preset 2**	**Preset 3**	**Customized setting 1**	**Customized setting 2**
ICG dye concentration, %	0.075	0.075	0.075	0.075	0.025	0.025
Red, Green, Blue, %	100,100,100	20,100,100	80,80,100	85,100,90	86,100,100	90,100,100
Hue, °	+2	+2	+2	+2	+2	+20
Saturation, %	90	90	90	90	90	100
Gamma	1.2	1.2	1.2	1.2	1.2	0.9
Screen distance, meter	1.2	1.2	1.2	1.2	1.2	1.2
Aperture, %	50	50	50	50	50	50
Endoillumination power, %	35	35	35	35	35	35

ICG, indocyanine green; DAVS, digitally assisted vitreoretinal surgery; Ver., version.

+2°, Saturation 90%, Gamma 1.2) and Customized Setting 2 (R 90, G 100, B 100%, Hue +20°, Saturation 100%, Gamma 0.9).

Other parameters, including endoillumination power, screen distance, and aperture, were identical in all groups. We consistently used plano contact lenses (Machemer Flat vitrectomy Lens OLV-5®, Ocular instruments, Inc., USA) when performing ILM peeling and located the endoilluminator in the mid-vitreous cavity in which the light pipe was not visible from the surgeon's visual field during the ILM peeling.

Data Analysis and Ophthalmologic Examination

Vitrectomy and ILM peeling were conducted after phacoemulsification, and intraocular lens (IOL) implantation was subsequently conducted. Retinal images were captured after ILM peeling using a microsurgical operating camera (MediLive Trio Eye, Panasonic, Germany) (**Figure 1**). Because retinal images were captured in the aphakic state, neither cataract nor IOL color affected the contrast of the captured retinal images. The RGB values of the images were analyzed using the Eyedropper tool of Adobe Photoshop CC 20.0.8 software (Adobe System, San Jose, CA, USA). RGB values were analyzed in masked images by two retinal specialists (SP and JD). The interobserver agreement for RGB values was satisfactory (interclass correlation coefficient = 0.922, $P < 0.001$). Color luminance and CCR were calculated according to previous studies (20). In summary, If the $R < 0.03928$, Rs is estimated by using Rs = R/12.92. If the R value was more than 0.03928, Rs is estimated by using $Rs = [(R + 0.055)/1.055]^{2.4}$. The Gs and Bs value can be estimated in the same manner. And then, the Color luminance and CCR are estimated by using the following: Color Luminance (L) = 0.2126Rs + 0.7152Gs + 0.0722Bs and CCR = (Lmax + 0.05)/(Lmin + 0.05), where Lmax = luminance of the brighter background and Lmin = luminance of the darker background. White balance was calibrated at the start of surgery.

All patients underwent full ophthalmologic examinations, including BCVA (logarithm of the minimal angle of resolution, logMAR), intraocular pressure (IOP) measurement, slit-lamp examination, and fundus examination at baseline and at every postoperative visit for at least for 12 months.

Statistical Analyses

Statistical analyses were performed using SPSS v.18.0 for Windows (SPSS Inc., Chicago, IL, USA). Quantitative data are expressed as mean ± standard deviation, and qualitative data are expressed as percentages. Mann-Whitney *U*-test and Kruskal-Wallis test were used to compare quantitative data, while Chi-square tests were used to compare qualitative data. Comparison of CCR between different color channels was analyzed using a Kendall's *W*-test and Wilcoxon signed-rank test. Multiple comparisons were adjusted by the Bonferroni method. $P < 0.05$ were considered statistically significant.

Considering our previous pilot studies, the required sample size to detect a statistical significance of 5%, a power of 80%, and a drop rate of 10% was 12 eyes (12 patients) per group.

RESULTS

The study included 50 eyes (50 patients) with ERM (n = 45 eyes) or MH (n = 5 eyes). **Table 2** shows patient clinical characteristics for the SOM (n = 25 eyes; 22 ERM and 3 MH), DAVS Ver. 1.1 (n = 12 eyes; 11 ERM and 1 MH), and DAVS Ver. 1.3 groups (n = 13 eyes; 12 ERM and 1 MH). Mean patient age was 68.3 ± 6.7 years (range, 61–82 years) in the SOM group, 69.3 ± 6.5 years (range, 60–83 years) in the DAVS Ver. 1.1 group, and 67.1 ± 6.2 (range, 61–80 years) in the DAVS Ver. 1.3 group, which did not differ between groups ($P > 0.05$). The groups did not differ in sex distribution, indication of surgery, baseline BCVA, IOP, or axial length ($P > 0.05$, respectively).

Measurement of Color Contrast Ratio in DAVS Ver. 1.1 With 0.075% ICG

During the first study period with DAVS Ver. 1.1, to determine the optimal color channels in the DAVS system, we compared the CCR among four different presets with 0.075% ICG dye. In macular images, the CCR differed among presets, with the highest CCR in Preset 3 and the lowest CCR in

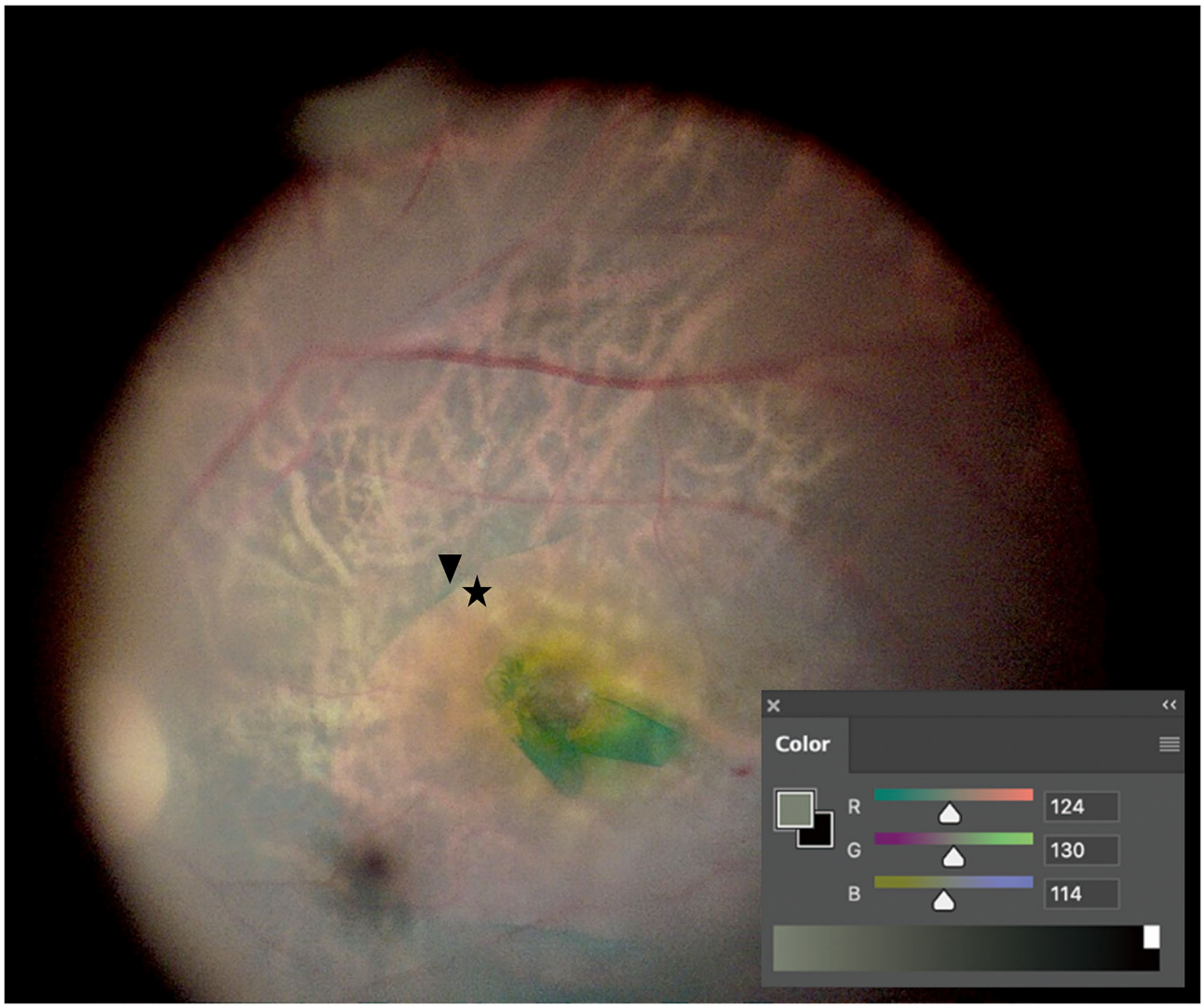

FIGURE 1 | Color contrast ratio (CCR) measurement. After internal limiting membrane (ILM) peeling, retinal images were captured. CCR was measured by comparing RGB values between the indocyanine green-stained area (arrowhead) and the ILM-peeled area (asterisk) using the Eyedropper tool of Photoshop.

Preset 1 (**Figures 2A,B**, $P < 0.01$). However, in the vitreous images, CCR did not differ among presets (**Figures 2C,D**, $P = 0.294$).

Measurement of Color Contrast Ratio in DAVS Ver. 1.3 With 0.025% ICG

During the second study period with DAVS Ver. 1.3, to determine if detailed customized settings enabled lowering of the ICG dye concentration, we used 0.025% ICG dye. As shown in **Table 1**, the parameters of Customized Setting 1 of DAVS Ver. 1.3 were similar to Preset 3 of DAVS Ver. 1.1. However, the macular CCR from Customized Setting 1 of DAVS Ver. 1.3 was lower than that of the Preset 3 of DAVS Ver. 1.1 (**Figures 3A,B,D**, $P < 0.01$).

Subsequently, we modified parameters of color settings, including hue values ($+2^{\circ}$ to $+20^{\circ}$), saturation (90% to 100%), and gamma (1.2 to 0.9), which were assigned as Customized Setting 2. The CCR of Customized Setting 2 was higher than that of Customized Setting 1 (**Figures 3B–D**, $P < 0.01$). Furthermore, the CCR of Customized Setting 2 of DAVS Ver. 1.3 with 0.025% ICG did not differ from that of Preset 3 of DAVS Ver. 1.1 with 0.075% ICG (**Figures 3A,C,D**, $P = 0.887$).

Comparison of Intraoperative Complication Rates and Postoperative Best-Corrected Visual Acuity

There was no difference in the ILM peeling time between the SOM with 0.075% ICG and Setting 2 of DAVS Ver. 1.3 groups with 0.025% ICG (3.3 ± 1.9 vs. 3.4 ± 0.8 min, $P = 0.361$). Regarding intraoperative complications, no iatrogenic retinal tears or retinal detachments occurred in any groups. Compared with baseline, the BCVA at 12 months was significantly improved: 0.33 ± 0.39 in the Customized Setting 2 of DAVS Ver. 1.3

TABLE 2 | Clinical characteristics of standard operating microscope and digitally assisted vitreoretinal surgery groups at baseline.

Variables	SOM ($n = 25$)	DAVS Ver. 1.1 ($n = 12$)	DAVS Ver. 1.3 ($n = 13$)	*P*-value*
Age, years	68.3 ± 6.7	69.3 ± 6.5	67.1 ± 6.2	0.749†
Male/female, *n*	10/15	7/5	3/10	0.199‡
Indication of surgery (ERM/MH)	22/3	11/1	12/1	0.656‡
BCVA, logMAR	0.76 ± 0.44	0.77 ± 0.61	0.54 ± 0.50	0.090†
IOP, mmHg	13.8 ± 2.7	15.0 ± 4.5	13.4 ± 2.7	0.708†
Axial length, mm	23.51 ± 0.81	23.85 ± 0.70	23.78 ± 1.19	0.204†

Data are shown as the mean ± standard deviation unless indicated otherwise.
BCVA, best-corrected visual acuity; ICG, indocyanine green; logMAR, logarithm of the minimal angle of resolution; IOP, intraocular pressure; SOM, standard operating microscope; DAVS, digitally assisted vitreoretinal surgery; Ver., version; ERM, epiretinal membrane; MH, macular hole.
**P-values were compared between SOM, DAVS version 1.1 and DAVS version 1.3 groups.*
†Kruskal-Wallis test.
‡Chi-square test.

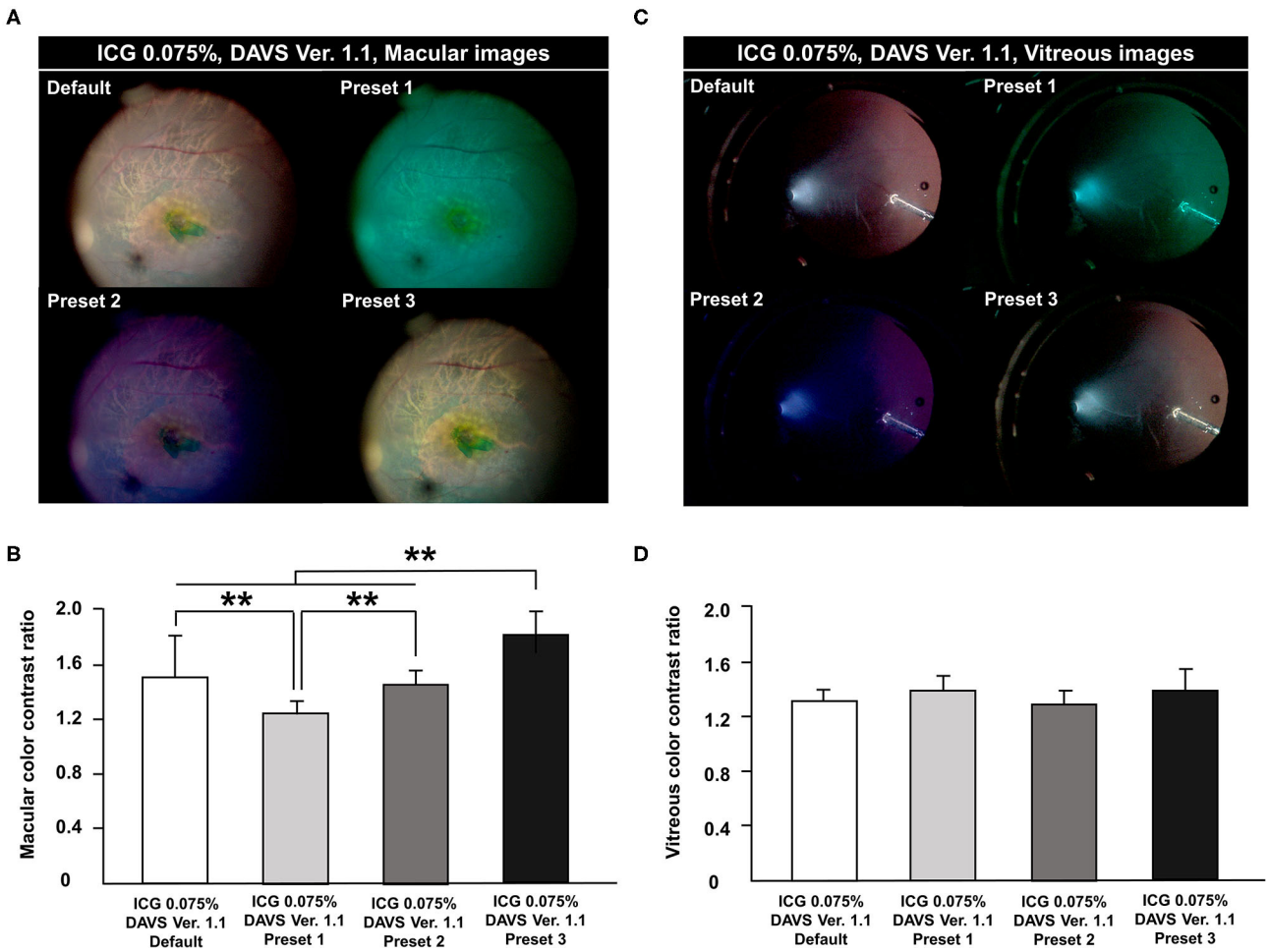

FIGURE 2 | Comparison of color contrast ratio (CCR) among channels in digitally assisted vitreoretinal surgery system (DAVS) Ver. 1.1. CCR was compared in macular and vitreous images from the DAVS Ver. 1.1 group. The following four channels were compared in each captured macular and vitreous image: Default [Red (R) 100%, Green (G) 100%, and Blue (B) 100%]; Preset 1 (R 20, G 100, B 100%); Preset 2 (R 80, G 80, B 100%); and Preset 3 (R 85, G 100, B 90%). **(A,B)** Macular CCR was different among the four channels ($P < 0.01$). CCR was highest in Preset 3 and lowest in Preset 1 ($P < 0.01$). **(C,D)** In vitreous images, CCR did not differ among the four settings ($P = 0.294$). **$P < 0.01$.

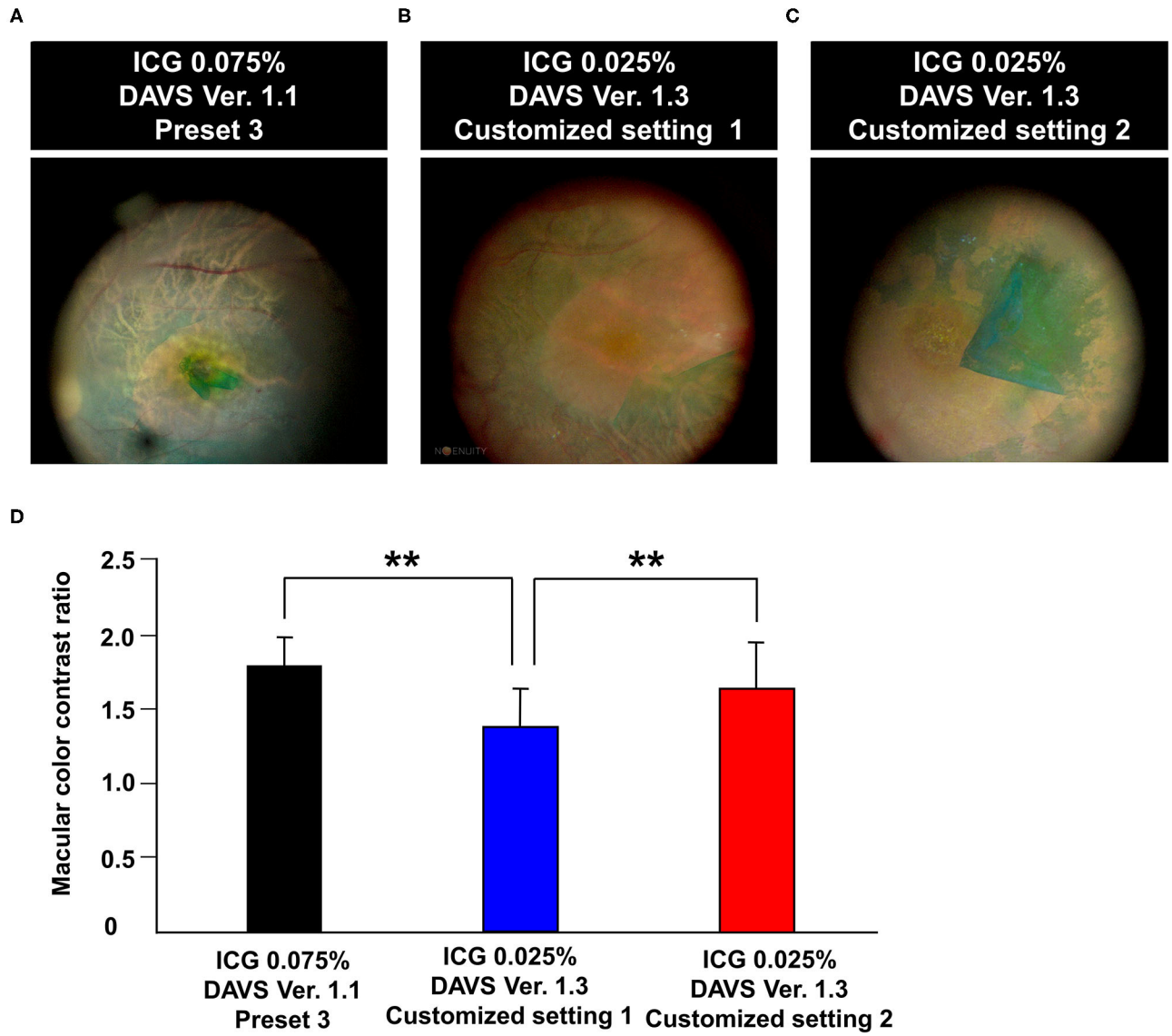

FIGURE 3 | Comparison of color contrast ratio (CCR) using different color settings of digitally assisted vitreoretinal surgery system (DAVS) in different indocyanine green (ICG) concentrations. **(A)** Macular image captured using Preset 3 of DAVS Ver. 1.1 with 0.075% ICG. **(B,C)** Macular image captured using Customized Settings 1 and 2 of DAVS Ver. 1.3 with 0.025% ICG. **(D)** CCR of Customized Setting 2 of DAVS Ver. 1.3 with 0.025% ICG did not differ from that of Preset 3 of DAVS Ver. 1.1 with 0.075% ICG ($P = 0.887$). $^{**}P < 0.01$.

with 0.025% ICG group and 0.36 ± 0.31 in the Preset 3 of DAVS Ver. 1.1 with 0.075% ICG group ($P < 0.05$, respectively). However, there was no significant difference in BCVA between the two groups at 12 months ($P = 0.406$). All of the MH cases from three groups showed MH closure at 12 months and did not require secondary surgery. BCVA at 12 months from the SOM group was 0.43 ± 0.05 logMAR, the BCVA from the DAVS Ver 1.1 with 0.075% ICG group was 0.40 logMAR, and the BCVA from the DAVS Ver 1.3 with 0.025% ICG group was 0.40 logMAR.

DISCUSSION

Since the advent of DAVS, this platform has been reported to provide a larger field of view at a higher magnification with accurate focus, better educational value, and a more ergonomically comfortable position for the operator than the SOM system (17, 18, 21–24). Importantly, Gonzalez-Saldivar and Chow (25) reported that DAVS provided superior depth of field and lateral resolution than did SOM when the aperture and display distance settings of DAVS were optimized. Although

several prior reports mentioned about the color channel function of DAVS (17–19), no previous studies have quantitatively measured macular color contrast according to different color channels or determined whether customized settings are able to lower ICG concentration.

ICG dye is commonly used for ILM visualization in macular surgery, and most surgeons use an ICG concentration of 0.1–0.5% (18, 26). However, several studies have reported the potential for ICG toxicity (**Supplementary Table 1**) (11, 27–30). Brief exposure of cultured human retinal pigment epithelial (RPE) cells to 0.1% decreases mitochondrial enzyme activity, suggesting the potential for toxicity (10). In macular surgeries, in 45% of cases, RPE atrophy occurred under 0.1% ICG at the site of a previous MH, which was confirmed by fundus photography (11), and RPE pigmentary changes were observed in 27% of patients with 0.25% ICG (31).

Despite its potential toxic effects, ICG is widely used for ILM staining in clinic. According to a previous meta-analysis based on comparative studies published between 2004 and 2014, 82.4% of studies used ICG. The study demonstrate that ICG is still one of the primary adjuvants used clinically for ILM peeling. In a previous study, comparing electrophysiologic and histological findings after injecting different concentrations of ICG (0.05, 0.5, and 2.5%) into the vitreous cavity of rabbits, ICG had a dose-dependent toxic effect, as demonstrated by decreased retinal function and morphology consistent with toxicity (32). Thus, it is important for retinal surgeons to use as little ICG as possible.

However, under the microscope, ILM visualization is difficult at lower concentrations such as 0.025% (**Supplementary Figure 1**). Furthermore, Kwok et al. reported that 50% of cases with 0.025% ICG required second ILM staining with 0.125% ICG due to poor ILM visualization (33). Thus, we sought to determine whether customized color settings could maximize visualization of the ICG-stained ILM, allowing the use of lower ICG concentrations.

During the first study period with DAVS Ver. 1.1, we determined which color channels allowed maximal color contrast in 0.075% ICG-stained ILM. Preset 3 had the highest CCR of the four evaluated color channels, likely because Preset 3 decreased the red and blue channels, emphasizing the green channel. This result suggested that green-emphasizing color channels are useful for visualization of the ICG-stained ILM.

Some reports have suggested that the blue channel increases visibility of the vitreous (17), which was not corroborated by the present study. Because the vitreous body is a transparent material and has no background, significant contrast would be difficult to visualize. However, it is possible that vitreous contrast varies depending on parameters of the surgical environment, such as the illuminator angle and location of the illuminator in the vitreous cavity.

Considering that the highest CCR was in Preset 3 of DAVS Ver. 1.1, we expected that using an ICG concentration lower than 0.075% for ILM visualization would be possible with the DAVS system. Thus, during the second study period with DAVS Ver. 1.3, we used 0.025% ICG and measured macular CCR. First, we used Customized Setting 1 of DAVS Ver. 1.3 similar to Preset 3 of DAVS Ver. 1.1, and subsequently compared the CCR between 0.025 and 0.075% ICG concentrations. The macular CCR from Customized Setting 1 of DAVS Ver. 1.3 was lower than that of Preset 3 of DAVS Ver. 1.1, likely due to the 3-fold decrease of ICG concentration. The above results suggest that adjustment of RGB channels alone was insufficient to visualize the ILM at 0.025% ICG. Rather, it was necessary to also adjust other parameters, such as hue, saturation, and gamma values. Thus, we modified the customized setting using other parameters.

Since the development of DAVS Ver. 1.2, customized settings of anterior, macular, and posterior image modes have been made available to optimize viewing experience during surgical procedural steps. Furthermore, not only RGB, but also hue, saturation, and gamma values can be easily modified to create customized settings for each surgical situation.

Various parameters related to color settings determine color perception including hue, saturation, and gamma values. Hue is used to distinguish colors, which is specified as between 0 and 360°. Saturation refers to the color intensity, with a higher saturation having more vivid color. Gamma is also important in digital image systems. While a high gamma setting can compress bright areas and increase black areas to create crisp and high-contrast images, a low gamma setting enables more detailed visualization in bright areas while still compressing shadow (34). Following the above principle, in Customized Setting 2, hue and saturation values were increased and gamma value was decreased to improve macular color contrast at 0.025% ICG. Interestingly, the present study demonstrated that Customized Setting 2 of DAVS Ver. 1.3 with 0.025% ICG exhibited a similar CCR to that of Preset 3 of DAVS Ver. 1.1 with 0.075% ICG. A recent questionnaire survey reported similar results that higher Hue parameter was correlated with better visualization (19). This suggested that the customized color settings available in the DAVS system enabled surgeons to lower the ICG concentration as much as 3-fold, which would be helpful for reduction of ICG toxicity.

This study has several limitations. First, the sample size was small in the DAVS groups. However, the sample size was sufficient for analysis by sample size calculation. Second, we could not directly compare CCR between the SOM and DAVS groups because the digital image resolution was not the same between the two systems. Third, because BBG and TB are not commercially available in Korea, we were unable to measure CCR using these dyes. Several cases have reported retinal toxicity resulting from the use of BBG dye during macular surgery (13–15). Although some studies have suggested a good safety profile for use of TB in macular surgeries (35, 36), a case study in which retinal toxicity occurred due to prolonged TB exposure has also been reported (37). Thus, it would be valuable to optimize instrument settings to maximize CCR during surgeries performed using BBG and TB to decrease the necessary dye concentration for ILM visualization, which we will evaluate in a future study. Fourth, although the same endoillumination power of 35% was used in the SOM and DAVS groups, this power is higher than is typically used for DAVS (24). In a future study, we will verify and optimize the settings

using a lower endoillumination power. Fifth, although high myopic patients were excluded to minimize the effect of myopia on CCR, variations in myopic state and RPE pigmentation between patients could affect the macular CCR. In the future, it will be necessary to evaluate the correlation between the pigmentation state and baseline color conditions. Sixth, though the DAVS Ver. 1.1 group was allocated to find the optimal settings among the various presets and to compare with the DAVS Ver. 1.3, the DAVS Ver. 1.1 is no longer commercially available in the real-world DAVS. However, the approach used in this study to determine the optimized customized settings could be helpful for surgeons to adjust to the next versions of the DAVS system in the future. Seventh, due to the small proportion of MH cases, postoperative toxicity assessment such as fundus autofluorescence was not evaluated. However, the authors would like to say that the purpose of this study was to determine the optimal color settings to lower the ICG concentration because BBG and TB are not commercially available in Korea. In the future, we will evaluate how the reduced ICG concentration enabled by the optimized use of the DAVS system could affect the RPE toxicity. Eight, we could not measure the direct correlation between the CCR and the surgeons' subjective visual perception. Instead, the ILM peeling time between the SOM with 0.075% ICG and Customized Setting 2 with 0.025% ICG groups was compared which was not statistically different. The above data could suggest that the customized settings of the DAVS determined by trial and error to acquire a higher CCR could be meaningful for the surgeons' visual perception.

In conclusion, this is the first report comparing the color contrast between different DAVS settings and different ICG concentrations. The study demonstrated that the customized color settings of the DAVS system enabled surgeons to lower ICG concentration used, which would be advantageous in macular surgery.

DATA AVAILABILITY STATEMENT

The data that support the findings of this study are available from the corresponding authors upon reasonable request.

ETHICS STATEMENT

The studies involving human participants were reviewed and approved by Institutional Review Board of Kyungpook National University Hospital (KNUH 01-015). The patients/participants provided their written informed consent to participate in this study.

AUTHOR CONTRIBUTIONS

SP, JD, JS, and DP contributed to the conception or design of the work. SP, JD, and DP contributed to the data collection, data analysis and/or interpretation. All authors contributed to the drafting of the article and critical review of the article.

FUNDING

This work was supported by Biomedical Research Institute grant, Kyungpook National University Hospital (2018). This research was supported by a grant of the Korea Health Technology R&D Project through the Korea Health Industry Development Institute (KHIDI), funded by the Ministry of Health and Welfare, Republic of Korea (Grant number: HI15C0001).

SUPPLEMENTARY MATERIAL

The Supplementary Material for this article can be found online at: https://www.frontiersin.org/articles/10.3389/fmed.2021.810070/full#supplementary-material

REFERENCES

1. Eckardt C, Eckardt U, Groos S, Luciano L, Reale E. Removal of the internal limiting membrane in macular holes. Clinical and morphological findings. *Ophthalmologe.* (1997) 94:545–51. doi: 10.1007/s003470050156
2. Brooks HL Jr. Macular hole surgery with and without internal limiting membrane peeling. *Ophthalmology.* (2000) 107:1939–48; discussion 1948–39. doi: 10.1016/S0161-6420(00)00331-6
3. Spiteri Cornish K, Lois N, Scott N, Burr J, Cook J, Boachie C, et al. Vitrectomy with internal limiting membrane (ILM) peeling versus vitrectomy with no peeling for idiopathic full-thickness macular hole (FTMH). *Cochrane Database Syst Rev.* (2013) 6:CD009306. doi: 10.1002/14651858.CD009306.pub2
4. Chang WC, Lin C, Lee CH, Sung TL, Tung TH, Liu JH. Vitrectomy with or without internal limiting membrane peeling for idiopathic epiretinal membrane: a meta-analysis. *PLoS ONE.* (2017) 12:e0179105. doi: 10.1371/journal.pone.0179105
5. ASRS (2017). *Preferences and Trends Survey: Global Trends in Retina.* American Society of Retina Specialists. Available online at: http://www.asrs.org/content/documents/2017-asrs-global-trends-in-retina-survey-results.pdf (accessed February 8, 2021).
6. Kadonosono K, Itoh N, Uchio E, Nakamura S, Ohno S. Staining of internal limiting membrane in macular hole surgery. *Arch Ophthalmol.* (2000) 118:1116–8. doi: 10.1001/archopht.118.8.1116
7. Feron EJ, Veckeneer M, Parys-Van Ginderdeuren R, Van Lommel A, Melles GR, Stalmans P. Trypan blue staining of epiretinal membranes in proliferative vitreoretinopathy. *Arch Ophthalmol.* (2002) 120:141–4. doi: 10.1001/archopht.120.2.141
8. Enaida H, Hisatomi T, Hata Y, Ueno A, Goto Y, Yamada T, et al. Brilliant blue G selectively stains the internal limiting membrane/brilliant blue G-assisted membrane peeling. *Retina.* (2006) 26:631–6. doi: 10.1097/00006982-200607000-00007
9. Shukla D, Kalliath J, Neelakantan N, Naresh KB, Ramasamy K. A comparison of brilliant blue G, trypan blue, and indocyanine green dyes to assist internal limiting membrane peeling during macular hole surgery. *Retina.* (2011) 31:2021–5. doi: 10.1097/IAE.0b013e318213618c
10. Sippy BD, Engelbrecht NE, Hubbard GB, Moriarty SE, Jiang S, Aaberg TMJr, et al. Indocyanine green effect on cultured human retinal pigment epithelial cells: implication for macular hole surgery. *Am J Ophthalmol.* (2001) 132:433–5. doi: 10.1016/S0002-9394(01)01061-3
11. Engelbrecht NE, Freeman J, Sternberg PJr, Aaberg TMSr, Aaberg TMJr, Martin DF, et al. Retinal pigment epithelial changes after macular hole surgery with indocyanine green-assisted internal limiting membrane

peeling. *Am J Ophthalmol.* (2002) 133:89–94. doi: 10.1016/S0002-9394(01)01293-4
12. Gandorfer A, Haritoglou C, Gandorfer A, Kampik A. Retinal damage from indocyanine green in experimental macular surgery. *Invest Ophthalmol Vis Sci.* (2003) 44:316–23. doi: 10.1167/iovs.02-0545
13. Jindal A, Pathengay A, Mithal K, Chhablani J, Pappuru RR, Flynn HW. Macular toxicity following brilliant blue G-assisted macular hole surgery - a report of three cases. *Nepal J Ophthalmol.* (2014) 6:98–101. doi: 10.3126/nepjoph.v6i1.10779
14. Almeida FP, De Lucca AC, Scott IU, Jorge R, Messias A. Accidental subretinal brilliant blue G migration during internal limiting membrane peeling surgery. *JAMA Ophthalmol.* (2015) 133:85–8. doi: 10.1001/jamaophthalmol.2014.3869
15. Venkatesh R, Aseem A, Jain K, Yadav NK. Combined brilliant blue G and xenon light induced outer retinal layer damage following macular hole surgery. *Indian J Ophthalmol.* (2020) 68:247–9. doi: 10.4103/ijo.IJO_1386_19
16. Chow DR. The evolution of endoillumination. *Dev Ophthalmol.* (2014) 54:77–86. doi: 10.1159/000360452
17. Kumar A, Hasan N, Kakkar P, Mutha V, Karthikeya R, Sundar D, et al. Comparison of clinical outcomes between "heads-up" 3D viewing system and conventional microscope in macular hole surgeries: a pilot study. *Indian J Ophthalmol.* (2018) 66:1816–9. doi: 10.4103/ijo.IJO_59_18
18. Talcott KE, Adam MK, Sioufi K, Aderman CM, Ali FS, Mellen PL, et al. Comparison of a three-dimensional heads-up display surgical platform with a standard operating microscope for macular surgery. *Ophthalmol Retina.* (2019) 3:244–51. doi: 10.1016/j.oret.2018.10.016
19. Melo AGR, Conti TF, Hom GL, Greenlee TE, Cella WP, Talcott KE, et al. Optimizing visualization of membranes in macular surgery with heads-up display. *Ophthalmic Surg Lasers Imaging Retina.* (2020) 51:584–7. doi: 10.3928/23258160-20201005-06
20. Kadonosono K, Arakawa A, Inoue M, Yamane S, Uchio E, Yamakawa T, et al. Internal limiting membrane contrast after staining with indocyanine green and brilliant blue G during macular surgery. *Retina.* (2013) 33:812–7. doi: 10.1097/IAE.0b013e3182807629
21. Eckardt C, Paulo EB. Heads-up surgery for vitreoretinal procedures: an experimental and clinical study. *Retina.* (2016) 36:137–47. doi: 10.1097/IAE.0000000000000689
22. Coppola M, La Spina C, Rabiolo A, Querques G, Bandello F. Heads-up 3D vision system for retinal detachment surgery. *Int J Retina Vitreous.* (2017) 3:46. doi: 10.1186/s40942-017-0099-2
23. Romano MR, Cennamo G, Comune C, Cennamo M, Ferrara M, Rombetto L, et al. Evaluation of 3D heads-up vitrectomy: outcomes of psychometric skills testing and surgeon satisfaction. *Eye.* (2018) 32:1093–8. doi: 10.1038/s41433-018-0027-1
24. Palacios RM, de Carvalho ACM, Maia M, Caiado RR, Camilo DAG, Farah ME. An experimental and clinical study on the initial experiences of Brazilian vitreoretinal surgeons with heads-up surgery. *Graefes Arch Clin Exp Ophthalmol.* (2019) 257:473–83. doi: 10.1007/s00417-019-04246-w
25. Gonzalez-Saldivar G, Chow DR. Optimizing visual performance with digitally assisted vitreoretinal surgery. *Ophthalmic Surg Lasers Imaging Retina.* (2020) 51:S15–21. doi: 10.3928/23258160-20200401-02
26. Kwok AK, Li WW, Pang CP, Lai TY, Yam GH, Chan NR, et al. Indocyanine green staining and removal of internal limiting membrane in macular hole surgery: histology and outcome. *Am J Ophthalmol.* (2001) 132:178–83. doi: 10.1016/S0002-9394(01)00976-X
27. Haritoglou C, Gandorfer A, Gass CA, Schaumberger M, Ulbig MW, Kampik A. The effect of indocyanine-green on functional outcome of macular pucker surgery. *Am J Ophthalmol.* (2003) 135:328–37. doi: 10.1016/S0002-9394(02)01969-4
28. Cheng SN, Yang TC, Ho JD, Hwang JF, Cheng CK. Ocular toxicity of intravitreal indocyanine green. *J Ocul Pharmacol Ther.* (2005) 21:85–93. doi: 10.1089/jop.2005.21.85
29. Posselt D, Rahman R, Smith M, Simcock PR. Visual outcomes following ICG assisted ILM peel for Macular Hole. *Eye.* (2005) 19:279–83. doi: 10.1038/sj.eye.6701455
30. Uemoto R, Yamamoto S, Takeuchi S. Changes in retinal pigment epithelium after indocyanine green-assisted internal limiting lamina peeling during macular hole surgery. *Am J Ophthalmol.* (2005) 140:752–5. doi: 10.1016/j.ajo.2005.04.035
31. Wolf S, Reichel MB, Wiedemann P, Schnurrbusch UEK. Clinical findings in macular hole surgery with indocyanine green-assisted peeling of the internal limiting membrane. *Graefes Arch Clin Exp Ophthalmol.* (2003) 241:589–92. doi: 10.1007/s00417-003-0673-1
32. Maia M, Margalit E, Lakhanpal R, Tso MO, Grebe R, Torres G, et al. Effects of intravitreal indocyanine green injection in rabbits. *Retina.* (2004) 24:69–79. doi: 10.1097/00006982-200402000-00011
33. Kwok AK, Lai TY, Yew DT, Li WW. Internal limiting membrane staining with various concentrations of indocyanine green dye under air in macular surgeries. *Am J Ophthalmol.* (2003) 136:223–30. doi: 10.1016/S0002-9394(02)02144-X
34. Pitas I. *Digital Image Processing Algorithms and Applications*. New York, NY: John Wiley & Sons (2000).
35. Haritoglou C, Eibl K, Schaumberger M, Mueller AJ, Priglinger S, Alge C, et al. Functional outcome after trypan blue-assisted vitrectomy for macular pucker: a prospective, randomized, comparative trial. *Am J Ophthalmol.* (2004) 138:1–5. doi: 10.1016/j.ajo.2004.03.005
36. Vote BJ, Russell MK, Joondeph BC. Trypan blue-assisted vitrectomy. *Retina.* (2004) 24:736–8. doi: 10.1097/00006982-200410000-00008
37. Bacsal KM, Chee SP. Trypan blue-associated retinal toxicity post complicated cataract surgery. *Eye.* (2006) 20:1310–1. doi: 10.1038/sj.eye.6702164

Conflict of Interest: The authors declare that the research was conducted in the absence of any commercial or financial relationships that could be construed as a potential conflict of interest.

frontiers in Medicine

ORIGINAL RESEARCH
published: 18 February 2022
doi: 10.3389/fmed.2021.750342

Oxymatrine Protects TGFβ1-Induced Retinal Fibrosis in an Animal Model of Glaucoma

*Ashmita Das[1], Onkar Kashyap[1], Amrita Singh[2], Jaya Shree[3], Kamta P. Namdeo[1] and Surendra H. Bodakhe[1]**

[1] Department of Pharmacology, SLT Institute of Pharmaceutical Sciences, Guru Ghasidas Vishwavidyalaya (A Central University), Bilaspur, India, [2] ISF College of Pharmacy, Moga, India, [3] Rungta Institute of Pharmaceutical Sciences and Research, Bhilai, India

Glaucoma has engulfed a huge population of the world into its claws of blindness as it remains asymptomatic until nearly 40% of the neurons are lost and the only option left is for patients to be subjected to symptomatic treatments or surgical methods, neither of which is completely effective in curing the disease as they do not restore the physiological dimensions at the neuronal level. Among the several factors that drive the pathophysiology of glaucoma, one is the involvement of fibrogenic factors, such as transforming growth factor β (TGFβ) which remodels the extracellular matrix (ECM) and, thus, the deposition of fibrotic material in the retina, resulting in the progression of primary open-angle glaucoma (POAG). The primary objectives of this study were to evaluate the protective effects of oxymatrine (OMT) in the steroid-induced glaucoma model in experimental rats and to determine the role of transforming growth factor β1 (TGFβ1) in the pathogenesis of glaucoma and its consequent inhibition due to the antioxidant and the antiinflammatory, and also the TGFβ1 antagonistic, behavior of OMT. To that end, we experimentally elucidated the role of OMT, a TGFβ1 antagonist, that is known to play antiinflammatory and antioxidant roles in the steroid-induced glaucoma model in experimental rats, and using the enzyme-linked immunosorbent assay (ELISA), we observed a direct inhibitory effect of OMT on the pathogenesis of glaucoma. The antioxidant and the antiinflammatory potentials of OMT were determined using several biochemical methods to determine the major antioxidants in the retinal layers, such as superoxide dismutase (SOD), glutathione peroxidase (GP_X), catalase (CAT), and glutathione (GSH), along with the nitrite and the malondialdehyde (MDA) concentration levels. As a result, OMT was found to reduce the total protein content in the retinal layers, a correlation that has not been previously reported. Moreover, the impacts of OMT on the major governing ATPases, namely Na^+/K^+ ATPase and Ca^{2+}ATPase, along with its impacts on the intracellular ionic concentrations of Na^+, K^+, and Ca^{2+}, were determined and were found to point toward OMT, restoring homeostasis in glaucomatous animals. A clearer picture of the changes during the treatment was obtained using retinal images of the live animals and of the lenticular changes in the sacrificed animal; these images provided data on the pathological pathways leading to glaucoma inception

OPEN ACCESS

Edited by:
Dong Ho Park, Kyungpook National University Hospital, South Korea

Reviewed by:
Ahmed Esmat Abdel Moneim, Helwan University, Egypt
Joanna Matowicka-Karna, Medical Univeristy of Bialystok, Poland
Regina Rodrigo, Principe Felipe Research Center (CIPF), Spain

***Correspondence:**
Surendra H. Bodakhe
drbodakhe@gmail.com

Specialty section:
This article was submitted to Ophthalmology, a section of the journal Frontiers in Medicine

Received: *30 July 2021*
Accepted: *18 November 2021*
Published: *18 February 2022*

Citation:
Das A, Kashyap O, Singh A, Shree J, Namdeo KP and Bodakhe SH (2022) Oxymatrine Protects TGFβ1-Induced Retinal Fibrosis in an Animal Model of Glaucoma. Front. Med. 8:750342. doi: 10.3389/fmed.2021.750342

and its consequent inhibition by OMT. The data reported in this study clearly indicate that OMT has a possible role in inhibiting the pathogenesis of glaucoma, and the data also permit the quantification of several biochemical parameters of concern.

Keywords: oxymatrine (OMT), TGFβ1, steroid induced glaucoma, retinal pathology, lenticular alterations, biochemical estimations

INTRODUCTION

Fibrotic disorders have been of increasing concern in the domain of ocular disorders, and the transforming growth factor β (TGFβ) plays a pivotal role in their progression. This multifunctional cytokine has been found to have a strong impact on the deposition and the expression of the extracellular matrix (ECM) and has been observed to be increased in aqueous humor (AH) and reactive optic nerve astrocytes of patients with primary open-angle glaucoma (POAG). TGFβ is a key player contributing to structural changes in the ECM of the trabecular meshwork (TM) and the optic nerve head (ONH), as characteristically seen in POAG, and TGFβ has a role in the production of protease inhibitors that hinder ECM degradation and cause an abnormal deposition of connective tissue that marks the onset of fibrotic disease (1–6). TGFβ1 has also been found to be elevated in the AH, along with TGFβ2, of patients with clinically active glaucoma and has also been found to be involved with the activation of thrombospondin-I *via* induction through dexamethasone (DEX) in TM cells, resulting in stress conditions (7). Moreover, TGFβ-mediated retinal fibrosis has been found to lead to an escalation in the intraocular pressure (IOP), which then causes pressure to be generated in the optic nerve neurons, as a result of which retinal ganglion cells (RGCs) die (8–10).

In the ONH, transforming growth factor β2 (TGFβ2)-induced changes are contributable to mechanobiological changes in the optic nerve axons that impair axonal transport and neurotrophic supply, thus leading to their continuous degeneration. The increase in the IOP further adds mechanical stress and strain to optic nerve axons and accelerates degenerative changes (11). Even though a variety of experimental findings have demonstrated the effective contribution of TGFβ2 in patients with glaucoma, the relationship between glaucoma and TGFβ1 has needed further investigation, which has led to the use of OMT, a TGFβ1 antagonist extracted from the roots of *Sophora flavescens Ait*, belonging to the family *Fabaceae* and a known savior for patients with fibrotic diseases (12–14).

Oxymatrine (OMT) has been chosen for this study because various researches and a literature review revealed it to be a potent inhibitor of TGFβ, an ECM protein extensively found in the TM and ONH and involved in the fibrotic pathway in glaucoma. Its accumulation in the TM causes mechanobiological alterations and finally leads to an increase in the IOP, subsequently contributing to glaucoma (8–10). In addition, OMT inhibits the inducible nitric oxide synthase (iNOS) and the nuclear factor kappa B, which are two important mediators of the inflammatory pathway associated with glaucoma progression (15, 16). OMT has further been found to inhibit the role of tumor necrosis factor alpha (TNFα), which enhances neurodegeneration by acting as a pressure enhancer on RGCs (15, 16). Even though the role of OMT in glaucoma retardation has yet to be reported, we here report, for the first time, that OMT may retard the development and the progression of glaucoma by acting on targets such as TGFβ and TNFα.

METHODS

Drug Solution and Dosing

Oxymatrine was obtained as a generous gift from Shaanxi Pioneer Biotech, China, whereas dorzolamide was purchased from Intas Pharmaceuticals Pvt. Ltd, India, and DEX from Alfa Aesar, Boston, USA. The other chemicals required for the biochemical analyses were purchased from various sources and were of standard analytical grade. The ELISA kit for TGFβ was purchased from Elabscience, Houston, TX, USA. A stock solution of 0.1% DEX was prepared by dissolving DEX in distilled water and filtering the solution in aseptic conditions. The resultant solution was administered to the animals four times daily for 21 days *via* the ophthalmic route at a dose of 100 μl or 0.1 ml per topical application (17). A stock solution of 1% OMT was prepared in distilled water, and consequent dilutions were made to produce solutions with 0.5 and 0.25% concentrations of OMT. The aseptically filtered solutions were administered to the animals once daily *via* the ophthalmic route at a dose of 50 μl per topical application for 21 days after the occurrence of DEX-induced glaucoma (18). All the ophthalmic solutions were prepared under aseptic conditions and finally filtered two times in an aseptic zone.

Experimental Animals

Experiments were carried out on male and female Sprague-Dawley rats, 8 to 10 weeks of age and weighing from 100 to 120 g, obtained from Chakraborti Enterprise, Narkeldanga, Kolkata- 700011, India. Before experimentation, the procedures were formally reviewed and approved by the Institutional Animal Ethics Committee (IAEC) (register number: 994/GO/Re/S/06/CPCSEA and reference number: 275/Pharmacy/2020) as per the guidance of the Committee for the Purpose of Control and Supervision for Experiments on Animals (CPCSEA), Government of India.

Experimental Design

Animals with normal IOPs and no visible ocular disturbances were chosen for the study and were randomly allotted to different experimental groups, with six animals in each group. During the experimental protocol, the animals in the normal group received distilled water at a dose of 100 μl, topical, for 15 days. Uveitic glaucoma was induced in animals by the administration of DEX

(0.1 ml of 0.1% solution, topical, i.e., ophthalmic route, four times daily, for 21 consecutive days) (17). The experimental animals allotted for the treatment groups received OMT at doses of 50 μl of 0.25, 0.5, or 1% solution once daily for 15 days *via* the topical route of administration. The experimental animals in the standard group were administered 100 μl of 1% of dorzolamide daily for 15 days *via* the topical route (19).

Evaluation of Intraocular Pressure

Before the inducing agent or the treatments were to be applied, we, with the help of a Tono-Pen tonometer (Reichert Technologies, Depew, USA), regularly checked the experimental rats for the degree of IOP generated in the eyes. To create a baseline, we checked all the rats for IOP before administration of the drugs; thereafter, we regularly checked the animals until the day of sacrifice (20).

Determination of the Lenticular Opacity

Assessment of the lenticular opacity was conducted through a photographic technique where the isolated lenses were washed immediately in double-distilled water and placed on graph paper. Photographs of the lenses were then taken using a cell phone camera (Photron Universal, Maharashtra, India) (21).

Picturization of the Retinal Images of the Experimental Rats

The experimental rats were exposed to anesthesia, and their retinas were picturized using fundoscopic examination with a Panoptic ophthalmoscope (Welch Allyn, Skaneateles Falls, USA), in which the retina was illuminated through the pupil (22).

Isolation of the Retinas and the Lenses From the Experimental Rats

The experimental rats were sacrificed using a high dose of anesthesia, after which the lenses and retinas were isolated using a posterior approach, washed with cold saline, and dried on a filter paper. The weighed retinas were homogenized with a 0.1-M phosphate buffer in nine volumes and centrifuged at 15,000 rpm for 5 min at 2°C−8°C using a refrigerated centrifuge (23). The supernatant was separated and utilized for further biochemical analysis with the help of a UV-visible spectrophotometer (Shimatzu, Japan).

Quantitative Estimates of the Antioxidants in the Retinal Layers

The concentrations of antioxidant, including CAT, SOD, GSH, and GP_X, were spectrophotometrically estimated, and the levels of lipid-layer damage were quantified using the MDA content in the retinal layers. The method detailed by Sinha (1972) was adopted for the determination of the CAT activity, which was measured using the rate of decomposition of hydrogen peroxide (H_2O_2) to water (H_2O) and was measured at 530 nm against a blank. The CAT activity was expressed as μM of H_2O_2consumed/min/mg protein (24). The activity of SOD in the biological samples was calculated based on photoinhibition of nitro blue tetrazolium (NBT). The enzymatic activity of SOD was recorded as U/mg, where one unit (U) of SOD describes the number of enzymes that have effectively reduced the photoreduction rate of NBT to 50% (25). The activity of the GPx was assayed using the methods described by Tappel (1978), which is a prime requisite for the catalyzed reduction in GSH into GSH and water in the presence of H_2O_2 and is expressed as μM of GSH oxidized/min/mg protein (26). Ellman's reagent was used to estimate the GSH level. The reaction between GSH and Ellman's reagent [(27), 5'-dithiobis (2-nitrobenzoic acid)] displays a yellow-colored product that was read at 412 nm spectrophotometrically (28). Lipid peroxidation was denoted as an analytical parameter for the damage inherited by the lipid bilayer and was quantified using the MDA content in the sample. The method defined by Ohkawa et al. (29) was used to estimate MDA levels during the course of its reaction with thiobarbituric acid (TBA). The consequent reaction between TBA and MDA produced a colored, stable chromogen product that was measured at 532 nm. The MDA content was expressed as nM/mg protein (29).

Estimates of Nitrite Levels

Assessment of the nitrite content in the retinal samples was performed following the method described by Green et al. (30). Sodium nitrite was utilized for the preparation of the standard curve. Nitrite content was expressed in nmoles/mg (30).

Quantitative Estimates of the Total Protein Content in the Retinal Layers

The total protein content in the retinal lysate was measured using the procedure penned down by Lowry et al. (31).

Quantitative Estimates of the Na^+/K^+ Atpase and the Ca^{2+}Atpase Activities in the Retinal Layers

The Na^+/K^+ ATPase and Ca^{2+}ATPase activities of the retina were quantified by employing the method of Manikandan et al. (32).

Estimates of the Ionic Contents

Isolated retinas were washed with cold distilled water and homogenized (1 % w/v) with distilled water. The homogenate was filtered, and the ionic contents were estimated. The Na^+, K^+, and Ca^{2+} contents in the samples were determined by spectrophotometry with diagnostic kits as per the procedure mentioned by Labcare Diagnostics Pvt. Ltd., India.

Estimates of TGFβ Levels in the Retinal Layers Using the ELISA

Commercially available and precoated ELISA kits (Elabscience, USA) were used for the *in vitro* quantitative determination of rat TGFβ concentrations in the retinal homogenates as per the manufacturer's instructions.

Statistical Analysis

All statistical analyses were performed using GraphPad Instat® (version 5.0) software, and the results were expressed as means ± standard errors of the mean (SEMs). A one-way ANOVA, followed by the Newmann–Keuls test, was used for comparing

TABLE 1 | Effect of OMT on the IOP.

Groups	Average IOP (mmHg)			
	Day zero	Day seven	Day fourteen	Day twenty-one
100 μl of distilled water(Normal)	19.67 ± 1.35	16.33 ± 0.66	17.50 ± 1.33	17.50 ± 1.33
100 μl of 0.1% DEX solution(DEX-induced glaucoma control)	20.50 ± 0.76	35.33 ± 0.42^{c}	42.17 ± 0.79^{c}	47.33 ± 0.667^{c}
50 μl of 0.25% OMT solution (treatment 1)	20.33 ± 1.05	27.17 ± 1.47^{ce}	24.33 ± 1.47^{bfi}	17.83 ± 0.70^{fi}
50 μl of 0.5% OMT solution(treatment 2)	20.50 ± 1.11	26.33 ± 2.70^{ce}	18.50 ± 0.76^{fi}	17.00 ± 0.57^{fi}
50 μl of 1% OMT solution(treatment 3)	21.67 ± 1.62	24.33 ± 1.76^{bfg}	17.33 ± 0.66^{fi}	17.00 ± 0.57^{fi}
100 μl of the commercial dose of dorzolamide solution(standard)	21.00 ± 0.73	32.00 ± 1.67^{c}	31.17 ± 1.81^{cf}	28.83 ± 1.13^{cf}

Values are expressed as means ± SEMs (n = 6). Data were analyzed using the two-way ANOVA, followed by Bonferroni's post hoc test and are expressed as $^{a}p < 0.05$, $^{b}p < 0.01$, and $^{c}p < 0.001$ when compared to the normal group, $^{d}p < 0.05$, $^{e}p < 0.01$, and $^{f}p < 0.001$ when compared to glaucoma control group, and $^{g}p < 0.05$, $^{h}p < 0.01$, and $^{i}p < 0.001$ when compared to the standard group. The values are expressed as non-significant values. ^{a,d,h}All the three represent comparisons made to the other groups with the normal group.

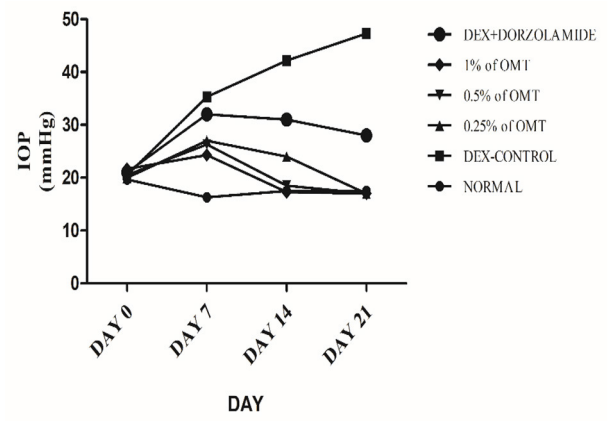

FIGURE 1 | Effects over time on the IOP. Values are expressed as mean (n = 6). Data were analyzed by two-way ANOVA followed by Bonferroni's *post hoc* test. Normal: 100 μl of distilled water; control: 0.1 ml of 0.1% DEX solution; treatment 1: 50 μl of 0.25% OMT solution; treatment 2: 50 μl of 0.5% OMT solution; treatment 3: 50 μl of 1% OMT solution; standard: 100 μl of 1% of dorzolamide solution.

the means of the different groups; similarly, a two-way ANOVA, followed by Bonferroni's test, was used for analyzing the data. The criterion for statistical significance was set at the $^{*}p < 0.05$, $^{**}p < 0.01$, and $^{***}p < 0.001$.

RESULTS

Effects on IOP

The experimental rats were regularly checked, with the help of the Tono-Pen tonometer (Reichert Technologies, Depew, USA), for the degree of IOP generated in the eyes. The IOP changes were recorded as the means of weekly changes and are represented in **Table 1** and **Figure 1**.

Administration of DEX to the animals in the glaucoma control group, as compared to the normal group, produced a significant ($p < 0.001$) elevation in the IOP approximately from the seventh day to the end of the experimental protocol. Topical administration of OMT at a 50-μl dose of 0.25, 0.5, or 1% notably inhibited the advance of IOP as compared to DEX-induced glaucoma control group and the standard group, ($p < 0.001$ and $p < 0.001$), respectively, in a time-dependent manner. After seven days of topical OMT administration at doses of 50 μl of 0.25% and 50 μl of 0.5%, a significant fall in the IOP was noted ($p < 0.001$) in comparison with the control group, whereas the group receiving treatment 3, that is, the group treated with 50 μl of 1% OMT, showed the best results in controlling the IOP in comparison with both the control and the standard groups, $p < 0.001$ and $p < 0.01$, respectively. From the 14 day to the 21st day of OMT administration, all three doses exhibited excellent control of the IOP, along with concurrent normalization of the IOP, when compared to the control and the standard groups, $p < 0.001$ and $p < 0.001$, respectively.

Effects on Oxidative Stress Markers in Retinal Extracts

Effects on Antioxidants

In the DEX-induced glaucoma control group, the levels of antioxidants, such as CAT, SOD, GPx, and GSH, were found to be decreased notably as compared to the normal group ($p < 0.001$) (**Figures 2A–D**). Subsequently, treatment with various doses of OMT resulted in a significant buildup in the levels of retinal antioxidants in contrast to the glaucoma control group. Two weeks of OMT administration at a dose of 50 μl of 0.25% OMT led to significant increases in some of the antioxidant levels, such as CAT ($p < 0.001$, $p < 0.001$, $p < 0.001$) and SOD ($p < 0.001$, $p < 0.01$, $p < 0.001$) when compared to the normal, glaucoma control, and standard groups, respectively, GPx ($p < 0.001$, $p < 0.001$) when compared to the glaucoma control and the standard groups, respectively, and GSH ($p < 0.001$, $p < 0.001$) when compared to the normal and standard groups, respectively, but with no significant variations from the glaucoma control group. The administration of 50 μl of 0.5% OMT led to marked increase in the antioxidant levels of CAT ($p < 0.001$, $p < 0.001$, $p < 0.001$), SOD ($p < 0.001$, $p < 0.001$, $p < 0.001$), GPx ($p < 0.05$, $p < 0.001$), and GSH ($p < 0.001$, $p < 0.01$, $p < 0.01$) when compared to the normal, glaucoma control, and standard groups, respectively. The administration of the highest dose of treatment, that is, 50 μl of 1% OMT, produced the most notable rises in the levels of the antioxidants in the retinal layers: CAT ($p < 0.001$, $p < 0.001$, $p < 0.001$), SOD ($p < 0.001$, $p < 0.001$, $p < 0.001$), and GPx ($p < 0.05$, $p < 0.001$, $p < 0.001$) when compared to the normal,

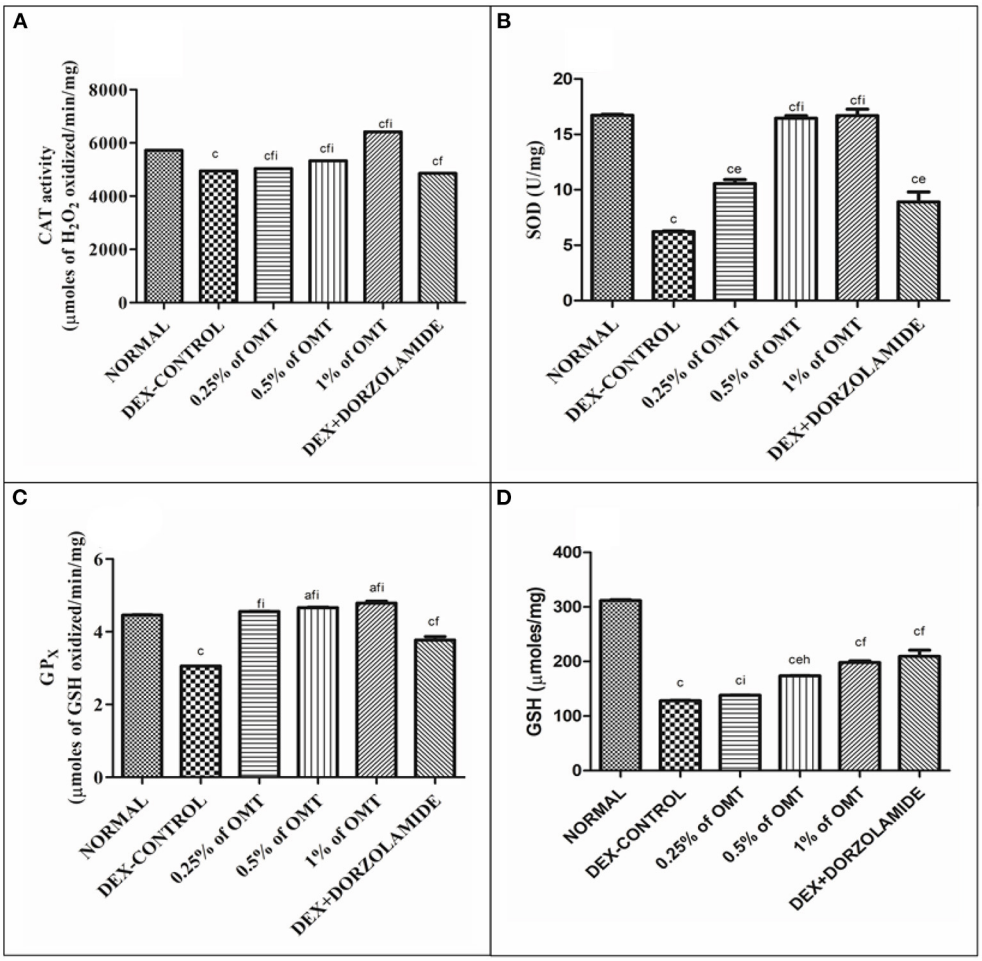

FIGURE 2 | Effects of various treatments of OMT on the levels of antioxidants: **(A)** CAT, **(B)** SOD, **(C)** GPX, and **(D)** GSH. Values are expressed as mean ± SEM (n = 6). Data were analyzed by one-way ANOVA and are expressed as ap < 0.05, bp < 0.01, cp < 0.001 when compared to normal group, dp < 0.05, ep < 0.01, fp < 0.001 when compared to DEX-induced glaucoma control group, and gp < 0.05, hp < 0.01, and ip < 0.001 when compared to standard group, respectively. Normal: 100 μl of distilled water; control: 0.1 ml of 0.1% DEX solution; treatment 1: 50 μl of 0.25% OMT solution; treatment 2: 50 μl of 0.5% OMT solution; treatment 3: 50 μl of 1% OMT solution; standard: 100 μl of 1% of dorzolamide solution.

glaucoma control, and standard groups, respectively, and GSH ($p < 0.001$, $p < 0.001$) when compared to the normal and glaucoma control groups, respectively with no significant variations from the standard group.

Effects of Various Treatments on Lipid Peroxidation and Nitrite Content in the Retinal Layers

The results (**Figures 3A,B**) demonstrate that the DEX control group significantly ($p < 0.001$) increased the MDA and nitrite content in the retina as compared to the normal group. The two weeks of OMT administration at the dose of 50 μl of 0.25% OMT led to a significant slash in the levels of lipid peroxidation quantified by the levels of MDA ($p < 0.001$, $p < 0.01$, $p < 0.001$) and nitrite ($p < 0.001$, $p < 0.001$, $p < 0.001$) as compared to the normal group, glaucoma control, and standard groups, respectively. 50μl of 0.5% OMT administration showed marked reduction in the levels of MDA ($p < 0.001$, $p < 0.001$, $p < 0.001$) and nitrite ($p < 0.001$, $p < 0.001$, $p < 0.001$) as compared to the normal group, glaucoma control, and standard groups, respectively. The highest dose of treatment, that is, 50μl of 1% OMT, exhibited the most notable decline in the levels of MDA ($p < 0.001$, $p < 0.001$, $p < 0.001$) and nitrite ($p < 0.001$, $p < 0.001$, $p < 0.001$) when compared to the normal group, glaucoma control, and standard groups, respectively. The standard group also displayed significant decline in the MDA levels ($p < 0.001$, $p < 0.001$) while a large increase exhibited in the nitrite concentrations ($p < 0.001$, $p < 0.001$) in the retinal layers when compared to the normal and glaucoma control groups, respectively.

Effects of Various Treatments on Retinal Protein Contents

The results (**Figure 4**) exhibit the remarkable remodeling of the total protein content in the retinal layers of the various experimental groups. The DEX control group significantly ($p < 0.001$) increased the total protein content in the lens as compared

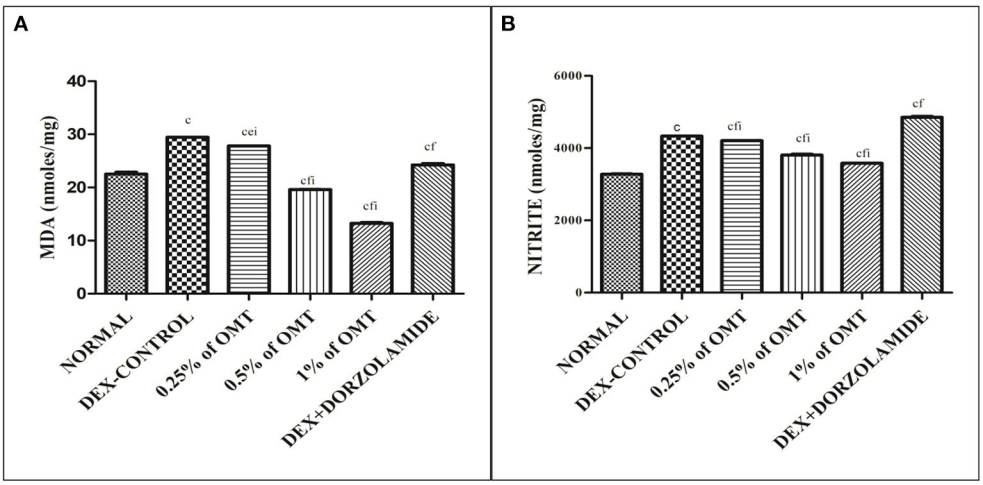

FIGURE 3 | Effects of various treatments on lipid peroxidation and nitrite content in the retinal extracts: **(A)** MDA and **(B)** nitrite. Values are expressed as mean ± SEM ($n = 6$). Data were analyzed by one-way ANOVA and are expressed as $^{a}p < 0.05$, $^{b}p < 0.01$, $^{c}p < 0.001$ when compared to normal group, $^{d}p < 0.05$, $^{e}p < 0.01$, $^{f}p < 0.001$ when compared to DEX-induced glaucoma control group, and $^{g}p < 0.05$, $^{h}p < 0.01$, $^{i}p < 0.001$ when compared to standard group, respectively. Normal: 100 μl of distilled water; control: 0.1 ml of 0.1% DEX solution; treatment 1: 50 μl of 0.25% OMT solution; treatment 2: 50 μl of 0.5% OMT solution; treatment 3: 50 μl of 1% OMT solution; standard: 100 μl of 1% of dorzolamide solution.

to the normal group. The two weeks of OMT administration at the dose of 50 μl of 0.25% OMT and 50 μl of 0.5% OMT in each of the respective experimental groups lead to a notable plunge in the levels of the total protein content ($p < 0.001$, $p < 0.05$) of the retinal layers, whereas treatment with 50 μl of 1% OMT led to an even more prominent decline in the protein content ($p < 0.001$, $p < 0.01$) as compared to the glaucoma control and standard groups respectively with no significant variation from the normal group. The standard group, however, raised the bar of the total protein concentration in the retinal layers ($p < 0.05$) when compared to the normal group but managed to reduce it significantly ($p < 0.001$) when compared to the glaucoma control group.

Effects of Various Treatments on ATPase Activity in the Retinal Extracts

Figures 5A,B reveal that the animals in the DEX control group had significantly ($p < 0.001$) increased Na^+/K^+ ATPase in their retinal layers, as compared to the normal group. Two weeks of OMT administration at a dose of 50 μl of 0.25% OMT led to a significant reduction in the levels of Na^+/K^+ ATPase ($p < 0.001$, $p < 0.001$, $p < 0.001$) and Ca^{2+}ATPase ($p < 0.001$, $p < 0.001$, $p < 0.001$) as compared to the normal, glaucoma control, and standard groups, respectively. Administration of 50 μl of 0.5% OMT led to an even more notable decline in the levels of Na^+/K^+ ATPase ($p < 0.001$, $p < 0.001$, $p < 0.001$) and Ca^{2+}ATPase ($p < 0.01$, $p < 0.001$, $p < 0.001$), as compared to the normal, glaucoma control, and standard groups, respectively. The treatment with the highest dose, that is, 50 μl of 1% OMT, led to the largest declines in the levels of Na^+/K^+ ATPase ($p < 0.001$, $p < 0.001$, $p < 0.001$) and Ca^{2+}ATPase ($p < 0.001$, $p < 0.001$, $p < 0.001$), as compared to the glaucoma control and standard groups, respectively. In the standard group, the levels of Na^+/K^+ ATPase and Ca^{2+}ATPase ($p < 0.001$, $p < 0.001$) were evidently reduced, as compared to the normal and glaucoma control groups, respectively.

Effects of Various Treatments on Na^+, K^+, Ca^{+2} ion Activities in the Retinal Extracts

Figures 6A–C reveal that the animals in the DEX control group had significantly increased Na^+ ($p < 0.01$), K^+ ($p < 0.001$), and Ca^{+2} ($p < 0.001$) in their retinal layers, as compared to the normal group, respectively. Two weeks of OMT administration at a dose of 50 μl of 0.25% OMT led to a significant reduction in the levels of Na^+ ($p < 0.01$, $p < 0.001$, $p < 0.001$), K^+ ($p < 0.001$, $p < 0.05$, $p < 0.001$), and Ca^{2+} ($p < 0.001$, $p < 0.05$), as compared to the normal, glaucoma control, and standard groups, respectively. The group receiving 50 μl of 0.5% OMT recorded remarkable drops in the levels of Na^+ ($p < 0.001$, $p < 0.001$, $p < 0.01$), K^+ ($p < 0.001$, $p < 0.001$, $p < 0.001$), and Ca^{2+} ($p < 0.001$, $p < 0.001$, $p < 0.001$), as compared to the normal, glaucoma control, and standard groups, respectively. The highest dose of treatment, that is, 50 μl of 1% OMT, led to the most notable decline in the levels of Na^+ ($p < 0.001$, $p < 0.001$, $p < 0.001$), K^+ ($p < 0.05$, $p < 0.001$, $p < 0.001$), and Ca^{2+} ($p < 0.001$, $p < 0.001$, $p < 0.001$), as compared to the glaucoma control and standard groups, respectively.

Effects of OMT on the Expression of TGFβ1

The animals in the DEX control group exhibited gigantic rises ($p < 0.001$) in the expression of TGFβ1 in their retinal layers, as compared to the normal group while dose-dependent decline in the expressions of TGFβ1 was observed in the various groups of animals treated with OMT (**Figure 7**). The animals that received a dose of 50 μl of 0.25% OMT demonstrated a notable inhibition ($p < 0.001$) when compared to the glaucoma control group, but had significantly higher expression ($p < 0.001$) when compared to the normal group; the animals that received a dose of 50 μl of

0.5% OMT exhibited sizable declines ($p < 0.001$) when compared to the control group, but failed to achieve normal levels ($p < 0.01$). The experimental animals that were treated with a dose of 50 μl of 1% OMT demonstrated the most notable fall in the TGFβ1 levels ($p < 0.001$, $p < 0.001$) when compared to the glaucoma control and standard groups, respectively. The most astonishing feature in the group of animals receiving 50 μl of 1% OMT was the restoration of normal levels of TGFβ1 in the retinal layers, which points to rehabilitation of homeostasis using OMT against dorzolamide, which was unable to restore normal levels of TGFβ1 in the retinal layers.

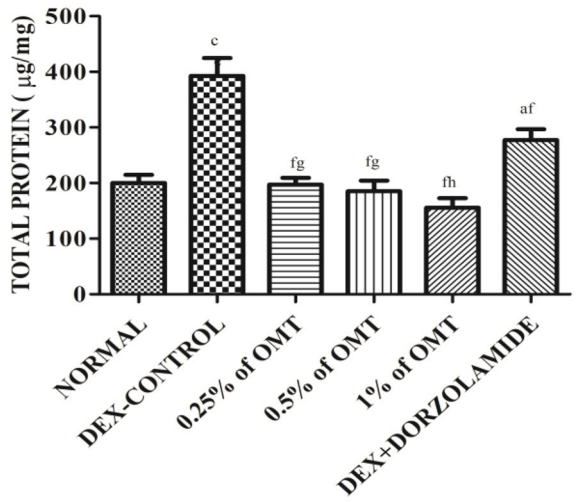

FIGURE 4 | Effects of various treatments on the retinal protein extracts. Values are expressed as mean ± SEM ($n = 6$). Data were analyzed by one-way ANOVA and are expressed as $^{a}p < 0.05$, $^{b}p < 0.01$, $^{c}p < 0.001$ when compared to normal group, $^{d}p < 0.05$, $^{e}p < 0.01$, $^{f}p < 0.001$ when compared to DEX-induced glaucoma control group, and $^{g}p < 0.05$, $^{h}p < 0.01$, $^{i}p < 0.001$ when compared to standard group, respectively. Normal: 100 μl of distilled water; control: 0.1 ml of 0.1% DEX solution; treatment 1: 50 μl of 0.25% OMT solution; treatment 2: 50 μl of 0.5% OMT solution; treatment 3: 50 μl of 1% OMT solution; standard: 100 μl of 1% of dorzolamide solution.

Effects of OMT on the Retinal Structure and Visual Field

The animals in the DEX-induced group exhibited a deposited fibrous network in the retinal vasculature, along with an increase in the lenticular opacity. The animals receiving 0.25% of OMT showed slight declines in amounts of the deposited fibrous network and in the lenticular opacity, as compared to the glaucoma control group whereas the group receiving 0.5% of OMT showed significant falls in amounts of deposited fibrous network deposition and subsequent increased clarity of the lens, as compared to the glaucoma control and standard group. The group receiving 1% of OMT exhibited complete restoration of the retinal vasculature, along with significant clarity of the lens, as compared to the glaucoma control and standard group (**Figure 8**).

DISCUSSION

Steroids are a class of antiinflammatory agents that find use in several systemic manifestations. Overindulgence in the application of topical or systemic steroids, however, is known to contribute to glaucomatous conditions, which can be detected by an increase in the IOP. Steroids, such as DEX, prednisolone, and others, are known to alter the ECM in ocular tissues *via* various pathways (7, 17, 27, 33–36). Inhibition of lysosomal

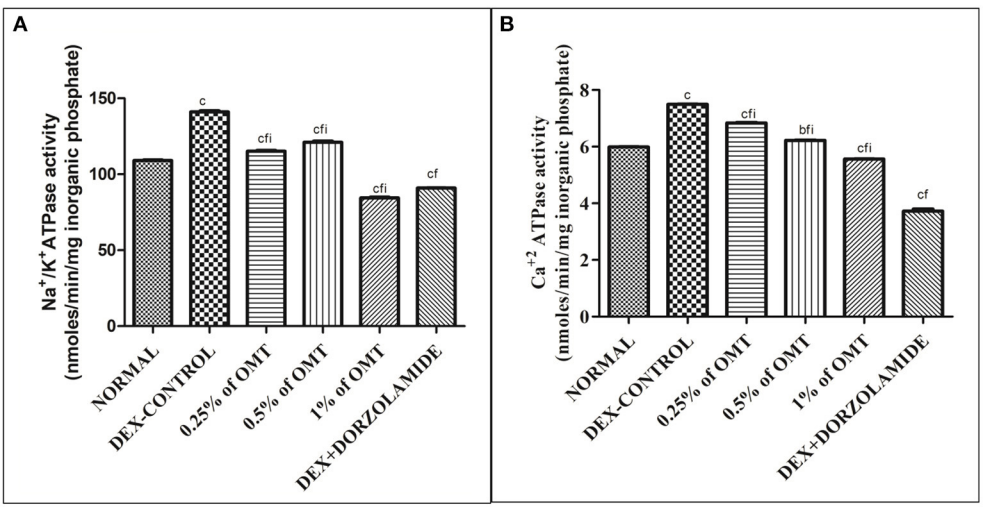

FIGURE 5 | Effects of various treatments on the ATPase activity in the retinal layers: **(A)** Na^{+}/K^{+} ATPase and **(B)** Ca^{+2} ATPase. Values are expressed as mean ± SEM ($n = 6$). Data were analyzed by one-way ANOVA and are expressed as $^{a}p < 0.05$, $^{b}p < 0.01$, and $^{c}p < 0.001$ when compared to normal group, $^{d}p < 0.05$, $^{e}p < 0.01$, and $^{f}p < 0.001$ when compared to DEX-induced glaucoma control group, and $^{g}p < 0.05$, $^{h}p < 0.01$, and $^{i}p < 0.001$ when compared to standard group, respectively. Normal: 100 μl of distilled water; control: 0.1 ml of 0.1% DEX solution; treatment 1: 50 μl of 0.25% OMT solution; treatment 2: 50 μl of 0.5% OMT solution; treatment 3: 50 μl of 1% OMT solution; standard: 100 μl of 1% of dorzolamide solution.

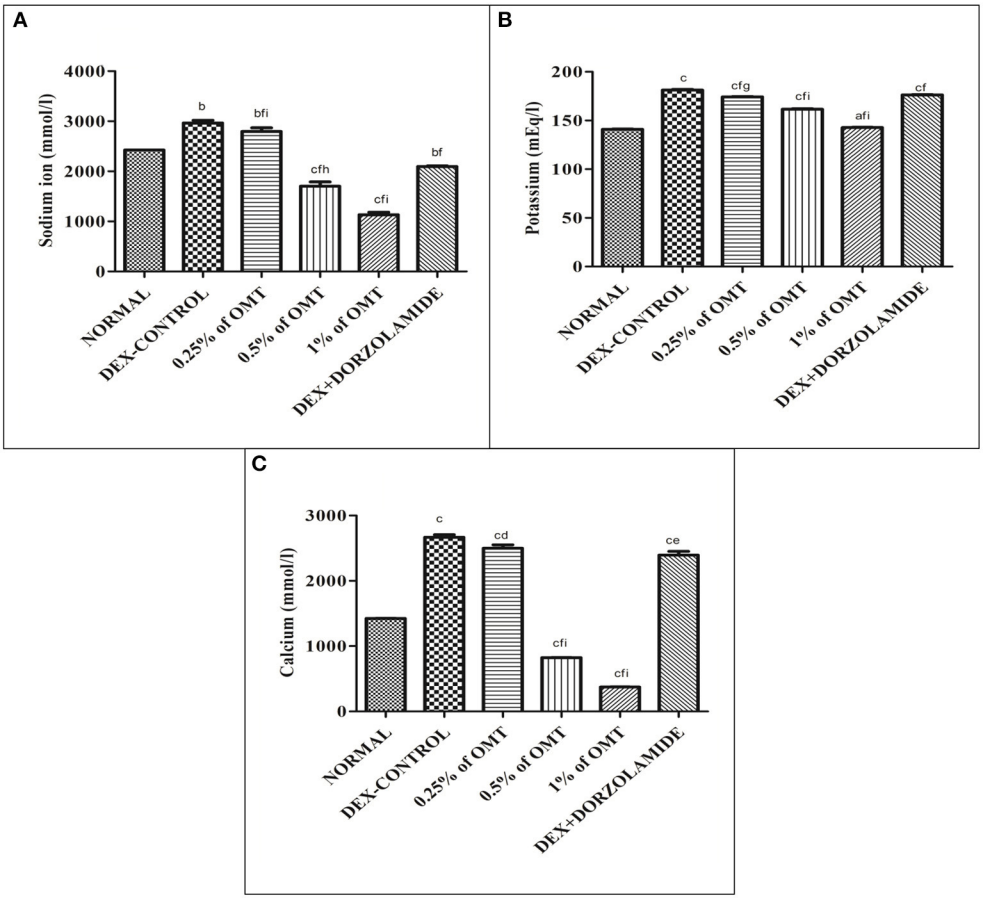

FIGURE 6 | Effects of various treatments on **(A)** Na^+, **(B)** K^+, **(C)** Ca^{+2} ion activities in the retinal extracts. Values are expressed as mean ± SEM ($n = 6$). Data were analyzed by one-way ANOVA and are expressed as $^{a}p < 0.05$, $^{b}p < 0.01$, $^{c}p < 0.001$ when compared to normal group, $^{d}p < 0.05$, $^{e}p < 0.01$, $^{f}p < 0.001$ when compared to DEX-induced glaucoma control group, and $^{g}p < 0.05$, $^{h}p < 0.01$, $^{i}p < 0.001$ when compared to standard group, respectively. Normal: 100 μl of distilled water; control: 0.1 ml of 0.1% DEX solution; treatment 1: 50 μl of 0.25% OMT solution; treatment 2: 50 μl of 0.5% OMT solution; treatment 3: 50 μl of 1% OMT solution; standard: 100 μl of 1% of dorzolamide solution.

hyaluronidase by steroids and the resultant activation of TGFβ is the key to retarding ECM degradation and enhancing fibrillar materials in the ocular vasculature with further benefaction into biological edema following a decline in the radius of the TM, thus causing an increase in the IOP (7, 17, 33, 36).

In this study, DEX (0.1%) was topically administered to the animals in the glaucoma control group four times daily at a dose of 0.1 ml for 21 days, and a significant hike in the IOP was noted, which is consistent with the results of studies previously conducted on humans and animals (5, 17, 34, 35). Diverse mechanisms have been used to explain the amplification of IOP by DEX. DEX increases the concentrations of thrombospondin I, integrin, laminin, and fibronectin, all of which happen to activate TGFβ signaling in ocular tissues, resulting in persistent fibrosis *via* cell–matrix interactions (7, 17, 27). In addition to its effects on the ECM, DEX can induce the activation of the endoplasmic reticulum and Golgi apparatus, finally boosting the DNA content in the TM. Modeling new channel debris due to reduced phagocytic activities at the TM further results in delayed clearance of the ocular vasculature, thus finally giving a clear picture of IOP enhancement (33, 36). The DNA damage caused by DEX administration enhances the release of reactive oxygen species (ROS) that further function in the activation and signaling of TGFβ (17, 37).

Dexamethasone administration in glaucomatous rats resulted in a steady amplification of the IOP whereas OMT administration resulted in a significant decline in and consequent normalization of the same. The treatment groups achieved IOP values similar to that found in the normal group, almost diminishing the effects of DEX; although the standard treatment did help reduce the IOP compared to the control group, it could not normalize the IOP value, thus clearly indicating the increased efficacy of OMT treatment when compared to dorzolamide treatment, even though the dorzolamide administered was a commercial preparation formulated with penetration enhancers. IOP regulation, however, is not the only requisite for inhibiting the progression of glaucoma; hence, biochemical parameters

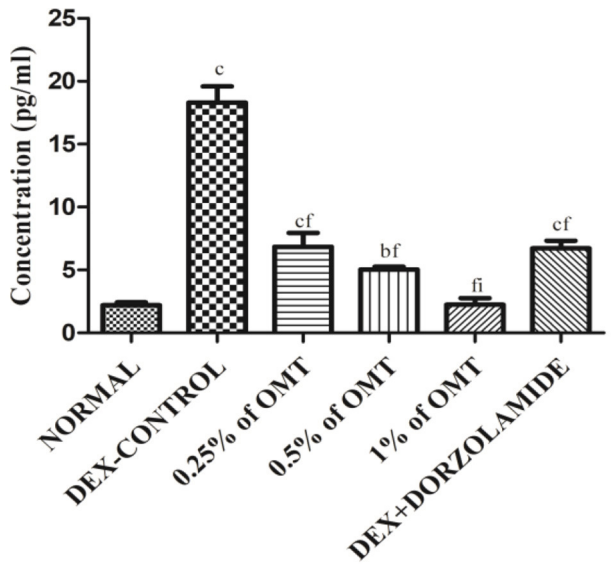

FIGURE 7 | Effects of OMT on the expression of TGFβ1. Values are expressed as mean ± SEM ($n = 6$). Data were analyzed by one-way ANOVA and are expressed as $^{a}p < 0.05$, $^{b}p < 0.01$, $^{c}p < 0.001$ when compared to normal group, $^{d}p < 0.05$, $^{e}p < 0.01$, $^{f}p < 0.001$ when compared to DEX-induced glaucoma control group, and $^{g}p < 0.05$, $^{h}p < 0.01$, $^{i}p < 0.001$ when compared to standard group, respectively. Normal: 100 μl of distilled water; control: 0.1 ml of 0.1% DEX solution; treatment 1: 50 μl of 0.25% OMT solution; treatment 2: 50 μl of 0.5% OMT solution; treatment 3: 50 μl of 1% OMT solution; standard: 100 μl of 1% of dorzolamide solution.

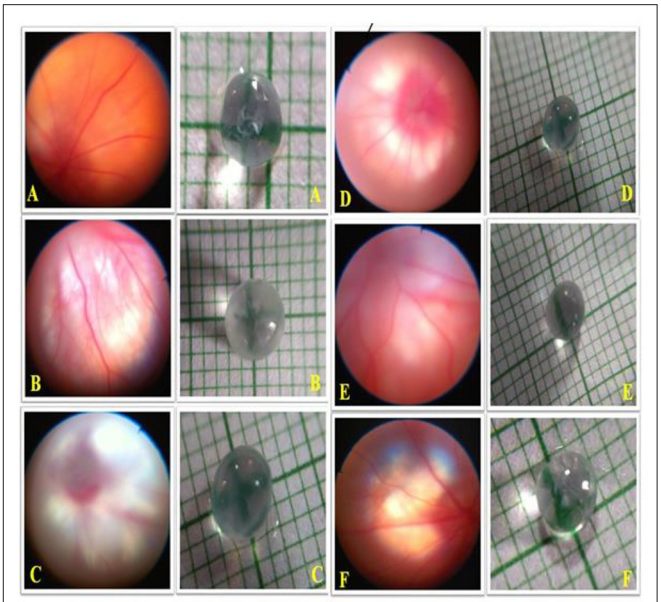

FIGURE 8 | Effects of OMT on the retinal structure and visual field. Normal group: **(A)** normal retinal vasculature along with normal visual field as indicated by lens opacity; **(B)** glaucoma control group: evident retinal fibrosis along with bilateral opacity in the lens upon DEX exposure; **(C)** standard group: restoration of retinal vasculature, however, without efficient detangling of the blood vessels and reduction in opacity as compared to the control group; **(D)** treatment 1 group: retinal fibrosis still evident with opacity in the lens; **(E)** treatment 2 group: significant restoration of retinal vasculature along with betterment in the visual field as indicated by the decline in lens opacity; **(F)** treatment 3 group: proper restoration of the retinal vasculature along with optimum lens clarity. Normal: 100 μl of distilled water; control: 0.1 ml of 0.1% DEX solution; treatment 1: 50 μl of 0.25% OMT solution; treatment 2: 50 μl of 0.5% OMT solution; treatment 3: 50 μl of 1% OMT solution; standard: 100 μl of 1% of dorzolamide solution.

and histopathology were investigated to determine the safest and most effective dose of OMT to inhibit the progression of glaucoma.

The activation of TGFβ, especially TGFβ1, leads to the concurrent downregulation of endogenous antioxidants such as GSH, SOD, GP_X, CAT, and ascorbic acid *via* a significant inhibitory impact on the mitochondrial membrane potential while simultaneously enhancing the ROS production that fosters an immediate reduction in the protective mechanisms of the TM cells and facilitates damage to the optic nerve disc and astrocytes (15, 19, 38, 39). All these effects that induced during the progression of glaucoma by DEX denote the withdrawal of the salubrious impacts of the antioxidant system and, thus, clearly define the role of DEX in TGFβ activation and the emergence of glaucoma in the glaucoma control group (40–45).

These studies denote the beneficial impacts of OMT administration on the glaucomatous experimental rats. OMT administration enhances the effects of various antioxidant systems, such as CAT, SOD, GP_X, and reduced GSH, present in the retinal layers while significantly delaying and reducing the rates of lipid peroxidation, as denoted by the decline in the MDA and the nitrite levels. Dorzolamide, being the standard drug candidate in this study, has been observed to heighten the nitrite levels, which is due to its effects on vasodilation mediated *via* the evolution of nitric oxide from nitrite. Dexamethasone, primarily being an antiinflammatory agent, does not crucially affect the nitrite levels when compared to its effects on other pathological enhancers; however, OMT has still been noticed to lower the nitrite levels to retard the generation of nitric oxide, thus clarifying its effects as an antiinflammatory agent. Oxymatrine has been studied to include various toxic molecules generated by TGFβ activation, thus reducing the consumption of antioxidant systems and their consequent elevations in diseased tissues (46). The profound antioxidant effects exerted by OMT further help to delay the rates of lipid peroxidation *via* inhibition of the MDA and the nitrite contents (12, 47). The antioxidant ability of OMT can be attributed to its chemical structure in which its oxygen atoms readily combine with the hydroxyl radicals in the diseased cells and function as a free radical scavenger, thus increasing the concentration of antioxidant systems and consequently decreasing the number of the ROS-activating agents, further inhibiting the generation of an immune response (12).

The total protein concentration is a crucial part of the AH drainage facility and has been shown to be increased in concentration in the glaucoma control group, suggesting a disruption in the optimum flow of AH. Though none of the studies previously conducted have reported any relationship

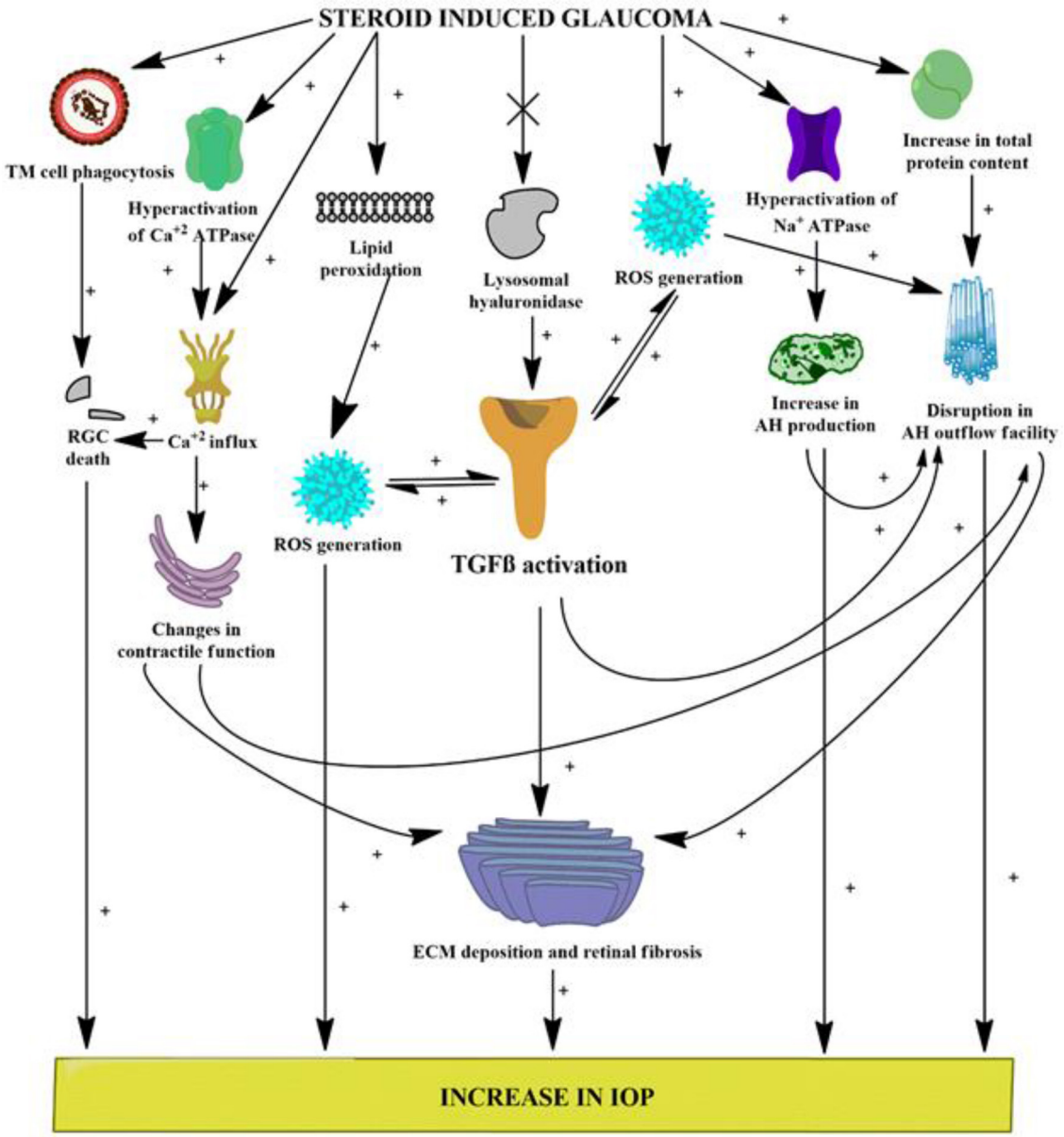

FIGURE 9 | Various possible targets served by DEX administration leading to glaucomatous conditions. [(+) indicates activation or increase; (x) indicates inhibition or decrease]. ROS, reactive oxygen species; RGCs, retinal ganglion cells; AH, aqueous humor; IOP, intraocular pressure; TGFβ, transforming growth factor β; iNOS, inducible nitric oxide synthase.

between OMT administration and the total protein content, studies have reported its efficacy in lowering the levels of matrix metalloproteinases (MMPs) and albumin, both of which are found to be upregulated in the retinal layers during glaucoma and are important regulators of the AH outflow facility (48, 49). Furthermore, TGFβ1 is known to elevate the levels of MMPs in the retinal layers and to provide systematically a distinct view of the relationship between TGFβ1 activation and the occurrence of fibrotic tangles (50). In this study, topical administration of OMT resulted in a profound reduction in the total protein concentration, thus emphasizing the antifibrotic effects of OMT, which has found a perfect role in decreasing the fibrogenic material deposited in the ECM (12).

Previously conducted studies have reported the effects of DEX in enhancing the Na^+/K^+ ATPase *via* an increase in the phosphorylation and subsequent endocytosis, thereby enhancing the pump function and increasing the AH production with an already depressed outflow facility, finally amplifying the IOP and the consequent increase in the intracellular concentrations of Na^+ and K^+ ions, resulting in an alteration of homeostasis

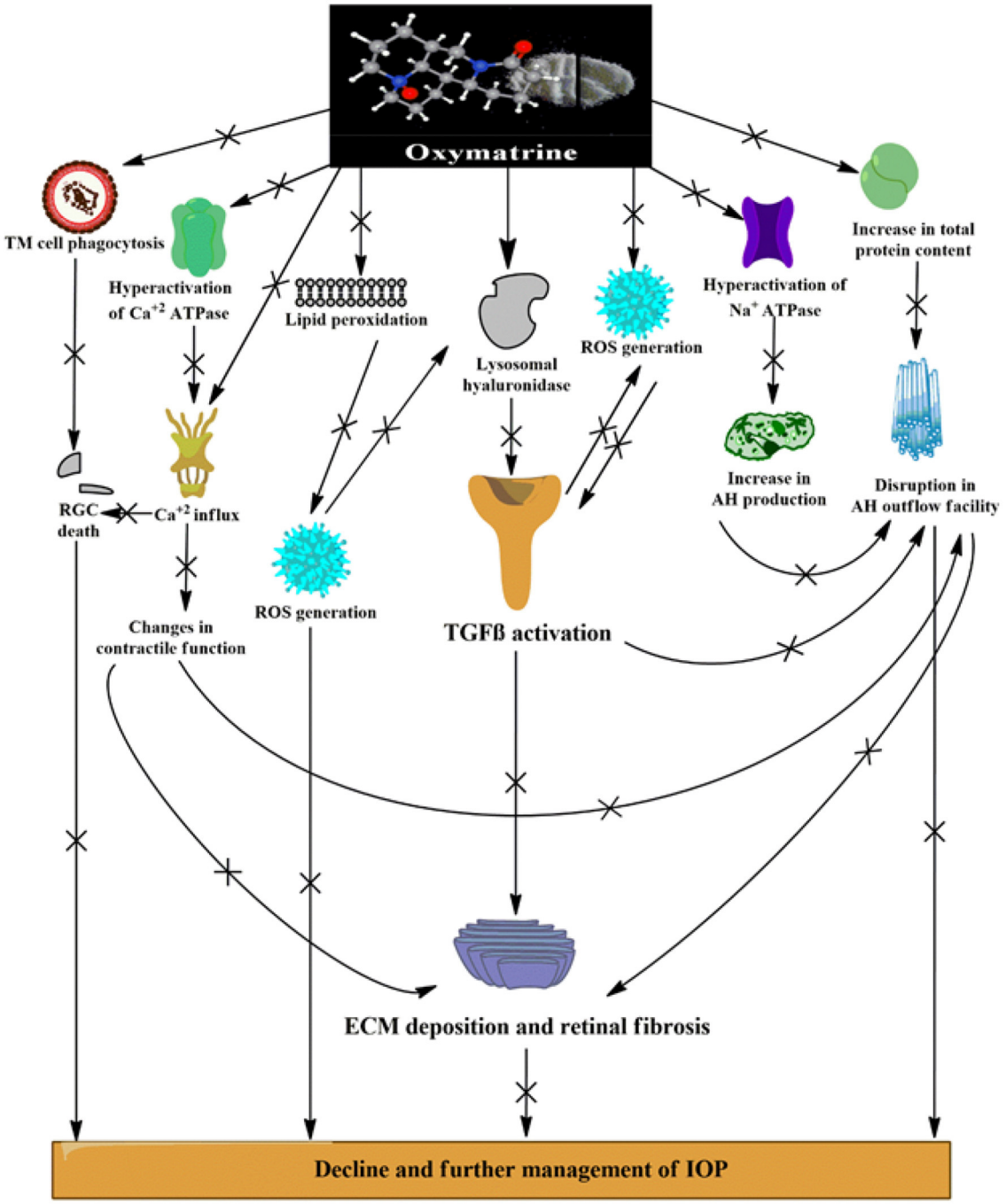

FIGURE 10 | Various possible targets served by OMT administration leading to effective management of IOP and mechanobiological alterations induced by DEX. [(+) indicates activation or increase; (x) indicates inhibition or decrease]. ROS, reactive oxygen species; RGCs, retinal ganglion cells; AH, aqueous humor; IOP, intraocular pressure; TGFβ-transforming growth factor β; iNOS, inducible nitric oxide synthase.

(51). In this study, OMT administration was shown to depress the Na^{+}/K^{+} ATPase activity, with a resultant decline in the related ionic concentrations in the retinal layers and a consequent normalization of activity, thereby shifting the focus to its underestimated roles in the regulation of pump functions and ionic balances. The extensive activities of Ca^{+2} ATPase in the progression of glaucoma have not yet been experimentally elucidated; however, significant rises in intracellular calcium levels and related neurodegeneration and oxidative stress have been previously demonstrated (18, 52). This study has set a

milestone in establishing a factual basis for the Ca^{+2} ATPase activity, which is amplified upon glaucoma induction in the control group animal, thereby forcing an enhanced entry of calcium ions, which is responsible the increased levels of ROS and the resultant excitotoxicity of the RGCs (18, 52). OMT administration has been found to lower the Ca^{+2} ATPase activity significantly, thus pointing toward its actions in reducing the intracellular calcium content. The resultant calcium overload causes excessive contractility due to an amplified actin–myosin interaction, leading to the deposition of fibrogenic materials and structural alterations (53). OMT is responsible for the decline in the levels of the inward L-type calcium current, especially during conditions of calcium overload, and this study also remains in sync with previous considerations as OMT caused prominent reductions in the rates of calcium overload and enhanced the restoration of homeostasis (41).

The results obtained from the ELISA analyses of TGFβ1 clearly defined an enhancement of the TGFβ1 levels in the retinal samples of the DEX-induced glaucoma control group whereas consistent treatment with OMT led to a dose-dependent decline, which is known to inhibit TGFβ1 selectively, thus putting enough emphasis on the impact of TGFβ1 hyperactivation in glaucoma and its resultant reduction. The relationships between the various biochemical parameters and TGFβ1 have been formerly elucidated, and a distinct correlation can thus be portrayed.

Pictures of the retinal vasculature and lens obtained from the DEX-induced glaucoma control animals showed evident retinal fibrosis and bilateral opacity in the lens upon DEX exposure whereas the standard group exhibited restoration of retinal vasculature, but without an efficient disentanglement of the blood vessels and reduction in opacity as compared to the control group. The groups receiving OMT showed dose-dependent effects on the retinal vasculature and lenticular opacity. The animal treated with OMT manifested proper restoration of the retinal vasculature along with optimum lens clarity; this is consistent with the biochemical estimates showing that the group receiving the highest dose of treatment experienced maximum beneficial effects.

CONCLUSION

The preclinical findings obtained from this study implicate an evident role of the TGFβ1 isoform in the progression of glaucoma, which might contribute to the various pathological alterations seen in patients with glaucoma (**Figure 9**). Elevations in oxidative stress, lipid peroxidation, nitrite level, and total protein content, inhibition of ECM-degrading enzymes, dysregulation in the pump activities and ionic levels, and alteration of the retinal vasculature *via* activation of TGFβ1 all work to fan the flames in the pathophysiology of glaucoma. The stipulated drug candidate used in this research, that is, OMT, was able to slow down the pathogenesis of glaucoma by not only lowering and further managing IOP but also substantially restoring the homeostasis of the retinal vasculature, which clearly identified the TGFβ1 isoform as a future target for therapies related to glaucoma inhibition (**Figure 10**).

DATA AVAILABILITY STATEMENT

The original contributions presented in the study are included in the article/supplementary material, further inquiries can be directed to the corresponding author/s.

ETHICS STATEMENT

The animal study was reviewed and approved by Institutional Animal Ethics Committee (IAEC), Committee for the Purpose of Control and Supervision for Experiments on Animals (CPCSEA), Government of India.

AUTHOR CONTRIBUTIONS

AD, KPN, and SB framed the study. AD, OK, and AS conducted the *in vivo* experiments and experimental analysis. AD and SB wrote the manuscript. SB, KPN, and JS analyzed all the experimental data and proofread the manuscript. All authors contributed to the article and approved the submitted version.

ACKNOWLEDGMENTS

We are greatly thankful to Shaanxi Pioneer Biotech, China, for providing a free sample of OMT and Elabscience, USA, for providing a generous gift TNFα ELISA kit. We are equally thankful to Dr. Rajesh R. Ugale and Miss Lopamudra P. Sarode for helping in the ELISA analysis. Finally, We devote their deepest gratitude to UGC-SAP, UGC-MRP, and AYUSH-EMR for providing the required instrumental facilities.

REFERENCES

1. Heldin CH, Miyazono K, Ten PD. TGF-β signalling from cell membrane to nucleus through SMAD proteins. *Nature.* (1997) 390:465–71. doi: 10.1038/37284
2. Junglas B, Kuespert S, Seleem AA, Struller T, Ullmann S, Bösl M, et al. Connective tissue growth factor causes glaucoma by modifying the actin cytoskeleton of the trabecular meshwork. *Am J Pathol.* (2012) 180:2386–403. doi: 10.1016/j.ajpath.2012.02.030
3. Verrecchia F, Mauviel A. Transforming growth factor-β and fibrosis. *World J Gastroenterol.* (2007) 13:3056–62. doi: 10.3748/wjg.v13.i22.3056
4. Wax MB, Tezel G, Edward PD. Clinical and ocular histopathological findings in a patient with normal pressure glaucoma. *Arch Ophthalmol.* (1998) 116:993–1001. doi: 10.1001/archopht.116.8.993
5. Weinreb RN, Aung T, Medeiros FA. The pathophysiology and treatment of glaucoma: a review. *JAMA.* (2014) 311:1901–11. doi: 10.1001/jama.2014.3192
6. Wordinger RJ, Sharma T, Clark AF. The role of TGF-β2 and bone morphogenetic proteins in the trabecular meshwork and

glaucoma. *J ocul pharmacol ther.* (2014) 30:154–62. doi: 10.1089/jop.2013.0220
7. Koch CFG, Ohlmanna A, Fuchshofera R. Welge-Lu?ssenb U, Tamm ER. Thrombospondin-1 in the trabecular meshwork: localization in normal and glaucomatous eyes, and induction by TGF-b1 and dexamethasone *in vitro*. *Exp Eye Res.* (2004) 79:649–63. doi: 10.1016/j.exer.2004.07.005
8. Kuehn MH, Fingert JH, Kwon YH. Retinal ganglion cell death in glaucoma: mechanisms and neuroprotective strategies. *Ophthalmol Clin North Am.* (2005) 18:383–95. doi: 10.1016/j.ohc.2005.04.002
9. Ozcan AA, Ozdemir N, Canataroglu A. The aqueous levels of TGF-β2 in patients with glaucoma. *Int Ophthalmol.* (2004) 25:19–22. doi: 10.1023/B:INTE.0000018524.48581.79
10. Surgucheva I, Surguchov A. Expression of caveolin in trabecular meshwork cells and its possible implication in pathogenesis of primary open angle glaucoma. *Mol Vis.* (2011) 17:2878–88.
11. Fuchshofer R, Yu A, Welge UL, Tamm ER. Bone morphogenetic protein-7 is an antagonist of transforming growth factor-β2 in human trabecular meshwork cells. *Investig Ophthalmol Vis Sci.* (2007) 48:715–26. doi: 10.1167/iovs.06-0226
12. Chen X, Sun R, Hu J, Mo Z, Yang Z, Liao D, et al. Attenuation of bleomycin-induced lung fibrosis by oxymatrine is associated with regulation of fibroblast proliferation and collagen production in primary culture. *Basic Clin Pharmacol Toxicol.* (2008) 103:278–86. doi: 10.1111/j.1742-7843.2008.00287.x
13. Wu CS, Piao XX, Piao DM, Jin YR, Li CH. Treatment of pig serum-induced rat liver fibrosis with Boschniakia rossica, oxymatrine and interferon-α. *World J Gastroenterol.* (2005) 11:122–6. doi: 10.3748/wjg.v11.i1.122
14. Wu XL, Zeng WZ, Jiang MD, Qin JP, Xu H. Effect of Oxymatrine on the TGFbeta-Smad signaling pathway in rats with CCl4-induced hepatic fibrosis. *World J Gastroenterol.* (2008) 14:2100–05. doi: 10.3748/wjg.14.2100
15. Vohra R, Tsai JC, Kolko M. The role of inflammation in the pathogenesis of glaucoma. *Surv Ophthalmol.* (2013) 58:311–20. doi: 10.1016/j.survophthal.2012.08.010
16. Williams PA, Marsh-Armstrong N, Howell GR. Neuroinflammation in glaucoma: a new opportunity. *Exp Eye Res.* (2017) 157:20–7. doi: 10.1016/j.exer.2017.02.014
17. Kasetti RB, Maddineni P, Patel P, Searby C, Sheffield VC, Zode GS. Transforming growth factor β2 (TGFβ2) signaling plays a key role in glucocorticoid-induced ocular hypertension. *J Biol Chem.* (2018) 293:9854–68. doi: 10.1074/jbc.RA118.002540
18. Crish SD, Calkins DJ. Neurodegeneration in glaucoma: progression and calcium dependent intracellular mechanisms. *Neuroscience.* (2011) 10:176. doi: 10.1016/j.neuroscience.2010.12.036
19. Aslan M, Cort A, Yucel I. Oxidative and nitrative stress markers in glaucoma. *Free Radic Biol Med.* (2008) 45:367–76. doi: 10.1016/j.freeradbiomed.2008.04.026
20. Wang WH, Millar JC, Pang LH, Wax MB, Clark AF. Noninvasive measurement of rodent intraocular pressure with a rebound tonometer. *Invest Ophthalmol Vis Sci.* (2005) 46:4617–21. doi: 10.1167/iovs.05-0781
21. Singh A, Bodakhe SH. Resveratrol delay the cataract formation against naphthalene-induced experimental cataract in the albino rats. *J Biochem Mol Toxicol.* (2019) 34:e22420.1–8. doi: 10.1002/jbt.22420
22. Schneiderman H. The Fundoscopic examination. Clinical methods: The history, physical, and laboratory examinations. *Butterworths.* (1990) 3:573–80.
23. Son HY, Kim H. Y HK. Taurine prevents oxidative damage of high glucose-induced cataractogenesis in isolated rat lenses. *J Nutr Sci Vitaminol.* (2007) 53:324–30. doi: 10.3177/jnsv.53.324
24. Sinha AK. Colorimetric assay of catalase. *Anal Biochem.* (1972) 47:389–94. doi: 10.1016/0003-2697(72)90132-7
25. Kakkar P, Das B, Viswanathan PN, A. modified spectrophotometric assay of superoxide dismutase. *Indian J Biochem Biophys.* (1984) 21:130–2.
26. Tappel AL. Glutathione peroxidase and hydroperoxides. *Methods Enzymol.* (1978) 52:506–13. doi: 10.1016/S0076-6879(78)52055-7
27. Dickerson JE, Thomassteely JR, English-wright JR, Clark AF. The effect of dexamethasone on integrin and laminin expression in cultured human trabecular meshwork. *Cells Exp Eye Res.* (1998) 66:731–8. doi: 10.1006/exer.1997.0470
28. Ellman GL. Tissue sulfhydryl groups. *Arch Biochem Biophys.* (1959) 82:70–7. doi: 10.1016/0003-9861(59)90090-6
29. Ohkawa H, Ohishi N, Yagi K. Assay for lipid peroxides in animal tissues by thiobarbituric acid reaction. *Anal Biochem.* (1979) 95:351–8. doi: 10.1016/0003-2697(79)90738-3
30. Green LC, Wagner DA, Glogowski J, Skipper PL, Wishnok JS, Tannenbaum SR. Analysis of nitrate, nitrite, and [15N] nitrate in biological fluids. *Anal Biochem.* (1982) 126:131–8. doi: 10.1016/0003-2697(82)90118-X
31. Lowry OH, Rosebrough NJ, Farr AL, Randall RJ. Protein measurement with the Folin phenol reagent. *J Biol Chem.* (1951) 193:265–75. doi: 10.1016/S0021-9258(19)52451-6
32. Manikandan R, Thiagarajan R, Beulaja S, Sudhandiran G, Arumugam M. Curcumin prevents free radical-mediated cataractogenesis through modulations in lens calcium. *Free Radic Biol Med.* (2010) 48:483–92. doi: 10.1016/j.freeradbiomed.2009.11.011
33. Kersey JP, Broadway DC. Corticosteroid induced glaucoma: a review of the literature. *Eye.* (2006) 20:407–16. doi: 10.1038/sj.eye.6701895
34. Lewis JM, Priddy T, Judd J, Gordon MO, Kass MA, Kolker AE, et al. Intraocular pressure response to topical dexamethasone as a predictor for the development of primary open-angle glaucoma. *Am J Ophthalmol.* (1988) 106:607–12. doi: 10.1016/0002-9394(88)90595-8
35. Palmberg PF, Mandell A, Wilensky JT, Podos SM, Becker B. The reproducibility of the intraocular pressure response to dexamethasone. *Am J ophthalmol.* (1975) 80:844–56. doi: 10.1016/0002-9394(75)90282-2
36. Phulke S, Kaushik S, Kaur S, Pandav SS. Steroid-induced Glaucoma: An Avoidable Irreversible Blindness. *Journal Curr Glaucoma Pract.* (2017) 11:67–72. doi: 10.5005/jp-journals-10028-1226
37. Fatma N, Kubo E, Toris CB, Stamer WD, Camras CB, Singh DP. Prdx6 attenuates oxidative stress- and tgfb-induced abnormalities of human trabecular meshwork cells. *Free Radic Res.* (2009) 43:783–95. doi: 10.1080/10715760903062887
38. Erb C, Heinke M. Oxidative stress in primary open-angle glaucoma. *Front Biosci.* (2011) E3:1524–33. doi: 10.2741/e353
39. Krsti J, Trivanovi D, Mojsilovi S, Santibanez JF. Transforming growth factor-beta and oxidative stress interplay: implications in tumorigenesis and cancer progression. *Oxid Med Cell Longev.* (2015) 1–15. doi: 10.1155/2015/654594
40. Ferreira SM, Lerner SFN, Brunzini R, Evelson PA, Llesuy SF. Oxidative stress markers in aqueous humor of glaucoma patients. *Am J Ophthalmol.* (2004) 137:62–9. doi: 10.1016/S0002-9394(03)00788-8
41. Gang CY, Shan J, Lei L, Jing-quan G, Zhi-ying S, Yan L, et al. Antiarrhythmic effects and ionic mechanisms of oxymatrine from sophora flavescens. *Phytother Res.* (2010) 24:1844–9. doi: 10.1002/ptr.3206
42. Kumar DM, Agarwal N. Oxidative stress in glaucoma: a burden of evidence. *J Glaucoma.* (2007) 16:334–43. doi: 10.1097/01.ijg.0000243480.67532.1b
43. Liu RM, Pravia KAG. Oxidative stress and glutathione in TGF-β-mediated fibrogenesis. *Free Radic Biol Med.* (2010) 48:1–15. doi: 10.1016/j.freeradbiomed.2009.09.026
44. Nucci C, Pierro DD, Varesi C, Ciuffoletti E, Russo R, Gentile R, et al. Increased malondialdehyde concentration and reduced total antioxidant capacity in aqueous humor and blood samples from patients with glaucoma. *Mol vis.* (2013) 19:1841–6.
45. Yildirim O, Ates NA, Ercan B, Lu NM,? nlu? AU, Tamer L, et al. Role of oxidative stress enzymes in open-angle glaucoma. *Eye.* (2005) 19:580–3. doi: 10.1038/sj.eye.6701565
46. Wu J, Pan L, Jin X, Li W, Li H, Chen J, et al. The role of oxymatrine in regulating TGF-β1 in rats with hepatic fibrosis. *Acta Cir Bras.* (2018) 33:207–15. doi: 10.1590/s0102-865020180030000002
47. Wang SB, Jia JP. Oxymatrine attenuates diabetes-associated cognitive deficits in rats. *Acta Pharmacol Sin.* (2014) 35:331–8. doi: 10.1038/aps.2013.158
48. Guo C, Han F, Zhang C, Xiao W, Yang Z. Protective effects of oxymatrine on experimental diabetic nephropathy. *Planta Med.* (2014) 80:269–76. doi: 10.1055/s-0033-1360369
49. Zhou YJ, Guo YJ, Yang XL, Ou ZL. Anti-cervical cancer role of matrine, oxymatrine and sophora flavescens alkaloid gels and its mechanism. *J Cancer.* (2018) 9:1357–136. doi: 10.7150/jca.22427
50. Wang J, Harris A, Prendes MA, Alshawa L, Gross JC, Wentz SM, et al. Targeting transforming growth factor-b signaling in primary open-angle glaucoma. *J Glaucoma.* (2017) 26:390–5. doi: 10.1097/IJG.0000000000000627
51. Hatou S, Yamada M, Mochizuki H, Shiraishi A, Joko T, Nishida T. The effects of dexamethasone on the NA,K-ATPase activity and pump

function of corneal endothelial cells. *Curr Eye Res.* (2009) 34:347–54. doi: 10.1080/02713680902829624
52. Niittykoski M, Kalesnykas G, Larsson KP, Kaarniranta K, Åkerman KEO, Uusitalo H. Altered calcium signaling in an experimental model of glaucoma. *Investig Ophthalmol Vis Sci.* (2010) 51:6387–93. doi: 10.1167/iovs.09-3816
53. Araie M, Mayama C. Use of calcium channel blockers for glaucoma. *Prog Retin Eye Res.* (2011) 30:54–71. doi: 10.1016/j.preteyeres.2010.09.002
54. Mukherjee S, Kolb MRJ, Duan F, Janssen LJ. Transforming growth factor–b evokes ca^{2+} waves and enhances gene expression in human pulmonary fibroblasts. *Am J Respir Cell Mol Biol.* (2012) 46:757–64. doi: 10.1165/rcmb.2011-0223OC
55. Ghanem AA, Arafa LF, El-Baz A. Oxidative stress markers in patients with primary open-angle glaucoma. *Curr Eye Res.* (2010) 35:295–301. doi: 10.3109/02713680903548970
56. Liu RM, Desai LP. Reciprocal regulation of tgf-β and reactive oxygen species: a perverse cycle for fibrosis. *Redox Biol.* (2015) 6:565–77. doi: 10.1016/j.redox.2015.09.009

Conflict of Interest: The authors declare that the research was conducted in the absence of any commercial or financial relationships that could be construed as a potential conflict of interest.

Advantages of publishing in Frontiers

OPEN ACCESS
Articles are free to read for greatest visibility and readership

FAST PUBLICATION
Around 90 days from submission to decision

HIGH QUALITY PEER-REVIEW
Rigorous, collaborative, and constructive peer-review

TRANSPARENT PEER-REVIEW
Editors and reviewers acknowledged by name on published articles

Frontiers
Avenue du Tribunal-Fédéral 34
1005 Lausanne | Switzerland

Visit us: www.frontiersin.org
Contact us: frontiersin.org/about/contact

REPRODUCIBILITY OF RESEARCH
Support open data and methods to enhance research reproducibility

DIGITAL PUBLISHING
Articles designed for optimal readership across devices

FOLLOW US
@frontiersin

IMPACT METRICS
Advanced article metrics track visibility across digital media

EXTENSIVE PROMOTION
Marketing and promotion of impactful research

LOOP RESEARCH NETWORK
Our network increases your article's readership